

# Arthritis & Rheumatology

An Official Journal of the American College of Rheumatology  
www.arthritisrheum.org and wileyonlinelibrary.com

## Editor

Daniel H. Solomon, MD, MPH, *Boston*

## Deputy Editors

Richard J. Bucala, MD, PhD, *New Haven*

Mariana J. Kaplan, MD, *Bethesda*

Peter A. Nigrovic, MD, *Boston*

## Co-Editors

Karen H. Costenbader, MD, MPH, *Boston*

David T. Felson, MD, MPH, *Boston*

Richard F. Loeser Jr., MD, *Chapel Hill*

## Social Media Editor

Paul H. Sufka, MD, *St. Paul*

## Journal Publications Committee

Amr Sawalha, MD, *Chair, Pittsburgh*

Susan Boackle, MD, *Denver*

Aileen Davis, PhD, *Toronto*

Deborah Feldman, PhD, *Montreal*

Donnamarie Krause, PhD, OTR/L, *Las Vegas*

Wilson Kuswanto, MD, PhD, *Stanford*

Michelle Ormseth, MD, *Nashville*

R. Hal Scofield, MD, *Oklahoma City*

## Editorial Staff

Kimberly M. Murphy, *Senior Director & Managing Editor, Delaware*

Lesley W. Allen, *Assistant Managing Editor, Virginia*

Ilani S. Lorber, *Assistant Managing Editor, Georgia*

Stefanie L. McKain, *Manuscript Editor, Georgia*

Rasa G. Hamilton, *Manuscript Editor, Florida*

Brian T. Robinson, *Manuscript Editor, Pennsylvania*

Christopher Reynolds, *Editorial Coordinator, Georgia*

Audra Jenson, *Assistant Editor, North Carolina*

## Associate Editors

Marta Alarcón-Riquelme, MD, PhD, *Granada*

Heather G. Allore, PhD, *New Haven*

Neal Basu, MD, PhD, *Glasgow*

Edward M. Behrens, MD, *Philadelphia*

Bryce Binstadt, MD, PhD, *Minneapolis*

Nunzio Bottini, MD, PhD, *San Diego*

John Carrino, MD, MPH, *New York*

Andrew Cope, MD, PhD, *London*

Adam P. Croft, MBChB, PhD, MRCP, *Birmingham*

Nicola Dalbeth, MD, FRACP, *Auckland*

Brian M. Feldman, MD, FRCPC, MSc, *Toronto*

Richard A. Furie, MD, *Great Neck*

J. Michelle Kahlenberg, MD, PhD, *Ann Arbor*

Benjamin Leder, MD, *Boston*

Yvonne Lee, MD, MMSc, *Chicago*

Katherine Liao, MD, MPH, *Boston*

Bing Lu, MD, DrPH, *Boston*

Stephen P. Messier, PhD, *Winston-Salem*

Rachel E. Miller, PhD, *Chicago*

Janet E. Pope, MD, MPH, *FRCPC, London, Ontario*

Lisa G. Rider, MD, *Bethesda*

Christopher T. Ritchlin, MD, MPH, *Rochester*

William Robinson, MD, PhD, *Stanford*

Carla R. Scanzello, MD, PhD, *Philadelphia*

Georg Schett, MD, *Erlangen*

Sakae Tanaka, MD, PhD, *Tokyo*

Maria Trojanowska, PhD, *Boston*

Betty P. Tsao, PhD, *Charleston*

Fredrick M. Wigley, MD, *Baltimore*

Edith M. Williams, PhD, MS, *Rochester*

## Advisory Editors

Ayaz Aghayev, MD, *Boston*

Joshua F. Baker, MD, MSCE, *Philadelphia*

Bonnie Bermas, MD, *Dallas*

Jamie Collins, PhD, *Boston*

Kristen Demoruelle, MD, PhD, *Denver*

Christopher Denton, PhD, FRCP, *London*

Anisha Dua, MD, MPH, *Chicago*

John FitzGerald, MD, *Los Angeles*

Lauren Henderson, MD, MMSc, *Boston*

Monique Hinchcliff, MD, MS, *New Haven*

Hui-Chen Hsu, PhD, *Birmingham*

Mohit Kapoor, PhD, *Toronto*

Seoyoung Kim, MD, ScD, MSCE, *Boston*

Vasileios Kytтарыs, MD, *Boston*

Carl D. Langefeld, PhD, *Winston-Salem*

Dennis McGonagle, FRCPI, PhD, *Leeds*

Julie Paik, MD, MHS, *Baltimore*

Amr Sawalha, MD, *Pittsburgh*

Julie Zikherman, MD, *San Francisco*

## AMERICAN COLLEGE OF RHEUMATOLOGY

Kenneth G. Saag, MD, MSc, *Birmingham*, **President**

Douglas White, MD, PhD, *La Crosse*, **President-Elect**

Carol Langford, MD, MHS, *Cleveland*, **Treasurer**

Deborah Desir, MD, *New Haven*, **Secretary**

Steven Echard, IOM, CAE, *Atlanta*, **Executive Vice-President**

© 2022 American College of Rheumatology. All rights reserved. No part of this publication may be reproduced, stored or transmitted in any form or by any means without the prior permission in writing from the copyright holder. Authorization to copy items for internal and personal use is granted by the copyright holder for libraries and other users registered with their local Reproduction Rights Organization (RRO), e.g. Copyright Clearance Center (CCC), 222 Rosewood Drive, Danvers, MA 01923, USA (www.copyright.com), provided the appropriate fee is paid directly to the RRO. This consent does not extend to other kinds of copying such as copying for general distribution, for advertising or promotional purposes, for creating new collective works or for resale. Special requests should be addressed to: permissions@wiley.com.

Access Policy: Subject to restrictions on certain backfiles, access to the online version of this issue is available to all registered Wiley Online Library users 12 months after publication. Subscribers and eligible users at subscribing institutions have immediate access in accordance with the relevant subscription type. Please go to onlinelibrary.wiley.com for details.

The views and recommendations expressed in articles, letters, and other communications published in Arthritis & Rheumatology are those of the authors and do not necessarily reflect the opinions of the editors, publisher, or American College of Rheumatology. The publisher and the American College of Rheumatology do not investigate the information contained in the classified advertisements in this journal and assume no responsibility concerning them. Further, the publisher and the American College of Rheumatology do not guarantee, warrant, or endorse any product or service advertised in this journal.

Cover design: Todd Machen

©This journal is printed on acid-free paper.

# Arthritis & Rheumatology

An Official Journal of the American College of Rheumatology  
www.arthritisrheum.org and wileyonlinelibrary.com

VOLUME 74 • November 2022 • NO. 11

<b>In This Issue</b> .....	A15
<b>Journal Club</b> .....	A16
<b>Clinical Connections</b> .....	A17
<b>Special Articles</b>	
Editorial: Immune Cell Signatures to Stratify Patients With Systemic Autoimmune Diseases: A Step Toward Individualized Medicine? <i>Takahisa Gono and Divi Cornec</i> .....	1727
Editorial: Transforming Rheumatology Practice With Technology: Products, Processes, People, and Purpose <i>Rebecca Grainger</i> .....	1730
Notes from the Field: VEXAS Syndrome and Disease Taxonomy in Rheumatology <i>Peter C. Grayson, David B. Beck, Marcela A. Ferrada, Peter A. Nigrovic, and Daniel L. Kastner</i> .....	1733
<b>Rheumatoid Arthritis</b>	
Smartphone-Assisted Patient-Initiated Care Versus Usual Care in Patients With Rheumatoid Arthritis and Low Disease Activity: A Randomized Controlled Trial <i>Bart Seppen, Jimmy Wiegel, Marieke M. ter Wee, Dirkjan van Schaardenburg, Leo D. Roorda, Michael T. Nurmohamed, Maarten Boers, and Wouter H. Bos</i> .....	1737
Heavy Chain Constant Region Usage in Antibodies to Peptidylarginine Deiminase 4 as a Marker of Disease Subsets in Rheumatoid Arthritis <i>E. Gómez-Bañuelos, J. Shi, H. Wang, M. I. Danila, S. L. Bridges Jr., J. T. Giles, G. P. Sims, F. Andrade, and E. Darrach</i> .....	1746
A Risk Score to Detect Subclinical Rheumatoid Arthritis-Associated Interstitial Lung Disease <i>Pierre-Antoine Juge, Benjamin Granger, Marie-Pierre Debray, Esther Ebstein, Fabienne Louis-Sidney, Joanna Kedra, Tracy J. Doyle, Raphaël Borie, Arnaud Constantin, Bernard Combe, René-Marc Flipo, Xavier Mariette, Olivier Vittecoq, Alain Saraux, Guillermo Carvajal-Alegria, Jean Sibilia, Francis Berenbaum, Caroline Kannengiesser, Catherine Boileau, Jeffrey A. Sparks, Bruno Crestani, Bruno Fautrel, and Philippe Dieudé</i> .....	1755
Serologic Biomarkers of Progression Toward Diagnosis of Rheumatoid Arthritis in Active Component Military Personnel <i>Matthew J. Loza, Sunil Nagpal, Suzanne Cole, Renee M. Laird, Ashley Alcalá, Navin L. Rao, Mark S. Riddle, and Chad K. Porter</i> .....	1766
Phase II/III Results of a Trial of Anti-Tumor Necrosis Factor Multivalent NANOBODY Compound Ozoralizumab in Patients With Rheumatoid Arthritis <i>Tsutomu Takeuchi, Masafumi Kawanishi, Megumi Nakanishi, Hironori Yamasaki, and Yoshiya Tanaka</i> .....	1776
<b>Spondyloarthritis</b>	
Characterization of Blood Mucosal-Associated Invariant T Cells in Patients With Axial Spondyloarthritis and of Resident Mucosal-Associated Invariant T Cells From the Axial Enteses of Non-Axial Spondyloarthritis Control Patients <i>Nicolas Rosine, Hannah Rowe, Surya Koturan, Hanane Yahia-Cherbal, Claire Leloup, Abdulla Watad, Francis Berenbaum, Jeremie Sellam, Maxime Dougados, Vishukumar Aimanianda, Richard Cuthbert, Charlie Bridgwood, Darren Newton, Elisabetta Bianchi, Lars Rogge, Dennis McGonagle, and Corinne Miceli-Richard</i> .....	1786
<b>Systemic Lupus Erythematosus</b>	
Choroid Plexus-Infiltrating T Cells as Drivers of Murine Neuropsychiatric Lupus <i>Erica Moore, Michelle W. Huang, Cara A. Reynolds, Fernando Macian, and Chaim Putterman</i> .....	1796

Longitudinal Immune Cell Profiling in Patients With Early Systemic Lupus Erythematosus <i>Takanori Sasaki, Sabrina Bracero, Joshua Keegan, Lin Chen, Ye Cao, Emma Stevens, Yujie Qu, Guoxing Wang, Jennifer Nguyen, Jeffrey A. Sparks, V. Michael Holers, Stephen E. Alves, James A. Lederer, Karen H. Costenbader, and Deepak A. Rao</i> . . . . .	1808
--	------

**Dermatomyositis**

Two Distinct Immune Cell Signatures Predict the Clinical Outcomes in Patients With Amyopathic Dermatomyositis With Interstitial Lung Disease <i>Yan Ye, Xueliang Zhang, Teng Li, Jiaqiang Ma, Ran Wang, Chunmei Wu, Runci Wang, Chunde Bao, Shuang Ye, Nan Shen, Qiang Guo, Qiong Fu, and Xiaoming Zhang</i> . . . . .	1822
---	------

**Autoimmune Disease**

Recombinant Zoster Vaccine Uptake and Risk of Flares Among Older Adults With Immune-Mediated Inflammatory Diseases in the US <i>Jessica Leung, Tara C. Anderson, Kathleen Dooling, Fenglong Xie, and Jeffrey R. Curtis</i> . . . . .	1833
---	------

**Sjögren’s Syndrome**

Strong Association of Combined Genetic Deficiencies in the Classical Complement Pathway With Risk of Systemic Lupus Erythematosus and Primary Sjögren’s Syndrome <i>Christian Lundtoft, Christopher Sjöwall, Solbritt Rantapää-Dahlqvist, Anders A. Bengtsson, Andreas Jönsen, Pascal Pucholt, Yee Ling Wu, Emeli Lundström, Maija-Leena Eloranta, Iva Gunnarsson, Eva Baecklund, Roland Jonsson, Daniel Hammenfors, Helena Forsblad-d’Elia, Per Eriksson, Thomas Mandl, Sara Bucher, Katrine B. Norheim, Svein Joar Auglaend Johnsen, Roald Omdal, Marika Kvarnström, Marie Wahren-Herlenius, Lennart Truedsson, Bo Nilsson, Sergey V. Kozyrev, Matteo Bianchi, Kerstin Lindblad-Toh, the DISSECT consortium, the ImmunoArray consortium, Chack-Yung Yu, Gunnel Nordmark, Johanna K. Sandling, Elisabet Svenungsson, Dag Leonard, and Lars Rönnblom</i> . . . . .	1842
---	------

**Pediatric Rheumatology**

Joint-Specific Memory and Sustained Risk for New Joint Accumulation in Autoimmune Arthritis <i>Margaret H. Chang, Alexandra V. Bocharnikov, Siobhan M. Case, Marc Todd, Jessica Laird-Gion, Maura Alvarez-Baumgartner, and Peter A. Nigrovic</i> . . . . .	1851
---	------

**Letters**

Duloxetine and Osteoarthritis, a Herd of Elephants in the Room: Comment on the Article by van den Driest et al <i>Alain Brailon</i> . . . . .	1859
Duloxetine May Have Clinical Value: Comment on the Article by van den Driest et al <i>Joel A. Block and Theodore Pincus</i> . . . . .	1859
Reply <i>Jacoline J. van den Driest, Dieuwke Schiphof, Patrick J. E. Bindels, Aafke R. Koffeman, Marc A. Koopmanschap, and Sita M. A. Bierma-Zeinstra</i> . . . . .	1860
Differences in Definitions and Prevalence of Hand Osteoarthritis: Comment on the Article by Eaton et al <i>Amanda E. Nelson, Todd A. Schwartz, Carolina Alvarez, and Yvonne M. Golightly</i> . . . . .	1861
Reply <i>Charles B. Eaton, Tim McAlindon, and Jeffrey Driban</i> . . . . .	1862

**Clinical Images**

Clinical Images: VEXAS Syndrome Presenting as Treatment-Refractory Polyarteritis Nodosa <i>Masaki Itagane, Hiroyuki Teruya, Tomohiro Kato, Naomi Tsuchida, Ayaka Maeda, Yohei Kirino, Yuri Uchiyama, Naomichi Matsumoto, and Mitsuyo Kinjo</i> . . . . .	1863
---	------

**Cover image:** The figure on the cover (from Itagane et al, pages 1863–1864) shows bone marrow aspirates in a patient with VEXAS (vacuoles, E1 enzyme, X-linked, autoinflammatory, somatic) syndrome. Numerous vacuoles were present in myeloid precursor cells.

# In this Issue

Highlights from this issue of *A&R* | By Lara C. Pullen, PhD

## Heavy Chain Region Constant Usage in Anti-PAD4 Antibodies Affects Disease Subsets in RA

Anti-peptidylarginine deiminase 4 (anti-PAD4) antibodies can have different constant regions, suggesting that the antibodies are generated in distinct immune microenvironments.

p. 1746

In this issue, Gómez-Bañuelos et al (p. 1746)

report the results of their exploration of the clinical associations of different isotypes and IgG subclasses of anti-PAD4 antibodies in rheumatoid arthritis (RA) patients. They found that anti-PAD4 IgG1, anti-PAD4 IgG3, and anti-PAD4 IgE antibodies identify discrete disease subsets in RA. The investigators found that anti-PAD4 IgG1 was more predictive of radiographic progression than the most utilized serologic clinical indicators and was independent of treatment or RA duration. The results suggest that heavy chain usage drives distinct effector mechanisms of anti-PAD4 antibodies in RA.

The investigators found that anti-PAD4 IgG1, anti-PAD4 IgG2, anti-PAD4 IgG3, anti-PAD4 IgG4, anti-PAD4 IgA, and anti-PAD4 IgE antibodies were more frequent in RA patients than in healthy controls. Moreover, anti-PAD4 IgG1, anti-PAD4 IgG3, and anti-PAD4 IgE were associated with distinct clinical features. Anti-PAD4 IgG1 was predictive of progressive radiographic joint damage, especially in RA patients without baseline joint damage or in those negative for anti-cyclic citrullinated peptide and/or rheumatoid factor. IgG1 was also associated with higher levels of C-reactive protein and interleukin-6 (the only interleukin tested in the study). RA patients with anti-PAD4 IgG3 had higher baseline joint damage scores, while those with anti-PAD4 IgE had higher Disease Activity Score in 28 joints, more frequent rheumatoid nodules, and interstitial lung disease. The researchers

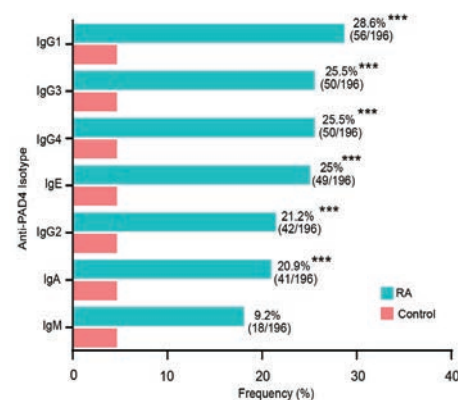


**Figure 1.** Frequency of anti-PAD4 antibody isotypes and IgG subclasses in RA patients and health controls. \*\*\* =  $P < 0.001$ , by Student's t-test.

corroborated anti-PAD4 IgG1 antibody associations with joint damage using an independent RA cohort.

## Combined Genetic Deficiencies in Classical Complement System Associated with Autoimmune Disease

In this issue, Lundtoft et al (p. 1842) report that a genetic pattern involving partial deficiencies of *C2* and *C4A* in the classical complement pathway is a strong

p. 1842

risk factor for systemic lupus erythematosus (SLE) and for primary

Sjögren's syndrome (SS). The observed genetic pattern included heterozygous *C2* deficiency in combination with a low copy number of *C4A*. The results emphasize the central role of the complement system in the pathogenesis of both SLE and primary SS and underscore the fact that partial deficiencies affecting multiple genes of the classical complement pathway may

increase the risk of disease substantially when present in combination.

Both *C2* and *C4A* are in the HLA region on chromosome 6. The 28-bp *C2* deletion rs9332736 exists in all populations of European descent but is relatively uncommon in African and Asian populations. The researchers found that SLE patients with heterozygous *C2* deficiency had reduced *C2* levels in plasma and impaired function of the classical complement pathway.

Investigators examined the effect of heterozygous *C2* deficiency and *C4* copy number variation on clinical manifestations and found that heterozygous *C2* deficiency, when present in combination with a low

*C4A* copy number, substantially increased the risk of SLE (odds ratio [OR] 10.2 [95% confidence interval (95% CI) 3.5–37.0]) and the risk of primary SS (OR 13.0 [95% CI 4.5–48.4]) when compared to individuals with 2 *C4A* copies and normal *C2*. The increased risk of disease for individuals who were heterozygous for the deletion and who also had a *C4A* copy number of 1 translated directly into a lower age at diagnosis for both SLE (median age 7 years younger) and primary SS patients (median age 12 years younger) when compared to patients with normal *C2*. In contrast, heterozygous *C2* deficiency did not affect the age of diagnosis among patients with 2 *C4A* copies.

# RZV Not Associated with Flares in IMID Patients

In October 2021, the Advisory Committee on Immunization Practices recommended recombinant zoster vaccine (RZV) for adults ages  $\geq 19$  years who are or will be immunodeficient or immunosuppressed due to disease or therapy. Previously, a cohort study of participants ages  $\geq 65$  years found vaccine effectiveness to be similar in individuals with immune-mediated inflammatory diseases (IMIDs) compared to the overall population. Some researchers, however, have hypothesized that vaccine adjuvants may trigger a disease flare in those with IMIDs, and prior literature has revealed

p. 1833

highly variable rates of flares, 1.5% – 16.4%.

In this issue, Leung et al (p. 1833) report results of their analysis of the association of presumed flares as defined by hospitalization/ER visit for a patient's IMID or steroid treatment with a short-acting oral glucocorticoid or parenteral glucocorticoid injection and RZV vaccination. They did not find an increase in presumed flares following RZV vaccination, suggesting that RZV vaccinations are safe for IMID patients ages  $\geq 50$  years.

Investigators identified IMID patients in the IBM MarketScan and CMS Medicare databases and found that most RZV vaccines in the US are administered to IMID patients in the pharmacy

setting and not in primary care or specialist offices for  $\geq 65$ -year-olds. Data indicate that 15% of adults 50–64 years of age and 43% of adults  $\geq 65$  years have received at least one dose of RZV. Thus, among IMID patients ages  $\geq 50$  years, a substantial proportion received RZV compared to general zoster coverage estimates. The researchers also found that, for all IMID subpopulations, second-dose completion rates within 6 months were not only high (~80%) but were higher in older age groups compared to younger age groups. They conclude that there appears to be excellent provider and patient acceptance of this vaccine to prevent herpes zoster and related complications.

## Journal Club

*A monthly feature designed to facilitate discussion on research methods in rheumatology.*

### Serologic Biomarkers of Progression Toward Diagnosis of RA in Active Component Military Personnel

Loza et al, *Arthritis Rheumatol.* 2022;74:1766–1775

New-onset rheumatoid arthritis (RA) presenting during mission deployment in active component military personnel could place both them and others at risk. Although elevations of inflammatory cytokines and autoantibodies can be present years preceding a diagnosis of RA, specific predictors for the onset of clinically defined RA within a short timeframe could help identify at-risk personnel before deployment. Loza et al used serum samples from the US Department of Defense Serum Repository, which were collected periodically from active component military personnel throughout their service, to analyze a broad array of protein biomarkers that enabled the building of classification models for predicting imminent diagnosis of RA.

In phase I of the analysis, random forest modeling was performed on SomaLogic SOMAscan serum analyte data from samples taken from 50 seropositive RA patients and 26 healthy control subjects obtained within 6 months before diagnosis. These were randomly separated into training and test sets, and an additional test set of samples from 22 patients with reactive arthritis was included. The random forest method employed included cross-validation steps to select model tuning parameters, the most influential analytes, and model coefficients. A 10-analyte model was confirmed in the test set that classified imminent RA diagnosis with moderate sensitivity and high specificity versus both the healthy controls and patients with reactive arthritis. Validation of the model was performed in phase II using serum samples analyzed by a different

analysis platform, with the model retrained in samples taken from the phase I group using random forest with an 8-analyte set that did not exactly match the previous 10-analyte set from phase I. The final model was confirmed in the phase II test set of seropositive RA samples, which were not included in phase I. Using this approach, the authors demonstrated that imminent diagnosis of seropositive RA, at least in the context of active military personnel, could be classified with moderate sensitivity and high specificity compared to both healthy controls and patients with reactive arthritis, based on a panel of cytokines measured in serum samples collected within 6 months before actual diagnosis.

#### Questions

1. What is currently known about the emergence of objective biomarkers in the years prior to full clinical presentation of RA?
2. Why did the authors focus on imminent diagnosis of RA rather than trying to predict chances of RA diagnosis at longer time intervals?
3. What steps were taken to minimize risks of over-modeling?
4. What are some of the advantages and disadvantages of switching between serum analysis platforms for phases I and II of the analysis?
5. What alternative methods could have been used to build and confirm the classification models?

# In this Issue

Highlights from this issue of *A&R* | By Lara C. Pullen, PhD

## Heavy Chain Region Constant Usage in Anti-PAD4 Antibodies Affects Disease Subsets in RA

Anti-peptidylarginine deiminase 4 (anti-PAD4) antibodies can have different constant regions, suggesting that the antibodies are generated in distinct immune microenvironments.

p. 1746

In this issue, Gómez-Bañuelos et al (p. 1746)

report the results of their exploration of the clinical associations of different isotypes and IgG subclasses of anti-PAD4 antibodies in rheumatoid arthritis (RA) patients. They found that anti-PAD4 IgG1, anti-PAD4 IgG3, and anti-PAD4 IgE antibodies identify discrete disease subsets in RA. The investigators found that anti-PAD4 IgG1 was more predictive of radiographic progression than the most utilized serologic clinical indicators and was independent of treatment or RA duration. The results suggest that heavy chain usage drives distinct effector mechanisms of anti-PAD4 antibodies in RA.

The investigators found that anti-PAD4 IgG1, anti-PAD4 IgG2, anti-PAD4 IgG3, anti-PAD4 IgG4, anti-PAD4 IgA, and anti-PAD4 IgE antibodies were more frequent in RA patients than in healthy controls. Moreover, anti-PAD4 IgG1, anti-PAD4 IgG3, and anti-PAD4 IgE were associated with distinct clinical features. Anti-PAD4 IgG1 was predictive of progressive radiographic joint damage, especially in RA patients without baseline joint damage or in those negative for anti-cyclic citrullinated peptide and/or rheumatoid factor. IgG1 was also associated with higher levels of C-reactive protein and interleukin-6 (the only interleukin tested in the study). RA patients with anti-PAD4 IgG3 had higher baseline joint damage scores, while those with anti-PAD4 IgE had higher Disease Activity Score in 28 joints, more frequent rheumatoid nodules, and interstitial lung disease. The researchers

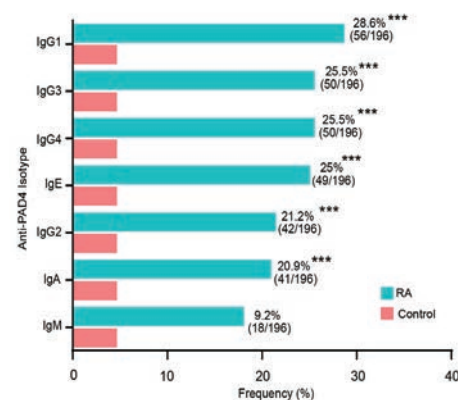


**Figure 1.** Frequency of anti-PAD4 antibody isotypes and IgG subclasses in RA patients and health controls. \*\*\* =  $P < 0.001$ , by Student's t-test.

corroborated anti-PAD4 IgG1 antibody associations with joint damage using an independent RA cohort.

## Combined Genetic Deficiencies in Classical Complement System Associated with Autoimmune Disease

In this issue, Lundtoft et al (p. 1842) report that a genetic pattern involving partial deficiencies of *C2* and *C4A* in the classical complement pathway is a strong

p. 1842

risk factor for systemic lupus erythematosus (SLE) and for primary Sjögren's syndrome (SS). The observed genetic pattern included heterozygous *C2* deficiency in combination with a low copy number of *C4A*. The results emphasize the central role of the complement system in the pathogenesis of both SLE and primary SS and underscore the fact that partial deficiencies affecting multiple genes of the classical complement pathway may

increase the risk of disease substantially when present in combination.

Both *C2* and *C4A* are in the HLA region on chromosome 6. The 28-bp *C2* deletion rs9332736 exists in all populations of European descent but is relatively uncommon in African and Asian populations. The researchers found that SLE patients with heterozygous *C2* deficiency had reduced *C2* levels in plasma and impaired function of the classical complement pathway.

Investigators examined the effect of heterozygous *C2* deficiency and *C4* copy number variation on clinical manifestations and found that heterozygous *C2* deficiency, when present in combination with a low

*C4A* copy number, substantially increased the risk of SLE (odds ratio [OR] 10.2 [95% confidence interval (95% CI) 3.5–37.0]) and the risk of primary SS (OR 13.0 [95% CI 4.5–48.4]) when compared to individuals with 2 *C4A* copies and normal *C2*. The increased risk of disease for individuals who were heterozygous for the deletion and who also had a *C4A* copy number of 1 translated directly into a lower age at diagnosis for both SLE (median age 7 years younger) and primary SS patients (median age 12 years younger) when compared to patients with normal *C2*. In contrast, heterozygous *C2* deficiency did not affect the age of diagnosis among patients with 2 *C4A* copies.

# RZV Not Associated with Flares in IMID Patients

In October 2021, the Advisory Committee on Immunization Practices recommended recombinant zoster vaccine (RZV) for adults ages  $\geq 19$  years who are or will be immunodeficient or immunosuppressed due to disease or therapy. Previously, a cohort study of participants ages  $\geq 65$  years found vaccine effectiveness to be similar in individuals with immune-mediated inflammatory diseases (IMIDs) compared to the overall population. Some researchers, however, have hypothesized that vaccine adjuvants may trigger a disease flare in those with IMIDs, and prior literature has revealed

p. 1833

highly variable rates of flares, 1.5% – 16.4%.

In this issue, Leung et al (p. 1833) report results of their analysis of the association of presumed flares as defined by hospitalization/ER visit for a patient's IMID or steroid treatment with a short-acting oral glucocorticoid or parenteral glucocorticoid injection and RZV vaccination. They did not find an increase in presumed flares following RZV vaccination, suggesting that RZV vaccinations are safe for IMID patients ages  $\geq 50$  years.

Investigators identified IMID patients in the IBM MarketScan and CMS Medicare databases and found that most RZV vaccines in the US are administered to IMID patients in the pharmacy

setting and not in primary care or specialist offices for  $\geq 65$ -year-olds. Data indicate that 15% of adults 50–64 years of age and 43% of adults  $\geq 65$  years have received at least one dose of RZV. Thus, among IMID patients ages  $\geq 50$  years, a substantial proportion received RZV compared to general zoster coverage estimates. The researchers also found that, for all IMID subpopulations, second-dose completion rates within 6 months were not only high (~80%) but were higher in older age groups compared to younger age groups. They conclude that there appears to be excellent provider and patient acceptance of this vaccine to prevent herpes zoster and related complications.

## Journal Club

*A monthly feature designed to facilitate discussion on research methods in rheumatology.*

### Serologic Biomarkers of Progression Toward Diagnosis of RA in Active Component Military Personnel

Loza et al, *Arthritis Rheumatol.* 2022;74:1766–1775

New-onset rheumatoid arthritis (RA) presenting during mission deployment in active component military personnel could place both them and others at risk. Although elevations of inflammatory cytokines and autoantibodies can be present years preceding a diagnosis of RA, specific predictors for the onset of clinically defined RA within a short timeframe could help identify at-risk personnel before deployment. Loza et al used serum samples from the US Department of Defense Serum Repository, which were collected periodically from active component military personnel throughout their service, to analyze a broad array of protein biomarkers that enabled the building of classification models for predicting imminent diagnosis of RA.

In phase I of the analysis, random forest modeling was performed on SomaLogic SOMAscan serum analyte data from samples taken from 50 seropositive RA patients and 26 healthy control subjects obtained within 6 months before diagnosis. These were randomly separated into training and test sets, and an additional test set of samples from 22 patients with reactive arthritis was included. The random forest method employed included cross-validation steps to select model tuning parameters, the most influential analytes, and model coefficients. A 10-analyte model was confirmed in the test set that classified imminent RA diagnosis with moderate sensitivity and high specificity versus both the healthy controls and patients with reactive arthritis. Validation of the model was performed in phase II using serum samples analyzed by a different

analysis platform, with the model retrained in samples taken from the phase I group using random forest with an 8-analyte set that did not exactly match the previous 10-analyte set from phase I. The final model was confirmed in the phase II test set of seropositive RA samples, which were not included in phase I. Using this approach, the authors demonstrated that imminent diagnosis of seropositive RA, at least in the context of active military personnel, could be classified with moderate sensitivity and high specificity compared to both healthy controls and patients with reactive arthritis, based on a panel of cytokines measured in serum samples collected within 6 months before actual diagnosis.

#### Questions

1. What is currently known about the emergence of objective biomarkers in the years prior to full clinical presentation of RA?
2. Why did the authors focus on imminent diagnosis of RA rather than trying to predict chances of RA diagnosis at longer time intervals?
3. What steps were taken to minimize risks of over-modeling?
4. What are some of the advantages and disadvantages of switching between serum analysis platforms for phases I and II of the analysis?
5. What alternative methods could have been used to build and confirm the classification models?

# Clinical Connections

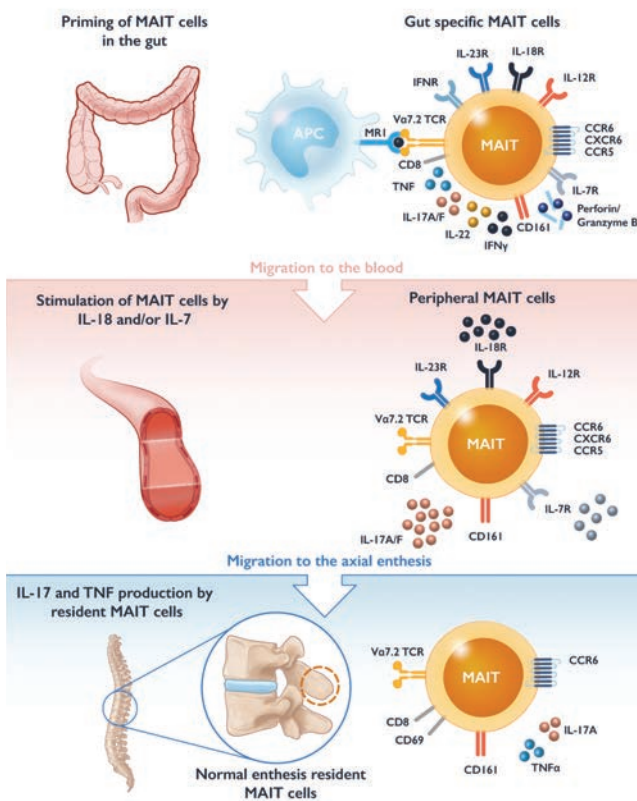
## Peripheral and Enthesal IL-17–Secreting MAIT Cells in Axial SpA

Rosine et al, *Arthritis Rheumatol.* 2022;74:1786–1795

### CORRESPONDENCE

**Corinne Miceli-Richard, MD, PhD:** corinne.miceli@aphp.fr

**Dennis McGonagle, PhD:** d.g.mcgonagle@leeds.ac.uk



### KEY POINTS

- MAITs can produce high amounts of IL-17A/F independently of IL-23 stimulation.
- Normal spinous process have resident MAITs able to produce TNF and IL-17A.
- MAITs cell could be a candidate cell type linking gut and axial inflammation in SpA.

### SUMMARY

Axial spondyloarthritis (AxSpA) shows strong associations with gut mucosal abnormalities that are frequently subclinical, but even so, such silent inflammation is associated with active axial inflammatory episodes. The normal intestine has numerous resident populations of both adaptive and innate lymphocytes, the latter of which includes mucosal-associated invariant T cells (MAITs). The MAIT population plays important roles in immunity and is regulated strongly by intestinal microbiota and B vitamin complex metabolites. It is suspected that MAITs may also traffic from the intestine to other sites. Rosine et al investigated MAITs in the blood in active AxSpA, and determined whether such cells were actually resident in the normal spinal enthesis tissue, a key target for skeletal pathology.

It was observed that blood MAIT cells were able to produce high amounts of interleukin-17A (IL-17A) and/or IL-17F depending on the type of cell stimulation.

Finally, it was shown that the normal spinous process enthesis also had resident MAITs in healthy controls and that these were more numerous than in the blood. Stimulation of MAITs resulted in production of key SpA-associated cytokines, including tumor necrosis factor (TNF) and IL-17A. Interestingly, IL-17 production in normal enthesis was independent of IL-23 stimulation, an observation that could at least partially explain the lack of demonstrated efficacy of IL-23 blocking agents in AxSpA. Collectively, these findings suggest novel pathways to understand and explore the immunology and therapy of the gut/enthesis axis in spondyloarthritis.

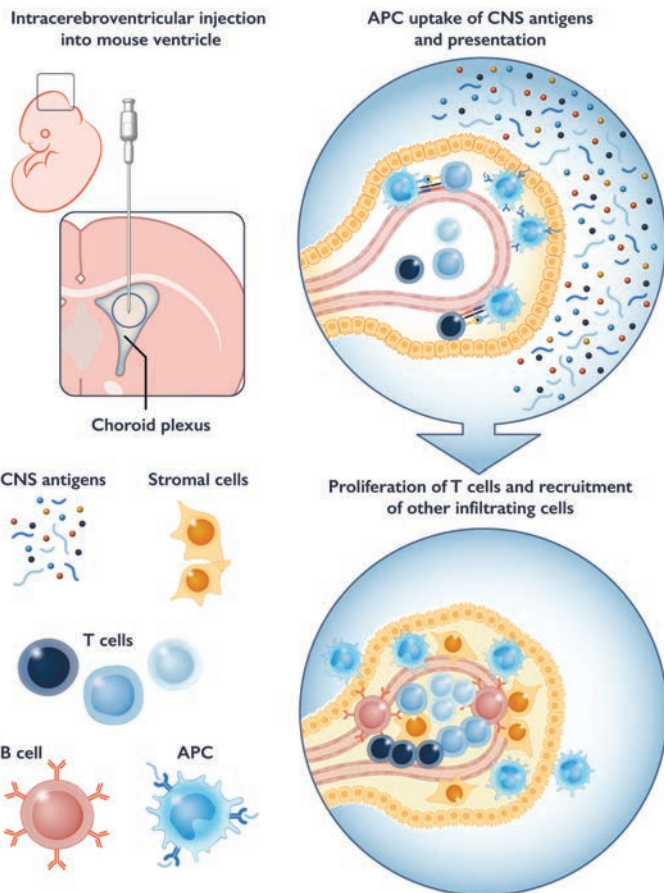


# Choroid Plexus–Infiltrating T Cells as Drivers of Murine Neuropsychiatric Lupus

Moore et al, *Arthritis Rheumatol.* 2022; 74:1796–1807

**CORRESPONDENCE**

**Chaim Putterman, MD:** [chaim.putterman@biu.ac.il](mailto:chaim.putterman@biu.ac.il)



**SUMMARY**

In autoimmune diseases such as systemic lupus erythematosus (SLE), T cells become dysfunctional and respond to the body’s own proteins rather than those of an invading pathogen. As a result, these cells migrate into various organs, where they can locally damage the tissue via various inflammatory pathways. However, their role in the central nervous system (CNS) manifestations, termed neuropsychiatric lupus, has not been previously evaluated. Furthermore, while T cells have been found to infiltrate into the choroid plexus (CP), a tissue in the CNS that forms the blood–cerebrospinal fluid barrier, little was previously known about their contribution to neuropsychiatric symptoms, such as memory dysfunction and depressive-like behavior. Moore et al demonstrated that CP-infiltrating T cells specifically drive neuropsychiatric lupus in the lupus mouse model (using MRL/lpr mice).

When MRL/lpr mice were depleted of CD4+ T cells, the treated mice had improved memory compared to controls. When CP-infiltrating T cells were injected into a brain ventricle of another mouse, the recipient mice had worse memory and depressive-like behavior compared to both the controls and the recipient mice injected with T cells from the spleen. These behavioral differences were found without any changes in the number of T cells or other immune cells in the CP of the injected mice. These CP-infiltrating T cells demonstrated enhanced activation upon exposure to CNS tissue rather than another organ, suggesting that these T cells specifically recognize proteins expressed in the CNS. These data demonstrate that T cells contribute to the mechanisms underlying neuropsychiatric lupus and, thus, may be a potential therapeutic target.

**KEY POINTS**

- T cells are integral to SLE disease.
- T cells extensively infiltrate the CP in the neuropsychiatric lupus mouse model.
- Adoptive transfer of CP-infiltrating T cells specifically worsened neuropsychiatric disease.
- CP-infiltrating T cells may specifically recognize CNS antigens.

**EDITORIAL**

# Immune Cell Signatures to Stratify Patients With Systemic Autoimmune Diseases: A Step Toward Individualized Medicine?

Takahisa Gono<sup>1</sup>  and Divi Cornec<sup>2</sup> 

Idiopathic inflammatory myopathies (IIMs) are a heterogeneous group of autoimmune disorders that mainly affect skeletal muscles with varying clinical manifestations, treatment responses, and prognoses (1). According to the EULAR/American College of Rheumatology classification criteria for IIMs, they are classified into polymyositis/immune-mediated necrotizing myopathy, dermatomyositis (DM), amyopathic dermatomyositis (ADM), and inclusion body myositis (2). A measurement for myositis-specific autoantibodies has been developed and is useful for the diagnosis and categorization of IIMs and the prediction of clinical course and prognosis in the fields of clinical practice as well as research (3,4). Among the myositis-specific autoantibodies, the anti-melanoma differentiation-associated protein 5 (MDA-5) antibody is strongly related to the development of ADM with rapidly progressive interstitial lung disease (RPILD) (5). This condition occasionally leads to fatal outcomes despite intensified combined immunosuppressive therapy with high-dose glucocorticoids, calcineurin inhibitors, and intravenous cyclophosphamide (6).

A recent study stratified patients with IIMs based on clinical parameters, with the aim of identifying predictors of mortality from ILD (7). After adjustment for the treatment regimen, 3 groups with different survival rates were identified among ILD patients positive for anti-MDA-5 antibodies (7). This study suggests that the clinical outcomes might depend on different immunophenotypes among patients with anti-MDA-5 antibodies. In this issue of *Arthritis & Rheumatology*, Ye et al investigated the heterogeneity of immunologic signatures and the relationship between immunologic features and clinical outcomes in patients who have ADM with ILD (ADM-ILD), using peripheral blood immunologic profiles by multi-color flow cytometry with hierarchical clustering analysis (8).

In this study, 82 ADM-ILD patients were enrolled. Of those patients, 78 (95%) were positive for anti-MDA-5 antibodies (8). The

outstanding part of the method in this study was to conduct a comprehensive analysis of 42 immune cell types from peripheral blood by flow cytometry and to stratify immunophenotypes using 2 kinds of unsupervised machine learning approaches: sparse partial least squares discriminant analysis and balanced random forest. Ye et al identified 2 clusters based on the stratification by immunophenotypes: cluster 1 was enriched in activated CD45RA+HLA-DR+CD8+ T cells with decreased CD56<sup>dim</sup> NK cell proportions, with a higher prevalence of RPILD and higher mortality rates; cluster 2 was the nonactivated T cell–dominant cluster showing favorable clinical outcomes with high survival rates. The immunophenotype of cluster 1 was an independent risk factor for mortality based on multivariable analysis using Cox proportional hazards regression models. On the other hand, clinical parameters such as the high-resolution computed tomography score and serum biomarkers including lactate hydrogenase and ferritin were not significant independent risk factors for mortality in patients with ADM-ILD. Ye et al showed that the immunophenotype was an independent risk factor associated with 1-year survival (8). This finding indicates that physicians should consider therapeutic regimens based on the immunophenotype of individual patients with ADM-ILD.

Accumulating recent evidence shows that most autoimmune diseases are highly heterogeneous and comprise distinct subsets of patients with common features. These subsets may be defined clinically based on the symptoms reported by the patients (9), as was recently shown for another systemic autoimmune disease, primary Sjögren's syndrome (10). Immune cell-based signatures have also been extensively studied to diagnose, classify, or stratify patients with different autoimmune diseases, but technical limitations of the flow cytometry approaches and of the supervised analyses strategies, study design pitfalls, and high heterogeneity of the results have precluded firm conclusions in most conditions

<sup>1</sup>Takahisa Gono, MD, PhD: Department of Allergy and Rheumatology, Nippon Medical School Graduate School of Medicine, and Scleroderma/Myositis Center of Excellence, Nippon Medical School Hospital, Tokyo, Japan; <sup>2</sup>Divi Cornec, MD, PhD: INSERM UMR1227 LBAI, Lymphocytes B, Autoimmunité et Immunothérapies, University of Brest, and Rheumatology Department, National Reference Center for Rare Systemic Autoimmune Diseases CERAINO, Brest University Hospital, Brest, France.

Author disclosures are available at <https://onlinelibrary.wiley.com/action/downloadSupplement?doi=10.1002%2Fart.42263&file=art42263-sup-0001-Disclosureform.pdf>.

Address correspondence via email to Divi Cornec, MD, PhD, at [divi.cornec@chu-brest.fr](mailto:divi.cornec@chu-brest.fr).

Submitted for publication March 24, 2022; accepted in revised form June 9, 2022.

(11). In the study by Ye et al, several of these limitations were addressed, as the authors used large panels of multicolor flow cytometry that allowed for a global overview of the immune cell profiles, including rare immune cell subsets, and they used unsupervised artificial intelligence–based clustering approaches to stratify the patients based on their biologic features (8). The 2 clusters of patients who were defined by this strategy were clearly distinct from a clinical standpoint, supporting the validity of this approach.

As we entered the era of system biology, other approaches have recently been deployed to invent a new taxonomy of systemic autoimmune diseases, based on multiomic characterization of patients, in order to define distinct biologically defined groups of patients. The PRECISESADS project was a European Council–supported consortium that studied a large and well-defined multicentric cohort of >2,000 patients with rheumatoid arthritis, systemic lupus erythematosus, systemic sclerosis, Sjögren’s syndrome, and undifferentiated connective tissue disease (<https://www.imi.europa.eu/projects-results/project-factsheets/precisesads>). This cohort was biologically characterized using state-of-the-art multiomic analyses (transcriptomic, genomic, epigenomic, proteomic, and metabolomic approaches, as well as deep immunophenotyping by standardized flow cytometry [12]), and innovative bioinformatics approaches were used to cluster the patients.

This ambitious project showed that, independent of the diagnosis made by the clinician, patients could be classified into distinct clusters defined by their biologic signature, paving the way for individualized treatment strategies targeting the main biologic pathways involved in the different clusters (13). Patients could also be classified according to their serum cytokine profiles leading to distinct immune cell and specifically B cell functional orientation (14). Within each clinically defined group of patients, a similar clustering based on biologic signatures could also be performed, suggesting that different treatment strategies may be evaluated for patients with different biologic features (15,16). For example, unsupervised analyses of total blood RNA sequencing data from the Sjögren’s syndrome cohort of the PRECISESADS project refined the so-called interferon signature in the disease: only half of the patients presented such a signature, and the association with other activated pathways defined 4 clusters of patients with distinct biologic and clinical features.

The next step will be to study these stratification strategies in longitudinal cohorts in order to evaluate whether these signatures are stable over time and are potentially related to the response to targeted therapies and to the prognosis of diseases. Another major challenge will be to evaluate these immune-related signatures within tissues targeted by the autoimmune process. Innovative and complementary tools to explore the immune system,

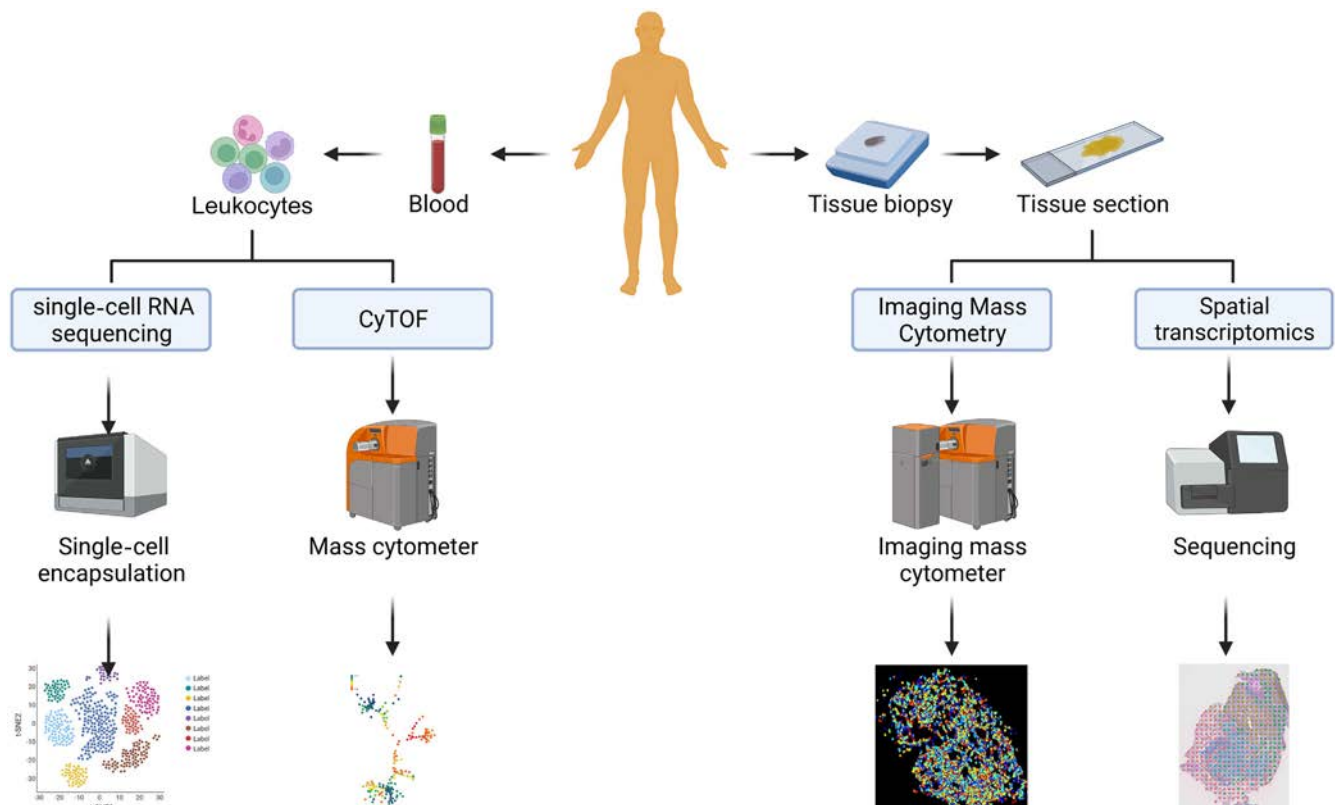


**Figure 1.** Combination of transcriptomic and deep immunophenotyping approaches to decipher the immune system in peripheral blood as well as in tissues targeted by the autoimmune process. Created with BioRender.com. CyTOF = cytometry by time-of-flight mass spectrometry.

e.g., single-cell RNA sequencing, spatial transcriptomics, mass cytometry, and imaging mass cytometry are currently being implemented in our research laboratories (Figure 1). We are opening new and exciting avenues to further stratify patients based on their combined clinical and biologic features to develop realistic and effective strategies for personalized therapy.

## ACKNOWLEDGMENT

The authors thank Soizic Garaud for editorial assistance.

## AUTHOR CONTRIBUTIONS

Drs. Gono and Cornec drafted the article, revised it critically for important intellectual content, and approved the final version to be published.

## REFERENCES

1. Lundberg IE, Fujimoto M, Vencovsky J, et al. Idiopathic inflammatory myopathies. *Nat Rev Dis Primer* 2021;7:86.
2. Lundberg IE, Tjärnlund A, Bottai M, et al. 2017 European League Against Rheumatism/American College of Rheumatology classification criteria for adult and juvenile idiopathic inflammatory myopathies and their major subgroups. *Arthritis Rheumatol* 2017;69:2271–82.
3. Gono T, Kuwana M. Current understanding and recent advances in myositis-specific and -associated autoantibodies detected in patients with dermatomyositis [review]. *Expert Rev Clin Immunol* 2020;16:79–89.
4. Gono T, Kuwana M. Inflammatory myopathies: choosing the right biomarkers to predict ILD in myositis [review]. *Nat Rev Rheumatol* 2016;12:504–6.
5. Sato S, Hoshino K, Satoh T, et al. RNA helicase encoded by melanoma differentiation-associated gene 5 is a major autoantigen in patients with clinically amyopathic dermatomyositis: association with rapidly progressive interstitial lung disease. *Arthritis Rheum* 2009;60:2193–200.
6. Sato S, Masui K, Nishina N, et al. Initial predictors of poor survival in myositis-associated interstitial lung disease: a multicentre cohort of 497 patients. *Rheumatol Oxf Engl* 2018;57:1212–21.
7. Gono T, Masui K, Nishina N, et al. Risk prediction modeling based on a combination of initial serum biomarker levels in polymyositis/dermatomyositis-associated interstitial lung disease. *Arthritis Rheumatol* 2021;73:677–86.
8. Ye Y, Zhang X, Li T, et al. Two distinct cell signatures predict the clinical outcomes in patients with amyopathic dermatomyositis with interstitial lung disease. *Arthritis Rheumatol* 2022;74:1822–32.
9. Escoda T, Jourde-Chiche N, Cornec D, et al. Toward a better clinical stratification of patients with autoimmune diseases to improve research and care within its biopsychosocial dimensions. *Rev Med Interne* 2022;43:71–4. In French.
10. Tarn JR, Howard-Tripp N, Lendrem DW, et al. Symptom-based stratification of patients with primary Sjögren's syndrome: multi-dimensional characterisation of international observational cohorts and reanalyses of randomised clinical trials. *Lancet Rheumatol* 2019;1:e85–94.
11. Alegria GC, Gazeau P, Hillion S, et al. Could lymphocyte profiling be useful to diagnose systemic autoimmune diseases? *Clin Rev Allergy Immunol* 2017;53:219–36.
12. Le Lann L, Jouve PE, Alarcón-Riquelme M, et al. Standardization procedure for flow cytometry data harmonization in prospective multicenter studies. *Sci Rep* 2020;10:11567.
13. Barturen G, Babaei S, Català-Moll F, et al. Integrative analysis reveals a molecular stratification of systemic autoimmune diseases. *Arthritis Rheumatol* 2021;73:1073–85.
14. Simon Q, Grasseau A, Boudigou M, et al. A proinflammatory cytokine network profile in Th1/Type 1 effector B cells delineates a common group of patients in four systemic autoimmune diseases. *Arthritis Rheumatol* 2021;73:1550–61.
15. Beretta L, Barturen G, Vigone B, et al. Genome-wide whole blood transcriptome profiling in a large European cohort of systemic sclerosis patients. *Ann Rheum Dis* 79:1218–26.
16. Soret P, Le Dantec C, Desvieux E, et al. A new molecular classification to drive precision treatment strategies in primary Sjögren's syndrome. *Nat Commun* 2021;12:3523.

**EDITORIAL**

# Transforming Rheumatology Practice With Technology: Products, Processes, People, and Purpose

Rebecca Grainger 

The recent decades of advances in rheumatology therapeutics translate into being able to aim for excellent outcomes for the majority of patients. We have an evidence base informing management and an ever-increasing range of treatments. Despite this, the field of rheumatology does not consistently achieve high-quality care at scale (1,2), and people from racial/ethnic minorities and of lower socioeconomic status disproportionately experience poor health outcomes (3). Perhaps harnessing the potential of digital technologies, which have transformed many aspects of modern life, can be the step change to extend high-quality rheumatology care to all? Digital health technologies (DHTs) that could enhance personalized care and ensure more consistent care across patient populations include mobile health applications, wearable devices, artificial intelligence and machine learning, digital therapeutics, telemedicine, and electronic health records (EHRs) (4). While each of these DHTs can be individually useful, integration would provide additional benefits. For example, organizing clinician- and patient-derived data into dashboards for clinicians would provide real-time insights on the quality of care and identify at-risk patients or areas for improvement in care pathways. Another opportunity includes the use of machine learning using routine EHR data to proactively identify patients at risk of poor outcomes who may require additional care (5). To inform such transformations will require an understanding of how and under what circumstances DHTs can support the achievement of the outcomes we want for our patients (do they work?), how we can avoid or minimize harm, including unintended consequences (are they safe?), and in what circumstances can these be implemented successfully into work practices and organizations (how does using this DHT affect clinical care and does clinical care still work well?).

In this issue of *Arthritis & Rheumatology*, Seppens et al report a randomized control trial (RCT) providing data on a patient-led, mobile app-supported care model that addresses some of these questions for people with rheumatoid arthritis (RA) with stable, low disease activity (6). In a metropolitan rheumatology practice in The Netherlands, participants were randomized to receive

usual care with appointments scheduled every 3 to 6 months (n = 53; usual care group) compared to participants in a group that self-reported weekly Routine Assessment of Patient Index Data 3 (RAPID3) results on a mobile application and had no routine appointments but the ability to initiate appointments for any perceived need (n = 50; app intervention group). At 12 months, RA disease activity (as measured by the Disease Activity Score in 28 joints using the erythrocyte sedimentation rate [DAS28-ESR]) increased slightly in both groups ( $\Delta$ DAS28-ESR was 0.27 for the app intervention group and 0.35 for the usual care group) with a mean difference in DAS28-ESR within the noninferiority limit:  $-0.04$  in favor of app group (95% confidence interval  $-0.39, 0.30$ ). This indicates that disease activity in participants in the app intervention group was not inferior to that of usual care. Furthermore, the coprimary outcome measure of the ratio of the total rate of consultations with rheumatologists (including in-person and via telephone) favored the app intervention with a ratio of 0.6. This equated to 38% fewer appointments for participants in the app intervention group.

Participants in both groups had longstanding RA (mean duration 11 years in the app intervention groups, and 9 years in the usual care group), low disease activity (mean  $\pm$  SD DAS28-ESR  $1.7 \pm 0.7$  in the app intervention group and  $1.5 \pm 0.7$  in the usual care group), with no changes in disease-modifying antirheumatic drugs (DMARDs) in the preceding 6 months. Over the 1-year follow-up period, ~20% of participants (n = 9) in each study arm had flares of RA, requiring a change in DMARD therapy. Participants in the app intervention group recorded their weekly self-monitoring only 60% of the time, which surprisingly was maintained during the 8 months of the study when the intended electronic reminder function did not function. There were no differences between participant groups in any of the secondary outcome measures of patient empowerment, patient-physician interaction, satisfaction with treatment, satisfaction with health care, or physician satisfaction, indicating that the positive

Rebecca Grainger, MB ChB (Dstn), PhD, FRACP: Department of Medicine, University of Otago, Wellington, Wellington, New Zealand.

Author disclosures are available at <https://onlinelibrary.wiley.com/action/downloadSupplement?doi=10.1002%2Fart.42259&file=art42259-sup-0001-DisclosureForm.pdf>.

Address correspondence via email to Rebecca Grainger, MB ChB (Dstn), PhD, FRACP, at [rebecca.grainger@otago.ac.nz](mailto:rebecca.grainger@otago.ac.nz).

Submitted for publication May 19, 2022; accepted in revised form June 2, 2022.

views of health care were maintained in the “arms-length” app intervention participants.

The findings of this study are novel in that it is the first RCT to combine patient-initiated appointments (to reduce the number of visits) with self-monitoring (to maintain disease control), and to report positive results; these findings suggest that this approach to organizing care may be suitable for some people with RA and is able to reduce the need for rheumatology care in The Netherlands. However, there are important points to consider, particularly regarding the adoption of similar care models in other settings. First, the mobile app had been locally developed and evaluated appropriately, informed by the Medical Research Council approach for complex interventions (7,8). An app is not the same as a medication, which can be prescribed locally based on data collected elsewhere. It seems inefficient for every health system or country to develop and evaluate a patient self-monitoring app for every relevant disease; further work is urgently required to understand the minimal essential features and functions and relevant persuasive design elements for an acceptable, useable, and effective patient self-monitoring app (9,10). This will reduce, but not eliminate, the local pre-implementation burden.

Second, the participant data uploaded to the electronic medical record (EMR) were not monitored by the rheumatologist, and participants initiated an appointment for only 10% of the occasions when the app had provided a flare notification. In real-world clinical care, safety net responses would be required for patients who do not complete self-monitoring or fail to contact a service when disease control appears to be worsening or lost. This would require the EMR to display summary data at a population level and highlight patients that need attention, and the service would need capacity in the rheumatology care team to monitor and take action when required.

Third, only 1 in 5 of the 458 potentially eligible clinic patients were enrolled in this study; 44% were not contactable via 2 phone calls, and 30% were not interested in participating. Since The Netherlands has high rates of mobile phone ownership and excellent network coverage, it would be reasonable to conclude that almost any eligible patient *could* have enrolled in the study but the majority did not. New models of care delivery may not appeal to all patients. The recruitment could confirm the tacit assumption that new care models will need to be *in addition to* current models. The administrative feasibility for this complexity will need to be addressed, particularly when the clinical oversight of patient self-reported data is required, along with safety net measures.

Finally, the follow-up period for this study was 1 year, although RA is a long-term condition. Previous studies have suggested that patient-led care in RA may maintain similar outcomes up to 6 years (11), but these positive longer-term outcomes will need to be confirmed. Nevertheless, this well-conducted RCT (and background body of work) provides proof of concept that in people with longstanding RA with low disease activity, patient self-monitoring via an app with patient-initiated follow up “works”

and is “safe,” at least over the short term, and reduces rheumatology health care usage.

What of other DHTs? The COVID-19 pandemic precipitated something of a natural experiment for telemedicine, also known as virtual visits. While we have all used informal telemedicine for years by way of phone calls to patients, formal telemedicine visits via telephone or videoconferencing have not been widely adopted. Evidence synthesis reported in 2017 concluded that there were insufficient data to draw conclusions on the effectiveness (or otherwise) of telemedicine in rheumatology (12). That notwithstanding, the pandemic led to an abrupt and unplanned move to telemedicine for many rheumatologists. This was widely perceived as an adequate interim care strategy, but the absence of physical examination remained a major limitation. Factors at the individual level (technology access, acceptance, and competence), organizational level (technology and staff to support virtual care), and system levels (regulation and reimbursement) will need to be addressed to facilitate the continuation of virtual care (13). The interest generated in virtual care has led to guidance documents for telemedicine in rheumatology that also outline research priorities (14,15). In addition, these summaries highlight that although virtual care will not be appropriate for everyone at all times, it is probably suitable for some clinical settings, provides logistic benefits to some patients, and may widen access to some groups (14,15). The opportunities for sustained adoption of virtual care for some patients, some of the time, should not be squandered. Advocacy for technology infrastructure, staff, regulatory changes, and reimbursement seem to be priorities along with the collection of real-world data on patient outcomes.

While additional studies examining clinical and patient-important outcomes for care incorporating DHTs in different health care settings and countries are definitely required, we also need the knowledge to inform successful implementation. Evaluations of DHT implementation usually focus on the technology (the product) and patient outcomes. It is equally important to attend to the impacts on clinical workflows (the processes) and impacts on health care providers and support staff (the people). Of course, any innovation must have a clear and meaningful purpose and evaluation. Approaches such as design thinking (16), quality improvement (17), and use of project and change management techniques (18), which are not often visible in the rheumatology literature, are likely to be required for more successful DHT implementation. DHT implementation that transforms care will be complex and most projects will not be entirely successful. Rather than considering new care models as static new states, we should expect to need iterative approaches to the design of technology-enabled models of care and have more flexible approaches to evaluating software in clinical settings.

We are going to need to move from the idea of implementing one piece of software, such as a mobile app, to considering the entire health information technology ecosystem and be prepared to implement a minimal viable product and innovate as required.

If we keep doing what we have always done, we will get what we have always got. If we are to achieve the best possible outcomes for all patients and improve equity of access and outcomes more of the time, we must continue to adapt and engage with new technology.

## AUTHOR CONTRIBUTIONS

Dr. Grainger drafted the article, revised it critically for important intellectual content, and approved the final version to be published.

## REFERENCES

- Izadi Z, Schmajuk G, Gianfrancesco M, et al. Significant gains in rheumatoid arthritis quality measures among RISE registry practices. *Arthritis Care Res (Hoboken)* 2022;74:219–28.
- Schmajuk G, Li J, Evans M, et al. RISE registry reveals potential gaps in medication safety for new users of biologics and targeted synthetic DMARDs. *Semin Arthritis Rheum* 2020;50:1542–8.
- Feldman CH, Ramsey-Goldman R. Widening disparities among patients with rheumatic diseases in the COVID-19 era: an urgent call to action. *Arthritis Rheumatol* 2020;72:1409–11.
- Solomon DH, Rudin RS. Digital health technologies: opportunities and challenges in rheumatology [review]. *Nat Rev Rheumatol* 2020;16:525–35.
- Norgeot B, Glicksberg BS, Trupin L, et al. Assessment of a deep learning model based on electronic health record data to forecast clinical outcomes in patients with rheumatoid arthritis. *JAMA Network Open* 2019;2:e190606.
- Seppen B, Weigel J, ter Wee MM, et al. Smartphone-assisted patient-initiated care in patients with rheumatoid arthritis and low disease activity: a randomized controlled trial. *Arthritis Rheumatol* 2022;74:1737–45.
- Seppen BF, L'ami MJ, Rico SD, et al. A smartphone app for self-monitoring of rheumatoid arthritis disease activity to assist patient-initiated care: protocol for a randomized controlled trial. *JMIR Res Protoc* 2020;9:e15105.
- Seppen BF, Weigel J, L'ami MJ, et al. Feasibility of self-monitoring rheumatoid arthritis with a smartphone app: results of two mixed-methods pilot studies. *JMIR Form Res* 2020;4:e20165.
- Najm A, Nikiphorou E, Kostine M, et al. EULAR points to consider for the development, evaluation and implementation of mobile health applications aiding self-management in people living with rheumatic and musculoskeletal diseases. *RMD Open* 2019;5:e001014.
- Najm A, Lempp H, Gossec L, et al. Needs, experiences, and views of people with rheumatic and musculoskeletal diseases on self-management mobile health apps: mixed methods study. *JMIR Mhealth Uhealth* 2020;8:e14351.
- Hewlett S, Kirwan J, Pollock J, et al. Patient initiated outpatient follow up in rheumatoid arthritis: six year randomised controlled trial. *BMJ* 2005;330:171.
- McDougall JA, Ferucci ED, Glover J, et al. Telerheumatology: a systematic review. *Arthritis Care Res (Hoboken)* 2017;69:1546–57.
- Chock YP, Putman M, Conway R, et al. Experience with telemedicine amongst rheumatology clinicians during the COVID-19 pandemic: an international survey. *Rheumatol Adv Pract* 2022;6:rkac039.
- De Thurah A, Bosch P, Marques A, et al. EULAR points to consider for remote care in rheumatic and musculoskeletal diseases. *Ann Rheum Dis* 2022;81:1065–71.
- Ahmed S, Grainger R, Santosa A, et al. APLAR recommendations on the practice of telemedicine in rheumatology. *Int J Rheum Dis* 2022;25:247–58.
- Ferreira FK, Song EH, Gomes H, et al. New mindset in scientific method in the health field: design thinking. *Clinics* 2015;70:770–2.
- Subash M, Liu LH, DeQuattro K, et al. The development of the rheumatology informatics system for effectiveness learning collaborative for improving patient-reported outcome collection and patient-centered communication in adult rheumatology. *ACR Open Rheumatology* 2021;3:690–8.
- Magid SK, Cohen K, Katzovitz LS. 21st Century Cures Act, an information technology-led organizational initiative. *HSS J* 2022;18:42–7.

**NOTES FROM THE FIELD****VEXAS Syndrome and Disease Taxonomy in Rheumatology**Peter C. Grayson,<sup>1</sup>  David B. Beck,<sup>2</sup> Marcela A. Ferrada,<sup>1</sup>  Peter A. Nigrovic,<sup>3</sup> and Daniel L. Kastner<sup>4</sup>**Introduction**

The discovery of VEXAS (vacuoles, E1 enzyme, X-linked, autoinflammatory, somatic) syndrome represents an important example of how genetics can reshape disease taxonomy in rheumatology. VEXAS syndrome is caused by mutations in *UBA1*, the master enzyme of ubiquitylation. Unlike most monogenic inflammatory diseases, VEXAS is not caused by heritable mutations in the germline; rather, it is caused by somatic mutations that originate in bone marrow stem cells, become lineage-restricted to myeloid cells in peripheral blood, and give rise to a complex inflammatory syndrome that begins in the fifth decade of life or later (1). Beyond the novelty of the disease itself, the pathophysiology of VEXAS syndrome demonstrates how the discovery of somatic mutations can disrupt the field of rheumatology, with potential to transform clinical diagnostics, disease classification, and the management of rheumatic diseases.

**Discovery of VEXAS syndrome**

VEXAS syndrome was discovered through the use of a genotype-first approach, whereby a large genetic database was analyzed for commonalities among patients, with minimal consideration of clinical phenotype (1). In contrast to prior approaches at monogenic disease discovery, VEXAS syndrome was not identified by focusing on early-onset inflammatory diseases or on seemingly rare instances in which unclassifiable inflammatory syndromes aggregate within an immediate family. Rather, unbiased analysis of whole-exome sequencing data from 2,560 patients at the National Institutes of Health led to the genetic identification of 3 patients with novel somatic mutations in codon 41 of *UBA1*. As genetic databases accumulate, similar unbiased efforts may

be useful for identifying genetic commonalities that uncover diseases that were initially difficult to recognize at the bedside.

Since *UBA1* is an X-linked gene, VEXAS syndrome is almost exclusively seen in men, as women are likely protected by a second functioning allele. The syndrome typically begins in adulthood with fever and the involvement of skin, cartilage, lungs, or blood vessels. Skin manifestations include leukocytoclastic vasculitis, medium-vessel vasculitis, and neutrophilic dermatosis. Cartilage manifestations include ear and nose chondritis. Pulmonary manifestations include alveolitis and exudative serositis. Arterial involvement can manifest as variable vessel vasculitis involving small, medium, or large arteries. Macrocytosis is usually present at diagnosis, and is followed by progressive bone marrow failure typified by anemia, thrombocytopenia, and lymphopenia (2). Thromboembolic events are also common. Late disease complications include transfusion dependence and evolution to myelodysplastic syndrome or multiple myeloma.

We have proposed the term hematoinflammatory diseases for conditions like VEXAS syndrome that are caused by somatic mutations in the blood that produce systemic inflammation with multiorgan involvement in association with bone marrow pathology (3). Hematoinflammatory diseases can manifest as premalignant conditions that result in myeloproliferation, myelodysplasia, or lymphoproliferation with the potential for malignant transformation. A goal in defining this class of diseases is to emphasize the importance of multidisciplinary clinical management involving rheumatology and hematology in the care of these patients. Erdheim-Chester disease, due to somatic mutations in *BRAF* in histiocytes, is another example of a hematoinflammatory disease, and, more broadly, diseases such as Felty's syndrome and clonal hematopoiesis may also be examples of similar pathophysiologies (4–6). With

Supported by the NIH Intramural Research Program, including the Intramural Research Program of the National Institute of Arthritis and Musculoskeletal and Skin Diseases and the National Human Genome Research Institute.

<sup>1</sup>Peter C. Grayson, MD, MSc, Marcela A. Ferrada, MD: National Institute of Arthritis and Musculoskeletal and Skin Diseases, NIH, Bethesda, Maryland; <sup>2</sup>David B. Beck, MD, PhD: Division of Rheumatology, Department of Medicine, and Center for Human Genetics and Genomics, New York University Grossman School of Medicine, New York, and the National Human Genome Research Institute, NIH, Bethesda, Maryland; <sup>3</sup>Peter A. Nigrovic, MD: Division of Immunology, Boston Children's Hospital, and the Division of

Rheumatology, Inflammation, and Immunity, Brigham and Women's Hospital, Boston, Massachusetts; <sup>4</sup>Daniel L. Kastner, MD, PhD: National Human Genome Research Institute, NIH, Bethesda, Maryland.

Author disclosures are available at <https://onlinelibrary.wiley.com/action/downloadSupplement?doi=10.1002%2Fart.42258&file=art42258-sup-0001-Disclosureform.pdf>.

Address correspondence via email to Peter C. Grayson, MD, MSc, at [peter.grayson@nih.gov](mailto:peter.grayson@nih.gov).

Submitted for publication January 5, 2022; accepted in revised form June 2, 2022.



increasing access to DNA sequencing, many more hematoinflammatory diseases are likely to be identified.

### Impact of VEXAS syndrome on disease taxonomy in rheumatology

The purpose of disease taxonomy is to integrate diseases with respect to each other in a way that guides clinical care and advances research. Ideally, disease taxonomy should reflect the pathophysiology and root cause of a disease when they are known. In practice, disease taxonomy is often partitioned into diagnostic criteria and classification criteria. Diagnostic criteria are sets of signs, symptoms, and tests developed for use in routine clinical care to assign an individual patient a medical diagnosis for the purpose of guiding clinical management. In contrast, classification criteria are used to identify homogeneous subsets of patients with a particular disease for inclusion in research studies. Developing systems of disease taxonomy in rheumatology is particularly challenging, albeit very important, given the substantial clinical heterogeneity observed in patients with individual rheumatic diseases, the high degree of clinical overlap shared among patients with different rheumatic diseases, and the limited understanding of the etiology of most of these diseases. In this context, VEXAS syndrome illustrates how rheumatologists of the future may incorporate novel taxonomic schema in clinical practice.

**Diagnostic criteria.** The identification of somatic mutations as a root cause of disease, as demonstrated in the taxonomy of VEXAS syndrome, is an advance that could disrupt diagnostic paradigms in rheumatology. In 2015, the American College of Rheumatology announced a decision to not endorse diagnostic criteria in rheumatic diseases (7). The reasoning was in part driven by the challenges of developing diagnostic criteria with consistent, near-perfect performance characteristics fit for use in clinical practice across different regions of the world. However, development of diagnostic criteria is possible for diseases in which there is a diagnostic gold standard. Since specific mutations in *UBA1* now constitute a diagnostic gold standard for VEXAS, development of scientifically valid diagnostic criteria to identify patients with VEXAS syndrome is within reach. Notably, germline mutations elsewhere in *UBA1* cause a different disease phenotype (spinal muscular atrophy) and thus, even for VEXAS, diagnostic criteria go beyond the mere presence of mutations in a specific gene.

Traditionally, assignment of a clinical diagnosis is a complex cognitive exercise driven largely by pattern recognition across a constellation of clinical symptoms. The genetic findings related to VEXAS syndrome illustrate how the incorporation of molecular diagnostics into clinical practice can result in new disease distinctions. A wide spectrum of inflammatory features is associated with VEXAS syndrome. Consequently, patients with VEXAS syndrome meet criteria for different clinical diagnoses, including relapsing

polychondritis, polyarteritis nodosa, Sweet syndrome, giant cell arteritis, systemic lupus erythematosus, adult-onset Still's disease, antineutrophil cytoplasmic antibody-associated vasculitis, myelodysplastic syndrome, multiple myeloma, and other conditions (1,8,9). Through the lens of molecular diagnostics, patients with VEXAS syndrome are stereotypically more similar to each other than they are to other patients with these respective clinical diagnoses. Moreover, diagnosing patients as having VEXAS syndrome through the use of a genetic biomarker creates opportunities for the development of novel therapeutic approaches that can target the fundamental pathophysiologic aspects of the disease.

Genetic data will likely provide alternative diagnostic boundaries in scenarios where diagnostic distinctions based on clinical assessment alone are suboptimal. Considering the variations in clinical manifestations of rheumatic diseases reveals opportunities for disruption in the process of diagnosis. Unique clinical symptoms tend to cluster within sets of clinical diagnoses. For example, inflammation in the large arteries, gastrointestinal tract, and axial skeleton can occur within an individual patient. Depending on the relative proportion of symptoms and the subjective interpretation of the health care provider, these patients can be assigned a clinical diagnosis of spondyloarthritis, various forms of vasculitis such as Behçet's disease or Takayasu arteritis, inflammatory bowel disease, or a combination of these diagnoses. The use of genetic data—either high-penetrance rare variants or cassettes of low-penetrance common variants (10)—to partition among phenotypically overlapping clinical diseases may lead to more objective and biologically meaningful diagnostic distinctions. Of particular interest is investigating the potential role of genetic data to define subsets of patients within clinically heterogeneous diseases, such as systemic lupus erythematosus, sarcoidosis, idiopathic vasculitis, and seronegative arthritis (Figure 1).

**Classification criteria.** Beyond diagnostics, VEXAS syndrome has implications for disease classification. The intent of most classification criteria is to define the largest subset of patients possible with disease features that are most representative of a clinical diagnosis for inclusion in clinical trials (11). Patients with atypical disease presentations are often excluded from classification criteria. In the future, classification criteria in rheumatology will need to consider to what extent a genetically defined subset of a clinical disease should be considered a unique disease entity. For example, discovery of VEXAS syndrome poses challenges for disease classification in relapsing polychondritis. Approximately 60% of patients with VEXAS syndrome meet the clinical criteria for relapsing polychondritis, while 8% of patients with relapsing polychondritis have VEXAS syndrome (1,12). How should future classification criteria in relapsing polychondritis address VEXAS syndrome? Should these patients be excluded from future studies of relapsing polychondritis? Among patients with relapsing polychondritis, patients with VEXAS syndrome are clinically and immunologically distinct, with higher mortality rates and different responses to treatment

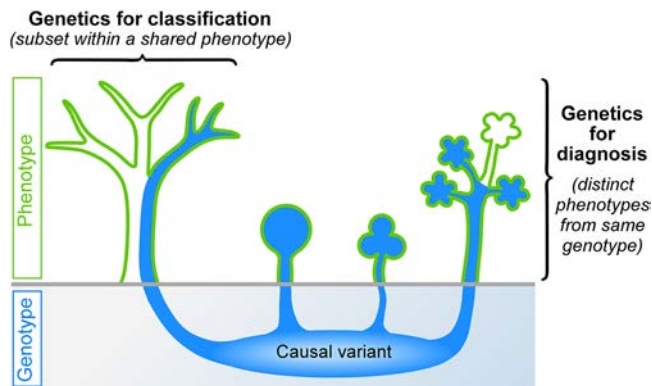


**Figure 1.** Distinct roles of genotype in disease taxonomy. Identification of a disease-causing pathogenic variant enables 2 improvements in the taxonomy of disease. First, identification of disease-causing variants permits the discovery of genetically defined biologic subsets within specific clinical syndromes, depicted here as blue branches within disease phenotypes represented by plants of different shapes, some of which always reflect the variant but others which can arise from other causes as well (genetics for classification). Second, identification of disease-causing variants permits the identification of the full clinical spectrum of a disease, exemplified here by 4 outwardly dissimilar phenotypes that can share a common origin (genetics for diagnosis). VEXAS (vacuoles, E1 enzyme, X-linked, autoinflammatory, somatic) syndrome exemplifies this principle, accounting for 8% of relapsing polychondritis but also accounting for cases of giant cell arteritis, polyarteritis nodosa, Sweet's syndrome, and myelodysplasia.

(12). Nevertheless, final common pathways may lead to chondritis in these patients regardless of the underlying cause of disease. Future classification criteria will need to address to what extent taxonomic relationships should be retained between clinically and genetically defined diseases.

### Clinical management and research findings in VEXAS syndrome

Promotion of genetics-based disease taxonomy in rheumatology does not imply that the clinical characterization of a disease is without value. Ultimately, integration of clinical and genetic profiling will improve patient care and lead to research advancements. In VEXAS syndrome, prompt recognition of clinical patterns of disease are essential to identify patients for genetic testing. The interplay between genetics and clinical symptoms also influences clinical outcomes. Almost all disease-defining genetic mutations in VEXAS syndrome are restricted to p.Met41 of *UBA1*, which serves as a start site for translation of the shorter cytoplasmic isoform of UBA-1 (1,13). Genetic alterations at codon 41 result in defects in cytoplasmic ubiquitylation (1). A genotype–phenotype relationship exists in VEXAS syndrome, whereby specific genetic mutations at p.Met41 are associated with clinical patterns of disease and the risk of death (8). Using clinical and genetic data in the development of survival models can aid in the identification of patients with VEXAS syndrome at highest risk for poor outcomes and can guide

decisions for the management of disease. VEXAS syndrome is a severe and progressive disease that is often refractory to treatment (1,14). Hematopoietic stem cell transplantation may be curative in select patients (15). Prioritization of candidates for such aggressive treatment measures in the future will likely rely on genetic and clinical risk stratification.

From a research standpoint, understanding the connection between genotype and clinical patterns of disease in patients with VEXAS syndrome will be instructive. Several recently discovered autoinflammatory diseases are the result of perturbations within the ubiquitin proteasome system (16). Identifying the mechanisms whereby damage to cellular clearance pathways or alteration of other functional aspects of ubiquitylation results in inflammation will uncover novel aspects of the innate immune system and likely lead to the development of novel therapeutics. The discovery of VEXAS syndrome raises many fundamental questions worth studying. Why do somatic mutations in *UBA1* in bone marrow cause inflammation primarily in cartilage, skin, lungs, and arteries? Why do these seemingly toxic mutations become lineage-restricted and clonally expand within the myeloid cell compartment? What are the additional mechanisms whereby subsets of patients with VEXAS syndrome develop progressive bone marrow failure and hematologic malignancies? Can the clonal burden of *UBA1* mutations in bone marrow or blood be used as a genetic biomarker to inform clinical management decisions? Does *UBA1* regulate inflammation outside of VEXAS syndrome, and if so, in which context? Monogenic diseases can result in heterogeneous systemic inflammatory syndromes, and the mechanisms that govern these relationships are likely to have broad implications in the field of medicine.

### Conclusion

Given the technical advancements in next-generation sequencing and the increasing clinical access to these technologies, the taxonomy of rheumatic diseases will likely be remodeled as genetic data become further integrated into clinical practice. The discovery of VEXAS syndrome illustrates how the identification of somatic mutations can provide diagnostic clarity about heterogeneous inflammatory syndromes in adult populations (Figure 1). However, perhaps even more remarkable and exciting are the ways in which VEXAS syndrome allow us to imagine the future of disease taxonomy in rheumatology.

### AUTHOR CONTRIBUTIONS




All authors drafted the article, revised it critically for important intellectual content, and approved the final version to be published.

### REFERENCES

1. Beck DB, Ferrada MA, Sikora KA, et al. Somatic mutations in *UBA1* and severe adult-onset autoinflammatory disease. *N Engl J Med* 2020;383:2628–38.

2. Obiorah IE, Patel BA, Groarke EM, et al. Benign and malignant hematologic manifestations in patients with VEXAS syndrome due to somatic mutations in UBA1. *Blood Adv* 2021;5:3203–15.
3. Grayson PC, Patel BA, Young NS. VEXAS syndrome. *Blood* 2021;137:3591–4.
4. Haroche J, Charlotte F, Arnaud L, et al. High prevalence of BRAF V600E mutations in Erdheim-Chester disease but not in other non-Langerhans cell histiocytoses. *Blood* 2012;120:2700–3.
5. Jaiswal S, Natarajan P, Ebert BL. Clonal hematopoiesis and atherosclerosis. *N Engl J Med* 2017;377:1401–2.
6. Savola P, Bruck O, Olson T, et al. Somatic STAT3 mutations in Feltz syndrome: an implication for a common pathogenesis with large granular lymphocyte leukemia. *Haematologica* 2018;103:304–12.
7. Aggarwal R, Ringold S, Khanna D, et al. Distinctions between diagnostic and classification criteria? [review]. *Arthritis Care Res (Hoboken)* 2015;67:891–7.
8. Georjin-Lavialle S, Terrier B, Guedon AF, et al. Further characterization of clinical and laboratory features occurring in VEXAS syndrome in a large-scale analysis of multicenter case-series of 116 French patients. *Br J Dermatol* 2022;186:564–74.
9. Koster MJ, Kourelis T, Reichard KK, et al. Clinical heterogeneity of the VEXAS syndrome: a case series. *Mayo Clin Proc* 2021;96:2653–9.
10. Manthiram K, Preite S, Dedeoglu F, et al. Common genetic susceptibility loci link PFAPA syndrome, Behcet's disease, and recurrent aphthous stomatitis. *Proc Natl Acad Sci U S A* 2020;117:14405–11.
11. Singh JA, Solomon DH, Dougados M, et al. Development of classification and response criteria for rheumatic diseases. *Arthritis Rheum* 2006;55:348–52.
12. Ferrada MA, Sikora KA, Luo Y, et al. Somatic mutations in *UBA1* define a distinct subset of relapsing polychondritis patients with VEXAS. *Arthritis Rheumatol* 2021;73:1886–95.
13. Poulter JA, Collins JC, Cargo C, et al. Novel somatic mutations in UBA1 as a cause of VEXAS syndrome. *Blood* 2021;137:3676–81.
14. Bourbon E, Heiblig M, Valentin MG, et al. Therapeutic options in VEXAS syndrome: insights from a retrospective series. *Blood* 2021;137:3682–4.
15. Diarra A, Duployez N, Fournier E, et al. Successful allogeneic hematopoietic stem cell transplantation in patients with VEXAS syndrome: a two center experience. *Blood Adv* 2022;6:998–1003.
16. Aksentijevich I, Zhou Q. NF- $\kappa$ B pathway in autoinflammatory diseases: dysregulation of protein modifications by ubiquitin defines a new category of autoinflammatory diseases. *Front Immunol* 2017;8:399.

# Smartphone-Assisted Patient-Initiated Care Versus Usual Care in Patients With Rheumatoid Arthritis and Low Disease Activity: A Randomized Controlled Trial

Bart Seppen,<sup>1</sup>  Jimmy Wiegel,<sup>1</sup>  Marieke M. ter Wee,<sup>2</sup> Dirkjan van Schaardenburg,<sup>3</sup> Leo D. Roorda,<sup>4</sup> Michael T. Nurmohamed,<sup>1</sup> Maarten Boers,<sup>5</sup>  and Wouter H. Bos<sup>6</sup>

**Objective.** We developed a smartphone application for patients with rheumatoid arthritis (RA) that allows them to self-monitor their disease activity in between clinic visits by answering a weekly Routine Assessment of Patient Index Data 3. This study was undertaken to assess the safety (noninferiority in the Disease Activity Score in 28 joints using the erythrocyte sedimentation rate [DAS28-ESR]) and efficacy (reduction in number of visits) of patient-initiated care assisted using a smartphone app, compared to usual care.

**Methods.** A 12-month, randomized, noninferiority clinical trial was conducted in RA patients with low disease activity and without treatment changes in the past 6 months. Patients were randomized 1:1 to either app-supported patient-initiated care with a scheduled follow-up consultation after a year (app intervention group) or usual care. The coprimary outcome measures were noninferiority in terms of change in DAS28-ESR score after 12 months and the ratio of the mean number of consultations with rheumatologists between the groups. The noninferiority limit was 0.5 difference in DAS28-ESR between the groups.

**Results.** Of the 103 randomized patients, 102 completed the study. After a year, noninferiority in terms of the DAS28-ESR score was established, as the 95% confidence interval (95% CI) of the mean  $\Delta$ DAS28-ESR between the groups was within the noninferiority limit:  $-0.04$  in favor of the app intervention group (95% CI  $-0.39, 0.30$ ). The number of rheumatologist consultations was significantly lower in the app intervention group compared to the usual care group (mean  $\pm$  SD  $1.7 \pm 1.8$  versus  $2.8 \pm 1.4$ ; visit ratio 0.62 [95% CI 0.47, 0.81]).

**Conclusion.** Patient-initiated care supported by smartphone self-monitoring was noninferior to usual care in terms of the  $\Delta$ DAS28-ESR and led to a 38% reduction in rheumatologist consultations in RA patients with stable low disease activity.

## INTRODUCTION

Patients with rheumatoid arthritis (RA) are routinely scheduled for follow-up appointments, but this format may not be sustainable. The American College of Rheumatology (ACR) workforce study estimates that by 2030 the number of projected rheumatologists will not even meet half the number of needed rheumatologists (1). The demand for more rheumatology health care providers is growing due to the increasing number of patients with RA and the overall increase in health care utilization. Additionally, the supply of health

care is dropping due to a decreasing rheumatology workforce (1,2). Therefore, we will need to provide more health care with the same capacity of people and resources (3,4). Currently in The Netherlands, most patients with RA consult their physician every 3 to 6 months, following the EULAR guidelines (5). This method may be inefficient as, on the one hand, 75% of patients are in a low disease activity state or their disease is in remission (6), and, on the other hand, flares often occur between outpatient clinic visits and can therefore still be missed and left untreated (7). Thus, the current process needs to be optimized to remain sustainable.

This trial was funded by AbbVie.

<sup>1</sup>Bart Seppen, MD, Jimmy Wiegel, MD, Michael T. Nurmohamed, MD, PhD: Reade Rheumatology, and the Department of Rheumatology, Amsterdam UMC, VU University Medical Center, Amsterdam, The Netherlands; <sup>2</sup>Marieke M. ter Wee, MSc, PhD: Department of Epidemiology and Data Science, Amsterdam UMC, VU University Medical Center, Amsterdam, The Netherlands; <sup>3</sup>Dirkjan van Schaardenburg, MD, PhD: Reade Rheumatology, and the Department of Rheumatology, Amsterdam UMC, Academic Medical Center, Amsterdam, The Netherlands; <sup>4</sup>Leo D. Roorda, MD, PhD: Reade Rehabilitation, Amsterdam, The Netherlands; <sup>5</sup>Maarten Boers, MD, PhD: Reade Rheumatology,

and the Department of Epidemiology and Data Science, Amsterdam UMC, VU University Medical Center, Amsterdam, The Netherlands; <sup>6</sup>Wouter H. Bos, MD, PhD: Reade Rheumatology, Amsterdam, The Netherlands.

Author disclosures are available at <https://onlinelibrary.wiley.com/action/downloadSupplement?doi=10.1002%2Fart.42292&file=art42292-sup-0001-Disclosureform.pdf>.

Address correspondence via email to Bart Seppen, MD at [b.seppen@reade.nl](mailto:b.seppen@reade.nl).

Submitted for publication January 12, 2022; accepted in revised form June 2, 2022.

As a solution, outpatient clinics could revert from preplanned visits to providing “health care on demand,” in which patients are expected to initiate health care themselves when needed. The effectiveness of patient-initiated care in patients with RA is still under investigation. Hewlett et al, Primdahl et al, and Poggenborg et al have shown that patients who self-initiate care (for 2 to 6 years) were clinically and psychologically at least as well and had fewer appointments than patients with physician-initiated regular appointments (8–10). However, a similar Swedish study showed that, although patient-initiated care was similar to traditional care in terms of clinical outcomes such as the Disease Activity Score in 28 joints using the erythrocyte sedimentation rate (DAS28-ESR) (11) after 18 months, the appointment frequency did not differ between both groups (12). In 2 of these studies, a general practitioner and a research nurse were used instead of the rheumatologist to monitor or follow up patients; thus, although health care costs may have been saved, health care usage may have been redirected rather than decreased (10,12). Furthermore, a potential downside of patient-initiated care is that information on RA disease activity may be lacking for longer time periods, which could complicate disease activity-guided management. This could be resolved by letting patients monitor themselves with electronic patient-reported outcomes (ePROs) in between clinic visits (self-monitoring), which can provide disease activity information between visits, allowing for better disease activity-guided management (13).

So far, self-monitoring of RA disease activity with ePROs has not been shown to improve patient satisfaction or disease activity (14), but improvements have been seen in terms of self-management skills, patient empowerment, patient-physician interaction, and physical activity (15–18). Several studies also demonstrate high acceptance rates of self-monitoring and high questionnaire completion during studies (14,19). In addition, self-monitoring can lead to a reduction in outpatient clinic visits by ~50% (20–22). To date, none of these studies have combined patient-initiated care (to reduce the number of visits) with self-monitoring (to maintain disease control).

The objective of this study was to assess the safety and efficacy of patient-initiated care combined with weekly ePRO self-monitoring through a smartphone application in patients with RA and low disease activity. We hypothesized that combining patient-initiated care with self-monitoring would lead to a lower number of outpatient clinic visits while maintaining other health care outcomes such as disease activity and patient satisfaction.

## PATIENTS AND METHODS

This was a 1-year, randomized, controlled, noninferiority clinical trial, with blinded outcome assessment. The protocol was registered on [www.trialregister.nl](http://www.trialregister.nl) (NL7715) and approved by the Medical Ethics Committee of the Vrije Universiteit Medical Center

Amsterdam. All patients provided oral and written informed consent prior to participation.

A detailed description of the methods of the trial has previously been published (23). Briefly, the inclusion criteria were as follows: 1)  $\geq 18$  years of age, 2) diagnosis of RA by a rheumatologist, 3) disease duration of  $\geq 2$  years, 4) DAS28-ESR score of  $< 3.2$  at the start of the study, 5) owner of a smartphone, 6) and ability to read and write Dutch. Patients with a disease duration of  $\geq 2$  years were anticipated to have sufficient experience with their own disease and flaring of their disease activity to allow for patient-initiated care. Patients were excluded if they had initiated or discontinued a conventional or biologic disease-modifying antirheumatic drug (DMARD) in the previous 6 months or if they participated in another intervention trial. Treating rheumatologists were asked for permission by an author (BS) to recruit, by telephone, all patients with previously low disease activity noted in the electronic medical record (EMR) who attended the outpatient clinic. Patients were called twice, and if no response was obtained, no further attempts to include the patient were made.

Patients were randomized 1:1 to the app intervention group or the usual care group, following a computer-generated random numbers sequence with a variable block size of 4, 6, or 8 in the online program Castor (24). The intervention consisted of weekly self-monitoring (completing a Routine Assessment of Patient Index Data 3 [RAPID3] questionnaire in a smartphone app designed for this purpose) with a single preplanned consultation at the end of the trial period (23,25). In the usual care group, preplanned outpatient clinic visits were continued at the discretion of the treating rheumatologist (usually every 3 to 6 months). After randomization, patients in the app intervention group received login credentials for the app. The first login was performed at Reade Rheumatology and Rehabilitation, to make sure this process was clear, and patients were shown the features of the app. Additionally, information about patient-initiated care was provided, patients were told they could contact the outpatient clinic when they deemed it necessary (in case of questions or symptoms). Patients in the usual care group were also allowed to contact the outpatient clinic if necessary. At the start and end of the trial, blinded assessment of the DAS28-ESR was performed by medical doctors or nurses, with no treatment relationship to the patient, who were called into the room during study visits. All medical doctors (PhD candidates) and nurses at Reade receive specific training for joint evaluations and have experience (multiple times per week) with joint evaluations.

The trial was performed at Reade, a secondary rheumatology care center in the region of Amsterdam in The Netherlands that employs 17 full- and part-time rheumatologists. Everyone in The Netherlands has access to health care services, as long as they have health insurance, which is a mandatory requirement for all Dutch residents (26). The Netherlands has excellent network coverage, reaching as high as 96.8% overall, and 100% in

Amsterdam; in addition, 97% of people have internet access at home and >87% of the Dutch adult population owns a smartphone (27–29). The mobile download speed currently ranks fifth worldwide (30).

**The smartphone application.** The app and its development following the Medical Research Council framework has been extensively described elsewhere (23,25). In brief, the app notified patients each week to complete their RAPID3 in the app. The results of the RAPID3 could be used by patients to monitor themselves during the year, to reflect on the course of their disease, and to contact the outpatient clinic in a timely manner in case of progressive complaints. Additionally, communication with the physician/nurse at the outpatient clinic was easier, as they also had access to their data. In the app, a RAPID3 algorithm was used to identify potential RA flares. An increase in the RAPID3 score by >2 points (from the previous data point) combined with a RAPID3 score of >4 led to a flare notification. The notification informed the patient about the possible flare, linked to self-management tips, and presented the advice to contact a rheumatology nurse if deemed necessary by the patient. Scores in the app were not used to trigger contact from clinician to patient. The data collected in the app was synchronized in real time with the EMR at Reade.

**Primary outcome measures.** The coprimary outcome measure was noninferiority in terms of change in DAS28-ESR after 12 months. The noninferiority limit was set at 0.5 difference in DAS28-ESR between the groups.

The second primary outcome measure was the number of visits with a rheumatologist. We recorded the number of consultations (by telephone and in person) with rheumatologists. The number of consultations (by telephone and in person) with nurses was evaluated as a secondary outcome.

**Secondary outcome measures.** *Patient empowerment.* The empowerment of patients was measured using the effective consumer scale 17 (EC-17). In the EC-17, patients score how often statements are true for them, to measure the patients' skills in managing their own health care. Each item is scored from 0 (never) to 4 (always), and ultimately the total score is converted to a scale out of 100 (higher is better) (31).

*Patient-physician interaction.* The patient-physician interaction was measured with the 5-item Perceived Efficacy in Patient-Physician Interactions (PEPPI-5). The PEPPI-5 is scored on a scale of 1 (not confident at all) to 5 (completely confident). The 5 items are added together to form a total score (out of a possible 25), with higher scores indicating more perceived efficacy in patient-physician interaction.

*Patient compliance.* To measure medication compliance, the 5-item Compliance Questionnaire for Rheumatology (CQR-5) was

used. The CQR-5 classifies patients as either “high” or “low” adherents.

*Patient satisfaction with treatment.* Satisfaction with treatment was measured with the 9-item Treatment Satisfaction Questionnaire for Medication (TSQM-9). The questionnaire measures satisfaction with treatment on 3 domains: effectiveness, convenience, and global satisfaction. TSQM scores have a range of 0 to 100, with higher scores indicating greater satisfaction.

*Patient satisfaction with health care.* Patient satisfaction with health care was measured on a 10-point Likert scale on 3 domains: ease of contacting our hospital, satisfaction with health care received, and likelihood of recommending our hospital. Higher scores indicate greater satisfaction.

*Physician satisfaction.* Physician satisfaction with the new form of health care delivery and the way the results were incorporated in the EMR was measured on a 10-point Likert scale (overall satisfaction) question and 6 5-point Likert scale statements. Physicians rated how much they agreed with the statements, ranging from 1 (not at all) to 5 (very much). Higher scores indicate greater satisfaction.

*Usability of the application.* Finally, the System Usability Scale was used to determine the usability of the app, the scale ranges from 0 to 100, in which a score of 52 indicates “OK” usability and 72 “good” usability (32,33). This outcome measure was accidentally not added to the protocol paper after it was suggested by the ethics review board.

**COVID-19 protocol amendments and power analysis.** Due to the global pandemic, inclusion was prematurely stopped in April 2020 after 103 inclusions and changes were made to the initial trial protocol accordingly. Inclusion was stopped because new patients that were randomized into the usual care group would also have been monitored at a distance by rheumatologist during the entire study following the COVID-19 contact restrictions. This would lead to 2 different control groups, which would complicate analyses and interpretation of the data. We reevaluated our power analysis in collaboration with a statistician (MB) and changed our noninferiority limit to 0.5 (initially 0.3), which is still below the minimally relevant change in DAS28-ESR score of 0.6 (which is often chosen as noninferiority cutoff) (22). The assumed SD of 0.6 in DAS28-ESR score for a group of RA patients remained unaltered. With these changes, 64 patients would be required to be 95% sure that the lower limit of a 95% confidence interval (95% CI) will be above the noninferiority limit of 0.5 if there were truly no difference between the standard and experimental treatment. Therefore, at the time of the inclusion stop, ample number of patients had been included to analyze the primary outcome measure.

At the start of the pandemic, for most patients, in-person visits were changed to (nonvideo) telephone consultations. Typically, only flares were seen in the outpatient clinic after COVID onset. However, this policy fluctuated with the number

of COVID-19 infections and hospital admissions in The Netherlands. Therefore, telephone consultations with the rheumatologist were also counted toward the end point of number of consultations with a rheumatologist.

**Statistical analysis.** All analyses were conducted using SPSS version 25. The distribution of all outcomes was visually assessed (histogram). Normally distributed data are presented by the mean  $\pm$  SD; otherwise, median and inner quartiles are reported. A 2-sided *P* value less than 0.05 was considered statistically significant; because we only had 2 separate hypotheses, we decided not to correct for multiple testing. All outcomes were analyzed on a per-protocol basis, as there was only 1 patient who dropped out of the study.

For the first primary outcome measure, noninferiority of the DAS28-ESR, the between-arm differences at follow-up of DAS28-ESR were analyzed by linear regression adjusted for the baseline value. For the second primary outcome measure, the number of visits with a rheumatologist, a Poisson distribution was assumed. Therefore, a (longitudinal) Poisson regression was performed, which analyzes the ratio of the total rate of outpatient visits and telephone consultations with a rheumatologist in the app intervention group

compared to the usual care group. As a secondary outcome measure, the separate ratios of the intervention group's number of telephone and in-person nurse consultations compared to that of the usual care group were evaluated. The assumptions of the regression models were evaluated.

For all other secondary outcome measures, continuous variables were compared to linear regression for normally distributed variables. In case the outcome variable was not normally distributed, the  $\Delta$  (12-month value – baseline value) was assessed, and if it was also not normally distributed, log transformation of the outcome was performed to see if the outcome became normally distributed. All outcomes were adjusted for age, sex, body mass index, education level, disease duration, and baseline score. Completion rates of the weekly questionnaires were presented as total numbers and percentages.

## RESULTS

Between May 2019 and April 2020, 103 patients provided written informed consent and were randomized to the app intervention group (*n* = 50) or the usual care group (*n* = 53) (Figure 1).

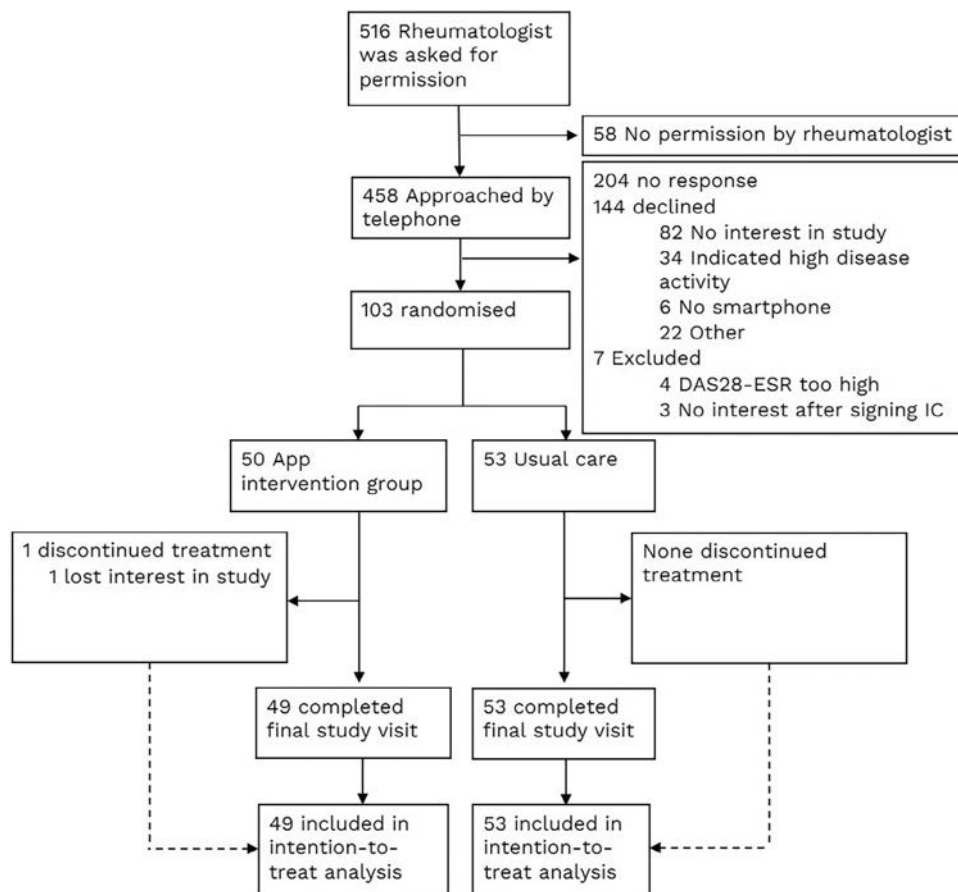


**Figure 1.** Consolidated Standards of Reporting Trials diagram of rheumatoid arthritis patient selection and flow of participants throughout the study of patient-initiated care assisted using a smartphone app versus usual care. DAS28-ESR = Disease Activity Score in 28 joints using the erythrocyte sedimentation rate; IC = informed consent.

**Table 1.** Baseline characteristics of the study patients\*

	App intervention group (n = 50)	Usual care group (n = 53)
Age, years	58 ± 13	57 ± 11
Male sex, no. (%)	22 (44)	21 (40)
BMI, kg/m <sup>2</sup>	26 ± 4.4	26 ± 4.5
Disease duration, median (IQR) years	11 (5–18)	9 (5–14)
Tertiary education, no. (%)†	28 (56)	27 (51)
DAS28-ESR score	1.7 ± 0.7	1.5 ± 0.7
RAPID3 score	2.3 ± 1.5	1.9 ± 1.4
ACPA-positive, no. (%)	33 (66)	40 (75)
RF-positive, no. (%)	29 (58)	33 (62)

\* Except where indicated otherwise, values are the mean ± SD. BMI = body mass index; IQR = interquartile range; DAS28-ESR = Disease Activity Score in 28 joints using the erythrocyte sedimentation rate; RAPID3 = Rapid Assessment of Patient Index Data 3; ACPA = anti-citrullinated protein antibody; RF = rheumatoid factor. † Higher vocational or university education.

At the end of the 12-month study period, 49 patients (98%) and 53 patients (100%) completed the final study visit in the app and usual care groups, respectively. Baseline characteristics of the 2 groups are presented in Table 1. The patients who were not interested in the study were slightly older (mean age 61 years), and 26% of them were male (versus 44% in the study).

The DAS28-ESR slightly increased in both groups ( $\Delta$ DAS28-ESR in app intervention group was 0.27 versus 0.35 in usual care group). Noninferiority was established, as the 95% CI of the mean difference in DAS28-ESR between the groups was within the non-inferiority limit:  $-0.04$  in favor of the intervention group (95% CI  $-0.39, 0.30$ ), adjusted for baseline DAS28-ESR (no significant confounders).

After 12 months, the number of rheumatologist telephone consultations and outpatient clinic visits was significantly lower in the app intervention group, with a total visit rate ratio of 0.6 (95% CI 0.47, 0.80) relative to the total number of visits in the usual care group ( $P < 0.001$ ). The total number of outpatient visits with nurses was also lower in the app intervention group (Table 2).

The proportion of in-person rheumatologist consultations to total number of rheumatologist consultations (both in-person and telephone consultations) changed pre- and post-COVID (after March 1, 2020). In the intervention group, the proportions changed from 0.15 (3 of 20) to 0.20 (13 of 65), and in the control group, the proportion changed from 0.59 (22 of 37) to 0.30 (34 of 112). This suggests that the control group would likely have had more in-person consultations without COVID and fewer telephone consultations.

The number of flare visits was 12 (in 11 patients) in the app intervention group and 18 (in 11 patients) in the control group. These consultations led to an intensification of treatment with DMARDs or steroids in 9 patients in both groups. For the app intervention group, 8 of 12 flare consultations were not preceded by a flare notification. During the study, there were 40 flare notifications, of which 36 did not lead to a consultation (10% of the prompts led to a consultation). Reasons for not contacting the outpatient clinic after a flare notification included the following: thought of flare but chose to wait and see ( $n = 20$ ), complaints caused by something else ( $n = 6$ ), did not think of flare/did not agree ( $n = 5$ ), other ( $n = 2$ ), or unknown ( $n = 3$ ).

During the study, there were no significant differences between groups in patient-reported disease activity (RAPID3), self-management (EC-17), patient-physician interaction (PEPPI-5), or medication adherence (CQR-5) at 12 months. Satisfaction with health care was high in both groups and not statistically different (Table 3).

Patients rated the usability of the app (out of a possible 100) with a median of 78 (interquartile range [IQR] 60–90) at 6 months and 80 (IQR 65–93) at 12 months, which indicates good-to-excellent usability of the app. The mean ± SD of completed questionnaires was 31 ± 14 out of a possible 52 (59%), which translates to 1 completed questionnaire every 1.7 weeks (or 12 days). The mean ± SD completion rates during the first, second, third, and fourth quarter of the year were 58 ± 7%, 59 ± 5%, 66 ± 6%, and 54 ± 6%, respectively. In total, 10 of 17 rheumatologists included patients in the study, and 9 of 10 completed the final evaluation (of the telemedicine platform). On average, physician

**Table 2.** Number of consultations per group and ratio of number of visits in the app intervention group compared to the usual care group\*

	App intervention group (n = 49)	Usual care group (n = 53)	Visit rate ratio (95% CI)†	P
Rheumatologist consultations				
Telephone	1.4 ± 1.6	1.8 ± 1.7	0.8 (0.59, 1.10)	0.16
Outpatient	0.3 ± 0.6	1.1 ± 0.8	0.3 (0.18, 0.54)	<0.001
Total	1.7 ± 1.8	2.8 ± 1.4	0.6 (0.47, 0.81)	<0.001
Nurse consultations				
Telephone	0.4 ± 0.8	0.5 ± 0.9	0.4 (0.41, 1.43)	0.40
Outpatient	0.1 ± 0.3	0.3 ± 0.6	0.3 (0.11, 0.81)	0.02
Total	0.4 ± 0.9	0.8 ± 1.1	0.6 (0.34, 0.95)	0.03

\* Values are the mean ± SD number of consultations per patient per year in each group, and the ratio (95% confidence interval [95% CI]) of the rate of visits in the app intervention group compared to the usual care group.

† Results of per-protocol analysis with a longitudinal Poisson regression are shown.



**Table 3.** Between-group differences in change from baseline value for the secondary outcome measures\*

	App intervention group (n = 49)†	Usual care (n = 53)‡	Estimated intervention effect (95% CI)§
RAPID3			
Baseline	2.3 ± 1.5	1.9 ± 1.4	–
Δ12 months	–0.2 ± 1.5	0.3 ± 1.4	–0.36 (–0.93, 0.21)
EC-17			
Baseline	80.3 ± 11.8	78.6 ± 10.4	–
Δ12 months	0.4 ± 11.7	1.3 ± 7.5	–0.33 (–3.75, 3.09)
PEPPI-5			
Baseline	21.7 ± 2.5	21.3 ± 2.8	–
Δ12 months	–0.5 ± 3.2	0.3 ± 2.5	–0.87 (–2.00, 0.26)
TSQM-9			
Medication effectiveness			
Baseline	73.8 ± 16.1	72.5 ± 21.2	–
Δ12 months	–0.6 ± 12.5	–1.6 ± 19.0	0.94 (–5.30, 7.17)
Medication convenience			
Baseline	77.0 ± 13.3	77.6 ± 14.7	–
Δ12 months	–1.4 ± 16.1	2.1 ± 12.9	–4.01 (–9.65, 1.63)
Medication global satisfaction			
Baseline	69.8 ± 14.5	71.2 ± 16.6	–
Δ12 months	1.5 ± 11.0	0.6 ± 13.0	0.10 (–4.58, 4.77)
Satisfaction with health care¶			
Ease of contact			
Baseline, median (IQR)	10 (9–10)	10 (10–10)	–
Δ12 months	–0.1 ± 0.6	–0.1 (0.8)	0.01 (–0.28, 0.29)
Health care received			
Baseline, median (IQR)	9 (8–9)	9 (8–9)	–
Δ12 months	–0.1 ± 1.4	0.0 ± 1.3	–0.10 (–0.62, 0.43)
Recommend hospital			
Baseline, median (IQR)	9 (8–10)	9 (8–10)	–
Δ12 months	–0.4 ± 1.8	–0.1 ± 1.4	–0.28 (–0.92, 0.37)
CQR-5, no. (%)#			
Baseline	32 (65)	40 (76)	–
12 months	30 (63)	40 (77)	0.54 (0.21, 1.42)

\* Except where indicated otherwise, values are the mean ± SD. Values at 12 months are the mean ± SD difference from baseline value. Lower Rapid Assessment of Patient Index Data 3 (RAPID3) scores indicate lower disease activity scores, while in all other outcome measures, higher scores are better. 95% CI = 95% confidence interval; EC-17 = effective consumer scale 17; PEPPI-5 = Perceived Efficacy in Patient-Physician Interaction Questionnaire 5; TSQM-9 = 9-item Treatment Satisfaction Questionnaire for Medication; IQR = interquartile range; CQR-5 = Compliance Questionnaire for Rheumatology 5.

† At 12 months, n = 48.

‡ At 12 months, n = 52.

§ Adjusted for age, sex, disease duration, body mass index, education level, and baseline value.

¶ Analysis of Δ (12-month value – baseline value) to create normal distribution.

# Classified as high medication adherence.

satisfaction was a 7.3 out of 10. Detailed results of the final evaluation are presented in Supplementary Table 1, available on the *Arthritis & Rheumatology* website at <http://onlinelibrary.wiley.com/doi/10.1002/art.42292>.

During the trial, 24 bug reports were made regarding 8 different bugs in the application. Most importantly, notifications did not work between July 2019 and February 2021 for most patients. Therefore, most patients received few or no reminders on the phone to complete their questionnaires during the study. In March 2020, automated email reminders were sent each week to patients to complete the questionnaire to minimize further impact of this bug. The adherence rate during the email reminders was similar (62%; 1,009 of 1,625) to that prior to the email reminders (58%; 537 of 923). Other bugs that were reported included the

following: the possibility to fill out a negative morning stiffness time, newly made password not working, not being able to log in, not receiving a token to log in, fingerprint login not working, badge icon (red reminder “1”) not disappearing after completing the questionnaire, and inability to send the questionnaire. These problems were resolved and were not recurrent.

## DISCUSSION

This randomized controlled trial compared app-assisted, patient-initiated care to usual care for patients with RA with low disease activity. Our findings show that the use of this intervention results in a significantly lower number (38%) of consultations with rheumatologists. Additionally, the intervention was noninferior to

usual care in terms of disease activity, and patient reported outcomes remained high in the app intervention group.

Our findings show that it is possible to optimize RA health care delivery by letting patients initiate consultations and self-monitor their disease. The inefficiency of the current system with preplanned consultations for disease monitoring is illustrated by the similar number of patient-initiated extra consultations that were planned in both groups. Our results are corroborated by previous studies that demonstrated the ability to maintain disease activity outcomes while lowering the number of outpatient clinic visits following a monitoring-at-a-distance protocol (of 51% after 2 years and 79% in 6 months) (20,21) and patient-initiated care (8–10). The results from Fredriksson et al contrast with our results, as they reported that patient-initiated care (without an app) did not lower the number of consultations in their population (12). This could have been a consequence of the frequent nurse monitoring visits in the study, which could have counteracted to the effect of patient-initiated care. Looking at the projected increase in health care demand and decrease in supply (or availability), the patient-initiated strategy combined with self-monitoring appears to be a very promising direction.

While health care utilization dropped, no difference was found in patient–physician interaction, health care satisfaction, self-efficacy, or treatment satisfaction between the intervention and control groups. The lack of improvement following an intervention using a smartphone app in these outcomes was also found by Lee et al (14) but contrasts with other studies (15,17,34). In our study, the secondary outcome measures were already at favorable levels at baseline, which suggests that patients with low disease activity value the current system of face-to-face consultations, which has been previously described (35). From a value-based health care perspective, the fact that these ePROs maintained favorable levels highlights that a similar quality of health care can be provided with less medical labor. In addition, patients have also acknowledged that prioritizing allocation of clinic visits, according to patient-generated RA disease activity via an app, would be acceptable and fair when demand exceeded capacity (35).

The flare notification did not function as desired, as most flare consultations were not preceded by a flare notification. In most cases, the flare notification was given during a rise in complaints. The notification might have helped patients to reflect on the cause of their complaints and self-manage their symptoms. However, with our current study design, it was not possible to evaluate the added effect and importance of weekly self-monitoring with the app in addition to patient-initiated care exclusively. The addition of a third arm (patient-initiated care without the app) was discussed but meant that information on disease activity would be lacking for a full year. This was deemed unethical and inconsistent with EULAR and ACR treatment protocols. Therefore, a design following a recent telemedicine study protocol was chosen (36). The value of smartphone apps and monitoring has previously

been indicated for patients and rheumatologists. Patients have been predominantly positive about online self-monitoring, indicating that it helps them assess the course of their disease, that they feel less dependent on the health care professional, and that it aids them in communication with their physician (23,37–39). In addition, rheumatologists with patients that self-monitor with ePROs are less likely to have difficulty estimating how patients were doing compared to rheumatologists who do not have access to ePRO data (40).

The average response rate (59%) to questionnaires was relatively low compared to the previously reported rates of 91% by Austin et al, 79% by Colls et al, and 69% by Seppen et al (calculated from response rates) (25,41,42). This could be due to the duration of the present study, which was  $\geq 6$  months longer than the aforementioned studies (although adherence did not steadily decline during this study), the lack of notifications during a major part of the study, or the overall persuasive design of the app (43). So far, it is unclear how often patients have to be monitored to be able to target consultations according to need. The burden for patients will need to be kept as low as possible, while still collecting sufficient data to make informed treatment decisions. The results of the present study suggest that weekly collection (with 60% actual completion) is sufficient to maintain low disease activity.

Strengths of the study include the randomized, controlled design with blinded outcome assessment and the number of participants. The study expands the population in which telemonitoring has been successfully tested, after Salaffi et al and Pers et al previously showed that such a system can also be deployed for intensive telemonitoring and treatment of patients with recently diagnosed active RA or patients that recently changed treatments (20,44). In theory, our results apply for many RA patients in affluent countries, namely those with a disease duration of  $>2$  years who are experiencing a low disease activity state ( $>70\%$  according to Haugeberg et al) (6) and have a smartphone. However, only 20% of the patients agreed to participate, and, specifically, women were less likely to participate. This illustrates that while health technology could be applicable to anyone, it is not adopted by everyone. This limited adoption is also reflected in the participating number of rheumatologists (10 of 17) and the somewhat neutral results of the physician satisfaction. Future research should focus on improving the adoption of health technologies by a larger population, which may be achieved with a more patient-centered design with more focus on involving the patient in health technology programs by health care providers (45).

There are limitations to this study. First, generalizability is limited for 2 reasons: 1) only 20% of the patients who were approached were randomized to a treatment group, which could have introduced a selection bias, and 2) inclusion was limited to patients who are able to use technology such as smartphones. Even though smartphone usage has widely spread ( $>90\%$  of adults in The Netherlands) (46), hospitals that use apps should

remain aware of patients who have insufficient eHealth literacy to participate in telemedicine care (47). In our study, very few people declined for this purpose, but to remain inclusive of all patients, traditional ways of providing health care should remain available, or patients should be trained on how to participate in the new form of health care (telemedicine). From anecdotal experience, patients easily learned how to use the app and were rapidly comfortable using it. For those who need some extra time, an eHealth walk-in clinic could be organized.

Second, our results show a decline in health care utilization but have not yet showed cost effectiveness of the intervention. Therefore, a cost effectiveness evaluation of this intervention will be performed to evaluate the economic effects of the intervention. Third, the use of the DAS28-ESR to compare disease activity at 2 time points has limitations. Since no DAS28-ESR data were collected between the study visits, it remains unclear what the DAS28-ESR of both groups was throughout the year. Therefore, it is possible that the DAS28-ESR was different in both groups over the course of the year. However, as illustrated by the RAPID3 results, disease activity of both groups appeared similar at all time points during the study. Looking at the real-life observational data from Müskens et al, the reduction in the number of visits continues after the first year, while the average disease activity does not deteriorate (it even slightly improves) (20). Fourth, testing 2 separate hypotheses using a *P* value of <0.05 might be considered a weakness. However, the noninferiority limit would also have been reached with a 97.5% CI, and the *P* value for number of visits was below 0.025, the Bonferroni threshold for multiple testing in case of 2 tests.

In conclusion, these findings suggest that self-initiated care combined with weekly self-monitoring in patients with RA with low disease activity is safe in terms of the DAS28-ESR, reduces the number of consultations with rheumatologists, and maintains high satisfaction with the health care received. Our intervention strategy may reduce the workforce that is needed per RA patient and could therefore decrease health care costs per patient, which will be evaluated in a separate analysis.

## AUTHOR CONTRIBUTIONS

All authors were involved in drafting the article or revising it critically for important intellectual content, and all authors approved the final version to be published. Dr. Seppen had full access to all of the data in the study and takes responsibility for the integrity of the data and the accuracy of the data analysis.

**Study conception and design.** Seppen, ter Wee, van Schaardenburg, Roorda, Nurmohamed, Boers, Bos.

**Acquisition of data.** Seppen, Wiegel.

**Analysis and interpretation of data.** Seppen, Wiegel, ter Wee, Nurmohamed, Boers, Bos.

## ROLE OF THE STUDY SPONSOR

This randomized controlled trial was an investigator-initiated study funded by AbbVie. AbbVie had no role in the design of this study, nor

during its execution, analysis, interpretation of the data, or decision to submit results.

## REFERENCES

1. Battafarano DF, Ditmyer M, Bolster MB, et al. 2015 American College of Rheumatology workforce study: supply and demand projections of Adult Rheumatology Workforce, 2015–2030. *Arthritis Care Res (Hoboken)* 2018;70:617–26.
2. Kilian A, Upton LA, Battafarano DF, et al. Workforce trends in rheumatology. *Rheum Dis Clin North Am* 2019;45:13–26.
3. Sheikh A, Sood HS, Bates DW. Leveraging health information technology to achieve the “triple aim” of healthcare reform. *J Am Med Inform Assoc* 2015;22:849–56.
4. Miloslavsky EM, Bolster MB. Addressing the rheumatology workforce shortage: a multifaceted approach. *Semin Arthritis Rheum* 2020;50:791–6.
5. Smolen JS, Breedveld FC, Burmester GR, et al. Treating rheumatoid arthritis to target: 2014 update of the recommendations of an international task force. *Ann Rheum Dis* 2016;75:3–15.
6. Haugeberg G, Hansen IJ, Soldal DM, et al. Ten years of change in clinical disease status and treatment in rheumatoid arthritis: results based on standardized monitoring of patients in an ordinary outpatient clinic in southern Norway. *Arthritis Res Ther* 2015;17:219.
7. Flurey CA, Morris M, Richards P, et al. It's like a juggling act: rheumatoid arthritis patient perspectives on daily life and flare while on current treatment regimes. *Rheumatology (Oxford)* 2014;53:696–703.
8. Poggenborg RP, Madsen OR, Dreyer L, et al. Patient-controlled outpatient follow-up on demand for patients with rheumatoid arthritis: a 2-year randomized controlled trial. *Clin Rheumatol* 2021;40:3599–604.
9. Primdahl J, Sorensen J, Horn HC, et al. Shared care or nursing consultations as an alternative to rheumatologist follow-up for rheumatoid arthritis outpatients with low disease activity—patient outcomes from a 2-year, randomised controlled trial. *Ann Rheum Dis* 2014;73:357–64.
10. Hewlett S, Kirwan J, Pollock J, et al. Patient initiated outpatient follow up in rheumatoid arthritis: six year randomised controlled trial. *BMJ* 2005;330:171.
11. Prevo ML, van't Hof MA, Kuper HH, et al. Modified disease activity scores that include twenty-eight-joint counts: development and validation in a prospective longitudinal study of patients with rheumatoid arthritis. *Arthritis Rheum* 1995;38:44–8.
12. Fredriksson C, Ebbevi D, Waldheim E, et al. Patient-initiated appointments compared with standard outpatient care for rheumatoid arthritis: a randomised controlled trial. *RMD Open* 2016;2:e000184.
13. US Department of Health and Human Services FDA Center for Drug Evaluation and Research, Center for Biologics Evaluation and Research, Center for Devices and Radiological Health. Guidance for industry: patient-reported outcome measures: use in medical product development to support labeling claims: draft guidance. *Health Qual Life Outcomes* 2006;4:79.
14. Lee YC, Lu F, Colls J, et al. Outcomes of a mobile app to monitor patient reported outcomes in rheumatoid arthritis: a randomized controlled trial. *Arthritis Rheumatol* 2021;73:1421–9.
15. Allam A, Kostova Z, Nakamoto K, et al. The effect of social support features and gamification on a Web-based intervention for rheumatoid arthritis patients: randomized controlled trial. *J Med Internet Res* 2015;17:e14.
16. Gossec L, Cantagrel A, Soubrier M, et al. An e-health interactive self-assessment website (Sanoia®) in rheumatoid arthritis. A 12-month randomized controlled trial in 320 patients. *Joint Bone Spine* 2018;85:709–14.

17. Shigaki CL, Smarr KL, Siva C, et al. RAHelp: an online intervention for individuals with rheumatoid arthritis. *Arthritis Care Res (Hoboken)* 2013;65:1573–81.
18. Van den Berg MH, Runday HK, Peeters AJ, et al. Using internet technology to deliver a home-based physical activity intervention for patients with rheumatoid arthritis: a randomized controlled trial. *Arthritis Rheum* 2006;55:935–45.
19. Colls J, Lee YC, Xu C, et al. Patient adherence with a smartphone app for patient-reported outcomes in rheumatoid arthritis. *Rheumatology (Oxford)* 2021;60:108–12.
20. Pers YM, Valsecchi V, Mura T, et al. A randomized prospective open-label controlled trial comparing the performance of a connected monitoring interface versus physical routine monitoring in patients with rheumatoid arthritis. *Rheumatology (Oxford)* 2021;60:1659–68.
21. Muskens WD, Rongen-van Dartel SA, Vogel C, et al. Telemedicine in the management of rheumatoid arthritis: maintaining disease control with less health-care utilization. *Rheumatol Adv Pract* 2021;5:rkaa079.
22. De Thurah A, Stengaard-Pedersen K, Axelsen M, et al. Tele-health followup strategy for tight control of disease activity in rheumatoid arthritis: results of a randomized controlled trial. *Arthritis Care Res (Hoboken)* 2018;70:353–60.
23. Seppen BF, L'Ami MJ, Rico SD, et al. A smartphone app for self-monitoring of rheumatoid arthritis disease activity to assist patient-initiated care: protocol for a randomized controlled trial. *JMIR Res Protoc* 2020;9:e15105.
24. CastorEDC. Castor, URL: <https://www.castoredc.com/>.
25. Seppen BF, Wiegel J, L'Ami MJ, et al. Feasibility of self-monitoring rheumatoid arthritis with a smartphone app: results of two mixed-methods pilot studies. *JMIR Form Res* 2020;4:e20165.
26. Schäfer W, Kroneman M, Boerma W, et al, on behalf of the World Health Organization. The Netherlands: health system review; 2010.
27. Centraal Bureau Statistiek, Internet; toegang, gebruik en faciliteiten; 2012–2019. URL: <https://www.cbs.nl/nl-nl/cijfers/detail/83429NED?dl=27A20>.
28. Vergelijk 4G dekking van alle providers. URL: <https://www.4gdekking.nl>
29. Van Ons. Digitaal in 2018–Hoe staan we ervoor? URL: <https://van-ons.nl/blog/digitale-strategie/digitaal-2018-hoe-staan-we-ervoor/>.
30. Speedtest. Speedtest Global Index: ranking mobile and fixed broadband speeds from around the world on a daily basis. Global Median Speeds Mau 2022. URL: <https://www.speedtest.net/global-index>.
31. Ten Klooster PM, Taal E, Siemons L, et al. Translation and validation of the Dutch version of the Effective Consumer Scale (EC-17). *Qual Life Res* 2013;22:423–9.
32. Bangor A, Kortum PT. An empirical evaluation of the System Usability Scale (SUS). *Int J Hum-Comput Int* 2008;24:574–94.
33. Brooke J. SUS: A quick and dirty usability scale. Redhatch Consulting Ltd: United Kingdom; 1996.
34. Mollard E, Michaud K. A mobile app with optical imaging for the self-management of hand rheumatoid arthritis: pilot study. *JMIR Mhealth Uhealth* 2018;6:e12221.
35. Grainger R, Townsley HR, Ferguson CA, et al. Patient and clinician views on an app for rheumatoid arthritis disease monitoring: function, implementation and implications. *Int J Rheum Dis* 2020;23:813–27.
36. De Jong MJ, van der Meulen-de Jong AE, Romberg-Camps MJ, et al. Telemedicine for management of inflammatory bowel disease (myIBDcoach): a pragmatic, multicentre, randomised controlled trial. *Lancet* 2017;390:959–68.
37. Renskers L, Rongen-van Dartel SA, Huis AM, et al. Patients' experiences regarding self-monitoring of the disease course: an observational pilot study in patients with inflammatory rheumatic diseases at a rheumatology outpatient clinic in The Netherlands. *BMJ Open* 2020;10:e033321.
38. Richter JG, Nannen C, Chehab G, et al. Mobile app-based documentation of patient-reported outcomes—3-months results from a proof-of-concept study on modern rheumatology patient management. *Arthritis Res Ther* 2021;23:121.
39. White KM, Ivan A, Williams R, et al. Remote measurement in rheumatoid arthritis: qualitative analysis of patient perspectives. *JMIR Form Res* 2021;5:e22473.
40. Bos WH, van Tubergen A, Vonkeman HE. Telemedicine for patients with rheumatic and musculoskeletal diseases during the COVID-19 pandemic: a positive experience in the Netherlands. *Rheumatol Int* 2021;41:565–73.
41. Austin L, Sharp CA, van der Veer SN, et al. Providing 'the bigger picture': benefits and feasibility of integrating remote monitoring from smartphones into the electronic health record. *Rheumatology (Oxford)* 2020;59:367–78.
42. Colls J, Lee YC, Xu C, et al. Patient adherence with a smartphone app for patient-reported outcomes in rheumatoid arthritis. *Rheumatology (Oxford)* 2020;60:108–12.
43. Kelders SM, Kok RN, Ossebaard HC, et al. Persuasive system design does matter: a systematic review of adherence to web-based interventions. *J Med Internet Res* 2012;14:e152.
44. Salaffi F, Carotti M, Ciapetti A, et al. Effectiveness of a telemonitoring intensive strategy in early rheumatoid arthritis: comparison with the conventional management approach. *BMC Musculoskelet Disord* 2016;17:146.
45. Solomon DH, Rudin RS. Digital health technologies: opportunities and challenges in rheumatology [review]. *Nat Rev Rheumatol* 2020;16:525–35.
46. Eurostat statistics. URL: <http://appsso.eurostat.ec.europa.eu/hui/submitViewTableAction.do>. 2017.
47. Rijksinstituut voor Volksgezondheid en Milieu. Niet iedereen kan regie voeren over eigen zorg. 2014.

# Heavy Chain Constant Region Usage in Antibodies to Peptidylarginine Deiminase 4 as a Marker of Disease Subsets in Rheumatoid Arthritis

E. Gómez-Bañuelos,<sup>1</sup> J. Shi,<sup>1</sup> H. Wang,<sup>1</sup> M. I. Danila,<sup>2</sup> S. L. Bridges Jr.,<sup>2</sup> J. T. Giles,<sup>3</sup> G. P. Sims,<sup>4</sup> F. Andrade,<sup>1</sup> and E. Darrah<sup>1</sup>

**Objective.** The study of autoantibody isotypes in autoimmune diseases is useful for identifying clinically relevant endotypes. This study was undertaken to study the prevalence and clinical significance of different isotypes and IgG subclasses of anti-peptidylarginine deiminase 4 (anti-PAD4) autoantibodies in individuals with rheumatoid arthritis (RA).

**Methods.** In 196 RA subjects and 64 healthy controls, anti-PAD4 antibody types were determined using enzyme-linked immunosorbent assay. We investigated associations between anti-PAD4 antibodies and clinical outcomes, and relevant features were confirmed in an independent RA cohort.

**Results.** Anti-PAD4 IgG1, anti-PAD4 IgG2, anti-PAD4 IgG3, anti-PAD4 IgG4, anti-PAD4 IgA, and anti-PAD4 IgE antibodies were more frequent in RA patients than healthy controls ( $P < 0.001$ ). Anti-PAD4 IgG1, anti-PAD4 IgG3, and anti-PAD4 IgE were associated with distinct clinical features. Anti-PAD4 IgG1 was predictive of progressive radiographic joint damage (odds ratio [OR] 4.88,  $P = 0.005$ ), especially in RA patients without baseline joint damage (40% versus 0%,  $P = 0.003$ ) or in those negative for anti-cyclic citrullinated peptide and/or rheumatoid factor (OR 32;  $P = 0.009$ ). IgG1 was also associated with higher levels of C-reactive protein ( $P = 0.006$ ) and interleukin-6 ( $P = 0.021$ ). RA patients with anti-PAD4 IgG3 had higher baseline joint damage scores (median Sharp/van der Heijde score 13 versus 7,  $P = 0.046$ ), while those with anti-PAD4 IgE had higher Disease Activity Score in 28 joints (median 4.0 versus 3.5,  $P = 0.025$ ), more frequent rheumatoid nodules (31% versus 16%,  $P = 0.025$ ), and more frequent interstitial lung disease (ground-glass opacification) (24% versus 9%,  $P = 0.014$ ). Anti-PAD4 IgG1 antibody associations with joint damage were corroborated in an independent RA cohort.

**Conclusion.** Anti-PAD4 IgG1, anti-PAD4 IgG3, and anti-PAD4 IgE antibodies identify discrete disease subsets in RA, suggesting that heavy chain usage drives distinct effector mechanisms of anti-PAD4 antibodies in RA.

## INTRODUCTION

Rheumatoid arthritis (RA) is a chronic autoimmune disease characterized by synovial joint inflammation leading to cartilage destruction and subchondral bone erosion (1). RA is a clinically heterogeneous disease with variable disease courses among patients. While several individual factors may interplay to determine disease progression and severity (2), autoantibodies, such as anti-citrullinated protein antibodies (ACPAs), are clinically useful tools for

defining RA endotypes with distinct clinical features and prognoses (3). Peptidylarginine deiminase 4 (PAD4), a key enzyme in the pathogenesis of RA, catalyzes the calcium-dependent citrullination of proteins, producing the main antigenic targets of ACPA in RA (4).

Antibodies targeting PAD4 are found in 24–45% of RA patients (5–8). These autoantibodies are associated with a subset of RA characterized by more severe joint damage, faster progression of joint erosions, and interstitial lung disease (ILD) (5–7,9). These phenotypes have been principally attributed to a subset of

The content is solely the responsibility of the authors and does not represent the official views of the National Institute of Arthritis and Musculoskeletal and Skin Diseases or the National Institutes of Health.

Supported by the Jerome L. Greene Foundation and National Institute of Arthritis and Musculoskeletal and Skin Diseases, NIH (grants R01-AR-050026, R01-AR-069569, R01-AR-079404, and R21-AR-079891), and by MedImmune, formerly the global biologics R&D arm of AstraZeneca.

Drs. Gómez-Bañuelos and Shi contributed equally to this work.

<sup>1</sup>E. Gómez-Bañuelos, MD, PhD, J. Shi, PhD, H. Wang, PhD, F. Andrade, MD, PhD, E. Darrah, PhD: Division of Rheumatology, Johns Hopkins University School of Medicine, Baltimore, Maryland; <sup>2</sup>M. I. Danila, MD, MSc, MSPH, S. L. Bridges Jr., MD, PhD (current address: Department of Medicine, Hospital for

Special Surgery and Department of Medicine, Weill Cornell Medical College, New York); Division of Clinical Immunology and Rheumatology, University of Alabama at Birmingham; <sup>3</sup>J. T. Giles, MD, MPH: Division of Rheumatology, College of Physicians and Surgeons, Columbia University, New York; <sup>4</sup>G. P. Sims, PhD: BioPharmaceuticals R&D, AstraZeneca, Gaithersburg, Maryland.

Author disclosures are available at <https://onlinelibrary.wiley.com/action/downloadSupplement?doi=10.1002%2Fart.42262&file=art42262-sup-0001-Disclosureform.pdf>.

Address correspondence via email to E. Darrah, PhD, at [edarrah1@jhmi.edu](mailto:edarrah1@jhmi.edu) or to F. Andrade, MD, PhD, at [andrade@jhmi.edu](mailto:andrade@jhmi.edu).

Submitted for publication April 29, 2021; accepted in revised form June 2, 2022.

anti-PAD4 antibodies that are cross-reactive to PAD3 (anti-PAD3/4) (5,6,10). Although the exact mechanism by which anti-PAD3/4 may result in a more severe disease course is unknown, this subset of anti-PAD4 antibodies increases the calcium sensitivity of PAD4 and enhances production of citrullinated antigens (6). Nevertheless, since anti-PAD3/4 are only found in 32–43% of anti-PAD4-positive RA patients (5,6), they do not entirely explain the clinical manifestations attributed to anti-PAD4. This suggests that additional types of anti-PAD4 antibodies may exist, which may further identify unique RA endotypes.

Ig exert their effects via 2 principal regions. The variable region determines antigen specificity and the constant region of the heavy chain (IgH) defines the effector functions of the antibody (e.g., complement activation, cell activation, placental transport) (11). Ig are classified into 5 major isotypes in humans according to their IgH constant region: IgA, IgM, IgE, IgD, and IgG. IgG is further subclassified into IgG1, IgG2, IgG3, and IgG4 (11,12). The distinct Ig types have different tissue distribution, Fc receptor affinities, and complement activation capacity (13). Therefore, different isotypes of antibodies against the same autoantigen may indicate distinct underlying pathogenic mechanisms, resulting in different clinical manifestations. Such studies in systemic lupus erythematosus have proven useful in identifying subsets of patients who have distinct clinical outcomes and pathogenic mechanisms (14,15).

Currently, it is known that PAD4 elicits IgG1 and IgG3 responses in RA patients (16), but IgA, IgM, and IgE responses have not been studied. Furthermore, there is no information regarding the association of different anti-PAD4 isotypes/subclasses with clinical manifestations in RA. Given that the anti-PAD4 autoantibody system is associated with RA outcomes, we studied the prevalence of anti-PAD4 IgA, anti-PAD4 IgE, anti-PAD4 IgM, and anti-PAD4 IgG subclasses and determined their association with clinical features in RA patients from 2 independent cohorts.

## PATIENTS AND METHODS

**Study subjects.** We studied sera samples from 196 RA subjects enrolled in the Evaluation of Subclinical Cardiovascular Disease and Predictors of Events in Rheumatoid Arthritis (ESCAPE RA) cohort, as previously described (6,17,18). Briefly, all RA subjects were classified according to the American College of Rheumatology 1987 revised RA criteria (19). Single-view anteroposterior radiography of the hands and posteroanterior radiography of the feet were obtained at study enrollment (baseline) and at a follow-up visit, which occurred at a mean  $\pm$  SD of  $39 \pm 4$  months after the baseline visit. Radiographs were scored using Sharp/van der Heijde scores (SHS) to quantify joint damage (20). Radiography was conducted at baseline for all 196 subjects, and follow-up radiography was conducted as well for 152 subjects. RA disease activity was calculated using the Disease Activity Score 28 joint assessment (DAS28) with C-reactive protein (CRP) levels (21). The Stanford Health Assessment Questionnaire (HAQ) was

used to assess disability (22). Current treatments and past treatments were determined using examiner-administered questionnaires. Participants ( $n = 176$ ) underwent multidetector row computed tomography of the chest at the baseline visit, and the presence and extent of ILD was scored as previously described (23). The healthy control group was composed of 64 healthy volunteers, recruited from the general population of Johns Hopkins. Written informed consent was obtained from all participants prior to participation. The study was approved by the Institutional Review Board of Johns Hopkins, and all study procedures were conducted in accordance with the Declaration of Helsinki.

For the confirmation cohort, we further tested serum samples from 135 subjects enrolled in the Consortium for the Longitudinal Evaluation of African Americans with Early Rheumatoid Arthritis (CLEAR) registry. The methods and procedures of the CLEAR-I and CLEAR-II registries have been described previously (24), and all CLEAR participants have been extensively genetically characterized (25).

### Determination of anti-PAD4 antibody isotypes and IgG subclasses.

Anti-PAD4 antibody isotypes and IgG subclasses were determined using an enzyme-linked immunosorbent assay. Briefly, Nunc MaxiSorp plates (Sigma) were coated overnight with recombinant PAD4 in 0.1M sodium carbonate buffer pH 9.6 phosphate buffered saline (PBS). Different concentrations of recombinant PAD4 were used to detect the different antibody subsets as follows: 1  $\mu$ g/ml for IgA and IgM; 2  $\mu$ g/ml for IgG1 and IgG3; and 3  $\mu$ g/ml for IgG2, IgG4, and IgE. Plates were blocked with 2% bovine serum albumin (BSA) in PBS for 1 hour at room temperature. Sera were diluted in 1% BSA/0.05% Tween 20 in PBS and incubated at room temperature for 2 hours in antigen-coated wells and wells without antigens for background subtraction in sera (IgE 1:10 dilution, IgG2 and IgG4 1:50 dilution, IgG1 and IgG3 1:100 dilution, IgA and IgM 1:250 dilution). Horseradish peroxidase (HRP)-conjugated anti-human IgG1 (1:5,000 dilution; catalog no. MH1715), IgG2 (1:2,500 dilution; catalog no. MH1722), IgG3 (1:5,000 dilution; catalog no. 05-3620), IgG4 (1:2,500 dilution; catalog no. MH1742), IgA (1:5,000 dilution; catalog no. PA1-74395), IgE (1:2,000 dilution; catalog no. SA5-10306), and IgM (1:10,000 dilution; catalog no. 05-4920; all from ThermoFisher) were used as secondary antibodies diluted in 1% BSA/0.05% Tween 20 in PBS. Anti-PAD4 antibody arbitrary units (AU) per milliliter were calculated for each background-corrected sample using a serial dilution of a human sera with high levels of each anti-PAD4 antibody subtype. We determined the cutoff value for anti-PAD4 antibody positivity using the 95th percentile of antibody levels in healthy controls.

**Statistical analysis.** We compared serum levels and positivity for different anti-PAD4 antibodies between RA subjects and healthy controls using Student's *t*-test and chi-square tests,

respectively. We calculated the intersections between the different anti-PAD4 isotypes present in each RA subject using UpSet function in the ComplexHeatmap R package (26) (version 2.13.1). The co-occurrence of anti-PAD4 isotypes was represented in a chord diagram generated using the circlize R package (version 0.4.12) (27). The significance of the co-occurrence of isotypes was tested using Jaccard/Tanimoto testing implemented in the R package Jaccard (version 0.1.0) (28). To evaluate patient demographic and clinical characteristics according to the presence of each anti-PAD4 isotype, Student's *t*-tests were used for group-wise comparisons of normally distributed continuous variables, Kruskal-Wallis testing was used for group-wise comparisons of nonnormally distributed variables, and either chi-square test or 2-sided Fisher's exact test was used as appropriate for group-wise comparisons of categorical variables.

The significance of comparisons between patient demographic and clinical characteristics according to the presence of anti-PAD4 isotypes was summarized in a heatmap using the  $-\log_2 P$  value. We explored the independent association between anti-PAD4 Ig level and radiographic progression (any progression and progression  $\geq 4$  units/year) using multivariable logistic regression, adjusting for covariates associated with the outcomes of interest and anti-PAD4 Ig levels in univariate modeling ( $P < 0.20$ ). Likelihood ratio testing was used to exclude noncontributing covariates from the models. We modeled differences in radiographic progression according to anti-PAD4 Ig status in subgroups defined by other RA-associated autoantibodies (i.e., RA and citrullinated peptide [anti-CCP]) and baseline radiographic erosion status (SHS score 0 versus  $>0$ ). Throughout, Stata/SE (version 16) was used, with 2-tailed  $\alpha = 0.05$ .

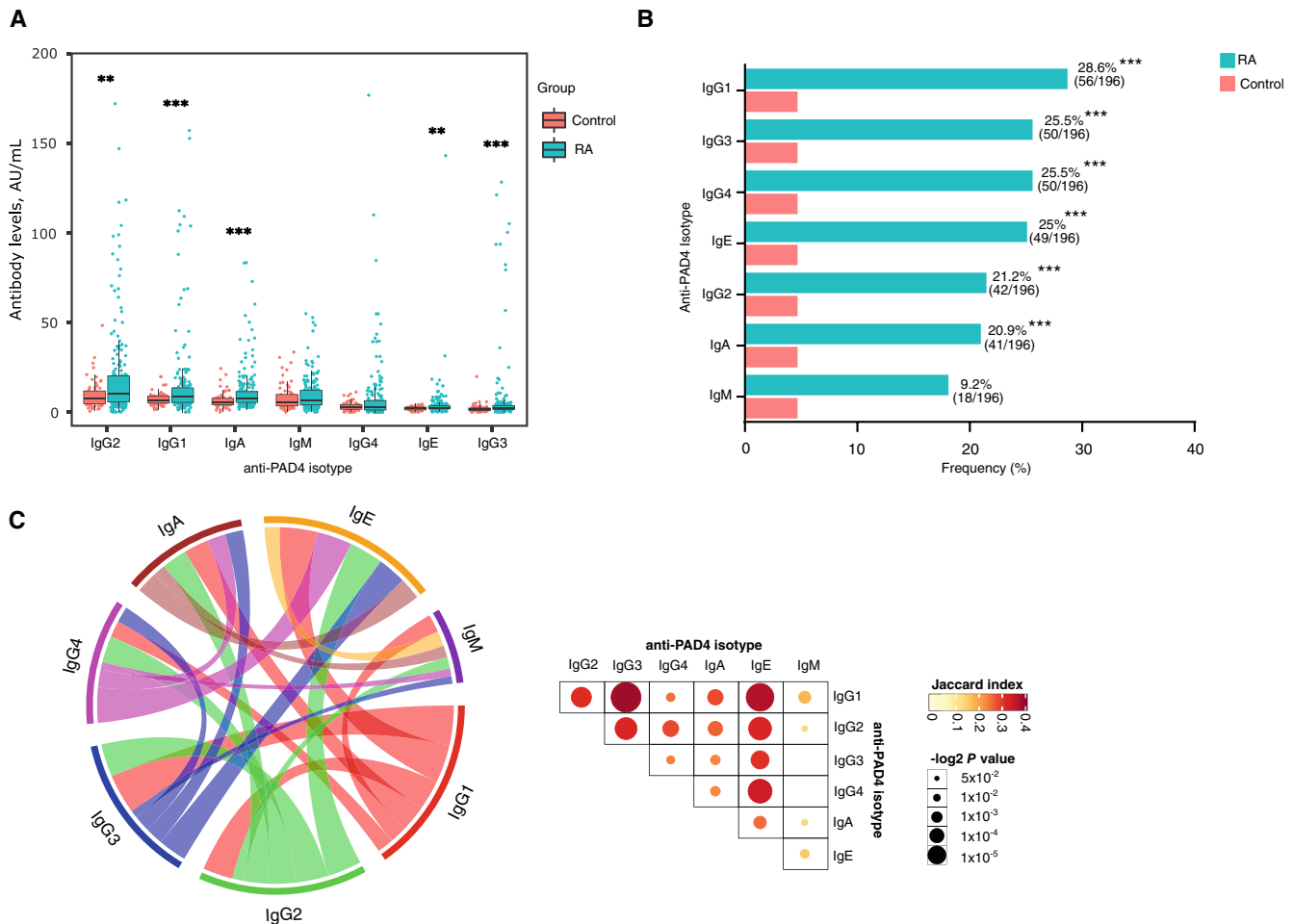


**Figure 1.** Rheumatoid arthritis (RA) serum is enriched in different anti-peptidylarginine deiminase 4 (anti-PAD4) antibody isotypes. **A**, Levels of anti-PAD4 antibody isotypes and IgG subclasses in serum samples from 196 RA subjects and 64 healthy controls. Symbols represent individual samples; data are presented as box plots with the line within the box showing the median, the boxes showing the interquartile range, and the whiskers showing the minimum and maximum values.  $** = P < 0.01$ ;  $*** = P < 0.001$ , by Student's *t*-test. **B**, Frequency of anti-PAD4 antibody isotypes and IgG subclasses in RA patients and healthy controls.  $*** = P < 0.001$  by Fisher's exact test. **C**, Left, Chord diagram showing the co-occurrence of anti-PAD4 antibody isotypes in samples from RA subjects. Each anti-PAD4 isotype and their respective link to other isotypes is represented by a different color. Line thickness is proportional to the Jaccard index, as shown in the matrix on the right. Right, Jaccard index matrix showing the similarities between anti-PAD4 isotype pair combinations. The color intensity represents the Jaccard's similarity coefficient, and the circle size represents the  $-\log_2 P$  value. AU = arbitrary unit.

## RESULTS

**Prevalence of different isotypes and subclasses of antibodies to PAD4 in RA.** In order to determine the prevalence of distinct anti-PAD4 antibodies in RA, we assayed sera from 196 RA subjects in the ESCAPE RA cohort and 64 healthy controls for IgG1, IgG2, IgG3, IgG4, IgA, IgE, and IgM antibodies against PAD4. Serum levels of anti-PAD4 isotypes and IgG subclasses were significantly higher in RA sera compared to healthy control sera, with the exceptions of IgG4 and IgM (Figure 1A). In the RA subjects, the most frequently detected anti-PAD4 antibody subset was IgG1 (28.6% [ $n = 56$ ]), followed by IgG3 (25.5% [ $n = 50$ ]), IgG4 (25.5% [ $n = 50$ ]), IgE (25.0% [ $n = 49$ ]), IgG2 (21.4% [ $n = 42$ ]), IgA (20.9% [ $n = 41$ ]), and IgM (9.2% [ $n = 18$ ]) (Figure 1B and Supplementary Table 1, available on the *Arthritis & Rheumatology* website at <http://onlinelibrary.wiley.com/doi/10.1002/art.42262>).

Each anti-PAD4 antibody was detected in 4.6% of healthy controls (3 of 65), with different individuals being positive for different subtypes (Figure 1B).

Considering all isotypes and IgG subclasses, 66% of RA subjects (129 of 196) were positive for any anti-PAD4 isotype. Of these, 59% of subjects (76 of 129) were positive for more than one antibody type, and 41% of subjects (53 of 129) were positive for a single antibody (Supplementary Figure 1A, <http://onlinelibrary.wiley.com/doi/10.1002/art.42262>). We further analyzed the co-occurrence of anti-PAD4 antibodies (Figure 1C and Supplementary Figure 1B) in RA by computing the different possible combinations. Combinations comprised of pairs of different types of anti-PAD4 antibodies were the most frequently observed (Supplementary Figure 1B, <http://onlinelibrary.wiley.com/doi/10.1002/art.42262>). The highest co-occurrences were between anti-PAD4 IgG1 and IgG3 (Jaccard index 0.377,  $P < 0.001$ ),

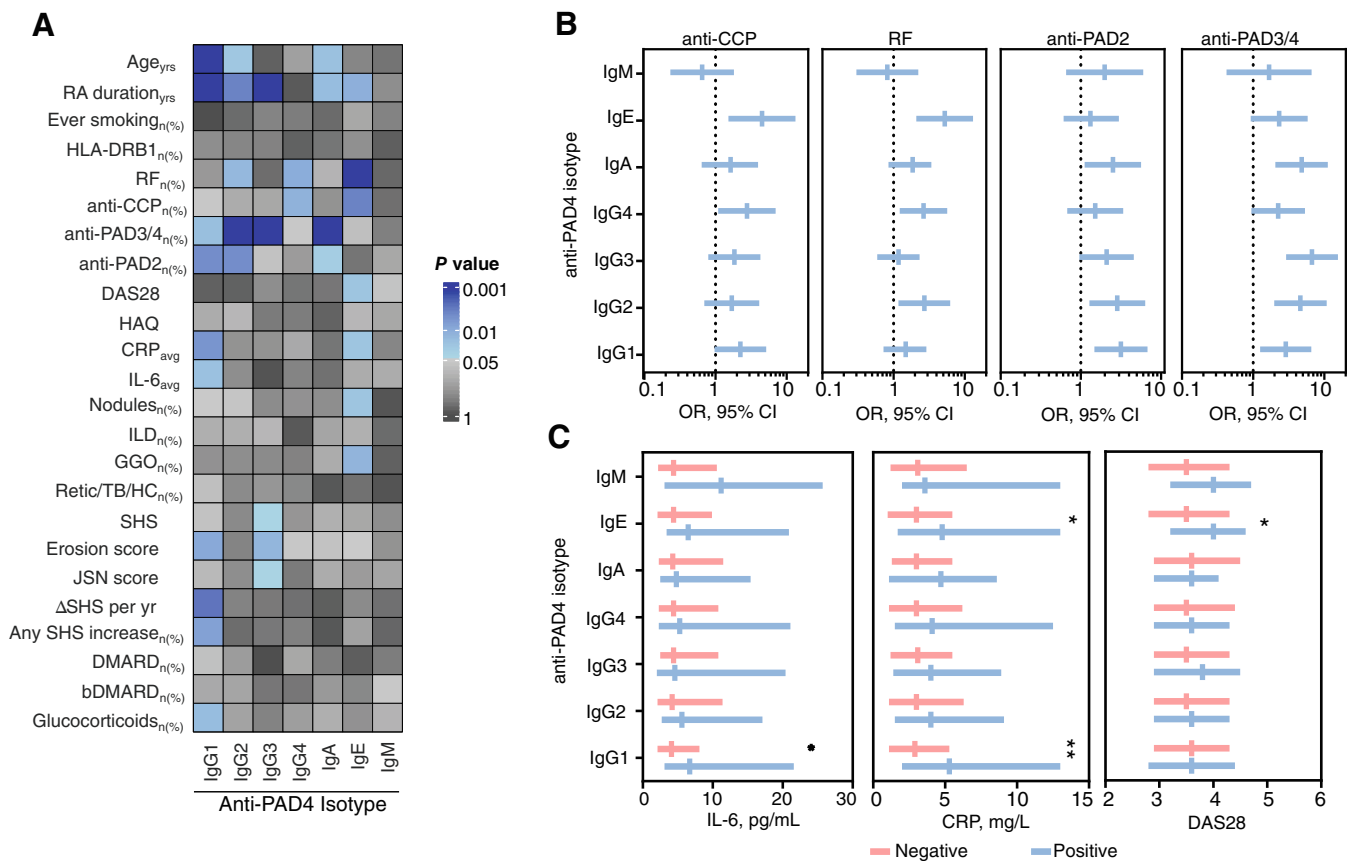


**Figure 2.** Clinical associations between anti-peptidylarginine deiminase 4 (anti-PAD4) antibody subsets in rheumatoid arthritis (RA). **A**, Heatmap showing demographic and clinical associations with anti-PAD4 antibody isotypes in RA ( $n = 196$ ). The color scale shows the  $-\log_2 P$  value, obtained from the comparison between the corresponding anti-PAD4 isotype-positive subjects and anti-PAD4 isotype-negative subjects, by Student's  $t$ -test or chi-square test as appropriate. Variables that were positively associated with the indicated anti-PAD4 isotype were considered significant. **B**, Associations between anti-PAD4 antibody subsets and other known serologic biomarkers. Bars show the odds ratio (OR) with 95% confidence interval (95% CI). **C**, Comparison of serum interleukin-6 (IL-6) levels, C-reactive protein (CRP) levels, and Disease Activity Score in 28 joints (DAS28) scores between RA patients who were negative for anti-PAD4 antibody subsets and RA patients who were positive for anti-PAD4 antibody subsets. Bars show the median and interquartile range. \* =  $P < 0.05$ ; \*\* =  $P < 0.01$ . Yrs = years; RF = rheumatoid factor; anti-CCP = anti-cyclic citrullinated peptide; HAQ = Health Assessment Questionnaire; avg = average; ILD = interstitial lung disease; GGO = ground-glass opacification; retic/TB/HC = reticulation/traction bronchiectasis/honeycombing; SHS = Sharp/van der Heijde score; JSN = joint space narrowing; bDMARD = biologic disease-modifying antirheumatic drug.



IgG1-IgE (Jaccard index 0.364,  $P < 0.001$ ), and IgG4-IgE (Jaccard index 0.338,  $P < 0.001$ ) (Figure 1C and Supplementary Table 2, <http://onlinelibrary.wiley.com/doi/10.1002/art.42262>). Importantly, IgM had the lowest co-occurrence with other antibody types (Figure 1C and Supplementary Table 2).

**Association of anti-PAD4 antibody isotypes and IgG subclasses with distinct clinical subsets in RA.** For a summary of demographic and clinical characteristics of ESCAPE RA subjects according to anti-PAD4 status, see Figure 2A and Supplementary Tables 3 and 4 (<http://onlinelibrary.wiley.com/doi/10.1002/art.42262>). RA patients positive for anti-PAD4 antibody isotypes, except IgG4 and IgM, had a longer disease duration than anti-PAD4-negative individuals (Figure 2A and Supplementary

Tables 3 and 4). White subjects were less likely to be positive for anti-PAD4 IgG1, anti-PAD4 IgA, or anti-PAD4 IgE (Supplementary Tables 3 and 4, <http://onlinelibrary.wiley.com/doi/10.1002/art.42262>). None of the anti-PAD4 antibodies were associated with HLA-DRB1 shared epitope (SE) alleles or smoking (Figure 2 and Supplementary Tables 3 and 4).

Anti-PAD4 IgG2, anti-PAD4 IgG4 and anti-PAD4 IgE were associated with classic seropositive RA (Figure 2A and Supplementary Tables 3 and 4, <http://onlinelibrary.wiley.com/doi/10.1002/art.42262>). Subjects positive for any of these isotypes had a higher frequency of rheumatoid factor (RF) compared to patients without these antibody types, and IgG4- or IgE-positive patients also had a higher frequency of anti-CCP antibodies. Importantly, subjects who were positive for anti-PAD4 IgA, anti-PAD4

**Table 1.** Demographic and clinical characteristics of RA patients according to whether or not there was radiographic progression\*

	No radiographic progression (n = 68)	Any radiographic progression (n = 85)	P
Age, mean $\pm$ SD years	58 $\pm$ 8	60 $\pm$ 8	0.080
Male	32 (47)	25 (29)	0.025
White	62 (91)	72 (85)	0.23
BMI, mean $\pm$ SD	28.0 $\pm$ 4.3	28.2 $\pm$ 5.5	0.88
Total fat, mean $\pm$ SD kg	29.2 $\pm$ 8.3	29.7 $\pm$ 11.4	0.73
Total lean, mean $\pm$ SD kg	47.4 $\pm$ 12.2	43.9 $\pm$ 10.2	0.057
Ever smoker	38 (56)	48 (56)	0.94
RA duration, median (IQR) years	6 (2.5–14.5)	12 (7–19)	<0.001
RF seropositivity of >40 units	39 (57)	53 (62)	0.53
Anti-CCP antibody seropositivity of >20 units	48 (71)	65 (76)	0.50
RF or anti-CCP antibody seropositivity	51 (75)	66 (78)	0.82
Anti-CCP antibody units among seropositive patients	145 (89–170)	142 (89–174)	0.89
Anti-PAD2 positive	17 (25)	13 (15)	0.15
Anti-PAD3/4 positive	3 (<1)	12 (14)	0.045
Any HLA-DRB1 SE allele	42 (62)	65 (76)	0.026
DAS28, median (IQR)	3.3 (2.8–4.2)	3.7 (3.1–4.5)	0.044
DAS, median (IQR)	3.0 (2.4–4.0)	3.4 (2.8–4.1)	0.022
Pain (100-mm VAS), median (IQR)	13 (5–24)	25 (12–47)	<0.001
Swollen joint count, median (IQR)	6 (2–9)	7 (5–10)	0.038
Tender joint count, median (IQR)	6 (2–12)	7 (3–13)	0.39
HAQ score (scale 0–3), median (IQR)	0.38 (0.00–0.94)	1.0 (0.50–1.38)	<0.001
CRP, median (IQR) mg/liter	1.6 (0.7–4.4)	3.0 (1.5–8.2)	0.006
Average CRP, median (IQR) mg/liter	1.8 (0.8–4.3)	4.6 (1.7–8.7)	<0.001
IL-6, median (IQR) pg/ml	2.4 (1.3–5.5)	4.5 (2.0–8.5)	0.008
Study average IL-6, median (IQR) pg/ml	3.4 (1.9–6.4)	5.6 (3.2–21.3)	0.001
Rheumatoid nodules	6 (1)	17 (20)	0.045
Nonbiologic DMARDs	58 (85)	74 (87)	0.82
bDMARDs	31 (46)	37 (44)	0.80
Glucocorticoids	24 (35)	31 (36)	0.88
Cumulative prednisone dose, median (IQR) gm	2.8 (0.0–7.8)	3.5 (0–10.0)	0.54
No. of prior DMARDs, median (IQR)	1 (0–2)	0 (1–3)	0.22
Baseline SHS of >0	41 (60)	73 (86)	<0.001
Anti-PAD4 IgG1 positive	11 (16)	30 (35)	0.008
Anti-PAD4 IgG2 positive	14 (21)	15 (18)	0.64
Anti-PAD4 IgG3 positive	19 (28)	20 (24)	0.53
Anti-PAD4 IgG4 positive	14 (21)	22 (26)	0.44
No. of anti-PAD4 isotypes, median (IQR)	1 (0–2)	1 (0–2)	0.26

\* Except where indicated otherwise, values are the number (%) of patients. RA = rheumatoid arthritis; BMI = body mass index; IQR = interquartile range; RF = rheumatoid factor; anti-CCP = anti-cyclic citrullinated peptide; anti-PAD2 = anti-peptidylarginine deiminase 2; SE = shared epitope; DAS28 = Disease Activity Score in 28 joints; VAS = visual analog scale; HAQ = Health Assessment Questionnaire; CRP = C-reactive protein; IL-6 = interleukin-6; bDMARDs = biologic disease-modifying antirheumatic drugs; SHS = Sharp/van der Heijde score.

IgG1, anti-PAD4 IgG2, or anti-PAD4 IgG3 were more likely to be positive for antibodies targeting other PAD isoenzymes (Figure 2A and Supplementary Tables 3 and 4, <http://onlinelibrary.wiley.com/doi/10.1002/art.42262>). Among these, IgA-, IgG1-, or IgG2-positive patients were more likely positive for anti-PAD2 antibodies, and those with anti-PAD4 IgA, anti-PAD4 IgG1, anti-PAD4 IgG2, or anti-PAD4 IgG3 had a higher frequency of anti-PAD3/4.

The associations of anti-PAD4 IgE, anti-PAD4 IgG1, and anti-PAD4 IgG3 with distinct clinical features of RA were unique among anti-PAD4 antibody types. Anti-PAD4 IgE positivity was associated with a higher DAS28 score (median 4.0 [interquartile range (IQR) 3.2–4.6] versus median 3.5 [IQR 2.8–4.3],  $P = 0.025$ ), higher CRP level (median 4.8 [IQR 1.7–13.0] versus median 3.0 [IQR 1.0–5.5],  $P = 0.025$ ), and extraarticular manifestations of RA, such as

radiographic evidence of ground-glass opacification in the lung (24% [10 of 42] versus 9% [12 of 134],  $P = 0.014$ ) and rheumatoid nodules (31% [14 of 45] versus 16% [21 of 131],  $P = 0.025$ ) (Figure 2 and Supplementary Table 4, <http://onlinelibrary.wiley.com/doi/10.1002/art.42262>). Anti-PAD4 IgG1 was associated with higher mean average CRP and IL-6 levels throughout the study (median 5.3 [IQR 2.0–13.0] versus median 2.9 [IQR 1.1–5.3],  $P = 0.006$  and median 6.7 [IQR 3.1–21.6] versus median 4.1 [IQR 2.1–8.1],  $P = 0.021$ , respectively), as well as more frequent use of glucocorticoids (52% [29 of 56] versus 34% [47 of 140],  $P = 0.018$ ) (Figures 2A and C).

Anti-PAD4 IgG1-positive patients had more erosive disease, had higher erosion scores (median 5 [IQR 1–26] versus median 2 [IQR 0–8],  $P = 0.010$ ), and were more prone to

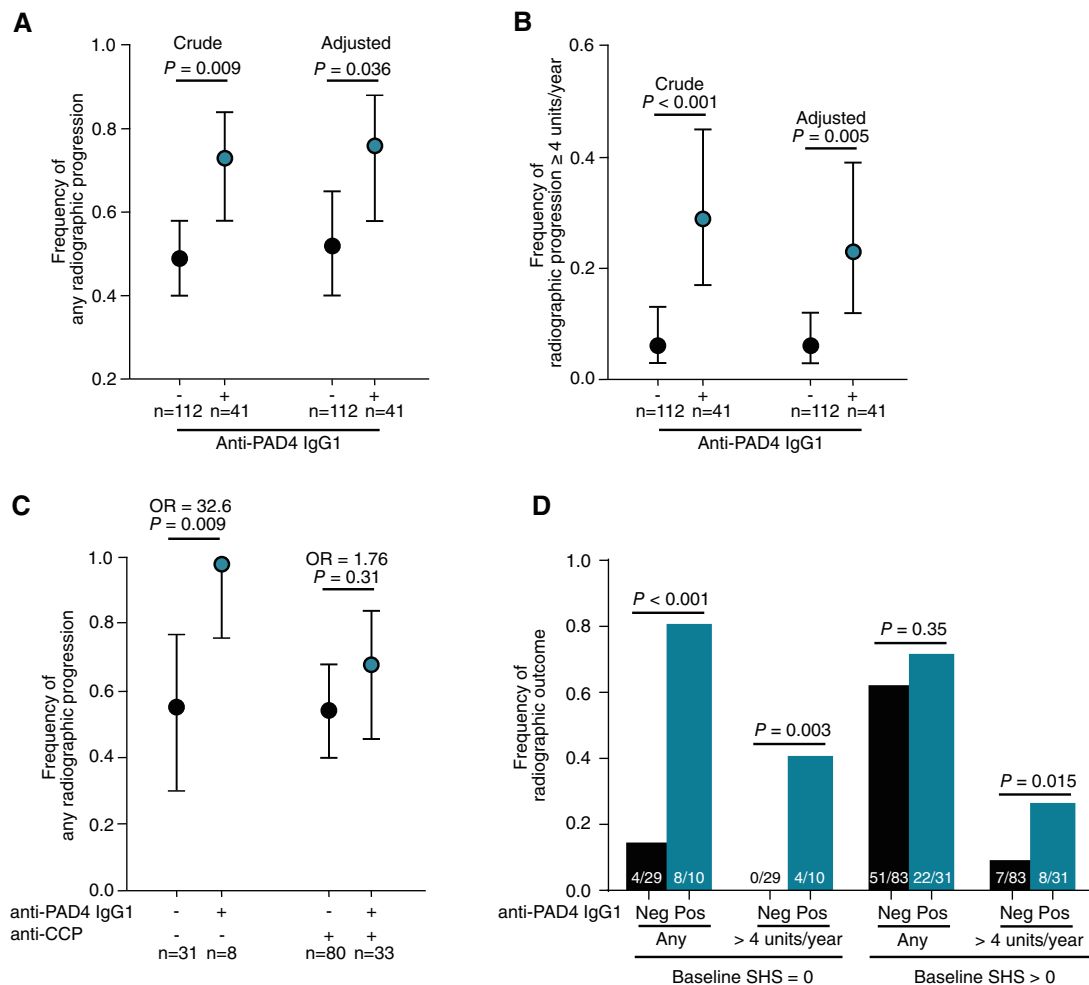


**Figure 3.** Radiographic progression according to anti-PAD4 IgG1 status. **A** and **B**, Frequency of any increase in SHS score, in crude models and models adjusted for sex, anti-PAD2 positivity, mean study average IL-6 level, baseline pain score, and baseline SHS score of  $>0$  (**A**) and frequency of radiographic progression of SHS score of  $\geq 4$  units/year, in crude models and models adjusted for mean study average IL-6 level (**B**). **C**, Frequency of any radiographic progression according to anti-PAD4 IgG1 and anti-CCP and/or RF status. ORs indicate the odds of any radiographic progression in the anti-PAD4 IgG1-positive group relative to the anti-PAD4 IgG1-negative group. Adjusted for sex, anti-PAD2, mean study average IL-6 level, baseline pain score, and baseline SHS score of  $>0$ . In **A–C**, black- and blue-shaded symbols with bars indicate the mean frequency with 95% confidence interval. **D**, Frequency of any radiographic progression according to anti-PAD4 IgG1 status and baseline SHS score. Disease duration, anti-PAD3/4 antibody level, HLA-DRB1, DAS28, swollen joint count, HAQ score, and rheumatoid nodules were not significant in multivariate analyses. Mean CRP levels were not co-modeled with mean study average IL-6 levels because they are collinear. See Figure 2 for definitions.

radiographic progression, as 73% of patients had an increase in SHS score over the course of the study, compared to 49% of anti-PAD4 IgG1-negative patients ( $P = 0.008$ ). Importantly, anti-PAD4 IgG1-positive patients also had a faster rate of radiographic progression than those who were anti-PAD4 IgG1-negative, with an increase in the SHS score per year (median increase 1.1 [IQR 0–4.2] versus median increase 0 [IQR 0–1.4], respectively,  $P = 0.003$ ) (Figure 2A and Supplementary Table 3, <http://onlinelibrary.wiley.com/doi/10.1002/art.42262>). Like anti-PAD4 IgG1, anti-PAD4 IgG3 was also associated with an increased burden of joint damage. Anti-PAD4 IgG3-positive patients had higher SHS scores (median 13 [IQR 2–85] versus median 7 [IQR 0–27],  $P = 0.046$ ), higher erosion scores (median 6 [IQR 0–31] versus median 2 [IQR 0–8],  $P = 0.015$ ), and higher joint space narrowing (JSN) scores (median 10 [IQR 0–54] versus median 4 [IQR 0–19],  $P = 0.045$ ) (Figure 2A and Supplementary Table 3) compared to anti-PAD4 IgG3-negative subjects. Neither anti-PAD4 IgG2, anti-PAD4 IgG4, anti-PAD4 IgA, nor anti-PAD4 IgM antibodies were associated with clinically relevant outcomes (Figure 2A and Supplementary Tables 3 and 4, <http://onlinelibrary.wiley.com/doi/10.1002/art.42262>).

**Role of anti-PAD4 IgG1 antibodies in radiographic progression in RA.** To analyze the predictive value of anti-PAD4 IgG subclass antibodies and possible covariates, we classified ESCAPE RA patients into 2 groups: subjects with any radiographic progression ( $n = 85$ ) or subjects with no radiographic progression ( $n = 68$ ). Among the anti-PAD4 IgG subclass of antibodies, only IgG1 antibodies were significantly associated with any radiographic progression (Table 1). Other variables associated with radiographic progression were disease duration, anti-PAD3/4, HLA-DRB1 SE alleles, swollen joint count, HAQ, CRP levels, IL-6 levels, rheumatoid nodules, pain scores, adiponectin levels, and baseline SHS scores (Table 1).

In the univariate analysis, anti-PAD4 IgG1-positive subjects were more likely to have any increase in SHS scores and an increase in SHS score of  $\geq 4$  units/year in comparison to anti-PAD4 IgG1-negative individuals (73% [ $n = 30$  of 41] versus 49% [ $n = 55$  of 112], respectively,  $P = 0.008$ ; and 29% [ $n = 12$  of

41] versus 6% [ $n = 7$  of 112], respectively,  $P < 0.001$ ) (Figures 3A and B and Supplementary Table 3, <http://onlinelibrary.wiley.com/doi/10.1002/art.42262>). After adjustment for baseline SHS scores, pain scores, IL-6 levels, and sex, subjects positive for anti-PAD4 IgG1 were 2.83 times more likely to have radiographic progression ( $P = 0.009$ ) and were 6.21 times more likely to have an increase in SHS score of  $\geq 4$  units/year (Table 2). Importantly, anti-PAD4 IgG1 alone was predictive of radiographic progression (odds ratio [OR] 2.93;  $P = 0.036$ ), and an increase in SHS score of  $\geq 4$  units/year (OR 4.88;  $P = 0.005$ ) (Table 2). Among RA patients who were negative for anti-CCP and/or RF, the odds of radiographic progression among anti-PAD4 IgG1-positive individuals was  $>32$ -fold higher ( $P = 0.009$ ) than those negative for anti-PAD4 IgG1 (Figure 3C). In contrast, anti-PAD4 IgG1 was not predictive of radiographic progression among individuals positive for RF and/or anti-CCP (OR = 1.76;  $P = 0.31$ ) (Figure 3C).

Anti-PAD4 IgG1 was also associated with incident radiographic progression, with 80% of anti-PAD4 IgG1-positive patients with baseline SHS score of 0 having radiographic progression during follow-up visits compared to only 13% of anti-PAD4 IgG1-negative individuals ( $P < 0.001$ ) (Figure 3D). Anti-PAD4 IgG1-positive patients with a baseline SHS score of 0 were also more likely to have an increase in SHS score of  $\geq 4$  compared to anti-PAD4 IgG1-negative patients (40% versus 0%,  $P = 0.003$ ) (Figure 3D). In RA patients with a baseline SHS score of  $>0$ , anti-PAD4 IgG1 was associated with an increase in SHS score of  $\geq 4$  units/year (25.8% versus 8.4%,  $P = 0.015$ ), but not with radiographic progression (Figure 3D).

To confirm the association between anti-PAD4 IgG1 and radiographic progression in a demographically distinct cohort, we tested additional serum samples from African American subjects enrolled in the CLEAR-I ( $n = 41$ ) and CLEAR-II cohorts ( $n = 94$ ) (Supplementary Table 5, <http://onlinelibrary.wiley.com/doi/10.1002/art.42262>). Of these, 28.9% of subjects (39 of 135) were positive for anti-PAD4 IgG1. Similar to the ESCAPE RA cohort, anti-PAD4 IgG1-positive subjects in the CLEAR cohorts had longer disease duration compared to anti-PAD4 IgG1-negative individuals (median 11.25 [IQR 1.9–24.3] years versus

**Table 2.** Multivariable predictors of any radiographic progression and radiographic progression of  $\geq 4$  SHS units/year\*

	Any radiographic progression				Radiographic progression of $\geq 4$ SHS units/year					
	Model 1	<i>P</i>	Model 2	<i>P</i>	Model 1	<i>P</i>	Model 2	<i>P</i>	Model 3	<i>P</i>
Anti-PAD4 IgG1	2.83	0.009	2.93	0.036	6.21	<0.001	5.39	0.006	4.88	0.005
Male sex	–	–	0.40	0.034	–	–	0.48	0.30	–	–
Anti-PAD2	–	–	0.26	0.023	–	–	0.34	0.19	–	–
Mean study average IL-6 level	–	–	1.06	0.010	–	–	1.04	0.002	1.03	0.004
Baseline pain score	–	–	1.03	0.006	–	–	1.01	0.52	–	–
Baseline SHS score $>0$	–	–	4.97	0.001	–	–	2.10	0.37	–	–
AUC (95% CI)	0.596 (0.528–0.663)	NA	0.817 (0.749–0.887)	NA	0.708 (0.591–0.824)	NA	0.868 (0.795–0.929)	NA	0.851 (0.777–0.915)	NA

\* Except where indicated otherwise, values are the odds ratio. SHS = Sharp/van der Heijde score; anti-PAD4 = anti-peptidylarginine deiminase 4; IL-6 = interleukin-6; AUC = area under the receiver operating characteristics curve; 95% CI = 95% confidence interval; NA = not applicable.

3.6 [1.2–16.7] years,  $P = 0.010$ ). Importantly, anti-PAD4 IgG1 was associated with significantly increased JSN score (median 54 [IQR 0–76] versus median 2 [IQR 0–47],  $P = 0.028$ ). In order to address whether anti-PAD4 IgG1 was predictive of more severe radiographic damage, we classified RA subjects according to the tertile of SHS scores, erosion scores, and JSN scores. As observed in ESCAPE RA trial, anti-PAD4 IgG1-positive subjects in the CLEAR cohorts were 2.4 times to 2.7 times more likely to have radiographic damage scores in the highest tertile for SHS scores, erosion scores, and JSN scores (Supplementary Table 6, <http://onlinelibrary.wiley.com/doi/10.1002/art.42262>).

## DISCUSSION

In this study, we explored the clinical associations of different isotypes and IgG subclasses of anti-PAD4 antibodies in RA patients. We found that the humoral response against PAD4 in RA is characterized by the usage of diverse IgH constant regions linked to different immune effector functions. Despite significant overlap among different anti-PAD4 antibodies, we observed that anti-PAD4 IgG1, anti-PAD4 IgG3, and anti-PAD4 IgE were associated with specific disease subsets. Interestingly, IgG subclasses known to have higher capacity to activate complement (i.e., IgG1 and IgG3) (13), may be used to identify anti-PAD4-positive patients with the worst joint damage burden. Importantly, anti-PAD4 IgG1 was strongly associated with rapid disease progression and higher serum IL-6 levels. Moreover, IgE anti-PAD4 antibodies were associated with a subset of RA patients characterized by higher frequencies of RF and anti-CCP, higher DAS28 score, higher CRP level, and extraarticular manifestations (ground-glass opacification and rheumatoid nodules). Taken together, these findings support the notion that different isotypes and IgG subclasses from a single autoantibody specificity are useful for identifying distinct disease subsets in RA.

Importantly, we found that anti-PAD4 IgG1 was more predictive of radiographic progression than the most commonly utilized serologic clinical indicators (i.e., RF and anti-CCP antibodies) independent of treatment or RA duration. Furthermore, anti-PAD4 IgG1 was associated with inflammatory response in RA, since this subset of patients has higher IL-6 levels and CRP levels compared to anti-PAD4 IgG1-negative individuals. Interestingly, this inflammatory response appears to be clinically silent, as there was no association with other components of the DAS28 (i.e., tender and swollen joint counts). It is intriguing that anti-PAD4 IgG1 was most significantly associated with erosive damage and the progression of erosive disease among RA patients who were seronegative for RF and/or anti-CCP. In addition, since anti-PAD4 IgG1 was strongly associated with incident radiographic progression among those with no erosive disease at baseline, it may be clinically useful for identifying a susceptible RA subgroup that would ordinarily not be detected as being at risk for radiographic progression using current predictors

(i.e., seropositivity and erosions at baseline) (29,30). We also note that this association appears to be consistent across racial/ethnic groups, as the ESCAPE RA cohort is predominantly White, while the confirmation cohort (subjects from the CLEAR registry) is African American.

Although anti-PAD4 IgE was not associated with articular damage, it was linked to an RA subset characterized by a higher frequency of extraarticular manifestations, which in turn are associated with worse disease outcomes. Rheumatoid nodules along with ILD are associated with a small but significantly higher risk for cardiovascular events and death in RA patients (31–33). Furthermore, the association with higher disease activity and RF and anti-CCP antibodies suggests that anti-PAD4 IgE indeed identifies an RA subset with a higher inflammatory milieu prone to develop extraarticular manifestations.

Although we identified anti-PAD4 antibody types that were associated with different clinical features in RA, our study has some limitations. We only evaluated levels of IL-6 in serum samples from RA patients, but analysis of other cytokines may help to dissect additional molecular mechanisms associated with anti-PAD4 isotypes. In addition, a larger longitudinal cohort study is necessary to confirm the association of anti-PAD4 IgG1 with radiographic progression, especially in seronegative RA, since this group was small in our cohort. Also, we do not have follow-up lung computed tomography data to evaluate the prognosis and evolution of anti-PAD4 IgE-positive RA with ground-glass opacification or ILD.

Mechanistically, the diverse array of class-switch recombination events leading to the development of anti-PAD4 antibodies with different constant regions suggests that these antibodies are generated in distinct immune microenvironments not limited to joints, but likely including mucosal-associated lymphoid tissue, such as that in the airways and the gut. This notion is consistent with the recent finding that anti-PAD4 antibodies are present in the sputum of RA patients (34). Moreover, the finding that some types of anti-PAD4, in particular IgG1 and IgE, are associated with radiographic progression and lung damage, respectively, suggest that these antibodies have mechanistic properties that promote target-tissue damage in RA. In summary, these data suggest that anti-PAD4 IgG1, anti-PAD4 IgG3, and anti-PAD4 IgE are promising mechanistic biomarkers associated with unique disease outcomes in RA patients.

## ACKNOWLEDGMENT

We would like to thank Dr. Joan Bathon (Columbia University) for providing access to serum samples from ESCAPE RA cohort participants.

## AUTHOR CONTRIBUTIONS

All authors were involved in drafting the article or revising it critically for important intellectual content, and all authors approved the final version to be published. Dr. Darrah had full access to all of the data in the

study and takes responsibility for the integrity of the data and the accuracy of the data analysis.

**Study conception and design.** Shi, Andrade, Darrah.

**Acquisition of data.** Gómez-Bañuelos, Shi, Wang, Danila, Bridges.

**Analysis and interpretation of data.** Gómez-Bañuelos, Giles, Sims, Andrade, Darrah.





## ADDITIONAL DISCLOSURES

Author Sims is an employee of AstraZeneca.

## REFERENCES

- Arend WP, Firestein GS. Pre-rheumatoid arthritis: predisposition and transition to clinical synovitis [review]. *Nat Rev Rheumatol* 2012;8:573–86.
- Suzuki T, Ikari K, Yano K, et al. PADI4 and HLA-DRB1 are genetic risks for radiographic progression in RA patients, independent of ACPA status: results from the IORRA cohort study. *PLoS One* 2013; 8:e61045.
- Malmstrom V, Catrina AI, Klareskog L. The immunopathogenesis of seropositive rheumatoid arthritis: from triggering to targeting [review]. *Nat Rev Immunol* 2017;17:60–75.
- Curran AM, Naik P, Giles JT, et al. PAD enzymes in rheumatoid arthritis: pathogenic effectors and autoimmune targets [review]. *Nat Rev Rheumatol* 2020;16:301–15.
- Navarro-Millan I, Darrah E, Westfall AO, et al. Association of anti-peptidyl arginine deiminase antibodies with radiographic severity of rheumatoid arthritis in African Americans. *Arthritis Res Ther* 2016;18:241.
- Darrah E, Giles JT, Ols ML, et al. Erosive rheumatoid arthritis is associated with antibodies that activate PAD4 by increasing calcium sensitivity. *Sci Transl Med* 2013;5:186ra65.
- Zhao J, Zhao Y, He J, et al. Prevalence and significance of anti-peptidylarginine deiminase 4 antibodies in rheumatoid arthritis. *J Rheumatol* 2008;35:969–74.
- Guderud K, Maehlen MT, Nordang GB, et al. Lack of association among peptidyl arginine deiminase type 4 autoantibodies, PADI4 polymorphisms, and clinical characteristics in rheumatoid arthritis. *J Rheumatol* 2018;45:1211–9.
- Halvorsen EH, Haavardsholm EA, Pollmann S, et al. Serum IgG antibodies to peptidylarginine deiminase 4 predict radiographic progression in patients with rheumatoid arthritis treated with tumour necrosis factor- $\alpha$  blocking agents. *Ann Rheum Dis* 2009;68:249–52.
- Seaman A, Darrah E, Infantino M, et al. Anti-peptidyl-arginine deiminase 3 (PAD3) antibodies as a promising marker to measure joint damage in patients with rheumatoid arthritis [review]. *Autoimmun Rev* 2016;15:776–80.
- Schroeder HW Jr, Cavacini L. Structure and function of immunoglobulins. *J Allergy Clin Immunol* 2010;125 Suppl 2:S41–52.
- Hjelholt A, Christiansen G, Sorensen US, et al. IgG subclass profiles in normal human sera of antibodies specific to five kinds of microbial antigens. *Pathog Dis* 2013;67:206–13.
- Vidarsson G, Dekkers G, Rispens T. IgG subclasses and allotypes: from structure to effector functions. *Front Immunol* 2014;5:520.
- Henault J, Riggs JM, Karnell JL, et al. Self-reactive IgE exacerbates interferon responses associated with autoimmunity. *Nat Immunol* 2016;17:196–203.
- Dema B, Charles N. Autoantibodies in SLE: specificities, isotypes and receptors [review]. *Antibodies (Basel)* 2016;5:2.
- Wang W, Li J. Predominance of IgG1 and IgG3 subclasses of autoantibodies to peptidylarginine deiminase 4 in rheumatoid arthritis. *Clin Rheumatol* 2011;30:563–7.
- Giles JT, Ling SM, Ferrucci L, et al. Abnormal body composition phenotypes in older rheumatoid arthritis patients: association with disease characteristics and pharmacotherapies. *Arthritis Rheum* 2008; 59:807–15.
- Darrah E, Giles JT, Davis RL, et al. Autoantibodies to peptidylarginine deiminase 2 are associated with less severe disease in rheumatoid arthritis. *Front Immunol* 2018;9:2696.
- Arnett FC, Edworthy SM, Bloch DA, et al. The American Rheumatism Association 1987 revised criteria for the classification of rheumatoid arthritis. *Arthritis Rheum* 1988;31:315–24.
- Van der Heijde D. How to read radiographs according to the Sharp/van der Heijde method. *J Rheumatol* 2000;27:261–3.
- Prevoo ML, van 't Hof MA, Kuper HH, et al. Modified disease activity scores that include twenty-eight-joint counts: development and validation in a prospective longitudinal study of patients with rheumatoid arthritis. *Arthritis Rheum* 1995;38:44–8.
- Wolfe F. A reappraisal of HAQ disability in rheumatoid arthritis. *Arthritis Rheum* 2000;43:2751–61.
- Giles JT, Darrah E, Danoff S, et al. Association of cross-reactive antibodies targeting peptidyl-arginine deiminase 3 and 4 with rheumatoid arthritis-associated interstitial lung disease. *PLoS One* 2014;9:e98794.
- Bridges SL Jr, Causey ZL, Burgos PI, et al. Radiographic severity of rheumatoid arthritis in African Americans: results from a multicenter observational study. *Arthritis Care Res (Hoboken)* 2010;62:624–31.
- Laufer VA, Tiwari HK, Reynolds RJ, et al. Genetic influences on susceptibility to rheumatoid arthritis in African-Americans. *Hum Mol Genet* 2019;28:858–74.
- Gu Z, Eils R, Schlesner M. Complex heatmaps reveal patterns and correlations in multidimensional genomic data. *Bioinformatics* 2016; 32:2847–9.
- Gu Z, Gu L, Eils R, et al. Circos Implements and enhances circular visualization in R. *Bioinformatics* 2014;30:2811–2.
- Chung NC, Miaojedow B, Startek M, et al. Jaccard/Tanimoto similarity test and estimation methods for biological presence-absence data. *BMC Bioinformatics* 2019;20 Suppl 15:644.
- Shiozawa K, Kawasaki Y, Yamane T, et al. Anticitrullinated protein antibody, but not its titer, is a predictor of radiographic progression and disease activity in rheumatoid arthritis. *J Rheumatol* 2012;39: 694–700.
- Guillemin F, Gerard N, van Leeuwen M, et al. Prognostic factors for joint destruction in rheumatoid arthritis: a prospective longitudinal study of 318 patients. *J Rheumatol* 2003;30:2585–9.
- Kaushik P, Solomon DH, Greenberg JD, et al. Subcutaneous nodules are associated with cardiovascular events in patients with rheumatoid arthritis: results from a large US registry. *Clin Rheumatol* 2015;34: 1697–704.
- Turesson C, O'Fallon WM, Crowson CS, et al. Occurrence of extra-articular disease manifestations is associated with excess mortality in a community based cohort of patients with rheumatoid arthritis. *J Rheumatol* 2002;29:62–7.
- Bongartz T, Nannini C, Medina-Velasquez YF, et al. Incidence and mortality of interstitial lung disease in rheumatoid arthritis: a population-based study. *Arthritis Rheum* 2010;62:1583–91.
- Demoruelle MK, Wang H, Davis RL, et al. Anti-peptidylarginine deiminase-4 antibodies at mucosal sites can activate peptidylarginine deiminase-4 enzyme activity in rheumatoid arthritis. *Arthritis Res Ther* 2021;23:163.

# A Risk Score to Detect Subclinical Rheumatoid Arthritis–Associated Interstitial Lung Disease

Pierre-Antoine Juge,<sup>1</sup>  Benjamin Granger,<sup>2</sup> Marie-Pierre Debray,<sup>3</sup> Esther Ebstein,<sup>4</sup> Fabienne Louis-Sidney,<sup>4</sup> Joanna Kedra,<sup>5</sup>  Tracy J. Doyle,<sup>6</sup> Raphaël Borie,<sup>7</sup> Arnaud Constantin,<sup>8</sup> Bernard Combe,<sup>9</sup> René-Marc Flipo,<sup>10</sup> Xavier Mariette,<sup>11</sup> Olivier Vittecoq,<sup>12</sup> Alain Saraux,<sup>13</sup>  Guillermo Carvajal-Alegria,<sup>13</sup> Jean Sibilia,<sup>14</sup> Francis Berenbaum,<sup>15</sup> Caroline Kannengiesser,<sup>16</sup> Catherine Boileau,<sup>17</sup> Jeffrey A. Sparks,<sup>18</sup>  Bruno Crestani,<sup>7</sup> Bruno Fautrel,<sup>5</sup> and Philippe Dieudé<sup>1</sup>

**Objective.** Patients at high risk of rheumatoid arthritis–associated interstitial lung disease (RA-ILD) would benefit from being identified before the onset of respiratory symptoms; this can be done by screening patients with the use of chest high-resolution computed tomography (HRCT). Our objective was to develop and validate a risk score for patients who have subclinical RA-ILD.

**Methods.** Our study included a discovery population and a replication population from 2 prospective RA cohorts (ESPOIR and TRANSLATE2, respectively) without pulmonary symptoms who had received chest HRCT scans. All patients were genotyped for *MUC5B* rs35705950. After multiple logistic regression, a risk score based on independent risk factors for subclinical RA-ILD was developed in the discovery population and tested for validation in the replication population.

**Results.** The discovery population included 163 patients with RA, and the replication population included 89 patients with RA. The prevalence of subclinical RA-ILD was 19.0% and 16.9%, respectively. In the discovery population, independent risk factors for subclinical RA-ILD were presence of the *MUC5B* rs35705950 T allele (odds ratio [OR] 3.74 [95% confidence interval (95% CI) 1.37, 10.39]), male sex (OR 3.93 [95% CI 1.40, 11.39]), older age at RA onset (for each year, OR 1.10 [95% CI 1.04, 1.16]), and increased mean Disease Activity Score in 28 joints using the erythrocyte sedimentation rate (for each unit, OR 2.03 [95% CI 1.24, 3.42]). We developed and validated a derived risk score with receiver operating characteristic areas under the curve of 0.82 (95% CI 0.70–0.94) for the discovery population and 0.78 (95% CI 0.65–0.92) for the replication population. Excluding *MUC5B* rs35705950 from the model provided a lower goodness of fit (likelihood ratio test,  $P = 0.01$ ).

**Conclusion.** We developed and validated a risk score that could help identify patients at high risk of subclinical RA-ILD. Our findings support an important contribution of *MUC5B* rs35705950 to subclinical RA-ILD risk.

## INTRODUCTION

Interstitial lung disease (ILD) is an extraarticular manifestation of rheumatoid arthritis (RA). Subclinical RA-associated ILD

(RA-ILD) is detected in 20–60% of RA patients when the method of systematic high-resolution computed tomography (HRCT) of the chest is used, and clinically significant RA-ILD presents in almost 10% of RA patients (1–6). The course of subclinical

The content is solely the responsibility of the authors and does not necessarily represent the official views of Harvard University, its affiliated academic health care centers, or the National Institutes of Health.

ESPOIR cohort (NCT03666091) was supported by the French Society of Rheumatology and INSERM, Merck Sharp and Dohme, Pfizer, AbbVie, Lilly, Fresenius, and Galapagos. TRANSLATE2 cohort (NCT04227535) was supported by the French Society of Rheumatology and Bristol Myers Squibb (IM101-647). Dr. Sparks' work was supported by the National Institute of Arthritis and Musculoskeletal and Skin Diseases, NIH (grants R01-AR-077607, P30-AR-070253, and P30-AR-072577), and the R. Bruce and Joan M. Mickey Research Scholar Fund.

<sup>1</sup>Pierre-Antoine Juge, MD, PhD, Philippe Dieudé, MD, PhD: Université de Paris, INSERM UMR 1152, F-75018, and Service de Rhumatologie, Hôpital Bichat-Claude Bernard, AP-HP, F-75018, Paris, France; <sup>2</sup>Benjamin Granger, MD: Sorbonne Université, Institut Pierre Louis d'Épidémiologie et de Santé Publique Département de Biostatistiques, INSERM UMR 1136, F-75013, and

Santé Publique et Information Médicale, Groupe Hospitalier Pitié-Salpêtrière, AP-HP, F-75013, Paris, France; <sup>3</sup>Marie-Pierre Debray, MD: Université de Paris, INSERM UMR 1152, F-75018, and Service de Radiologie, Hôpital Bichat-Claude Bernard, AP-HP, F-75018, Paris, France; <sup>4</sup>Esther Ebstein, MD, Fabienne Louis-Sidney, MD: Service de Rhumatologie, Hôpital Bichat-Claude Bernard, AP-HP, F-75018, Paris, France; <sup>5</sup>Joanna Kedra, MD, Bruno Fautrel, MD, PhD: Sorbonne Université, Institut Pierre Louis d'Épidémiologie et de Santé Publique Département de Biostatistiques, INSERM UMR 1136, F-75013, and Service de Rhumatologie, Groupe Hospitalier Pitié-Salpêtrière, AP-HP, F-75013, Paris, France; <sup>6</sup>Tracy J. Doyle, MD: Division of Pulmonary and Critical Care Medicine, Department of Medicine, Brigham and Women's Hospital, Boston, Massachusetts; <sup>7</sup>Raphaël Borie, MD, PhD, Bruno Crestani, MD, PhD: Université de Paris, INSERM UMR 1152, F-75018, Service de Pneumologie A, Centre de compétences maladies pulmonaires rares, Hôpital Bichat-Claude Bernard, AP-HP, F-75018, Paris, France; <sup>8</sup>Arnaud Constantin, MD, PhD: Université

RA-ILD is heterogeneous, with some patients having disease progression to pulmonary symptoms and decreased respiratory function (7,8). Once clinically significant, RA-ILD is associated with high levels of morbidity and mortality, with a median survival ranging from 3 years to 8 years (1,9,10).

For patients in whom a diagnosis of RA-ILD is clinically suspected, HRCT of the chest is a useful screening tool to confirm the diagnosis of ILD and to assess ILD both qualitatively (by reviewing the pattern of interstitial pneumonia) and quantitatively (by determining the extent of ILD) (11–14). However, for patients who lack respiratory symptoms and have a particularly high risk of disease, screening for ILD is challenging (11,15). Therefore, improving ways to determine risk of progression in patients with subclinical RA-ILD could be of great value, especially because recently developed therapeutic interventions could help reduce the decline of lung function in patients with progressive disease (16).

To date, RA-ILD-associated risk factors have been investigated in patients with clinically significant disease in retrospective case-control or register studies (17–19). Clinical RA-ILD-associated risk factors consistently observed across many studies include male sex, older age, tobacco smoking, high RA activity, extraarticular features, and longer RA disease duration (1,2,20–23). Positivity for RA autoantibodies (rheumatoid factor [RF] and/or anti-citrullinated protein antibodies [ACPAs]) remains controversial because no consistent association was observed in recent large studies (23–25). The *MUC5B* rs35705950 genetic variant has been identified as a major RA-ILD risk factor, associated with 3-fold higher odds of presence of RA-ILD compared with RA without ILD (23). In a recent study comparing patients with and those without reported clinical RA-ILD from the FinnGen study—a collection of data from prospective epidemiologic and disease-based cohorts and hospital biobank samples in Finland—the presence of the *MUC5B* rs35705950 variant was associated with an increased lifetime risk of clinical RA-ILD, highlighting the importance of genetic predisposition in the occurrence of RA-ILD (19). However, the FinnGen study design included patients with symptomatic RA-ILD (i.e., ILD identified in health care registries), which did not allow for the identification of specific risk factors for subclinical ILD.

The identification of high-risk RA patients who may benefit from HRCT screening at an early and subclinical stage of the disease is an important unmet need in RA-ILD (26). Consequently, we aimed to develop and validate a risk score for subclinical ILD in patients with RA.

## PATIENTS AND METHODS

**Study populations and study design.** This cross-sectional study included a discovery and a replication population of patients with RA from 2 prospective cohorts.

All patients included in the study met either the ACR 1987 classification criteria for RA (27) or the 2010 ACR/EULAR classification criteria for RA (28). To meet the World Health Organization guidelines for screening of a high-risk patient from an asymptomatic population (29), patients with RA were considered to be asymptomatic at the time of chest HRCT scan screening according to a definition that reflected a real-life situation in rheumatology. According to this definition, patients should have no history of ILD and no pulmonary signs or respiratory symptoms (i.e., dyspnea, cough, clubbing, and crackles at lung auscultation), as demonstrated from systematic questioning and physical examination by a senior rheumatologist. Patients with RA-ILD or with symptoms suggestive of ILD were not included in the study. The 6-minute walk test was not performed.

The discovery population consisted of patients from the prospective French ESPOIR cohort ([ClinicalTrials.gov](https://clinicaltrials.gov/ct2/show/study/NCT03666091) identifier: NCT03666091). The ESPOIR cohort included patients with early RA who were included as participants from January 2003 to April 2005 (30); patients included in the ESPOIR cohort were evaluated every 6 months in the first 2 years and then yearly. For our discovery population, we included patients who had agreed to undergo a chest HRCT for research purposes between year 9 and year 12 of their follow-up.

The replication population consisted of patients from the independent prospective TRANSLATE2 cohort ([ClinicalTrials.gov](https://clinicaltrials.gov/ct2/show/study/NCT04227535) identifier NCT04227535). For our replication population, we included patients who were being investigated for RA-ILD in the TRANSLATE2 study who had received consecutive and

Toulouse III–Paul Sabatier, INSERM UMR 1043, F-31024, and Service de Rhumatologie, Hôpital Purpan, F-31024, Toulouse, France; <sup>9</sup>Bernard Combe, MD, PhD: Université de Montpellier and Département de Rhumatologie, Hôpital Lapeyronie, F-34000, Montpellier, France; <sup>10</sup>René-Marc Flipo, MD, PhD: Université de Lille, and Service de Rhumatologie, Hôpital Salengro, F-59000, Lille, France; <sup>11</sup>Xavier Mariette, MD, PhD: Université Paris-Saclay, INSERM UMR 1184, CEA, F-94270, and Service de Rhumatologie, Hôpital Bicêtre, AP-HP, F-94270, Le Kremlin Bicêtre, France; <sup>12</sup>Olivier Vittecoq, MD, PhD: Rouen University Hospital, Service de Rhumatologie, CIC-CRB 1404, F-76000, and Normandy University, UNIROUEN, INSERM, U1234, FR-76000, Rouen, France; <sup>13</sup>Alain Saraux, MD, PhD, Guillermo Carvajal-Alegriax, MD, PhD: Université de Bretagne Occidentale, INSERM UMR 1227, F-29200, and Service de Rhumatologie, Hôpital de la Cavale Blanche, F-2900, Brest, France; <sup>14</sup>Jean Sibilia, MD, PhD: Université de Strasbourg, INSERM UMR S1109, F-67000, and Service de Rhumatologie, RESO: Centre de Référence des Maladies Autoimmunes Systémiques Rares Est Sud-Ouest, Hôpital De Haute-pierre, F-67000, Strasbourg, France; <sup>15</sup>Francis Berenbaum, MD, PhD: Sorbonne

Université, CRSA, INSERM UMR 938, F-75012, Service de Rhumatologie, Hôpital Saint-Antoine, AP-HP, F-75012, Paris, France; <sup>16</sup>Caroline Kannengiesser, PharmD, PhD: Université de Paris, INSERM UMR 1152, F-75018, Département de Génétique Moléculaire, Hôpital Bichat-Claude Bernard, AP-HP, FR-75018, Paris, France; <sup>17</sup>Catherine Boileaux, PharmD, PhD: Département de Génétique Moléculaire, Hôpital Bichat-Claude Bernard, AP-HP, FR-75018, Université de Paris, INSERM UMR 1148, Paris, F-75018, France; <sup>18</sup>Jeffrey A. Sparks, MD, MMSc: Division of Rheumatology, Inflammation, and Immunity, Brigham and Women's Hospital, and Harvard Medical School, Boston, Massachusetts.

Author disclosures are available at <https://onlinelibrary.wiley.com/action/downloadSupplement?doi=10.1002%2Fart.42162&file=art42162-sup-0001-Disclosureform.pdf>.

Address correspondence via email to Philippe Dieudé, MD, PhD, at [philippe.dieude@aphp.fr](mailto:philippe.dieude@aphp.fr).

Submitted for publication November 19, 2021; accepted in revised form May 10, 2022.

systematic chest HRCT from February 2020 to February 2021 at Bichat Hospital (Paris, France).

For patients in both the discovery and replication populations, chest HRCT scans were centrally read by an experienced radiologist and pulmonologist (MPD and RB), who remained blinded with regard to patient phenotype and genotype data. Results from the chest HRCT scans were classified as ILD, no ILD, or not interpretable, and ILD extension and pattern were evaluated according to previously reported criteria (31). Inconsistencies between the individual reviewers were resolved by consensus. Only patients with interpretable chest HRCT scans were included in the analyses.

The institutional review boards (ethics committee of Montpellier, France, no. 020307, Northern and Western French Ethic Committee III no. 2019-31) approved all protocols, and all patients provided written informed consent. This study was performed without direct patient and public involvement.

**Genotyping.** Included patients underwent genotyping for the *MUC5B* rs35705950 variant and subtyping to identify the presence of the shared epitope of HLA-DRB1, as previously described (32,33).

**Data collection.** In the discovery step, we prospectively collected potential predictors for subclinical RA-ILD (a list of all collected data is provided in the Supplementary Appendix, available on the *Arthritis & Rheumatology* website at <https://onlinelibrary.wiley.com/doi/10.1002/art.42162>). Baseline clinical and biologic data were collected at time of patient inclusion. All longitudinal variables were systematically collected at every follow-up visit (every 6 months during the first 2 years of RA and then yearly) (33). For variables that were found to be independently associated with RA-ILD in the discovery step, we systematically collected these retrospective variables at inclusion of the replication population from their medical records. Detailed information is provided in the Supplementary Appendix.

**Statistical analysis.** We used R program version 4.1.1 for all statistical analyses. We used GraphPad Prism 9.0 to create graphics in Figure 1 and in the supplementary figures. Further details on all methods are provided in the Supplementary Appendix.

*Identification of independent risk factors for subclinical RA-ILD.* For the discovery population (ESPOIR cohort), we tested the association of each collected variable with subclinical RA-ILD occurrence in bivariate and then multivariate analysis by logistic regression. Odds ratios (ORs) or effect sizes and 95% confidence intervals (95% CIs) were estimated. *P* values less than 0.05 were considered statistically significant. Because of the low number of missing data (<1%) (Supplementary Table 1, available on the *Arthritis & Rheumatology* website at <https://onlinelibrary.wiley.com/doi/10.1002/art.42162>), no imputation methods were used.

*Construction of a risk score for subclinical RA-ILD.* According to the categorized multivariate model in the discovery population (in which which continuous variables are transformed into categorical variables), we generated an aggregate-weighting score for each independent risk factor for subclinical RA-ILD (no missing data). For each patient, a risk score for subclinical RA-ILD was calculated by summing the weighted scores of each independent risk factor. We calculated performance of the risk score, which included calculating the area under the receiver operating characteristic (ROC) curve (AUC), sensitivity, specificity, and likelihood ratio for a proposed total cutoff value providing a sensitivity of  $\geq 70\%$ . The risk score was developed according to the transparent reporting of a multivariable prediction model for individual prognosis or diagnosis (TRIPOD) guidelines (Supplementary Table 2, available on the *Arthritis & Rheumatology* website at <https://onlinelibrary.wiley.com/doi/10.1002/art.42162>) (34).

*Validation in an independent cohort.* We tested the risk score for validation in the replication population. We calculated the performance of all corresponding risk scores, which included calculations of sensitivity, specificity, likelihood ratio, and ROC curve analysis with AUC calculation based on the proposed corresponding cutoff values for each total risk score.

## RESULTS

**Study populations.** The discovery population (ESPOIR cohort) included 163 patients (see flow chart in Supplementary Figure 1, available on the *Arthritis & Rheumatology* website at <https://onlinelibrary.wiley.com/doi/10.1002/art.42162>). Patients from the discovery population received chest HRCT between year 9 and year 12 of follow-up. Among the 163 patients, 35 (21.5%) were men, 150 (92.6%) were White, the median age at RA onset was 49.4 years (interquartile range [IQR] 41.2–55.1), 96 (58.9%) were positive for ACPAs, 128 (78.5%) were positive for RF, 77 (47.2%) were ever smokers, and the *MUC5B* rs35705950 T risk allele frequency was 11.3% (Table 1). Chest HRCT scan was performed after a median RA disease duration of 13.9 years (IQR 13–14.1). At the time of chest HRCT, the median Disease Activity Score in 28 joints using the erythrocyte sedimentation rate (DAS28-ESR) over the follow-up was 2.9 (IQR 2.4–3.7). Among the 163 patients, 138 (84.7%) had received methotrexate (MTX), 66 (40.5%) had received a biologic disease-modifying antirheumatic drug (bDMARD), and 32 (19.6%) had moderate to high tobacco smoking exposure (Table 1). Subclinical RA-ILD was detected in 31 (19.0%) of 163 patients. Missing data are provided in Supplementary Table 1. Characteristics of the patients who were not included in the analysis (i.e., refusal to participate or uninterpretable HRCT scan) are summarized in Supplementary Table 3 (available on the *Arthritis & Rheumatology* website at <https://onlinelibrary.wiley.com/doi/10.1002/art.42162>).



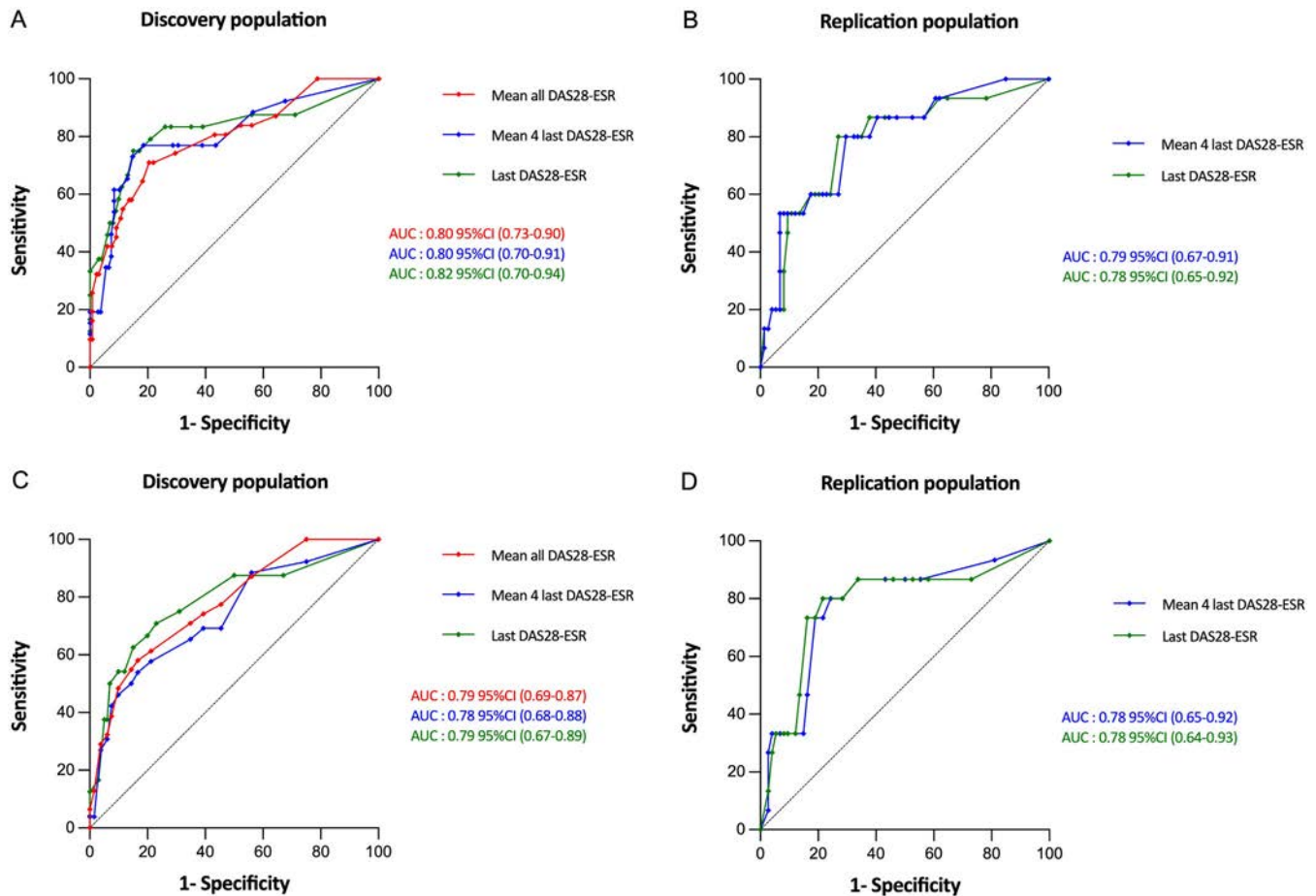


**Figure 1.** Performance of the proposed risk scores for detection of subclinical rheumatoid arthritis-associated interstitial lung disease in the discovery and replication populations. Results are shown as area under the receiver operating characteristic curves (AUCs) (with 95% confidence intervals [95% CIs]) in the full model (including *MUC5B* rs35705950) (A and B) and in the simplified model (without *MUC5B* rs35705950) (C and D). Curves labeled “mean all DAS28-ESR” represent models that used the mean of all Disease Activity Score in 28 joints using the erythrocyte sedimentation rate (DAS28-ESR) values over the follow-up until chest high-resolution computed tomography (HRCT) was performed to calculate the risk score. Curves labeled “mean 4 last DAS28-ESR” represent models that used the mean of the last 4 DAS28-ESR values available before chest HRCT to calculate the risk score. Curves labeled “mean last DAS28-ESR” represent models that used mean of the last DAS28-ESR value before chest HRCT to calculate the risk score.

The replication population (TRANSLATE2 cohort) included 89 patients, and their characteristics are summarized in Table 2. Subclinical RA-ILD was detected in 15 (16.9%) of 89 patients.

**Identification of independent risk factors for subclinical RA-ILD. Bivariate analysis.** Compared with patients with RA without ILD, those with subclinical RA-ILD more frequently carried the *MUC5B* rs35705950 T risk allele (minor allele frequency of 19% versus 9.5%,  $P = 0.02$ ), were more frequently men (38.7% versus 17.4%,  $P = 0.01$ ), were older at RA onset (median age 56.2 years [IQR 50.6–61.4] versus 47.6 years [IQR 38.5–53.7],  $P < 0.0001$ ), had higher DAS28-ESR (median 3.4 [IQR 2.7–4.1] versus 2.9 [IQR 2.3–3.5],  $P = 0.03$ ), and had higher scores for the Health Assessment Questionnaire (median 0.6 [IQR 0.3–1.1] versus 0.4 [IQR 0.2–0.6],  $P = 0.007$ ) over the follow-up (Table 1). Patients with subclinical RA-ILD had numerically higher

body mass index (BMI), longer tobacco smoking exposure (pack-years), and higher mean C-reactive protein level during the follow-up compared with results shown in RA patients without ILD; however, differences between RA patients with and those without ILD were not statistically significant (Table 1). We detected no differences in the ACPA or RF positivity rates or ACPA or RF titers according to RA-ILD status versus RA without ILD status, presence versus absence of the shared epitope for HLA-DRB1 status, or level of exposure to MTX or bDMARD (Table 1). The relatively small number of patients with RA-ILD did not allow subanalyses according to the HRCT patterns.

**Multivariate analysis.** Logistic regression analysis identified 4 variables independently associated with subclinical RA-ILD: the *MUC5B* rs35705950 T risk allele (OR 3.74 [95% CI 1.37, 10.39]) ( $P = 0.01$ ), male sex (OR 3.93 [95% CI 1.40, 11.39]) ( $P = 0.01$ ), older age at RA onset (for each year, OR 1.1 [95% CI 1.04, 1.16])

**Table 1.** Characteristics of patients with RA in the discovery sample (ESPOIR)\*

Characteristic	Patient group			OR or ES or HR (95% CI)	P†
	Overall RA (n = 163)	RA-ILD (n = 31)	RA without ILD (n = 132)		
Characteristic at RA onset					
Male sex	35 (21.5)	12 (38.7)	23 (17.4)	2.99 (1.28, 7.01)	0.01
White race/ethnicity	150 (92.6)	27 (87.1)	123 (93.9)	2.28 (0.64, 8.11)	0.25
Age, median (IQR) years	49.4 (41.2–55.1)	56.2 (50.6–61.4)	47.6 (38.5–53.7)	−0.84 (−1.24, −0.43)‡	<0.0001
BMI median (IQR) kg/m <sup>2</sup>	24.0 (21.5–27.4)	24.9 (23.0–28.9)	23.7 (21.4–27.0)	−0.23 (−0.62, −0.17)‡	0.11
Ever smoker	77 (47.2)	17 (54.8)	60 (45.5)	1.46 (0.66, 3.20)	0.42
Smoking exposure, median (IQR) pack-years	0 (0–15)	8 (0–20)	0 (0–13)	−0.37 (−0.77, 0.03)‡	0.11
DAS28-ESR, median (IQR)	5.2 (4.5–6.1)	5.5 (4.7–6.2)	5.1 (4.4–6.0)	−0.04 (−0.43, 0.36)‡	0.48
CRP, median (IQR) mg/dl	10.0 (4.0–22.8)	9.0 (4.5–20.5)	10.0 (4.0–22.5)	0.07 (−0.33, 0.43)‡	0.69
ACPA positive	96 (58.9)	20 (64.5)	76 (57.6)	1.34 (0.59, 3.02)	0.55
ACPA titer, median (IQR) units/ml	394 (0.0–500)	429 (0–500)	325 (0–500)	−0.10 (−0.50, 0.29)‡	0.68
RF positive	128 (78.5)	24 (77.4)	104 (78.8)	0.92 (0.36, 2.36)	0.81
RF titer, median (IQR) units/ml	30 (5–95)	50 (5–161)	16 (6–43)	−0.16 (−0.55, 0.24)‡	0.33
ANA positive	61 (37.4)	10 (32.3)	51 (38.6)	0.76 (0.33, 1.74)	0.54
Sicca syndrome	111 (68.1)	19 (61.3)	92 (69.7)	0.69 (0.31, 1.55)	0.40
Erosive status	29 (17.8)	7 (11.1)	22 (17.7)	1.46 (0.56–3.80)	0.44
Total SHS, median (IQR)	2.0 (0.0–4.0)	2.0 (0.0–4.0)	2.0 (0.0–4.0)	−0.19 (−0.61, 0.23)‡	0.59
HAQ score, median (IQR)	1.0 (0.5–1.5)	1.1 (0.5–1.4)	1.0 (0.5–1.5)	−0.07 (−0.47, 0.32)‡	0.83
HLA-DRB1*SE allele presence					0.93
0	68 (42.8)	14 (45.2)	54 (42.2)	1 (referent)	
1	65 (40.9)	13 (42.0)	52 (40.6)	0.96 (0.41, 2.25)	
2	26 (16.4)	4 (12.9)	22 (17.2)	0.70 (0.21, 2.37)	
MUC5B rs35705950 GT/TT genotype, %	11.3	19	9.5	2.91 (1.22, 6.95)	0.02
Longitudinal variables at time of chest HRCT scan					
RA duration, median (IQR) years	13.9 (13–14.1)	13.9 (13.3–14)	13.9 (13–14.1)	0.82 (0.55, 1.22)§	0.30
Smoking status trajectory					
Never-stop/low	131 (80.4)	22 (71.0)	109 (82.6)	1 (referent)	0.21
Maintained/moderate-high	32 (19.6)	9 (29.0)	23 (17.4)	1.94 (0.79, 4.75)	
DAS28-ESR, median (IQR)	2.9 (2.4–3.7)	3.4 (2.7–4.1)	2.9 (2.3–3.5)	−0.47 (−0.87, −0.07)‡	0.03
CRP, median (IQR) mg/dl	5.8 (3.9–9.2)	6.6 (3.9–9.2)	5.8 (4.1–8.7)	−0.38 (−0.78, 0.01)‡	0.42
CRP trajectory					
None-low	147 (90.2)	25 (80.6)	122 (92.4)	1 (referent)	0.09
Moderate-high	16 (9.8)	6 (19.4)	10 (7.6)	2.93 (0.91, 8.79)	
HAQ score, median (IQR)	0.4 (0.2–0.8)	0.6 (0.3–1.1)	0.4 (0.2–0.6)	−0.01 (−0.4, 0.39)‡	0.007
MTX exposure	138 (84.7)	27 (87.1)	111 (84.1)	1.28 (0.40, 4.03)	0.79
MTX exposure trajectory					
None-low	51 (31.3)	12 (38.7)	39 (29.6)	1 (referent)	0.64
Moderate	76 (46.6)	13 (41.9)	63 (47.7)	0.67 (0.28, 1.62)	
High	36 (22.1)	6 (19.4)	30 (22.7)	0.65 (0.22, 1.93)	
bDMARD exposure	66 (40.5)	14 (45.2)	52 (39.4)	1.27 (0.58, 2.79)	0.68
TNF inhibitor exposure	54 (33.1)	14 (45.2)	40 (30.3)	1.89 (0.85, 4.21)	0.14
Glucocorticoid exposure trajectory					0.84
None-low	60 (36.8)	13 (41.9)	47 (35.6)	1 (referent)	
Moderate	30 (18.4)	5 (16.2)	25 (18.9)	0.72 (0.23, 2.26)	
High	73 (44.8)	13 (41.9)	60 (45.5)	0.78 (0.33, 1.85)	
ILD pattern on chest HRCT					
UIP and probable UIP	–	4 (12.9)	–	–	–
NSIP	–	4 (12.9)	–	–	–
Indeterminate	–	23 (74.2)	–	–	–
Extent of ILD on chest HRCT					
<5%	–	7 (22.6)	–	–	–
5–10%	–	15 (48.4)	–	–	–
>10%	–	9 (29.0)	–	–	–
Pulmonary function test results, median (IQR)					
FVC, % predicted	–	110 (91.8–117)	–	–	–
FEV <sub>1</sub> , % predicted	–	96 (90.3–113)	–	–	–

(Continued)

**Table 1.** (Cont'd)

Characteristic	Patient group			OR or ES or HR (95% CI)	P†
	Overall RA (n = 163)	RA-ILD (n = 31)	RA without ILD (n = 132)		
TLC, % predicted	-	104 (92.3–108.3)	-	-	
DLco, % predicted	-	77 (62–80)	-	-	

\* Except where indicated otherwise, results (qualitative variables) are the number (%); quantitative variables are shown as median and interquartile range (IQR). The odds ratio (OR) with 95% confidence interval (95% CI) represents the likelihood of a qualitative variable being higher in the rheumatoid arthritis-associated interstitial lung disease (RA-ILD) group than in the RA without ILD group. Erosive status indicates presence of articular erosions due to RA. The effect size (ES) with 95% CI represents the effect size of a quantitative variable being higher in the RA-ILD group than in the RA without ILD group. BMI = body mass index; DAS28-ESR = Disease Activity Score in 28 joints using the erythrocyte sedimentation rate; CRP = C-reactive protein; ACPA = anti-citrullinated peptide antibody; RF = rheumatoid factor; ANA = antinuclear antibody; SHS = modified Sharp/van der Heijde score of radiographic progression; HAQ = Health Assessment Questionnaire; HLA-DRB1\*SE = HLA-DRB1 shared epitope; HRCT = high-resolution computed tomography; MTX = methotrexate; bDMARD = biologic disease-modifying antirheumatic drug; TNF = tumor necrosis factor; UIP = usual interstitial pneumonia; NSIP = nonspecific interstitial pneumonia; FVC = forced vital capacity, FEV<sub>1</sub> = forced expiratory volume in 1 second; TLC = total lung capacity; DLco = diffusing capacity for carbon monoxide.

† Results from the bivariate analysis.

‡ ES with 95% CI.

§ Hazard ratio (HR) with 95% CI.

( $P < 0.001$ ), and increased mean DAS28-ESR over the follow-up (for each unit increase, OR 2.03 [95% CI 1.24, 3.42]) ( $P = 0.006$ ) (Table 3).

#### Development of a risk score for subclinical RA-ILD.

We represented the performance of the multivariate model from the discovery population by ROC curve analysis, in which the AUC was calculated as 0.81 (95% CI 0.73, 0.90) (Supplementary Figure 2, available on the *Arthritis & Rheumatology* website at

<https://onlinelibrary.wiley.com/doi/10.1002/art.42162>). We had similar findings when we used categorized variables to determine performance (Supplementary Appendix), with the AUC calculated as 0.80 (95% CI 0.73, 0.9) (Figure 1A). The corresponding risk matrix is provided in Table 4. The probability (OR) for subclinical RA-ILD ranged from 2 (0.3–5.7) for female patients not carrying the *MUC5B* rs35705950 T risk allele and  $\leq 49$  years of age at RA onset and with a mean DAS2-ESR  $\leq 2.9$  over follow-up to 94.9 (72.1–99.3) for male patients carrying the

**Table 2.** Characteristics of patients with RA in the replication population (TRANSLATE2)\*

Characteristic	Patient group		
	Overall RA (n = 89)	RA-ILD (n = 15)	RA without ILD (n = 74)
Male sex	23 (25.8)	7 (46.7)	16 (21.6)
RA duration, median (IQR) years	11 (5–18)	9 (4.5–11.5)	12 (6–18)
Age at RA onset			
Median (IQR) years	46.0 (34.0–55.0)	50.0 (43.5–57.5)	42.5 (30.5–53.8)
$\leq 49$ years	53 (59.6)	5 (33.3)	48 (64.9)
50–58 years	11 (12.4)	4 (26.7)	7 (9.5)
$> 58$ years	25 (28.1)	6 (40.0)	19 (25.7)
ACPA positive	84 (94.4)	14 (93.3)	70 (94.6)
RF positive	66 (75.9)	11 (73.3)	55 (76.4)
Ever smoker	48 (59.3)	8 (61.5)	40 (58.8)
<i>MUC5B</i> rs35705950 GT/TT genotype, %	17.4	26.7	15.5
All DAS28-ESR values during the 4 years before HRCT			
Median (IQR)	3.1 (2.2–4.6)	4.8 (4.0–5.1)	2.9 (2.0–3.9)
$< 2.9$	29 (32.6)	1 (6.6)	28 (37.8)
2.9–4.3	37 (41.6)	4 (26.7)	33 (44.6)
$> 4.3$	23 (25.8)	10 (66.7)	13 (17.6)
Last 4 DAS28-ESR values available before HRCT			
Median (IQR)	3.5 (2.4–4.4)	4.7 (4.2–5.0)	3.2 (2.3–4.1)
$< 2.9$	31 (34.8)	1 (6.6)	30 (40.5)
2.9–4.3	35 (39.4)	4 (26.7)	31 (41.9)
$> 4.3$	23 (25.8)	10 (66.7)	13 (17.6)
Last DAS28-ESR value available before HRCT			
Median (IQR)	3.1 (2.2–4.6)	4.8 (4.0–5.1)	2.9 (2.0–3.9)
$< 2.9$	40 (45.0)	2 (13.3)	38 (51.4)
2.9–4.3	22 (24.7)	2 (13.3)	20 (27.0)
$> 4.3$	27 (30.3)	11 (73.4)	16 (21.6)

\* Except where indicated otherwise, values are the number (%). See Table 1 for definitions.

**Table 3.** Independent risk factors associated with subclinical RA-ILD in the discovery population (ESPOIR)\*

	Model with MUC5B rs35705950		Categorized model with MUC5B rs35705950		Weighted coefficient with MUC5B rs35705950		Model without MUC5B rs35705950		Categorized model without MUC5B rs35705950		Weighted coefficient without MUC5B rs35705950	
	OR (95% CI)	P†	OR (95% CI)	P†	OR (95% CI)	P†	OR (95% CI)	P†	OR (95% CI)	P†	OR (95% CI)	P†
<b>MUC5B rs35705950</b>												
GG	1 (referent)		1 (referent)		0		NA		NA		NA	
GT/TT	3.74 (1.37–10.39)	0.01	3.52 (1.28–9.77)	0.01	27		NA		NA		NA	
Sex												
Female	1 (referent)		1 (referent)		0		1 (referent)		NA		NA	
Male	3.93 (1.40–11.39)	0.01	3.59 (1.26–10.42)	0.02	28		3.8 (1.4–10.6)	<0.01	NA		NA	
Age at RA onset												
Per year change	1.10 (1.04–1.16)	<0.001	–				1.1 (1.0–1.2)	0.001	–		–	
≤49 years	–		1 (referent)		0		–		1 (referent)		–	
50–58 years	–		3.10 (1.08–9.66)	0.04	25		–		2.68 (0.97–7.89)	0.06	–	
>58 years	–		9.98 (3.04–36.36)	<0.001	50		–		8.81 (2.8–30.09)	<0.001	–	
Mean DAS28-ESR												
Per unit change	2.03 (1.24–3.42)	0.006	–				1.9 (1.2–3.2)	0.01	–		–	
<2.9	–		1 (referent)		0		–		1 (referent)		–	
2.9–4.3	–		2.83 (1.02–8.46)	0.05	23		–		2.54 (0.94–7.36)	0.07	–	
>4.3	–		5.93 (1.45–24.78)	0.01	39		–		5.93 (1.4–23.47)	0.01	–	

\* A categorized model is a model in which continuous variables are transformed into categorical variables. NA = not applicable. See Table 1 for other definitions.  
 † Results from the multivariate analysis.

**Table 4.** Association matrices for risk scores associated with the risk of subclinical RA-ILD in the discovery population\*

Risk matrix variable	DAS28-ESR <2.9		DAS28-ESR 2.9–4.3		DAS28-ESR >4.3	
	Female	Male	Female	Male	Female	Male
Model with <i>MUC5B</i> rs35705950						
≤49 years (GG)	2.0 (0.3, 5.7)	7.1 (1.0, 18.6)	6.7 (1.2, 16.5)	21.3 (3.2, 50.3)	12.5 (2.0, 29.7)	34.9 (5.9, 71.4)†
≤49 years (GT/TT)	6.7 (1.4, 17.6)	21.3 (5.4, 48.0)	20.3 (5.2, 38.2)	48.9 (16.0, 80.1)†	33.5 (6.3, 59.4)†	65.4 (16.3, 90.8)‡
50–58 years (GG)	6.2 (1.5, 15.6)	19.9 (4.5, 41.6)	18.9 (5.9, 30.6)	46.8 (15.0, 71.7)†	31.6 (8.3, 57.1)†	63.4 (18.1, 87.5)‡
50–58 years (GT/TT)	18.9 (3.8, 50.1)	46.8 (13.0, 80.8)†	45.2 (15.6, 71.7)†	75.6 (39, 94.6)§	62 (17.9, 87.4)‡	86.0 (40.7, 97.7)§
>58 years (GG)	16.7 (5.0, 39.1)	42.9 (20.6, 72.0)†	41.4 (15.0, 69.5)†	72.7 (35.6, 92.3)‡	58.3 (25.1, 84.8)‡	84.0 (48.3, 97.2)§
>58 years (GT/TT)	41.4 (17.4, 76.6)†	72.7 (46.9, 92.7)‡	71.4 (40.8, 91.7)‡	90.4 (66.9, 98.3)§	83.1 (47.3, 96.8)§	94.9 (72.1, 99.3)§
Model without <i>MUC5B</i> rs35705950						
≤49 years	3.6 (0.8, 7.1)	11.9 (3.3, 24.7)	8.6 (2.3, 17.6)	25.6 (7.2, 53.7)†	17.5 (4.0, 40.4)	43.6 (9.7, 81.8)†
50–58 years	9.1 (2.2, 20.3)	26.6 (8.8, 53.5)†	20.2 (7.9, 35.8)	48.0 (21.7, 73.8)†	36.3 (10.1, 66.2)†	67.4 (22.0, 91.5)‡
>58 years	24.6 (8.0, 51.2)	54.4 (26.8, 79.3)‡	45.4 (20.2, 71.9)†	75.2 (45.2, 93.7)§	65.1 (35.3, 91.1)‡	87.2 (59.1, 98.3)§

\* Risk matrix models were stratified by the presence or absence of each independent risk factor for subclinical RA-ILD (age at RA onset, *MUC5B* rs35705950 genotype [GG or GT/TT], DAS28-ESR disease activity scores, and sex). See Table 1 for definitions.

† High risk level for RA-ILD.

‡ Higher level of risk for RA-ILD.

§ Highest level of risk for RA-ILD.

*MUC5B* rs35705950 T risk allele and >58 years of age at RA onset and with a mean DAS28-ESR >4.3 over follow-up (Table 4).

To generate a risk score for subclinical RA-ILD, we attributed a weighted coefficient to each independent risk factor, which led to a total risk score ranging from 0 to 144 (Table 3). In a model in which we used a total risk score cutoff of 51 for defining subclinical RA-ILD, the sensitivity was 71.0% and the specificity was 79.6% (Supplementary Table 4, available on the *Arthritis & Rheumatology* website at <https://onlinelibrary.wiley.com/doi/10.1002/art.42162>).

To simplify the score for use in daily clinical practice, we aimed to estimate the best approximation of the mean DAS28-ESR over follow-up. The last 4 DAS28-ESR values obtained from each patient before they underwent chest HRCT scan (i.e., 4 years before the chest HRCT scan) provided a good estimate of the mean DAS28-ESR for all values available over the entire follow-up, with an AUC of 0.80 (95% CI 0.70, 0.91) (not significantly different from the model with all available DAS28-ESR values, bootstrap  $P = 0.08$ ). For the model with the last 4 DAS28-ESR values and with total risk score cutoff of 51 for defining subclinical RA-ILD, the sensitivity was 73.1% and the specificity was 85.2% (Figure 1A, Supplementary Table 4). We then validated the score based on the last 4 DAS28-ESR values obtained from each patient before chest HRCT in the replication cohort. In this validation model, the AUC was 0.79 (95% CI 0.67, 0.91) (Figure 1B); the sensitivity and specificity values based on a total risk score cutoff of 51 are listed in Supplementary Table 4.

When we evaluated the last DAS28-ESR value available within the year before chest HRCT scan in the discovery population, we found that the performance was similar and not significantly different from the model with all available DAS28-ESR values (bootstrap  $P = 0.23$ ). In this model for detection of

subclinical RA-ILD based on a total risk score cutoff of 51, the AUC was 0.82 (95% CI 0.70, 0.94) (Figure 1A), the sensitivity was 75.0%, and the specificity was 85.0% (Supplementary Table 4). We then validated the score derived from the last DAS28-ESR value in the replication population; in the validated model, the AUC was 0.78 (95% CI 0.65, 0.92) (Figure 1B). The sensitivity, specificity, and likelihood ratios based on a total risk score cutoff of 51 are listed in the Supplementary Table 4.

Because *MUC5B* rs35705950 genotyping is not available yet in daily practice, we created a simplified model that excluded *MUC5B* rs35705950. Male sex (OR 3.8 [95% CI 1.4, 10.6]) ( $P < 0.01$ ), older age at RA onset (OR 1.1 [95% CI 1.0, 1.2]) ( $P = 0.001$ ), and increased mean DAS28-ESR value over the follow-up (OR 1.9 [95% CI 1.2, 3.2]) ( $P = 0.01$ ) were independently associated with subclinical RA-ILD (Table 3). A new weighted coefficient was attributed to each independent risk factor, which led to a total risk score that ranged from 0 to 113 (Table 3). The corresponding risk matrix is provided in Table 4.

The performance of the ROC curve for the simplified model was comparable to the full model (bootstrap  $P = 0.25$ ), with an AUC of 0.79 (95% CI 0.69, 0.87) (Figure 1C). When we included the mean of the last 4 DAS28-ESR values available in the 4 years before the chest HRCT, performance of the risk score for the simplified model was comparable between the discovery population (AUC 0.78 [95% CI 0.68, 0.88]) and after validation in the replication population (AUC 0.78 [95% CI 0.65, 0.92]) (Figure 1C; see also Supplementary Table 5, available on the *Arthritis & Rheumatology* website at <https://onlinelibrary.wiley.com/doi/10.1002/art.42162>) (not significantly different from the model with all available DAS28-ESR values, bootstrap  $P = 0.21$ ). The simplified risk score derived from the last DAS28-ESR value available within the year before the chest HRCT scan was similar to the score derived from

the last 4 DAS28-ESR values (not significantly different from the model with all available DAS28-ESR values, bootstrap  $P = 0.42$ ) in both the discovery and replication populations, with an AUC of 0.79 (95% CI 0.67, 0.89) and 0.78 (95% CI 0.64, 0.93), respectively (Figures 1C and D). Corresponding sensitivity and specificity values in the model based on a total risk score cutoff value of 25 for defining subclinical RA-ILD were 75.0% and 69.0%, respectively, in the discovery population and 86.7% and 47.3%, respectively, in the replication population (Supplementary Table 5).

Of note, if the ROC AUCs of the models with and without *MUC5B* rs35705950 were found comparable (bootstrap  $P = 0.25$ ) (Figure 1), the model that included *MUC5B* rs35705950 had better goodness of fit than the model without, with an Akaike's information criterion value of 133 and 138, respectively (likelihood ratio test,  $P = 0.01$ ).

## DISCUSSION

A scoring system that allows stratification of patients at high risk for RA-ILD before the onset of their pulmonary symptoms (i.e., subclinical RA-ILD) may help clinicians identify patients who would most benefit from chest HRCT screening.

In this study, we proposed and validated a risk score for subclinical RA-ILD that included 4 variables (sex, age at RA onset, RA disease activity using DAS28-ESR, and the *MUC5B* rs35705950 genetic variant). Although the risk score without *MUC5B* rs35705950 was found to be appropriate to discriminate patients with subclinical RA-ILD, the model with *MUC5B* rs35705950 had better performance, suggesting an important contribution of the genetic variant to the overall risk of subclinical RA-ILD. In our study, the contribution of *MUC5B* rs35705950, a common variant with a relatively high magnitude of association, to risk of subclinical RA-ILD was similar to that previously reported for clinical RA-ILD (23). Indeed, in both our present study and our earlier study, the odds of RA-ILD developing in patients carrying the *MUC5B* rs35705950 T risk allele was at least 3 times greater than in those carrying the GG genotype (23). Of note, a similar magnitude of association was reported in individuals with interstitial lung abnormalities and without RA (35). Our findings are in good agreement with the results of the FinnGen epidemiologic cohort (19) and support a pivotal role of the *MUC5B* rs35705950 variant for both clinical and subclinical RA-ILD risk stratification and add to the possible interest for genotyping the risk variant in future clinical practice (36).

The performance of the risk score when the last DAS28-ESR value available in the year before the chest HRCT scan was used was similar to the performance when the mean DAS28-ESR over follow-up was used. This finding is concordant with the previously reported effect of the increase in annual DAS28 on the risk of incident RA-ILD within the year before RA-ILD onset (21). Estimation of the risk for subclinical RA-ILD using only the last DAS28-ESR

available makes our risk score easy to use for daily practice. However, the performance of our risk score cannot be directly compared with the performance of other scores because of the different study design (i.e., a systematic exploration of asymptomatic patients by chest HRCT) and the integration of different variables in our model (i.e., the *MUC5B* rs35705950 variant and DAS28-ESR). Of interest, a risk score for clinical RA-ILD defined in a recent case-control study identified both male sex and disease activity (i.e., Clinical Disease Activity Index score >28 and ESR >80 mm/hour) as independent risk factors, which reinforces their contribution to the excess risk for ILD in patients with RA (17). In their case-control study, Paulin et al also identified smoking and the presence of extraarticular manifestations as predictors of ILD among patients with RA. However, in a nested case-control study that matched incident RA-ILD cases to RA non-ILD controls on age, sex, RA duration, RF, and time from exposure assessment to RA-ILD, the investigators identified obesity, CRP level, functional status, and heavy smoking as potential risk factors for RA-ILD (37). Even if our study was not designed to assess the impact of RA treatments, MTX use was not found to contribute to the risk of subclinical RA-ILD, which is consistent with previous studies that concluded that MTX was not a risk factor for RA-ILD (22,25,38).

Our study has some limitations. The relatively low occurrence of RA-ILD in the discovery population and the relatively small sample size may have decreased the power to detect other RA-ILD risk factors (17,37). Conversely, if such factors were not identified in our study because of lack of power, the magnitude of their likely association would be small, with a limited contribution to the excess risk for subclinical RA-ILD. In addition, the limited sample size did not allow us to perform subanalyses to identify risk factors for specific HRCT patterns. Indeed, the potential of including *MUC5B* rs35705950 in a future risk score for patients at high risk of subclinical usual interstitial pneumonia-type RA should be considered according to the restricted association demonstrated between the risk variant and the usual interstitial pneumonia pattern shown on HRCT scan of the chest of patients with RA-ILD (23). In our study, the ACPA positivity rate was different between the discovery and replication populations (58.9% versus 94.4%, respectively), which could be the consequence of sampling bias. However, this difference should not affect the performance of the risk score, as the discovery stage did not identify ACPA status as an independent risk factor for subclinical RA-ILD. Lastly, several patients included in the ESPOIR cohort did not agree to participate in this cross-sectional study, which may have implied a selection bias. However, the characteristics of patients included in the study and those not included were not different. In addition, the prevalence of subclinical RA-ILD in our discovery population was comparable to that previously reported in the literature (1-6). Our risk score was developed and validated in patients having established RA with a mean disease duration of 10 years. The predictive value of our risk score will need validation for early or

longstanding RA. Therefore, future large prospective studies are needed to investigate 1) the effects of other potential risk factors, including smoking, BMI, RF-positive and ACPA-positive status, and serum biomarkers (39), on the risk score for subclinical RA-ILD, 2) the performance of our risk score for other RA durations, notably at RA onset, and 3) the identification of risk score for a specific HRCT pattern and progression to clinical lung fibrosis.

In conclusion, this is the first study that identified and validated a risk score (with and without inclusion of *MUC5B* rs35705950) that would allow the identification of patients at high risk for subclinical RA-ILD who are eligible for chest HRCT screening. The fact that the highest-performance model was the one that included *MUC5B* rs35705950 in the risk score illustrates the significant contribution of this genetic variant to the risk of subclinical RA-ILD. These findings could help clinicians in their daily practice and could affect future recommendations of RA-ILD screening.

## ACKNOWLEDGMENTS

We thank the participating patients for their contributions to this work, Nathalie Rincheval for expert monitoring and data management, and the investigators who recruited and followed the patients.

## AUTHOR CONTRIBUTIONS

All authors were involved in drafting the article or revising it critically for important intellectual content, and all authors approved the final version to be published. Dr. Juge had full access to all of the data in the study and takes responsibility for the integrity of the data and the accuracy of the data analysis.

**Study conception and design.** Juge, Granger, Debray, Kedra, Borie, Crestani, Fautrel, Dieudé.

**Acquisition of data.** Juge, Debray, Borie, Kannengiesser, Boileau, Crestani, Fautrel, Dieudé.

**Analysis and interpretation of data.** Juge, Granger, Ebstein, Louis-Sidney, Kedra, Doyle, Borie, Constantin, Combe, Flipo, Mariette, Vittecoq, Sarau, Carvajal-Alegria, Sibilia, Berenbaum, Kannengiesser, Boileau, Sparks, Crestani, Fautrel, Dieudé.


## REFERENCES

- Bongartz T, Nannini C, Medina-Velasquez YF, et al. Incidence and mortality of interstitial lung disease in rheumatoid arthritis: a population-based study. *Arthritis Rheum* 2010;62:1583–91.
- Koduri G, Norton S, Young A, et al. Interstitial lung disease has a poor prognosis in rheumatoid arthritis: results from an inception cohort. *Rheumatology* 2010;49:1483–9.
- Gabbay E, Tarala R, Will R, et al. Interstitial lung disease in recent onset rheumatoid arthritis. *Am J Respir Crit Care Med* 1997;156:528–35.
- Reynisdottir G, Karimi R, Joshua V, et al. Structural changes and antibody enrichment in the lungs are early features of anti-citrullinated protein antibody-positive rheumatoid arthritis. *Arthritis Rheumatol* 2014;66:31–9.
- Salaffi F, Carotti M, Di Carlo M, et al. High-resolution computed tomography of the lung in patients with rheumatoid arthritis: prevalence of interstitial lung disease involvement and determinants of abnormalities. *Medicine (Baltimore)* 2019;98:e17088.
- Chen J, Shi Y, Wang X, et al. Asymptomatic preclinical rheumatoid arthritis-associated interstitial lung disease. *Clin Dev Immunol* 2013;2013:406927.
- Robles-Perez A, Luburich P, Rodriguez-Sanchon B, et al. Preclinical lung disease in early rheumatoid arthritis. *Chron Respir Dis* 2016;13:75–81.
- Gochuico BR, Avila NA, Chow CK, et al. Progressive preclinical interstitial lung disease in rheumatoid arthritis. *Arch Intern Med* 2008;168:159–66.
- Hyltdgaard C, Ellingsen T, Hilberg O, et al. Rheumatoid arthritis-associated interstitial lung disease: clinical characteristics and predictors of mortality. *Respiration* 2019;98:455–60.
- Raimundo K, Solomon JJ, Olson AL, et al. Rheumatoid arthritis-interstitial lung disease in the United States: prevalence, incidence, and healthcare costs and mortality. *J Rheumatol* 2019;46:360–9.
- Spagnolo P, Ryerson CJ, Putman R, et al. Early diagnosis of fibrotic interstitial lung disease: challenges and opportunities. *Lancet Respir Med* 2021;9:1065–76.
- Vij R, Strek ME. Diagnosis and treatment of connective tissue disease-associated interstitial lung disease. *Chest* 2013;143:814–24.
- Kanne JP. Interstitial lung disease (ILD): imaging finding, and the role of imaging in evaluating the patient with known or suspected ILD. *Semin Roentgenol* 2010;45:3.
- Bradley B, Branley HM, Egan JJ, et al. Interstitial lung disease guideline: the British Thoracic Society in collaboration with the Thoracic Society of Australia and New Zealand and the Irish Thoracic Society. *Thorax* 2008;63 Suppl:v1–58.
- Hansell DM, Goldin JG, King TE Jr, et al. CT staging and monitoring of fibrotic interstitial lung diseases in clinical practice and treatment trials: a position paper from the Fleischner Society. *Lancet Respir Med* 2015;3:483–96.
- Flaherty KR, Wells AU, Cottin V, et al. Nintedanib in progressive fibrosing interstitial lung diseases. *N Engl J Med* 2019;381:1718–27.
- Paulin F, Doyle TJ, Mercado JF, et al. Development of a risk indicator score for the identification of interstitial lung disease in patients with rheumatoid arthritis. *Reumatol Clin (Engl Ed)* 2021;17:207–11.
- Mena-Vazquez N, Perez Albaladejo L, Manrique-Ariza S, et al. Analysis of clinical-analytical characteristics in patients with rheumatoid arthritis and interstitial lung disease: case-control study. *Reumatol Clin (Engl Ed)* 2021;17:197–202.
- Palomaki A, FinnGen Rheumatology Clinical Expert Group, Palotie A, et al. Lifetime risk of rheumatoid arthritis-associated interstitial lung disease in *MUC5B* mutation carriers. *Ann Rheum Dis* 2021;80:1530–6.
- Kelly CA, Saravanan V, Nisar M, et al. Rheumatoid arthritis-related interstitial lung disease: associations, prognostic factors and physiological and radiological characteristics—a large multicentre UK study. *Rheumatology* 2014;53:1676–82.
- Sparks JA, He X, Huang J, et al. Rheumatoid arthritis disease activity predicting incident clinically apparent rheumatoid arthritis-associated interstitial lung disease: a prospective cohort study. *Arthritis Rheumatol* 2019;71:1472–82.
- Kiely P, Busby AD, Nikiphorou E, et al. Is incident rheumatoid arthritis interstitial lung disease associated with methotrexate treatment? Results from a multivariate analysis in the ERAS and ERAN inception cohorts. *BMJ Open* 2019;9:e028466.
- Juge PA, Lee JS, Ebstein E, et al. *MUC5B* Promoter variant and rheumatoid arthritis with interstitial lung disease. *N Engl J Med* 2018;379:2209–19.
- Hyltdgaard C, Hilberg O, Pedersen AB, et al. A population-based cohort study of rheumatoid arthritis-associated interstitial lung disease: comorbidity and mortality. *Ann Rheum Dis* 2017;76:1700–6.

25. Juge PA, Lee JS, Lau J, et al. Methotrexate and rheumatoid arthritis associated interstitial lung disease. *Eur Respir J* 2020;57:2000337.
26. Kelly C, Emery P, Dieude P. Current issues in rheumatoid arthritis-associated interstitial lung disease. *Lancet Rheumatol* 2021;3: E798–807.
27. Arnett FC, Edworthy SM, et al. The American Rheumatism Association 1987 revised criteria for the classification of rheumatoid arthritis. *Arthritis Rheum* 1988;31:315–24.
28. Aletaha D, Neogi T, Silman AJ, et al. 2010 rheumatoid arthritis classification criteria: an American College of Rheumatology/European League Against Rheumatism collaborative initiative. *Arthritis Rheum* 2010;62:2569–81.
29. World Health Organization. Screening programmes: a short guide. Increase effectiveness, maximize benefits and minimize harm. Geneva: World Health Organization; 2020.
30. Combe B, Rincheval N, Berenbaum F, et al. Current favourable 10-year outcome of patients with early rheumatoid arthritis: data from the ESPOIR cohort. *Rheumatology (Oxford)* 2021;60:5073–9.
31. Raghu G, Remy-Jardin M, Myers JL, et al. Diagnosis of idiopathic pulmonary fibrosis. An official ATS/ERS/JRS/ALAT clinical practice guideline. *Am J Respir Crit Care Med* 2018;198:e44–68.
32. Seibold MA, Wise AL, Speer MC, et al. A common MUC5B promoter polymorphism and pulmonary fibrosis. *N Engl J Med* 2011;364: 1503–12.
33. Combe B, Benessiano J, Berenbaum F, et al. The ESPOIR cohort: a ten-year follow-up of early arthritis in France: methodology and baseline characteristics of the 813 included patients. *Joint Bone Spine* 2007;74:440–5.
34. Collins GS, Reitsma JB, Altman DG, et al. Transparent reporting of a multivariable prediction model for individual prognosis or diagnosis (TRIPOD): the TRIPOD Statement. *Eur J Clin Invest*. 2015;45:204–14.
35. Hunninghake GM, Hatabu H, Okajima Y, et al. MUC5B promoter polymorphism and interstitial lung abnormalities. *N Engl J Med* 2013;368: 2192–200.
36. Sparks JA. Towards clinical significance of the MUC5B promoter variant and risk of rheumatoid arthritis-associated interstitial lung disease. *Ann Rheum Dis* 2021;80:1503–4.
37. Kronzer VL, Huang W, Dellariipa PF, et al. Lifestyle and clinical risk factors for incident rheumatoid arthritis-associated interstitial lung disease. *J Rheumatol* 2021;48:656–63.
38. Ibfelt EH, Jacobsen RK, Kopp TI, et al. Methotrexate and risk of interstitial lung disease and respiratory failure in rheumatoid arthritis: a nationwide population-based study. *Rheumatology (Oxford)* 2021; 60:346–52.
39. Doyle TJ, Patel AS, Hatabu H, et al. Detection of rheumatoid arthritis-interstitial lung disease is enhanced by serum biomarkers. *Am J Respir Crit Care Med* 2015;191:1403–12.



# Serologic Biomarkers of Progression Toward Diagnosis of Rheumatoid Arthritis in Active Component Military Personnel

Matthew J. Loza,<sup>1</sup>  Sunil Nagpal,<sup>1</sup> Suzanne Cole,<sup>1</sup> Renee M. Laird,<sup>2</sup> Ashley Alcalá,<sup>2</sup> Navin L. Rao,<sup>1</sup> Mark S. Riddle,<sup>3</sup> and Chad K. Porter<sup>4</sup>

**Objective.** To identify a panel of serum biomarkers that could specifically identify imminent cases of rheumatoid arthritis (RA) before diagnosis.

**Methods.** Serum samples were collected at 4 time points from active component US military personnel, including 157 anti-citrullinated protein antibody (ACPA)–seropositive and 50 ACPA–seronegative RA subjects, 100 reactive arthritis (ReA) subjects, and 76 healthy controls. The cohorts were split into 2 phases, with samples tested on independent proteomic platforms for each phase. Classification models of RA diagnosis based on samples obtained within 6 months prior to diagnosis were developed both in univariate analyses and by multivariate random forest modeling of training sample sets and testing sample sets from each phase.

**Results.** Increases in serum analytes, including C-reactive protein levels, serum amyloid A, and soluble programmed cell death 1 (PD-1), were observed in seropositive RA subjects at the time point closest to diagnosis, up to several years before diagnosis. Only a small fraction of RA subjects had levels above the 95th percentile of healthy control levels until the time period within 6 months of diagnosis. For classification of RA diagnosis using samples obtained within 6 months prior to diagnosis, soluble PD-1 provided superior specificity compared to ReA cases (>89%), with a sensitivity of 48% for RA classification. An 8-analyte model provided superior sensitivity (69%), with comparable specificity relative to ReA (>82%).

**Conclusion.** Our findings demonstrate that imminent RA diagnosis could be classified with high specificity, relative to healthy controls and ReA cases, using a panel of cytokines measured in serum samples collected within 6 months before actual diagnosis.

## INTRODUCTION

Rheumatoid arthritis (RA) is a chronic autoimmune disease of unknown etiology that affects ~1% of the population worldwide. The disease is characterized by inflammation of synovial joints and manifests as symmetric polyarthritis and synovial hyperplasia, leading to the destruction of bone and cartilage (1).

Clinical studies have shown that a window of opportunity exists in early, recently diagnosed RA when the disease is more responsive to both conventional and biologic disease-modifying

antirheumatic drugs (bDMARDs) (2–5). Therefore, aggressive treatment of early RA may result in stronger response and long-term disease remission. Indeed, in early RA, DMARD treatment has been shown to reduce disease progression as assessed by radiologic scores (6). Once the disease is established, the probability of achieving clinical remission is substantially reduced, with increased risk of irreversible joint damage.

Anti-citrullinated protein antibody (ACPA) levels and inflammatory cytokine levels can be elevated in individuals years before diagnosis and may be predictive of future RA diagnosis (7–14).

The views expressed in this article are those of the authors and do not necessarily reflect the official policy or position of the Department of the Navy, Department of Defense, the Department of Veterans Affairs, nor the US government. This is a US government work. There are no restrictions on its use. There were no financial conflicts of interests among any of the authors.

Some authors are employees of the US government. This work was prepared as part of their official duties. Title 17 U.S.C. §105 provides that "Copyright protection under this title is not available for any work of the United States Government." Title 17 U.S.C. §101 defines a US government work as a work prepared by a military service member or employee of the US government as part of that person's official duties.

Supported by Janssen Research and Development, LLC, under a Cooperative Research and Development Agreement (NMR 9245). This article is the result of work supported with resources and the use of facilities at the VA Sierra Nevada Health Care System.

<sup>1</sup>Matthew J. Loza, PhD, Sunil Nagpal, PhD, Suzanne Cole, MS, Navin L. Rao, PhD: Immunology, Janssen Research & Development, Spring House, Pennsylvania; <sup>2</sup>Renee M. Laird, PhD, PMP, Ashley Alcalá, MPH, CPH: Henry M. Jackson Foundation for Military Medicine, Bethesda, Maryland; <sup>3</sup>Mark S. Riddle, MD, DrPH: Enteric Diseases Department, Naval Medical Research Center, Silver Spring, Maryland, Reno-School of Medicine, University of Nevada, and VA Sierra Nevada Health Care System, Reno, Nevada; <sup>4</sup>Chad K. Porter, PhD, MPH: Enteric Diseases Department, Naval Medical Research Center, Silver Spring, Maryland.

Author disclosures are available at <https://onlinelibrary.wiley.com/action/downloadSupplement?doi=10.1002%2Fart.42260&file=art42260-sup-0001-Disclosureform.pdf>.

Address correspondence via email to Matthew J. Loza, PhD, at [mloza@its.jnj.com](mailto:mloza@its.jnj.com).

Submitted for publication January 3, 2022; accepted in revised form June 2, 2022.

Soluble programmed cell death 1 (PD-1) has previously been shown to be elevated in patients with arthralgia and those with newly diagnosed RA, particularly in ACPA-seropositive patients (15). These results suggest the possibility that serum biomarkers could be used to identify the imminent development of full clinical presentation of RA.

We utilized data from the US Defense Medical Surveillance System (DMSS) and serum samples from the US Department of Defense Serum Repository (DoDSR) to identify RA biomarkers that appear before RA diagnosis. Reactive arthritis (ReA), which is also of interest to the military for the evaluation of personnel prior to active deployment, served as a disease control to evaluate the specificity of RA biomarkers. The goal of this study was to identify a panel of biomarkers that could aid in identifying imminent RA cases prior to full clinical presentation, when irreversible joint damage may already be underway, and reduce the risk of such individuals being deployed to physically demanding missions where disability could put them and others at risk.

## PATIENTS AND METHODS

**Study design.** A nested, case-control study was designed that included US military personnel diagnosed as having RA or ReA and age- and sex-matched healthy comparator subjects. A total of 500 subjects with RA, 500 subjects with ReA, and 500 healthy controls who were frequency matched to the RA subjects and ReA subjects were identified from the DMSS as previously described by Porter et al (16). A total of 74.8% of RA subjects had >2 RA-related medical visits, with a median number of days between the first encounter and last encounter of 426 days (interquartile range [IQR] 83–1,238 days) for all cases. For subjects with only 2 encounters, the median number of days was 48 days (IQR 16–115 days). Data regarding the potential initiation of treatments after medical encounters were not available. This study was approved by the ethics review committee of the Naval Medical Research Center in Silver Spring, Maryland (approval no. NMRC.2014.0012) in compliance with the Declaration of Helsinki and all federal regulations governing the protection of human volunteers.

**Serum samples.** For each RA subject, ReA subject, and healthy control subject identified, up to 4 frozen serum samples were obtained from the DoDSR (16). All identifiable information was removed before investigator receipt of data or samples. For RA subjects and ReA subjects, sample D was the first sample available in the repository. For RA subjects, sample A was the first sample available within 30 days of diagnosis or, if that was not available, the first sample collected before diagnosis. Samples B and C were interim samples approximately evenly distributed across the subject's service time. For ReA, samples A and B represented the first available sample after an initial ReA diagnosis and before an initial ReA diagnosis, respectively, and sample C was an interim sample collected between samples B and D. Time points for healthy control

subjects were matched to RA subject samples and ReA subject samples as previously described (16).

Sample A serum from RA cases was tested for levels of ACPA using a commercial cyclic citrullinated peptide 2 (CCP-2) assay (Bio-Rad). Cases with >5 units/ml in the CCP-2 assay were classified as ACPA seropositive.

Samples were selected for inclusion in 1 of 2 sample sets: phase I for building predictive models for RA diagnosis and phase II for model confirmation (Supplementary Figure 1, available on the *Arthritis & Rheumatology* website at <http://onlinelibrary.wiley.com/doi/10.1002/art.42260>). The phase I sample set consisted of all serum samples from 88 randomly selected ACPA-seropositive RA subjects, 50 ReA subjects, and 50 healthy controls. The phase II sample set consisted of samples A and B from 69 ACPA-seropositive RA subjects, 50 ACPA-seronegative RA subjects, and 50 ReA subjects. In addition, 50 sample A sera from seropositive RA subjects (39 samples collected 0 to <0.5 years before diagnosis and 11 samples collected after diagnosis) and 26 sample A sera from healthy controls from phase I were included in the phase II set.

**Serum analyte analysis.** Phase I serum samples from all 4 time points from RA subjects, ReA subjects, and healthy controls were analyzed for soluble PD-1 levels on the Meso Scale Discovery platform, as previously described (15). The assay has a sensitivity of 6.4 pg/ml. Data were  $\log_2$ -transformed for all analyses.

Phase I serum samples collected at all time points from RA cases and those collected at time points A and B from ReA subjects and healthy controls were analyzed by SomaLogic Inc. using the aptamer-polymerase chain reaction-based SOMAscan version 3.2 platform for a panel of 497 analytes. Serum analyte levels were recorded as relative fluorescence units (RFUs), were cross-plate calibrated, and were median normalized. Analyte levels were transformed to the  $\log_2$  ratio of normalized RFUs to the geometric mean of the healthy control cohort.

Because of unavailability of the SOMAscan platform at the time of confirmation study planning, the Olink Proteomics platform was selected for the analysis of the phase II serum sample set. Samples were analyzed by Olink analysis service in Boston using 4 Olink Target 96 assay panels (Cardiometabolic v.3602, Development v.3511, Inflammation v.3021, and Oncology-II v.7004) that measure relative levels of 362 unique analytes. Data are reported as the  $\log_2$ -transformation of an arbitrary unit of relative expression.

**Statistical analysis.** Generalized linear model analyses were used to test for significance of differences in mean serum analyte levels between time points (with subject ID as a random factor) within a group, to test the significance of differences compared to the timeframe of <0.5 years before diagnosis within an individual group, and to test the significance of the differences between groups at a specific time point/timeframe. Fold statistics represent the ratio of the geometric mean of the test group over

the geometric mean for a specific reference group (non-log-transformed data), with values <1 transformed to opposite of the reciprocal. Multiple testing correction was performed using the Benjamini-Hochberg false discovery rate (FDR) method.

Serum levels of selected analytes were evaluated as univariate predictors of a seropositive RA diagnosis based on serum measurements after diagnosis, between 0 to <0.5 years, 0.5 to <1 year, 1 to <2 years, 2 to <5 years, and  $\geq 5$  years prediagnosis. Specificity of model performance was evaluated according to the proportion of healthy controls and ReA subjects also classified as positive in the respective timeframes. A positive prediction was based on high levels of the analytes, defined a priori as levels >95th percentile of healthy controls for the respective timeframe.

For multivariate modeling, the seropositive RA subjects and healthy control subjects from phase I and phase II who had samples collected within 6 months prior to diagnosis were randomly separated with ~66% in the training set and ~33% in the testing set for model development and validation, respectively. The phase II samples were used for confirmation of the phase I multivariate model, with samples analyzed using the Olink platform. See Supplementary Methods and Supplementary Figure 2 (<http://onlinelibrary.wiley.com/doi/10.1002/art.42260>) for details regarding the selection of training samples and testing samples.

Predictive models were developed using the random forest method (R version 4.6-12 software CRAN [Comprehensive R Archive Network]) (17) with model cross-validation for the selection of tuning parameters implemented by caret (R version 6.0-77 CRAN) (18). Case samples were defined as samples collected within 0.5 years before diagnosis from RA subjects. Healthy control samples were defined as samples from healthy control subjects. The final models were applied to all available samples to model the

probability of RA diagnosis, with classification according to cutoffs determined from the training model.

## RESULTS

**Overview of subjects and serum samples.** Demographic characteristics of RA subjects, ReA subjects, and healthy control subjects in the overall study and in the serum sample sets are shown in Table 1. RA subjects and ReA subjects were predominately male, consistent with the active component military population. There was a higher proportion of Black subjects among RA subjects than ReA subjects. RA subjects were older than ReA subjects (mean 37 and 30 years, respectively, in the overall study). These demographic characteristics were similar in the overall study population and in the 2 serum sample sets across groups, with the exception of ReA subjects with samples in the serum sample sets being younger on average than the overall study population.

The timing of sample collection relative to diagnosis is shown in Supplementary Table 1 (<http://onlinelibrary.wiley.com/doi/10.1002/art.42260>).

**Soluble PD-1 and SOMAscan platform analytes in the phase I sample set.** In the RA group, ReA group, and healthy control group, serum levels of soluble PD-1 across the 4 time points are shown in Figure 1A. Soluble PD-1 levels remained stable over the 4 time points in healthy controls subjects. Levels of soluble PD-1 were similar in the RA group, ReA group, and healthy control group at the most distant time points. In RA subjects, soluble PD-1 levels significantly increased at time point B ( $P = 0.0026$ ) and were elevated compared to healthy

**Table 1.** Demographic characteristics of cases included in the phase I and phase II serum sample sets\*

	No. of subjects	Age at diagnosis		Male sex, %	Race, White/Black/Hispanic/ Other, %
		Mean $\pm$ SD years	Median (range) years		
Overall study					
RA	500	37.4 $\pm$ 7.1	37 (24–58)	61	56/25/10/8
ReA	500	30.2 $\pm$ 7.6	29 (18–56)	92	70/11/10/9
Healthy control, combined	500	31.3 $\pm$ 6.7	31 (20–50)	91	64/16/11/9
RA control	250	34.6 $\pm$ 5.6	35 (23–50)	84	63/17/12/8
ReA control	250	28.0 $\pm$ 6.1	26 (20–48)	98	65/16/10/9
Phase I serum set					
CCP-2+ RA	88	35.2 $\pm$ 7.5	34 (24–54)	64	55/25/10/10
ReA	50	25.8 $\pm$ 4.9	25 (20–38)	96	84/4/10/2
Healthy control, combined	50	27.9 $\pm$ 6.3	26 (20–43)	92	70/10/10/10
RA control	25	31.7 $\pm$ 5.4	30 (23–41)	88	72/12/8/8
ReA control	25	24.2 $\pm$ 4.7	23 (20–43)	96	68/8/12/12
Phase II serum set					
ACPA+ RA†	69	40.3 $\pm$ 6.6	37 (24–54)	65	52/33/10/4
Phase I set	50	35.9 $\pm$ 7.7	35 (24–53)	74	46/28/14/12
CCP-2– RA	50	34.9 $\pm$ 6.4	33.5 (25–49)	52	62/20/12/6
ReA	50	27.1 $\pm$ 5.4	25 (21–44)	100	58/16/14/12
Healthy control	26	26.9 $\pm$ 5.4	26 (20–40)	92	46/12/8/8

\* RA = rheumatoid arthritis; ReA = reactive arthritis; CCP-2 = cyclic citrullinated peptide 2; ACPA = anti-citrullinated protein antibody.

† The remaining seropositive cases were not included in the phase I set.

control samples at time point B ( $P = 0.0011$ ). Soluble PD-1 levels further increased at time point A (closest to diagnosis) compared to time point B ( $P < 0.0001$ ). In contrast, soluble PD-1 levels in ReA subjects did not increase from time point D through time point A, but rather a small decrease was observed after diagnosis (time point A) compared to earlier time points.

Table 2 shows the statistics for analytes measured using the SOMAscan platform with an FDR of  $<0.05$  and a  $>1.5$ -fold change between samples collected at time points A and D in the RA group. Acute-phase-associated C-reactive protein (CRP) levels (Figure 1A) and serum amyloid A (SAA)- and interferon (IFN)-induced chemokines CXCL10 (Figure 1A), CXCL11, and

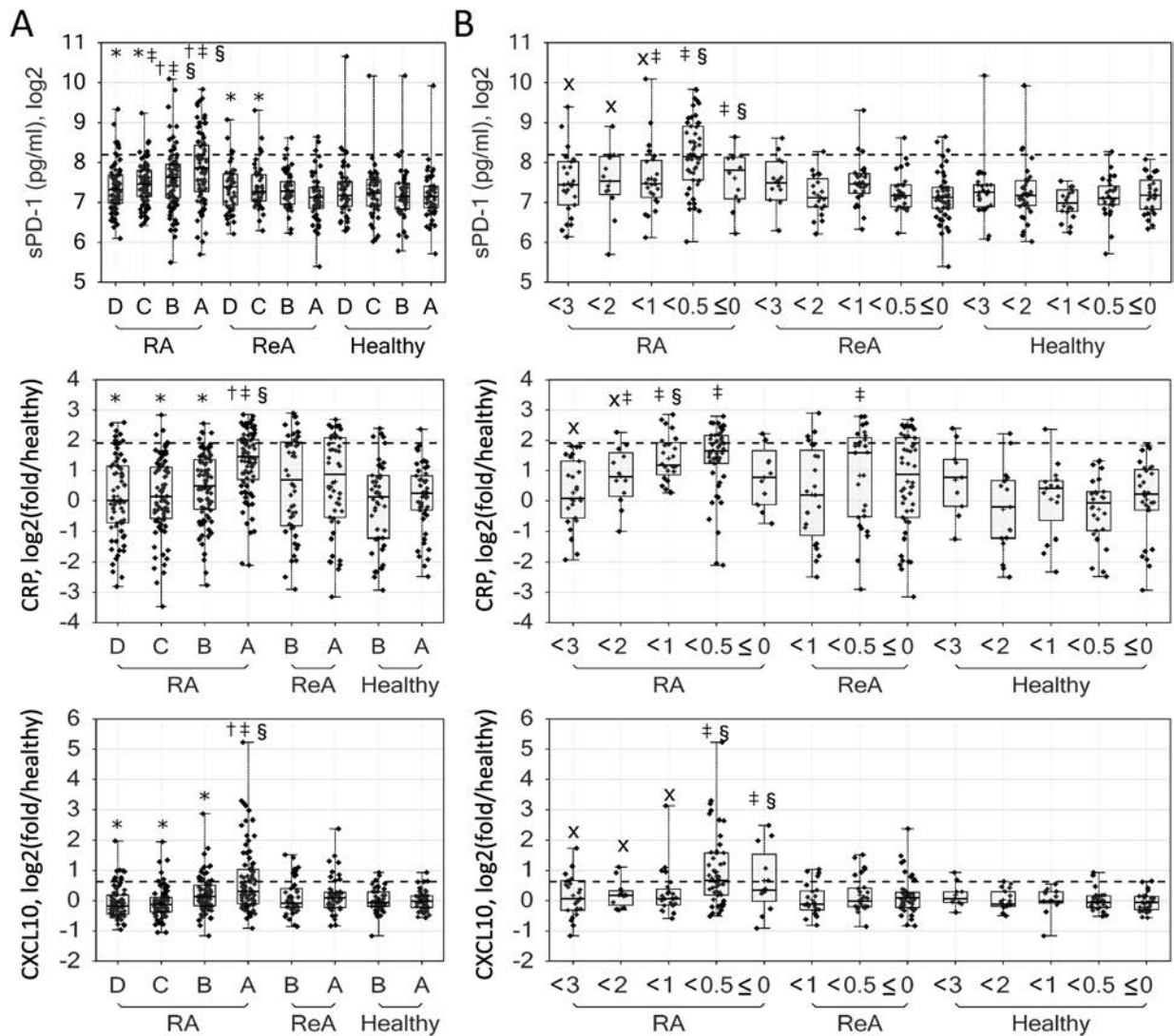


**Figure 1.** Soluble programmed cell death 1 (sPD-1) levels, C-reactive protein (CRP) levels, and inducible protein 10/CXCL10 levels by time point and years before diagnosis in the phase I sample set. Serum levels of soluble PD-1 (top), CRP (middle), and inducible protein 10/CXCL10 (bottom) ( $\log_2$ -transformed) are shown for samples collected at indicated time points by disease group (A) and for samples collected between the indicated years before diagnosis by disease group (B). In A, sample D was the first sample available in the repository; for rheumatoid arthritis (RA) subjects, sample A was the first sample available within 30 days of diagnosis or the first sample before diagnosis and samples B and C were interim samples approximately evenly distributed across the subject's service time; for reactive arthritis (ReA) subjects, samples A and B represented the first available sample after and before an initial ReA diagnosis, respectively and sample C was an interim sample between samples B and D; for healthy subjects, time points were matched to RA and ReA subject samples. In B, the time points are separated according to year intervals before the time of diagnosis (restricted to  $\leq 3$  years before diagnosis), with the  $\leq 0$  time point representing samples collected at or after diagnosis. Dashed lines show the 95th percentile of levels in the healthy control cohort. Data are shown as box plots; symbols represent individual samples. Each box represents the 25th to 75th percentiles. Lines inside the boxes represent the median. Lines outside the boxes represent the 10th and 90th percentiles. \* =  $P < 0.05$  compared to time point A. † =  $P < 0.05$  compared to healthy control samples; ‡ =  $P < 0.05$  compared to time point B within group and within subject; § =  $P < 0.05$  for RA compared to ReA within the time point; X =  $P < 0.05$  compared to samples collected  $<0.5$  years before diagnosis within group. + = mean.

**Table 2.** Elevated serum analytes in RA patients at time point A (closer to initial diagnosis) compared to other time points, and comparison between groups at time point A in the phase I sample set\*

	RA†				Time point A					
	Time point A vs. D		Time point B vs. D		RA vs. healthy control		ReA vs. healthy control		RA vs. ReA	
	Fold-change	P	Fold-change	P	Fold-change	P	Fold-change	P	Fold-change	P
CRP	2.11	<10 <sup>-4</sup>	1.19	0.0829	2.24	<10 <sup>-4</sup> ‡	1.43	0.0364	1.57	0.0032
CXCL11	2.04	<10 <sup>-4</sup>	1.39	0.0001‡	2.12	<10 <sup>-4</sup> ‡	1.49	0.0151	1.43	0.0138
CXCL10	1.68	<10 <sup>-4</sup>	1.24	0.0013‡	1.58	<10 <sup>-4</sup> ‡	1.12	0.2963	1.41	0.0007‡
CXCL13	1.57	<10 <sup>-4</sup>	1.1	0.1804	1.55	0.0001‡	1.05	0.7193	1.48	0.0004
SAA	2.21	<10 <sup>-4</sup>	1.27	0.0481	2.06	0.0032‡	2.02	0.0106	1.02	0.9438
C3a	1.76	<10 <sup>-4</sup>	1.46	0.0001‡	1.24	0.0268	1.18	0.1265	1.05	0.6181
MMP-3	1.78	<10 <sup>-4</sup>	1.24	0.0002‡	1.24	0.041	1.31	0.0230	-1.06	0.5966
Haptoglobin, mixed type	1.57	<10 <sup>-4</sup>	1.06	0.6048	1.41	0.0546	1.24	0.2903	1.14	0.4622
ITIH-4	1.55	<10 <sup>-4</sup>	1.35	0.0007‡	1.21	0.1760	1.37	0.0471	-1.13	0.3697
ApoER3	1.55	<10 <sup>-4</sup>	1.54	<10 <sup>-4</sup> ‡	-1.09	0.2703	1.01	0.9359	-1.10	0.2330
TIMP-3	1.52	<10 <sup>-4</sup>	1.29	<10 <sup>-4</sup> ‡	1.11	0.3478	1.32	0.0325	-1.18	0.1376
Hepcidin	1.51	0.0004	1.28	0.0294	-1.16	0.4325	-1.15	0.5276	-1.01	0.9428
α <sub>1</sub> -antichymotrypsin complex	1.51	<10 <sup>-4</sup>	1.28	0.004	1.17	0.1054	1.34	0.0073	-1.15	0.1531

\* Fold-change values represent the ratio of the geometric mean of the test over the reference group, with values <1 transformed to opposite of the reciprocal. ReA = reactive arthritis; CRP = C-reactive protein; SAA = serum amyloid A; MMP-3 = matrix metalloproteinase 3; ITIH-4 = inter-α trypsin inhibitor heavy chain H4; ApoER3 = apolipoprotein E receptor 3; TIMP-3 = tissue inhibitor of metalloproteinases.

† Analytes from the SOMAscan platform with a false discovery rate (FDR) <0.05 and a fold change >1.5 at time point A compared to time point D in the rheumatoid arthritis (RA) group from the phase I sample set.

‡ Indicates P value with an FDR <0.05.

CXCL13 had significant within-subject changes from time point D to time point A in the RA group and levels were also significantly higher at time point A in RA subjects compared to the healthy

control subjects (FDR <0.05). CRP levels, CXCL10 levels, and CXCL13 levels were also significantly higher in RA subjects compared to ReA subjects at time point A (FDR <0.05), with a similar

**Table 3.** Subjects predicted for imminent diagnosis of RA in the phase I set according to the time of serum biomarker evaluation\*

	After diagnosis	0 to <0.5 years before diagnosis	0.5 to <1 year before diagnosis	1 to <2 years before diagnosis	2 to <5 years before diagnosis	≥5 years before diagnosis
Soluble PD-1†						
ACPA+ RA	12 (8)	50 (48)	24 (17)	12 (8)	92 (10)	159 (8)
ReA	52 (6)	29 (3)	28 (11)	19 (5)	46 (11)	29 (3)
Healthy control	28 (0)	27 (4)	20 (0)	36 (8)	55 (5)	34 (6)
CRP†						
ACPA+ RA	12 (25)	50 (38)	24 (25)	12 (8)	91 (4)	145 (8)
ReA	50 (30)	27 (33)	23 (17)	-	-	-
Healthy control	28 (0)	26 (0)	15 (7)	17 (6)	13 (23)	1 (NA)‡
CXCL10†						
ACPA+ RA	12 (42)	50 (50)	24 (17)	12 (17)	91 (20)	145 (8)
ReA	50 (18)	27 (22)	23 (17)	-	-	-
Healthy control	28 (4)	26 (8)	15 (0)	17 (0)	13 (15)	1 (NA)‡
RF 10-analyte model§						
ACPA+ RA	12 (50)	50 (76)	24 (29)	12 (17)	91 (19)	145 (8)
Training	-	33 (91)	-	-	-	-
Testing	-	17 (47)	-	-	-	-
ReA	50 (18)	27 (22)	23 (13)	-	-	-
Healthy control	28 (0)	26 (0)	15 (0)	17 (0)	14 (0)	1 (NA)‡
Training	-	18 (0)	-	-	-	-
Testing	-	8 (0)	-	-	-	-

\* Values are the number (%) of subjects in whom a diagnosis of RA could be predicted based on the evaluation of the indicated serum analyte in samples collected within the indicated timeframe. ACPA = anti-citrullinated protein antibody (see Table 2 for other definitions).

† Cutoff for positive prediction of RA diagnosis was set as the 95th percentile of the healthy group distribution (across all available time points) for serum levels of the indicated biomarker measured using the Meso Scale Discovery platform (soluble programmed cell death 1 [PD-1]) or SOMAscan platform (CRP, CXCL10).

‡ Not available (NA) was reported when there were <5 cases within the actual group for the indicated time of serum biomarker evaluation.

§ Random forest (RF) model for SOMAscan (plus PD-1) 10-analyte panel (cutoff >80% probability), calculated for all available cases in the respective group or stratified by training/testing set for the ACPA+ RA group.

**Table 4.** AUC for the prediction of RA evaluated within 0.5 years before diagnosis\*

	RA vs. healthy control	RA vs. ReA
Phase I set, SOMAscan		
Soluble PD-1	0.85 (0.74–0.91)	0.82 (0.70–0.90)
CRP	0.88 (0.78–0.94)	0.57 (0.41–0.70)
CXCL10	0.80 (0.68–0.88)	0.72 (0.58–0.82)
RF 10-analyte model†	NA	0.83 (0.71–0.90)
Training	0.97 (0.93–1.00)	NA
Testing	0.90 (0.76–1.00)	NA
Phase II set, Olink		
CFHR-5	0.78 (0.65–0.86)	0.40 (0.25–0.53)
CXCL10	0.83 (0.71–0.90)	0.77 (0.60–0.87)
RF 8-analyte model†	NA	0.82 (0.68–0.96)
Training	0.79 (0.64–0.93)	NA
Testing	0.81 (0.67–0.96)	NA

\* Values are the area under the receiver operating characteristic curve (AUC) (95% confidence interval) for the prediction of rheumatoid arthritis (RA) within 6 months of actual diagnosis in RA cases compared to the indicated reference group for the indicated predictor evaluated within the 0 to <0.5-year timeframe. Sample sizes for RA, healthy control, and reactive arthritis (ReA) groups were 50, 27, and 29 for the MSD platform; 50, 26, and 21 for the SOMAscan platform; and 58, 26, and 18 for the Olink platform, respectively. All AUC values were significant at  $P < 0.05$ , except for the AUC for C-reactive protein (CRP) level in RA versus ReA cases, and the AUC for complement factor h-related protein 5 (CFHR5) in RA versus ReA cases. PD-1 = programmed cell death 1; NA = not applicable.

† Random forest (RF) model for SOMAscan 10-analyte panel and Olink 8-analyte panel, split by the subset used to train the model (for RA compared to healthy control) and the application of the model to the reserved testing subsets.

trend ( $P < 0.05$ ) for CXCL11 levels but not for SAA. Among these 5 analytes, levels of CXCL10 and CXCL11 were also higher (FDR <0.05) at time point B compared to time point D in the RA group. Levels of additional acute-phase proteins, including  $\alpha$ 1-antichymotrypsin, C3a, haptoglobin, and hepcidin, plus levels of matrix metalloproteinase 3, were also significantly higher (FDR <0.05) at time point A compared to time point D in the RA group, but the levels at time point A were not significantly higher compared to healthy controls. Osteomodulin levels were significantly lower (FDR <0.05) at time point A compared to time point D in the RA group, with levels at time point A being significantly lower than in the healthy control group.

A refined view of the prediagnosis data focusing on the 3-year period before diagnosis (Figure 1B) showed that mean soluble PD-1 levels were stable between 3 and 0.5 years before diagnosis in RA cases, although mean concentrations were higher than those in the healthy control group during this timeframe. Mean soluble PD-1 levels then increased 50% in RA cases in the 0.5 years before diagnosis. CRP level increases became apparent between 1 and 2 years before diagnosis and were significant compared to healthy control levels at this time span ( $P < 0.05$ ), with levels increasing through <0.5 years before diagnosis. Samples postdiagnosis were not significantly different than those from healthy controls. The increase in CXCL10 levels in RA cases was not observed until <0.5 years before diagnosis, but these levels did not decrease postdiagnosis, as was observed for CRP levels.

**Univariate classification in phase I.** The percentage of subjects predicted to be diagnosed with RA based on high levels (i.e., >95th percentile of healthy control levels) of soluble PD-1,

CRP, and CXCL10 in serum samples from various timeframes are shown in Table 3. A higher proportion of seropositive RA subjects had high levels of soluble PD-1 (48%), CRP (38%), and CXCL10 (50%) <0.5 years before diagnosis compared to healthy control subjects in the respective timeframe (4%, 0%, and 8%, respectively). In ReA subjects, soluble PD-1 specificity remained high but specificity was reduced for CRP levels and CXCL10 levels, with 3%, 33%, and 22% of ReA case samples from <0.5 years before diagnosis having high levels, respectively. For samples collected between 0.5 and <1 year before diagnosis, the model sensitivity for classifying RA diagnosis dramatically decreased to <25% for any of the analytes.

Across a range of predictor cutoffs, the area under the receiver operating characteristic curve (AUC) for samples collected <0.5 years before diagnosis ranged from 0.80 (CXCL10) to 0.88 (CRP level) for RA subjects compared to healthy controls and ranged from 0.57 (CRP) to 0.82 (soluble PD-1) for RA subjects compared to ReA subjects (Table 4 and Supplementary Figure 3, <http://onlinelibrary.wiley.com/doi/10.1002/art.42260>). For example, choosing a less restrictive CRP level cutoff of 1.22 (log<sub>2</sub>-transformed) RFUs increased the sensitivity for RA diagnosis to 76% (from 38% compared to more than the 95th percentile of healthy controls) while reducing the specificity compared to healthy controls to 90% and the specificity compared to ReA cases to 44%.

**Phase I multivariate modeling for the prediction of RA diagnosis.** Multivariate models for the prediction of RA diagnosis were generated using random forest modeling and were based on serum samples collected <0.5 years before diagnosis. An initial model was generated including all 498 analytes in the

**Table 5.** Subjects predicted for imminent diagnosis of RA in the confirmation phase II sample set according to the time of serum biomarker evaluation\*

	After diagnosis	0 to <0.5 years before diagnosis	0.5 to <1 year before diagnosis	1 to <2 years before diagnosis	2 to <5 years before diagnosis	≥5 years before diagnosis
<b>CFHR-5†</b>						
ACPA+ RA	11 (45)	58 (34)	14 (29)	25 (44)	27 (22)	44 (9)
ACPA- RA	12 (33)	35 (31)	0 (NA)‡	2 (NA)‡	45 (18)	0 (NA)‡
ReA	49 (45)	18 (39)	8 (13)	17 (24)	6 (0)	0 (NA)‡
Healthy control	-	26 (4)	-	-	-	-
<b>CXCL10†</b>						
ACPA+ RA	11 (36)	58 (34)	14 (21)	25 (20)	27 (19)	44 (2)
ACPA- RA	12 (17)	35 (6)	0 (NA)‡	2 (NA)‡	45 (0)	0 (NA)‡
ReA	49 (8)	18 (11)	8 (0)	17 (6)	6 (0)	0 (NA)‡
Healthy control	-	26 (4)	-	-	-	-
<b>RF 8-analyte model (0.85 cutoff)§</b>						
ACPA+ RA	11 (45)	58 (69)	14 (21)	25 (28)	27 (22)	44 (16)
Training	-	27 (74)	-	-	-	-
Testing	-	20 (60)	-	-	-	-
ACPA <sup>high</sup>	-	11 (73)	-	-	-	-
CCP-2- RA	12 (25)	35 (14)	0 (NA)‡	2 (NA)‡	45 (9)	0 (NA)‡
ReA	49 (29)	18 (17)	8 (13)	17 (18)	6 (17)	0 (NA)‡
Healthy control	-	26 (4)	-	-	-	-
<b>RF 8-analyte model (0.95 cutoff)§</b>						
ACPA+ RA	11 (18)	58 (50)	14 (14)	25 (28)	27 (11)	44 (5)
Training	-	27 (44)	-	-	-	-
Testing	-	20 (45)	-	-	-	-
ACPA <sup>high</sup>	-	11 (73)	-	-	-	-
CCP-2- RA	12 (25)	35 (9)	0 (NA)‡	2 (NA)‡	45 (9)	0 (NA)‡
ReA	49 (20)	18 (11)	8 (0)	17 (12)	6 (17)	0 (NA)‡
Healthy control	-	26 (0)	-	-	-	-

\* Values are the number (%) of cases (within the total number of cases for the indicated group) in whom a diagnosis of rheumatoid arthritis (RA) could be predicted based on evaluation of the indicated serum biomarker from the indicated timeframe. CFHR-5 = complement factor h-related protein 5; ACPA = anti-citrullinated protein antibody; ReA = reactive arthritis; CCP-2 = cyclic citrullinated peptide 2.

† Cutoff for positive prediction of RA diagnosis was set as the 95th percentile of the healthy group distribution (across all available time points) for serum levels of the indicated cytokine measured using Olink proteomics platforms.

‡ Not available (NA) was reported when there were <5 cases within the actual group for the indicated time of serum biomarker evaluation.

§ Random forest (RF) model for Olink 8-analyte panel (cutoff >0.85 or >0.95 probability), calculated for all available cases in a respective group, or stratified by training or testing set for the ACPA+ RA group and the ACPA<sup>high</sup> cases from phase I sample set that were excluded from training.

training set of 33 subjects from the seropositive RA group and 18 subjects from the healthy control group. The AUC for the selected model was 0.93 (95% confidence interval [95% CI] 0.86–0.99). The top 10 most important analytes in this initial training model, based on mean decreases in Gini coefficients (aggrecan, CRP, CXCL9, CXCL10, CXCL13, fibrinogen D-dimer, interleukin-7 [IL-7], granulocyte-macrophage colony-stimulating factor [GM-CSF], stem cell factor soluble receptor, soluble PD-1), were included in the final modeling for the training set, yielding an AUC of 0.97 (95% CI 0.93–1.00) for the selected model (Table 4). Applying this model to the testing set yielded an AUC of 0.90 (95% CI 0.76–1.00). This final phase I 10-analyte model was applied to all available samples across groups and timeframes to calculate the probability of positive RA diagnosis using the model. The AUC for the comparison of RA and ReA for samples collected in the timeframe of <0.5 years before diagnosis was 0.83 (95% CI 0.71–0.90).

The proportion of cases that would be classified for RA diagnosis based on a serum sample from the indicated timeframe with a probability cutoff of >0.80 are shown in Table 5. In the seropositive RA group for samples collected <0.5 years before diagnosis, 76% of all cases were above the cutoff (model sensitivity), whereas no subjects in the healthy control group were above the cutoff. The specificity relative to ReA diagnosis was lower, with 22% of ReA subjects above the cutoff for samples collected <0.5 years prediagnosis. Lower sensitivity was observed for samples collected further from diagnosis, with only 8% sensitivity for an RA diagnosis detected using samples collected ≥5 years before diagnosis (compared to 29% using samples collected between 0.5 and <1 year prediagnosis). Model sensitivity also decreased for the evaluation of samples collected after diagnosis. Model sensitivities and specificities for the prediction of RA using samples collected within 0.5 years of diagnosis at various probability cutoff points are shown in Supplementary Figure 3 (<http://onlinelibrary.wiley.com/doi/10.1002/art.42260>).

**Model confirmation for RA diagnosis prediction.** The phase II set of serum samples was analyzed using the Olink platform for confirmation of the phase I 10-analyte model. However, 4 analytes in the model were not available on the Olink platform. Comparing samples analyzed using both SOMAscan and Olink platforms, the top correlations of these 4 analytes (CRP level, D-Dimer, GM-CSF, and soluble PD-1) with measurements on the Olink platform were complement factor h-related protein 5 (CFHR-5), CXCL9, CXCL10, and SAA4, with Spearman's correlation coefficients of 0.65, 0.71, 0.47, and 0.54, respectively. CFHR-5 and SAA4 were added into the analyte set for model retraining with an 8-analyte predictor set.

The model was trained with 27 serum samples collected <0.5 years before diagnosis from seropositive RA cases and 14 samples from healthy controls, resulting in a selected model with an AUC of 0.79 (95% CI 0.64–0.93) and probability cutoff of 0.85 (Table 4). This model was applied to the seropositive RA testing set of samples collected <0.5 years before diagnosis, with an AUC of 0.83 (95% CI 0.69–0.97). The proportion of cases positively classified for evaluation based on samples from various timeframes is shown in Table 5.

For all seropositive RA subjects, including the training set and testing set and the ACPA-high cases that were excluded from training, the sensitivity for proper classification of RA diagnosis was 69%, with 4% of samples from healthy controls and 17% of samples from ReA subjects collected <0.5 years before diagnosis classified as positive. Positive classification of RA diagnosis decreased between 16% and 28% for the evaluation of seropositive RA subject samples collected during the timeframes of between 0.5 and <1 year through >5 years before diagnosis. The model did not successfully classify seronegative RA subjects based on either samples collected <0.5 years before diagnosis or those collected post-diagnosis, with 14% and 25% positivity, respectively.

The confirmation model had only slightly lower sensitivity for RA cases based on the timeframe of <0.5 years before diagnosis for sample collection (69%) compared to the phase I model (76%) but had better performance with respect to sensitivity for RA cases in the respective, independent testing sets (60% and 47%). To achieve 100% specificity, as observed in the phase I model, an alternate probability cutoff of 0.95 could be used in the phase II model, with sensitivity reduced to 50% (Supplementary Figure 3, <http://onlinelibrary.wiley.com/doi/10.1002/art.42260>). Although improving specificity from 96% to 100% may seem modest, in the context of the low incidence rate of RA diagnosis in the general population, the implications on positive predictive values (PPVs) are dramatic (<1% versus 100% PPV) (data not shown). There were no significant associations of sex or race with the prediction of imminent RA diagnosis based on serum samples collected between 0 and <0.5 years before diagnosis (Supplementary Table 2, <http://onlinelibrary.wiley.com/doi/10.1002/art.42260>).

In the phase I set, univariate models using SOMAscan analytes also had higher sensitivities compared to Olink analytes in

the phase II set (e.g., for CXCL10 [50% versus 34%]) and had similar specificities for healthy controls and ReA subjects and similar specificities compared to later timeframes for seropositive RA cases (Table 5). In the phase II analysis, CXCL10 was also specific with respect to seronegative RA, with only 6% of seronegative cases predicted as positive for RA on samples collected between 0 and <0.5 years before diagnosis. Predictions for RA diagnoses were also presented for the CFHR-5 univariate analysis from the phase II sample set, with similar patterns compared to CRP levels in the phase I sample set, albeit with lower sensitivity for seropositive RA based on samples collected <0.5 years before diagnosis, with neither model providing significant discrimination between RA and ReA (Table 4 and Table 5).

## DISCUSSION

Leveraging the longitudinal collection of serum samples from US active component military personnel, we were able to evaluate changes in serum proteomic profiles up to 10 years before diagnosis in individuals who were eventually diagnosed as having RA or ReA.

The most specific predictor of seropositive RA diagnosis in both univariate and multivariate modeling was serum-soluble PD-1, although sensitivity was limited to identifying ~50% of seropositive RA cases when testing samples collected <0.5 years before diagnosis. Prediction for RA diagnosis was very specific, with <5% of ReA cases and healthy control subjects predicted for RA diagnosis based on serum collected <0.5 years before diagnosis. However, soluble PD-1 could be a useful predictor of RA diagnosis only when samples were collected close to diagnosis, as even samples tested 0.5 to <1 year before diagnosis greatly diminished sensitivity to 17%. Samples collected >1 year before diagnosis had sensitivity <10%. Elevations of soluble PD-1 levels were also lower in samples collected after diagnosis, when the recently diagnosed patients would have been able to receive antiinflammatory or immunosuppressant treatments. As a univariate predictor, CXCL10 had similar sensitivity to soluble PD-1 for RA diagnosis but the specificity of CXCL10 for ReA diagnosis was weaker. CRP level had weaker sensitivity and lower specificity for RA diagnosis than either soluble PD-1 and CXCL10.

Multivariate predictors achieved superior sensitivity for seropositive RA diagnosis compared to soluble PD-1 (69% versus 48%), but at the expense of reduced specificity for ReA (83% versus 96%). Given that most cases of ReA are triggered by bacterial infections, it is possible that healthy individuals who have inflammatory responses to infection mimicking the ReA profile might also be predicted for RA diagnosis. However, this moderate reduction in specificity could be offset if ACPA seropositivity was corequired, as most imminent ReA cases and healthy individuals are seronegative for ACPA. Indeed, when evaluating reactivity to specific citrullinated peptide antigens, positive reactivity preceded or was concurrent with the time point, demonstrating positive prediction of RA diagnosis for most of those



subjects who were reactive to at least 1 citrullinated peptide antigen (data not shown).

The generalizability of these findings from active component military personnel to the general population is not straightforward. The short time from detectable elevation in both acute-phase analytes (e.g., CRP level, CFHR-5) and lymphocyte-associated analytes (e.g., soluble PD-1, CXCL10) to RA diagnosis may be a consequence of military discipline and associated physical rigors, in which personnel should be required to have a medical examination at the first signs of disability caused by RA, in addition to required periodic medical screenings. Consistent with age restrictions for active component military personnel, this cohort of RA cases had younger age at RA diagnosis (median 37 years) (16) compared to the median age at onset of 58 years in the general population (19). Despite moderate overrepresentation of men and Black race in the seropositive RA military cohort compared to the general population, there was not a significant association between sex or race and the sensitivities for the prediction of imminent RA diagnosis.

Early intervention, even months before identifiable clinical disease, could stop disease progression and potentially irreversible joint damage. Although ACPA seropositivity provides strong support for RA diagnoses, seropositivity can be observed more than a decade before the onset of disease (7,11). CRP level is nonspecific and is elevated across a range of inflammatory conditions. A specific test with sufficient sensitivity, as presented here, could potentially help to confirm imminent identifiable clinical disease in at-risk individuals, particularly those with known ACPA seropositivity. A critical follow-up study prior to such application should confirm the performance of the tests in the general (nonmilitary) population, including specificity compared to additional inflammatory conditions.

Specifically for active component military personnel, those previously identified as ACPA seropositive could be regularly screened for RA predictors, particularly before operational deployment. This could reduce the risk of putting personnel with a high probability of imminent debilitating arthritis into a situation that jeopardizes the mission. The specificity of the tests for RA compared to ReA could be important in determining whether a patient's arthralgia would lead to a chronic lifelong disability (i.e., RA) compared to a more transient, albeit debilitating condition (i.e., ReA), in which the patient could potentially return to active component military service.

Contributing to the biologic understanding of the clinical onset of RA, it has been established that a break in tolerance allowing for autoantibody production can occur years before the clinical onset of arthralgia and RA (7,11). In the current study, significant elevations of mean CRP levels, soluble PD-1 levels, and CXCL10 levels were observable within 2, 1, and <0.5 years before diagnosis, respectively, in seropositive RA cases. However, high levels relative to levels in healthy controls were only observed in a small proportion of cases (<25%) with samples collected at timeframes >0.5 years before diagnosis, with the

greatest elevations occurring within 0.5 years of diagnosis. These observations suggest that systemic inflammatory responses begin to increase starting <2 years before diagnosis, after ACPA seropositivity is established. Of note, soluble PD-1 demonstrated the highest specificity for RA relative to ReA, perhaps indicating a specific role of highly activated, PD-1-expressing T cells, including peripheral helper T cells, found in the synovium of RA cases (20,21) as well as pre-RA cases (15).

Other analytes that were elevated at the time point closest to diagnosis included additional acute-phase proteins (SAA, haptoglobin, hepcidin, inter- $\alpha$ -trypsin inhibitor heavy chain 4) and interferon-induced lymphocyte chemoattractants (CXCL9, CXCL11, and CXCL13). The prediction model contained acute-phase proteins (CRP, fibrinogen D-Dimer), IFN-induced chemokines (CXCL9, CXCL10, CXCL13), the lymphocyte survival factor IL-7, and GM-CSF, which supports maturation and activation of monocytes that in turn are sources of CXCL9 and CXCL10. High levels of PD-1-expressing T cells, namely follicular helper T cells and peripheral helper T cells, are sources of CXCL13 (20). In the model, aggrecan is the only analyte that decreases closer to diagnosis. It is an integral matrix-associated protein in cartilage that protects type II collagen from proteolytic cleavage (22). Citrullinated aggrecan, which can be found in the cartilage of RA patients, is a target of autoreactive T cells (23) and ACPA (24) in some RA patients.

Although increases in levels of inflammatory cytokines may occur earlier compared to ACPA seropositivity, as previously reported in an independent military cohort (7), high levels of RA-specific cytokines are only observed close to diagnosis. In this prior study (7), a predictor with at least 10 analytes elevated at any time (up to 10 years) prediagnosis yielded 96% specificity, but with very low sensitivity (16%) for seropositive RA diagnosis. The inability to attain both high sensitivity and specificity is likely a consequence of including samples collected months or many years prediagnosis rather than restricting sample collection to a more restrictive timeframe immediately preceding diagnosis.

Our case definitions relied on International Classification of Diseases, Ninth Revision, Clinical Modification (ICD-9-CM) codes without accessing patient records, which is why our primary analyses focused on RA subjects who were selected according to ACPA seropositivity. It is possible that disease misclassification due to reliance on ICD-9-CM codes could have limited the upper bound of sensitivity (25), particularly when evaluating ACPA seronegative subjects.

Despite expected overmodeling in phase I multivariate modeling from double-usage of the training set, as demonstrated by the modest reduction in AUC in the testing set, a well-performing model emerged for confirmation in the phase II set. The risk of overmodeling in phase II was minimized by the sample selection strategy for training and testing sets, together with modifications to the model constituents and proteomic platform used. Indeed, the model AUC numerically increased between training and testing, confirming that the approach successfully limited overmodeling.

Modeling was also attempted to achieve greater specificity for RA diagnosis within 6 months compared to the reference of >3 years before diagnosis, including multinomial models that also included the healthy control cohort. Despite improved specificity of >95% for samples collected >3 years before diagnosis, specificity compared to healthy controls was reduced (data not shown), with modest decreases in specificity compared to healthy controls that was unacceptable for practical utility.

In summary, we have demonstrated that the imminent diagnosis of RA could be classified with high specificity compared to healthy control subjects and ReA subjects based on a panel of cytokines measured in serum samples collected within 6 months prior to actual diagnosis. The predictive power diminishes dramatically when evaluating serum samples collected at time points further from diagnosis, limiting the practical utility of any diagnostic test to identifying only cases that would develop into clinically diagnosed RA in the very near term of <6 months. Although potential applications in the general population may be limited, practical applications in active component military personnel could be envisioned.

## AUTHOR CONTRIBUTIONS

All authors were involved in drafting the article or revising it critically for important intellectual content, and all authors approved the final version to be published. Dr. Loza had full access to all of the data in the study and takes responsibility for the integrity of the data and the accuracy of the data analysis.

**Study conception and design.** Loza, Nagpal, Laird, Alcalá, Rao, Riddle, Porter.

**Acquisition of data.** Loza, Nagpal, Cole, Laird, Alcalá, Rao, Riddle, Porter.

**Analysis and interpretation of data.** Loza, Nagpal, Laird, Riddle, Porter.

## ROLE OF THE STUDY SPONSOR

Janssen Research and Development had a role in the study design and in the collection, analysis, and interpretation of the data, the writing of the manuscript, and the decision to submit the manuscript for publication. Publication of this article was contingent upon approval by Janssen.

## REFERENCES

- Komatsu N, Takayanagi H. Inflammation and bone destruction in arthritis: synergistic activity of immune and mesenchymal cells in joints. *Front Immunol* 2012;3:77.
- Breedveld F. The value of early intervention in RA—a window of opportunity. *Clin Rheumatol* 2011;30 Suppl:S33–39.
- Cush JJ. Early rheumatoid arthritis—is there a window of opportunity? *J Rheumatol Suppl* 2007;80:1–7.
- Bosello S, Fedele AL, Peluso G, et al. Very early rheumatoid arthritis is the major predictor of major outcomes: clinical ACR remission and radiographic non-progression. *Ann Rheum Dis* 2011;70:1292–5.
- Kim D, Choi CB, Lee J, et al. Impact of early diagnosis on functional disability in rheumatoid arthritis. *Korean J Intern Med* 2017;32:738–46.
- Kyburz D, Gabay C, Michel BA, et al. The long-term impact of early treatment of rheumatoid arthritis on radiographic progression: a population-based cohort study. *Rheumatology (Oxford)* 2011;50:1106–10.
- Deane KD, O'Donnell CI, Hueber W, et al. The number of elevated cytokines and chemokines in preclinical seropositive rheumatoid arthritis predicts time to diagnosis in an age-dependent manner. *Arthritis Rheum* 2010;62:3161–72.
- Del Puente A, Knowler WC, Pettitt DJ, et al. The incidence of rheumatoid arthritis is predicted by rheumatoid factor titer in a longitudinal population study. *Arthritis Rheum* 1988;31:1239–44.
- Hughes-Austin JM, Deane KD, Derber LA, et al. Multiple cytokines and chemokines are associated with rheumatoid arthritis-related autoimmunity in first-degree relatives without rheumatoid arthritis: Studies of the Aetiology of Rheumatoid Arthritis (SERA). *Ann Rheum Dis* 2013;72:901–7.
- Karlson EW, Chibnik LB, Tworoger SS, et al. Biomarkers of inflammation and development of rheumatoid arthritis in women from two prospective cohort studies. *Arthritis Rheum* 2009;60:641–52.
- Kelmenson LB, Wagner BD, McNair BK, et al. Timing of elevations of autoantibody isotypes prior to diagnosis of rheumatoid arthritis. *Arthritis Rheumatol* 2020;72:251–61.
- Kokkonen H, Söderström I, Rocklöv J, et al. Up-regulation of cytokines and chemokines predates the onset of rheumatoid arthritis. *Arthritis Rheum* 2010;62:383–91.
- Nielen MM, van Schaardenburg D, Reesink HW, et al. Simultaneous development of acute phase response and autoantibodies in preclinical rheumatoid arthritis. *Ann Rheum Dis* 2006;65:535–7.
- Rantapää-Dahlqvist S, de Jong BA, Berglin E, et al. Antibodies against cyclic citrullinated peptide and IgA rheumatoid factor predict the development of rheumatoid arthritis. *Arthritis Rheum* 2003;48:2741–9.
- Guo Y, Walsh AM, Canavan M, et al. Immune checkpoint inhibitor PD-1 pathway is down-regulated in synovium at various stages of rheumatoid arthritis disease progression. *PLoS One* 2018;13:e0192704.
- Porter CK, Riddle MS, Laird RM, et al. Cohort profile of a US military population for evaluating pre-disease and disease serological biomarkers in rheumatoid and reactive arthritis: rationale, organization, design, and baseline characteristics. *Contemp Clin Trials Commun* 2020;17:100522.
- Liaw A, Wiener M. Classification and Regression by randomForest. *R News* 2002;2:18–22.
- Kuhn M. Caret package. *J Stat Softw* 2008;285.
- Innala L, Berglin E, Moller B, et al. Age at onset determines severity and choice of treatment in early rheumatoid arthritis: a prospective study. *Arthritis Res Ther* 2014;16:R94.
- Rao DA, Gurish MF, Marshall JL, et al. Pathologically expanded peripheral T helper cell subset drives B cells in rheumatoid arthritis. *Nature* 2017;542:110–4.
- Greisen SR, Rasmussen TK, Stengaard-Pedersen K, et al. Increased soluble programmed death-1 (sPD-1) is associated with disease activity and radiographic progression in early rheumatoid arthritis. *Scand J Rheumatol* 2014;43:101–8.
- Pratta MA, Yao W, Decicco C, et al. Aggrecan protects cartilage collagen from proteolytic cleavage. *J Biol Chem* 2003;278:45539–45.
- Law SC, Street S, Yu CH, et al. T-cell autoreactivity to citrullinated autoantigenic peptides in rheumatoid arthritis patients carrying HLA-DRB1 shared epitope alleles. *Arthritis Res Ther* 2012;14:R118.
- Glant TT, Ocsko T, Markovics A, et al. Characterization and localization of citrullinated proteoglycan aggrecan in human articular cartilage. *PLoS One* 2016;11:e0150784.
- Kim SY, Servi A, Polinski JM, et al. Validation of rheumatoid arthritis diagnoses in health care utilization data. *Arthritis Res Ther* 2011;13:R32.

# Phase II/III Results of a Trial of Anti-Tumor Necrosis Factor Multivalent NANOBODY Compound Ozoralizumab in Patients With Rheumatoid Arthritis

Tsutomu Takeuchi,<sup>1</sup> Masafumi Kawanishi,<sup>2</sup> Megumi Nakanishi,<sup>2</sup> Hironori Yamasaki,<sup>2</sup> and Yoshiya Tanaka<sup>3</sup>

**Objective.** To assess the efficacy and safety of subcutaneous administration of 30 mg or 80 mg of ozoralizumab plus methotrexate (MTX) in patients with rheumatoid arthritis (RA) whose disease remained active despite MTX therapy.

**Methods.** In this multicenter, double-blind, parallel-group, placebo-controlled phase II/III trial, 381 patients were randomized to receive placebo, ozoralizumab 30 mg, or ozoralizumab 80 mg, plus MTX subcutaneously injected every 4 weeks for 24 weeks. The primary end points were the response rates based on the American College of Rheumatology 20% improvement criteria (ACR20) at week 16 and change in the Sharp/van der Heijde score ( $\Delta$ SHS) from baseline to week 24.

**Results.** The proportion of patients with an ACR20 response at week 16 was significantly higher ( $P < 0.001$ ) in both ozoralizumab groups (79.6% for 30 mg, 75.3% for 80 mg), compared with placebo (37.3%); these improvements were observed from the first week of treatment. The proportion of the patients with structural nonprogression ( $\Delta$ SHS  $\leq 0$ ) was significantly higher in both ozoralizumab groups than in the placebo group. For some secondary end points, significantly greater improvements were observed starting from as early as day 3. Serious adverse events occurred in 4 patients in the ozoralizumab 30-mg group and 5 patients in the ozoralizumab 80-mg group.

**Conclusion.** In patients with active RA who received ozoralizumab in combination with MTX, the signs and symptoms of RA were significantly reduced as compared with the outcomes in those receiving placebo. Ozoralizumab demonstrated acceptable tolerability with no new safety signals when compared with other antibodies against tumor necrosis factor.

## INTRODUCTION

Rheumatoid arthritis (RA) treatment has greatly improved the management of RA through a standardized treatment algorithm, treat-to-target strategy, and drugs such as biologic disease-modifying antirheumatic drugs (bDMARDs) and targeted synthetic DMARDs. Despite advances in disease management, there is still an unmet therapeutic need in RA, as current therapeutic agents sometimes only achieve partial response, and only 20–25% of patients achieve complete remission (1,2).

Tumor necrosis factor (TNF) is deeply implicated in the pathogenesis of RA (3). Ozoralizumab is a next-generation anti-TNF antibody. It is a 38-kd trivalent NANOBODY compound (Ablynx originally discovered and performed initial development of the

NANOBODY compound ozoralizumab, and NANOBODY is a registered trademark of Ablynx NV, an affiliate of Sanofi) consisting of the 2 humanized anti-human TNF VHH antibodies and 1 humanized anti-human serum albumin (HSA) VHH antibody. VHH antibodies are derived from a special type of heavy-chain antibody naturally produced by llamas and other camelids (4,5). Ozoralizumab demonstrates inhibitory activity against human TNF and demonstrates a specific binding ability to HSA, which leads to potent neutralization of the action of TNF and prolonged serum half-life by interacting with serum albumin (6–10). Murine surrogate NANOBODY molecules have been shown to accumulate in inflamed tissue in a mouse collagen-induced arthritis model (6). This accumulation in inflamed tissue is expected to occur with the equivalent compound in humans.

Supported by Taisho Pharmaceutical Co., Ltd.

<sup>1</sup>Tsutomu Takeuchi, MD, PhD: Keio University School of Medicine, Tokyo, and Saitama Medical University, Saitama, Japan; <sup>2</sup>Masafumi Kawanishi, MS, Megumi Nakanishi, MS, Hironori Yamasaki, PhD: Taisho Pharmaceutical Co., Ltd., Tokyo, Japan; <sup>3</sup>Yoshiya Tanaka, MD, PhD: University of Occupational and Environmental Health Japan, Kitakyushu, Japan.

Author disclosures are available at <https://onlinelibrary.wiley.com/action/downloadSupplement?doi=10.1002%2Fart.42273&file=art42273-sup-0001-Disclosureform.pdf>.

Address correspondence via email to Yoshiya Tanaka, MD, PhD, at [tanaka@med.uoeh-u.ac.jp](mailto:tanaka@med.uoeh-u.ac.jp).

Submitted for publication March 7, 2022; accepted in revised form June 10, 2022.

Here, we report the first results of a phase II/III trial (JapicCTI identifier: 184029) to evaluate the efficacy and safety of 2 dosage regimens of ozoralizumab concomitant with methotrexate (MTX) therapy, compared with placebo, in patients with active RA who had an inadequate response to MTX treatment alone.

### PATIENTS AND METHODS

**Trial design.** The phase II/III results of the anti-TNF multivalent NANOBODY compound ozoralizumab in patients with RA (OHZORA) trial (JapicCTI identifier: 184029) was a multicenter, randomized, placebo-controlled, parallel-group confirmatory trial with a 24-week double-blind treatment period (period A) followed by a 28-week open-label treatment period (period B). Period A was conducted between September 2018 and March 2020 at 78 sites in Japan.

In period A, RA patients were randomly allocated in a 2:2:1 ratio to receive ozoralizumab 30 mg, ozoralizumab 80 mg, or placebo under double-blind conditions, administered subcutaneously every 4 weeks concomitant with MTX therapy (6–16 mg/week) for 24 weeks. The dosage and administration method were determined based on the previous phase I/II study (ClinicalTrials.gov identifier: NCT01007175). At week 16, patients who met the early escape criteria (<20% improvement from baseline in tender joint count in 68 joints [TJC68] and swollen joint count in 66 joints [SJC66]) were moved to the ozoralizumab 30-mg group from the placebo group and from the ozoralizumab

30-mg group to the 80-mg group under double-blind conditions, starting from week 20. The double-blind treatment period was followed by a 28-week open-label period, with the patients receiving placebo rerandomized (at a 1:1 ratio) to receive treatment with 30 mg or 80 mg of ozoralizumab.

**Ethics approval.** This clinical trial was conducted in accordance with the ethics principles according to the Declaration of Helsinki Act on Securing Quality, Efficacy and Safety of Products Including Pharmaceuticals and Medical Devices; and Japan’s Ministerial Ordinance on Good Clinical Practice for Drugs.

**Patients.** This trial sample included Japanese RA patients ages 20–75 years who had an inadequate response to MTX and met the American College of Rheumatology (ACR)/EULAR 2010 classification criteria for RA (11). The inclusion criteria included active RA (TJC68 score ≥6, SJC66 score ≥6, and high-sensitivity C-reactive protein [hsCRP] level of ≥0.6 mg/dl or erythrocyte sedimentation rate [ESR] ≥28 mm/hour), MTX treatment at least 12 weeks prior to the baseline visit, and no change in MTX dose (6–16 mg/week) for at least 6 weeks prior to the baseline visit. Patients with abnormal findings on chest radiography suggestive of a malignant tumor, infection, or interstitial pneumonia were excluded. Patients with active tuberculosis were excluded, and patients with latent tuberculosis were excluded except when anti-tuberculosis pharmacotherapy with isoniazid had been started in advance.

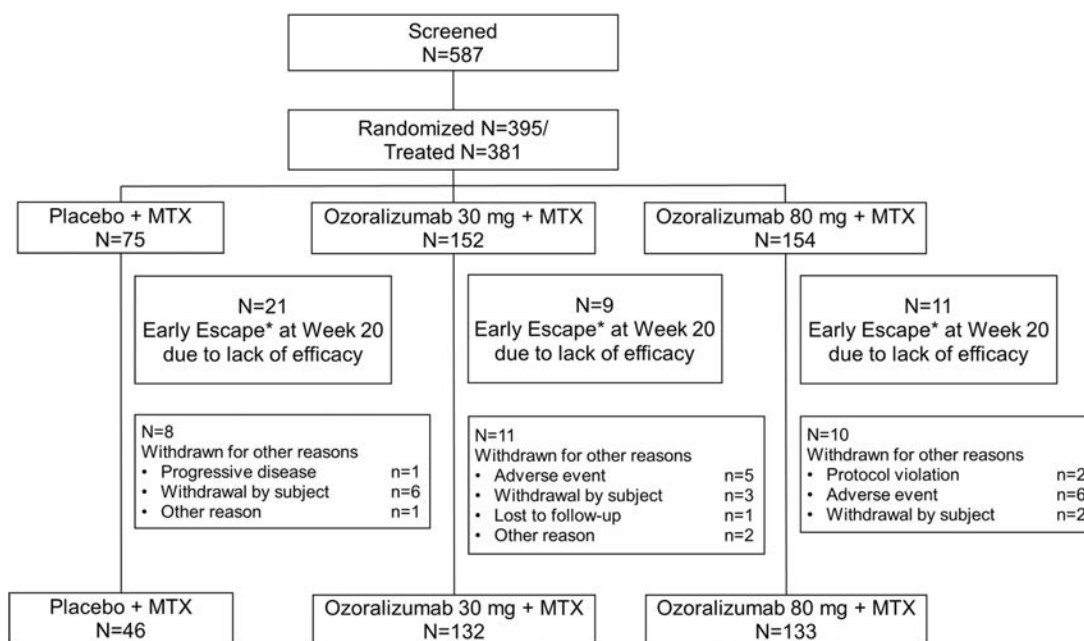


**Figure 1.** Flow chart showing the disposition of patients into groups to receive either placebo and methotrexate (MTX), ozoralizumab 30 mg and MTX, or ozoralizumab 80 mg and MTX. Early escape (\*) indicates that when improvements from baseline in tender joint count and swollen joint count at week 16 were <20%, the patient was transferred to the open-label follow-up trial (after administration of the investigational drug) at week 20.

**Outcomes.** The primary efficacy end points were the ACR criteria for 20% improvement in disease activity (ACR20) response rate at week 16 and a change from baseline in the Sharp/van der Heijde score (SHS) at week 24 ( $\Delta$ SHS). Radiography was performed at the baseline visit and at week 24 (or treatment discontinuation or week 20, for early escape). Bone erosion and joint space narrowing (JSN) were centrally and independently scored by 2 blinded radiologists (third-party assessors, as needed). To evaluate structural progression, we used  $\Delta$ SHS and the proportion of patients with structural nonprogression ( $\Delta$ SHS  $\leq 0$ ), structural remission ( $\Delta$ SHS  $\leq 0.5$ ), and  $\Delta$ SHS less than or equal to smallest detectable change (SDC) (12,13). In this trial, the SDC in SHS at week 24 was 1.0.

Secondary efficacy end points included ACR50/70 response, Disease Activity Score in 28 joints using the CRP level (DAS28-CRP), patient global assessment of disease activity (PtGA) score using a visual analogue scale [VAS], patient's assessment of pain using a VAS, Simplified Disease Activity Index (SDAI), Boolean remission, Health Assessment Questionnaire disability index (HAQ-DI), erosion score, and JSN score. In addition, pharmacodynamic end points such as hsCRP and ESR were evaluated (for all secondary end points and pharmacodynamics, see Supplementary Information, available on the *Arthritis & Rheumatology* website at <http://onlinelibrary.wiley.com/doi/10.1002/art.42273>).

**Safety assessments.** For the assessment of safety, adverse events (AEs) (including injection site reactions, severe AEs [SAEs], and AEs of special interest), body weight, vital signs,

and laboratory test results were evaluated. For the assessment of immunogenicity, we measured plasma anti-ozoralizumab antibodies and plasma ozoralizumab-neutralizing antibodies during administration of the first dose, at week 8, and at week 24 (at week 20 for patients who met the early escape criteria).

**Statistical analysis.** Sample size ( $n = 148$  for 30 mg and 80 mg ozoralizumab and  $n = 74$  for placebo) was calculated according to the results of phase II studies. The ACR20 response rates (at week 16, i.e., the primary end point) between the ozoralizumab 30 mg, ozoralizumab 80 mg, and placebo groups were assumed to be 66%, 66%, and 40%, respectively. An allocation ratio of 2:2:1 was planned for the ozoralizumab 30-mg group, ozoralizumab 80-mg group, and placebo group with 2-sided significance levels of 2.5% and statistical power of 90%, allowing for a dropout rate and exclusion rate of 10%.

In efficacy and pharmacodynamics evaluations, the full analysis set was used as the primary analysis set (for full analysis set definition, see Supplementary Information, <http://onlinelibrary.wiley.com/doi/10.1002/art.42273>). Comparisons between the placebo group and ozoralizumab group were conducted using a Cochran-Mantel-Haenszel test with history of TNF inhibitor (TNFi) usage as a stratification factor for the ACR20 response rate (week 16), and analysis of covariance, with baseline values and history of TNFi usage as covariates for  $\Delta$ SHS (week 24). For the primary analysis, the 2-sided significance level was set at 2.5% and the 2-sided confidence coefficient was set at 95%. To analyze the primary end point, multiplicity adjustment was conducted using a closed testing procedure (see

**Table 1.** Demographic characteristics and disease status of the patients at baseline assigned to receive MTX and either placebo, ozoralizumab 30 mg, or ozoralizumab 80 mg (full analysis set)\*

	Placebo (n = 75)	Ozoralizumab		Total (n = 381)
		30 mg (n = 152)	80 mg (n = 154)	
Sex, female, no. (%)	57 (76.0)	105 (69.1)	123 (79.9)	285 (74.8)
Age, years	54.3 $\pm$ 12.1	54.8 $\pm$ 11.2	55.5 $\pm$ 10.9	55.0 $\pm$ 11.2
Age <65 years, no. (%)	56 (74.7)	119 (78.3)	116 (75.3)	291 (76.4)
Weight, kg	58.4 $\pm$ 13.5	60.0 $\pm$ 12.8	57.6 $\pm$ 11.6	58.7 $\pm$ 12.5
Disease duration, years	7.6 $\pm$ 7.4	6.8 $\pm$ 6.4	7.8 $\pm$ 7.5	7.4 $\pm$ 7.1
MTX dosage, mg/week	10.2 $\pm$ 3.0	10.0 $\pm$ 2.9	10.1 $\pm$ 2.7	10.1 $\pm$ 2.8
Glucocorticoid use, no. (%)	37 (49.3)	62 (40.8)	64 (41.6)	163 (42.8)
DAS28-CRP	5.1 $\pm$ 1.0	5.2 $\pm$ 1.1	5.1 $\pm$ 0.9	5.1 $\pm$ 1.0
DAS28-ESR	5.8 $\pm$ 1.0	5.9 $\pm$ 1.0	5.8 $\pm$ 0.9	5.8 $\pm$ 1.0
TJC68	15.5 $\pm$ 9.6	16.6 $\pm$ 8.8	15.6 $\pm$ 8.9	16.0 $\pm$ 9.0
SJC66	13.2 $\pm$ 8.5	13.8 $\pm$ 7.2	12.8 $\pm$ 6.4	13.3 $\pm$ 7.2
SHS	32.2 $\pm$ 50.2	25.0 $\pm$ 30.9	27.6 $\pm$ 37.4	27.5 $\pm$ 38.0
Erosion score	17.8 $\pm$ 28.0	14.2 $\pm$ 16.4	15.2 $\pm$ 18.8	15.3 $\pm$ 20.1
JSN score	14.5 $\pm$ 23.1	10.7 $\pm$ 15.5	12.4 $\pm$ 19.4	12.1 $\pm$ 18.8
hs-CRP level, mg/dl	1.3 $\pm$ 1.7	1.6 $\pm$ 2.0	1.3 $\pm$ 1.8	1.4 $\pm$ 1.9
ESR, mm/hour	36.4 $\pm$ 17.3	40.3 $\pm$ 22.3	38.6 $\pm$ 20.6	38.8 $\pm$ 20.7
Seropositive RA, no. (%)†	64 (85.3)	140 (92.1)	136 (88.3)	340 (89.2)

\* Except where indicated otherwise, values are the mean  $\pm$  SD. MTX = methotrexate; DAS28-CRP = Disease Activity Score in 28 joints using the C-reactive protein level; ESR = erythrocyte sedimentation rate; TJC68 = tender joint count in 68 joints; SJC66 = swollen joint count in 68 joints; SHS = Sharp/van der Heijde score; JSN = joint space narrowing; hsCRP = high-sensitivity CRP.

† Seropositive rheumatoid arthritis (RA) indicates an anti-citrullinated protein antibody level  $\geq 4.5$  units/ml and/or rheumatoid factor  $>15$  IU/ml.

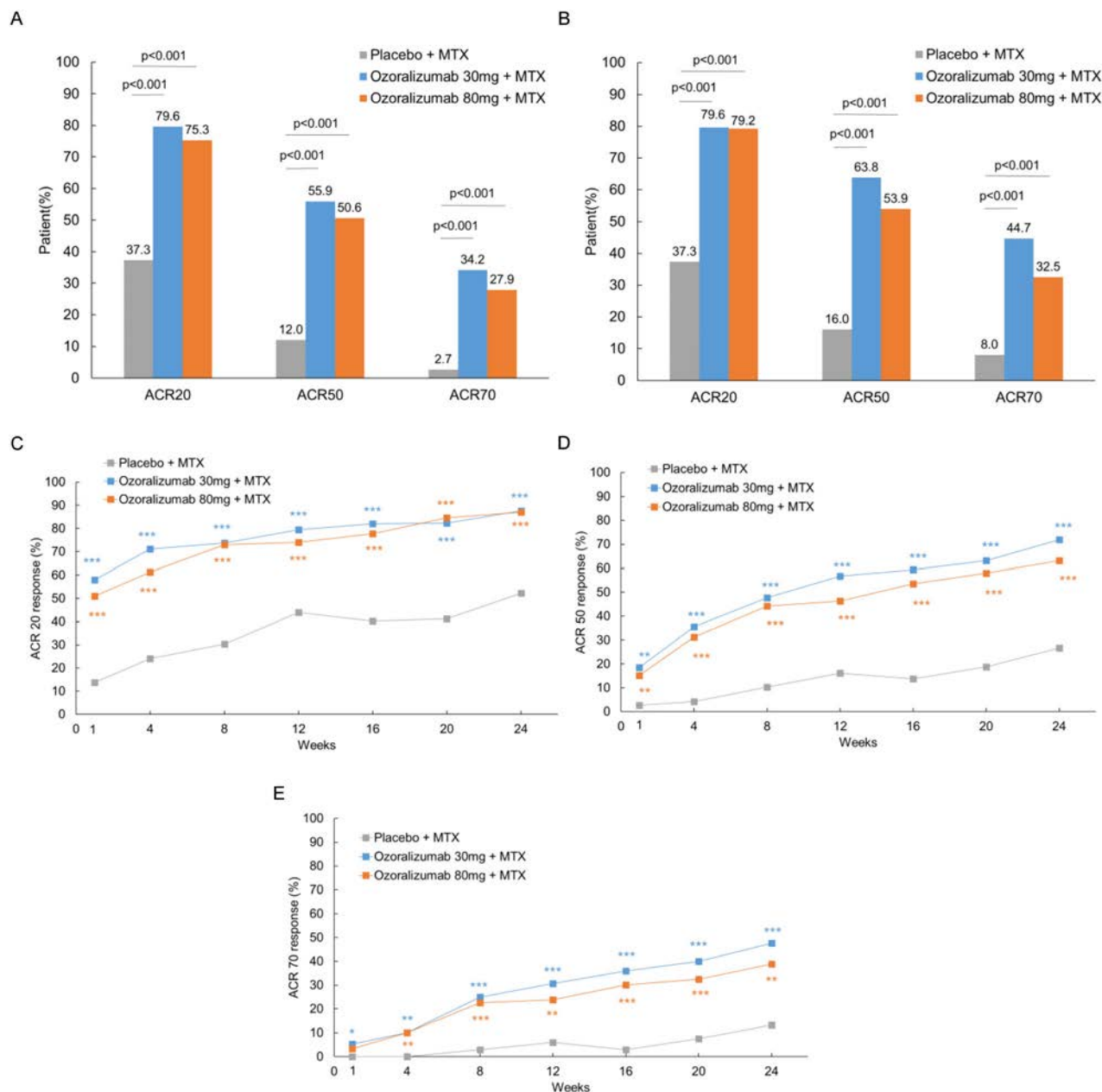


**Figure 2.** Treatment response rates based on the American College of Rheumatology 20% (ACR20), ACR50, and ACR70 improvement criteria up to week 24. **A** and **B**, ACR20, ACR50, and ACR70 improvement response rates at week 16 (**A**) and week 24 (**B**). **C–E**, Changes in ACR20 (**C**), ACR50 (**D**), and ACR70 (**E**) response rates over time. Cochran-Mantel-Haenszel test results were used as a stratification factor based on tumor necrosis factor inhibitor usage history. \* =  $P < 0.05$ ; \*\* =  $P < 0.01$ ; \*\*\* =  $P < 0.001$  versus placebo + methotrexate (MTX).

Supplementary Information, <http://onlinelibrary.wiley.com/doi/10.1002/art.42273>. For the second analysis, the 2-sided significance level was set at 5%.

The last observation carried forward method was used for missing ACR20 data and missing data for other secondary end points at weeks 16 and 24 (including early escape at week 24). A linear extrapolation method was used for SHS, erosion score, and JSN score at week 24.

The safety analysis set was used as the analysis set in the safety and immunogenicity assessments (for safety analysis set definition, see Supplementary Information, <http://onlinelibrary.wiley.com/doi/10.1002/art.42273>).

AEs were defined according to the Japanese version of the Medical Dictionary for Regulatory Activities, version 22.1. For details regarding the evaluation of immunogenicity, see Supplementary Information. Statistical analyses were performed using SAS 9.4 software.

**RESULTS**

**Patient demographic and baseline clinical characteristics.** In this trial, 587 patients were screened, and 395 patients were randomized to the placebo group,

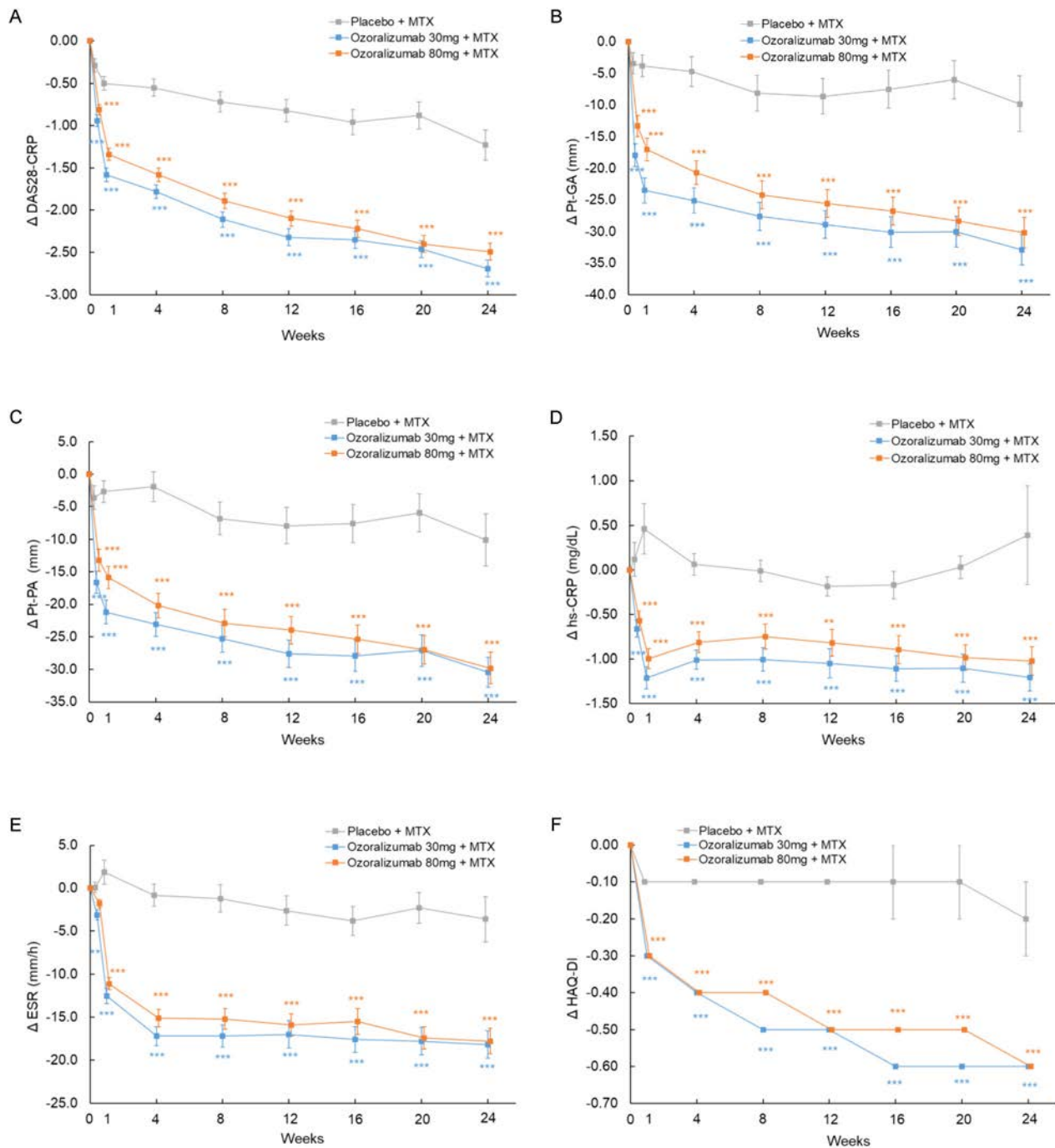


**Figure 3.** Changes from baseline in various parameters over time, including change in Disease Activity Score in 28 joints using the C-reactive protein level (DAS28-CRP) (A), patient global assessment of disease activity (PtGA) (B), patient's assessment of pain (Pt-PA) (C), high-sensitivity CRP (hsCRP) level (D), erythrocyte sedimentation rate (ESR) (E), and Health Assessment Questionnaire disability index (HAQ-DI) (F), from weeks 0 to 24. Statistical comparisons were determined with an analysis of covariance using the status of prior tumor necrosis factor inhibitor usage and baseline values as covariates. Symbols with error bars show the mean  $\pm$  SEM. \*\* =  $P < 0.01$ ; \*\*\* =  $P < 0.001$  versus placebo + methotrexate (MTX).

ozoralizumab 30 mg-group, and ozoralizumab 80-mg group. Drugs were administered according to the allocation of 381 patients (placebo [ $n = 75$ ], ozoralizumab 30 mg [ $n = 152$ ], and ozoralizumab 80 mg [ $n = 154$ ]). Early escape criteria applied to 21 patients in the placebo group, 9 patients in the ozoralizumab

30-mg group, and 11 patients in the ozoralizumab 80-mg group. A total of 29 patients discontinued for reasons other than early escape. The overall rate of trial continuation up to week 24 (including patients who met the early escape criteria at week 20) was 92.4% (Figure 1). Among patients included in the full analysis set

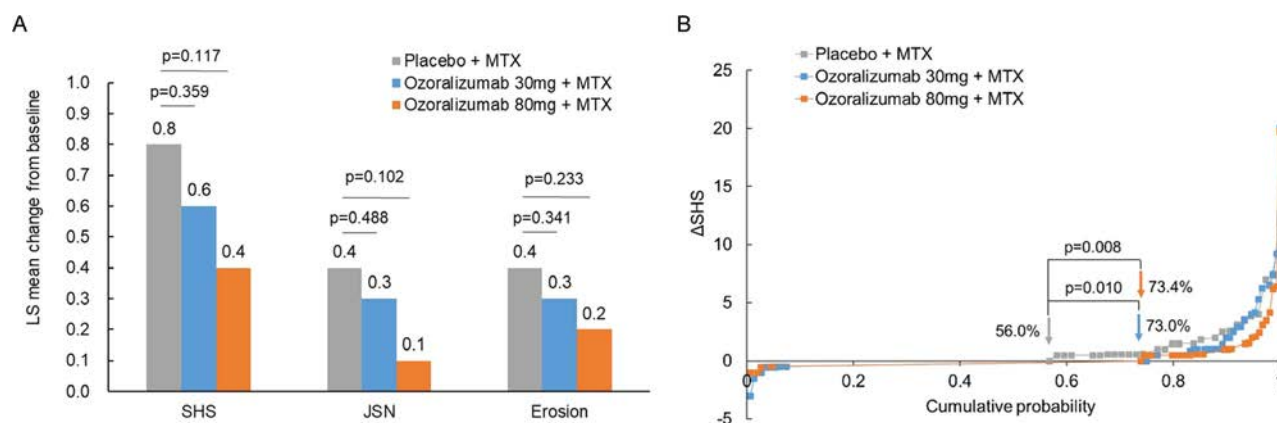


**Figure 4.** Progression of structural damage (EXTRAP). **A**, Least squares (LS) mean change from baseline to week 24 in Sharp/van der Heijde (SHS) score, joint space narrowing (JSN) scores, and erosion scores. Statistical comparisons were determined by analysis of covariance using the status of prior tumor necrosis factor inhibitor usage and baseline values as covariates. **B**, Cumulative probability of change in SHS score at week 24 compared with baseline values. Percentages indicate rates of nonprogression ( $\Delta$ SHS  $\leq 0$ ) in each treatment group. *P* values were calculated by chi-square test without continuity correction or multiplicity adjustment. MTX = methotrexate.

used in this trial, the mean disease duration was 7.4 years, the mean DAS28-CRP at baseline was 5.13, and the mean SHS score was 27.46. Among the included patients, 89.2% were seropositive for rheumatoid factor and/or anti-citrullinated protein antibodies. When other indices were included, there was no major difference in the mean values (Table 1).

**Efficacy. ACR20 and ACR50/70 response.** The ACR20 response rate at week 16 was 37.3% in the placebo group, 79.6% in the ozoralizumab 30-mg group, and 75.3% in the ozoralizumab 80-mg group. The intergroup difference compared with the placebo group was mean 42.1 (95% confidence interval [95% CI] 28.7–53.7;  $P < 0.001$ ) in the ozoralizumab 30-mg group and mean 37.9 (95% CI 24.4–49.7;  $P < 0.001$ ) in the ozoralizumab 80-mg group, indicating a significantly higher improvement rate in the ozoralizumab groups compared with the placebo group (Figure 2A). In the post hoc analysis using nonresponder imputation, the ACR20 response rate was also significantly higher in the ozoralizumab groups than in the placebo group (Supplementary Table 1, <http://onlinelibrary.wiley.com/doi/10.1002/art.42273>). Similarly, at week 24, a significantly higher ACR20 response rate was found in the ozoralizumab groups than in the placebo group (Figure 2B). Furthermore, the onset of ACR20 response with ozoralizumab was rapid (Figure 2C). A similar result compared with the ACR20 was found for ACR50/70, with a rapid onset of response in the ozoralizumab groups, and significantly higher ACR50/70 response rates than in the placebo group at both weeks 16 and 24 (Figures 2A–E).

**Other clinical measures and physical function.** The ozoralizumab groups showed rapid improvement in DAS28-CRP compared with the placebo group at day 3 (Figure 3A). Furthermore, the ozoralizumab groups showed a significantly better response to PtGA and patient's assessment of pain than the placebo group

(Figures 3B and C). Similarly, rapid reduction was observed for both hsCRP level and ESR (Figures 3D and E). A significant improvement in the other secondary efficacy end points and pharmacodynamic end points were observed in the ozoralizumab groups compared with the placebo group (Supplementary Figure 1 and Supplementary Table 2, <http://onlinelibrary.wiley.com/doi/10.1002/art.42273>). At week 24, the proportions of patients who achieved an SDAI of  $\leq 3.3$  was 5.3% in the placebo group, 25.0% in the ozoralizumab 30-mg group, and 23.4% in the ozoralizumab 80-mg group, indicating a significantly higher remission rate in the ozoralizumab groups compared with the placebo group. Boolean remission rates and other indices of clinical remission rate were also significantly higher than that in the placebo group (Supplementary Table 2, <http://onlinelibrary.wiley.com/doi/10.1002/art.42273>). Improvement in HAQ DI scores in the ozoralizumab groups was observed from week 1 (Figure 3F), and the rates of achieving an HAQ DI score of  $\leq 0.5$  at week 24 were significantly higher in both ozoralizumab groups than in the placebo group (Supplementary Table 2).

For all parameters, responses in the ozoralizumab groups were comparable, irrespective of the dose. In the post hoc analysis, there were no clear relationship between serum albumin level and efficacy.

**Structural progression.** The change from the baseline in SHS score (least squares mean) at week 24 was 0.8 in the placebo group, 0.6 in the ozoralizumab 30-mg group, and 0.4 in the ozoralizumab 80-mg group. While the amount of change tended to be lower in the ozoralizumab groups than in the placebo group, no statistically significant inhibition of progression was observed (Figure 4A). On the other hand, the change in SHS score was lower in the ozoralizumab groups than in the placebo group (Figure 4B), and the proportion of patients with structural nonprogression up to week 24 was 56.0% in the



**Table 2.** Summary of safety through week 24 in patients receiving methotrexate and either placebo, ozoralizumab 30 mg, or ozoralizumab 80 mg\*

	Placebo (n = 75)	Ozoralizumab	
		30 mg (n = 152)	80 mg (n = 154)
AE	47 (62.7)	116 (76.3)	111 (72.1)
Adverse drug reactions	14 (18.7)	42 (27.6)	39 (25.3)
AE leading to death	0 (0)	0 (0)	1 (0.6)
Other serious AE except death	2 (2.7)	4 (2.6)	4 (2.6)
AE leading to discontinuation	1 (1.3)	5 (3.3)	6 (3.9)
AE leading to suspension or a dose reduction of the study drug	2 (2.7)	8 (5.3)	11 (7.1)
Intensity			
Mild	42 (56.0)	101 (66.4)	101 (65.6)
Moderate	8 (10.7)	35 (23.0)	29 (18.8)
Severe	2 (2.7)	3 (2.0)	5 (3.2)
AEs of special interest			
Infections and infestations	28 (37.3)	64 (42.1)	62 (40.3)
Serious infection other than tuberculosis	2 (2.7)	7 (4.6)	3 (1.9)
Tuberculosis	0 (0)	0 (0)	1 (0.6)
HZ	0 (0)	2 (1.3)	3 (1.9)
Malignant tumors	0 (0)	1 (0.7)	1 (0.6)
ILD	0 (0)	2 (1.3)	1 (0.6)
Injection site reaction	1 (1.3)	3 (2.0)	2 (1.3)

\* Values are the number (%) of patients. AE = adverse event; HZ = herpes zoster; ILD = interstitial lung disease.

placebo group, compared to 73.0% in the ozoralizumab 30-mg group and 73.4% in the ozoralizumab 80-mg group. A significant difference was observed in both ozoralizumab groups compared with the placebo group. Also, a significant difference was observed in those with structural remission at week 24. The proportion of patients in whom the change in SHS score from baseline was lower than the SDC was significantly reduced in ozoralizumab 80-mg group compared with the placebo group (Supplementary Table 2, <http://onlinelibrary.wiley.com/doi/10.1002/art.42273>).

**Safety.** The occurrence of AEs up to 24 weeks (up to 20 weeks in early escape) is shown in Table 2. The incidence of AEs was 62.7% in the placebo group, 76.3% in the ozoralizumab 30-mg group, and 72.1% in the ozoralizumab 80-mg group. There was no clinical difference depending on the dose of ozoralizumab in the incidence of either AEs or adverse reactions. Infection had the highest incidence among AEs. The majority of AEs were mild to moderate; the onset of an SAE was rare. An AE that resulted in death was observed in 1 patient in the ozoralizumab 80-mg group, in whom disseminated tuberculosis had developed. It was determined to have had a causal relationship with the investigational drug. In the placebo group, 2 patients (2.7%) had serious AEs other than death (perforated appendicitis and pneumonia), 4 patients (2.6%) in the ozoralizumab 30-mg group (pelvic fracture, diabetes mellitus, lung adenocarcinoma, and interstitial lung disease [ILD]), and 4 patients (2.6%) in the ozoralizumab 80-mg group (ovarian carcinoma/uterine carcinoma, renal abscess,

cerebellar hemorrhage, and ILD). The incidence of injection site reaction was low, and the severity was mild.

During the 24-week treatment period, the generation of a new anti-ozoralizumab antibody response or an increase in existing anti-ozoralizumab antibody response was observed in 43 patients in the ozoralizumab 30-mg group (28.3%), and 41 patients in the ozoralizumab 80-mg group (26.6%). Among them, 2 patients in the 30-mg group (1.3%), and 4 patients in the 80 mg group (2.6%) were positive for neutralizing antibodies. The presence of anti-ozoralizumab antibodies showed no consistent trend in the efficacy or safety of the investigational drug, regardless of dose. Among neutralizing antibody-positive patients, there was no incidence of trial discontinuation due to exacerbation of the underlying illness, and no specific AEs occurred with this drug.

## DISCUSSION

This phase II/III trial in RA patients who had an inadequate response to MTX demonstrated that both 30-mg and 80-mg ozoralizumab groups achieved statistically significant improvements in ACR20 response, which was one of the primary end points, compared with the placebo group. Furthermore, significant improvements were observed in the ozoralizumab groups compared with the placebo group in terms of other clinical symptoms, such as DAS28-CRP, PtGA, and patient's assessment of pain. Moreover, a significant HAQ DI response was observed in the ozoralizumab groups compared with the placebo group. Most evaluation indices relating to clinical

symptoms and physical function showed improvement starting as early as 3 days or 1 week after ozoralizumab administration. The efficacy of ozoralizumab 30 mg was comparable to 80 mg of ozoralizumab. Several other clinical trials of antirheumatic biologic treatments have demonstrated no dose-dependency in efficacy above a certain dose (14,15). In the present trial, there was no major difference between dosages in terms of efficacy, and the 30-mg dose was considered sufficient for achieving the maximal clinical efficacy of ozoralizumab with concomitant MTX.

Of note, the MTX dosage used in this study, which was within the dosage range approved in Japan, is lower (10 mg on average and a maximum approved dosage of 16 mg/week) than typical dosages in North America and Europe. More robust MTX treatment regimens may leave less room for improvement from baseline in ACR20 response. However, even using more stringent criteria, such as ACR50/70, ozoralizumab showed significant improvement. Also, it is remarkable that the difference in ACR responses between the placebo group and ozoralizumab groups was comparable or greater than responses in previous trials of TNFi in Japanese patients conducted at even lower MTX doses (6–8 mg) (14,16). Finally, it has been shown that MTX–polyglutamate concentrations between Japanese RA patients receiving a lower dose of MTX and those in North America receiving a higher dose were comparable, in part, because of the lower body mass index and body weight of Japanese RA patients (17).

Ozoralizumab is an antibody with a structure that greatly differs from that of conventional IgG antibodies. The rate of absorption of subcutaneously injected drugs is highly dependent on molecular weight (18–20). In addition, VHH antibodies have demonstrated good tissue penetration (21–24). Furthermore, since serum albumin accumulates in inflammatory tissue in RA and other diseases, serum albumin–mediated drug transport has also been reported (25–27). Due to its structural characteristics (e.g., low molecular weight, HSA binding ability), ozoralizumab is predicted to quickly accumulate in the inflamed tissue. In this trial, an improvement was observed in terms of biochemical indices and clinical symptoms and physical function from day 3. Thus, it was found that ozoralizumab causes a change in biochemical indices soon after administration. As a result, early improvement was observed in indices of disease activity and in subjective indices, such as PtGA and patient's assessment of pain.

The change in SHS score from baseline, which was another primary end point (to evaluate prevention of structural damage in the joints), was not significantly different between the ozoralizumab groups and placebo group. We attribute this result to less change in SHS in the placebo group, compared with the change in SHS observed in phase III trials of other anti-TNFi (14,16). In recent years, the treatment of RA has improved; there has been

an overall declining trend in the progression of structural damage in patients (28,29). There are examples of similar trends in trials conducted in Japanese patients (30). However, regarding the proportion of patients without progression of structural damage and those who achieved structural remission, a significant response was observed in both ozoralizumab groups compared with the placebo group. Significant changes in SHS scores from baseline were not demonstrated at a group level. Thus, prevention of joint destruction by ozoralizumab was not demonstrated. However, a significant difference was demonstrated in terms of the proportion of patients with structural nonprogression, suggesting that ozoralizumab prevents or reduces progression of structural damage to joints in the majority of patients with active RA.

Our trial also included patients who had previously received antirheumatic biologic treatments. The subpopulation analysis showed no difference in terms of ACR20 response rates between patients with and those without previous use of antirheumatic biologic treatments (Supplementary Table 3, <http://onlinelibrary.wiley.com/doi/10.1002/art.42273>). Moreover, this trial also included a small number of patients who had discontinued the use of therapeutic drugs (anti-TNF antibody) due to secondary ineffectiveness. All of those who received treatment with ozoralizumab achieved an ACR20 response, which suggests that ozoralizumab might improve the condition of patients with secondary ineffectiveness to other anti-TNF antibodies. It is thought that this could be attributed to the characteristic structure of ozoralizumab. It is necessary to understand the actual effect on patients who previously received bDMARDs with further evaluation in the future.

New expression or induction of anti-ozoralizumab antibodies was observed in 28.3% of patients in the ozoralizumab 30-mg group and in 26.6% of patients in the ozoralizumab 80-mg group. At week 16, 81.4% (30-mg group) and 67.5% (80-mg group) of these patients achieved an ACR20 response. This finding indicates that the effect of antidrug antibodies on the investigational drug is limited; it is expected that efficacy and safety would be maintained in many subjects, but longer-term observation is required to determine whether the development of antidrug antibodies affects the efficacy (including the prevention of structural damage) and safety of ozoralizumab.

Ozoralizumab had good tolerability up to 24 weeks. Most AEs were mild or moderate. The incidences of AE in the ozoralizumab 30-mg and 80-mg groups were comparable. AEs observed during administration of ozoralizumab were comparable to that of other TNFi approved by regulators in terms of frequency and type (14,16,31).

Treatment with bDMARDs has the potential to increase the risk of infections, including tuberculosis. In this trial, 11 cases of serious infection (including 1 case of tuberculosis in the ozoralizumab 80-mg group) were reported in ozoralizumab groups, compared with 2 cases reported in the placebo group. Overall, the

frequency of serious infections reported in this trial, including tuberculosis, was consistent with other TNFi, such as infliximab, etanercept, adalimumab, and golimumab in the Japanese population (32–35).

This trial has limitations, including the fact that it is a clinical trial that included only Japanese patients who had an inadequate response to prior therapy with MTX. The sample size was small, with inclusion/exclusion criteria that included history of MTX use and disease activity. The unique genetic, environmental, and medical background of the Japanese population may affect the efficacy and safety of biologic agents in RA patients (36). In addition, since this trial was not designed to be active-controlled, it is impossible to compare the results with other biologic agents. In this trial, eligibility criteria for active RA included TJC levels, SJC levels, and CRP levels, but not the number of bone erosions. This may have been a reason for the difficulty in assessing radiographic progression. Here we present an interim analysis of the results up to week 24. The safety and efficacy of ozoralizumab requires further assessment in the open-label period, up to week 52 of the trial.

Ozoralizumab, at doses of 30 mg and 80 mg once every 4 weeks, demonstrated significant therapeutic effects on clinical symptoms and physical functions, as well as the prevention of structural damage to the joints, in RA patients who had inadequate response to MTX. The onset of therapeutic effects was rapid after administration. Ozoralizumab was well tolerated in the trial period. The efficacy and tolerability of ozoralizumab were comparable between 30-mg and 80-mg doses.

## ACKNOWLEDGMENTS

We would like to thank the patients who were involved in this trial, as well as the investigators and the trial team. Ablynx originally discovered and performed initial development of the NANOBODY compound ozoralizumab. (NANOBODY is a registered trademark of Ablynx NV. Ablynx is an affiliate of Sanofi.)

## AUTHOR CONTRIBUTIONS

All authors were involved in drafting the article or revising it critically for important intellectual content, and all authors approved the final version to be published. Dr. Tanaka had full access to all of the data in the study and takes responsibility for the integrity of the data and the accuracy of the data analysis.

**Study conception and design.** Takeuchi, Nakanishi, Yamasaki, Tanaka  
**Acquisition of data.** Nakanishi.

**Analysis and interpretation of data.** Takeuchi, Kawanishi, Nakanishi, Yamasaki, Tanaka.

## ROLE OF THE STUDY SPONSOR

Taisho Pharmaceutical Co., Ltd. was involved in the study design and in the collection, analysis, and interpretation of the data, the writing of the manuscript, and the decision to submit the manuscript for


publication. Publication of this article was contingent upon approval by Taisho Pharmaceutical Co., Ltd.

## REFERENCES

- Zampeli E, Vlachoyiannopoulos PG, Tzioufas AG. Treatment of rheumatoid arthritis: unraveling the conundrum. *J Autoimmun* 2015;65:1–18.
- Smolen JS, Aletaha D, Barton A, et al. Rheumatoid arthritis. *Nat Rev Dis Primers* 2018;4:18001.
- McInnes IB, Buckley CD, Isaacs JD. Cytokines in rheumatoid arthritis - shaping the immunological landscape [review]. *Nat Rev Rheumatol* 2016;12:63–8.
- Harmsen MM, De Haard HJ. Properties, production, and applications of camelid single-domain antibody fragments. *Appl Microbiol Biotechnol* 2007;77:13–22.
- Khodabakhsh F, Behdani M, Rami A, et al. Single-domain antibodies or nanobodies: a class of next-generation antibodies. *Int Rev Immunol* 2018;37:316–22.
- Coppieters K, Dreier T, Silence K, et al. Formatted anti-tumor necrosis factor  $\alpha$  VHH proteins derived from camelids show superior potency and targeting to inflamed joints in a murine model of collagen-induced arthritis. *Arthritis Rheum* 2006;54:1856–66.
- Beirmaert E, Desmyter A, Spinelli S, et al. Bivalent llama single-domain antibody fragments against tumor necrosis factor have picomolar potencies due to intramolecular interactions. *Front Immunol* 2017;8:867.
- Van Faassen H, Ryan S, Henry KA, et al. Serum albumin-binding VHHs with variable pH sensitivities enable tailored half-life extension of biologics. *FASEB J* 2020;34:8155–71.
- Dennis MS, Zhang M, Meng YG, et al. Albumin binding as a general strategy for improving the pharmacokinetics of proteins. *J Biol Chem* 2002;277:35035–43.
- Ishiwatari-Ogata C, Kyuuma M, Ogata H, et al. Ozoralizumab, a humanized anti-TNF $\alpha$  NANOBODY compound, exhibits efficacy not only at the onset of arthritis in a human TNF transgenic mouse but also during secondary failure of administration of an anti-TNF $\alpha$  IgG. *Front Immunol* 2022;13:853008.
- Aletaha D, Neogi T, Silman AJ, et al. 2010 rheumatoid arthritis classification criteria: an American College of Rheumatology/European League Against Rheumatism collaborative initiative. *Arthritis Rheum* 2010;62:2569–81.
- Bland JM, Altman DG. Statistical methods for assessing agreement between two methods of clinical measurement. *Lancet* 1986;1:307–10.
- Bruynesteyn K, Boers M, Kostense P, et al. Deciding on progression of joint damage in paired films of individual patients: smallest detectable difference or change. *Ann Rheum Dis* 2005;64:179–82.
- Yamamoto K, Takeuchi T, Yamanaka H, et al. Efficacy and safety of certolizumab pegol plus methotrexate in Japanese rheumatoid arthritis patients with an inadequate response to methotrexate: the J-RAPID randomized, placebo-controlled trial. *Mod Rheumatol* 2014;24:715–24.
- Aletaha D, Bingham CO III, Tanaka Y, et al. Efficacy and safety of sirukumab in patients with active rheumatoid arthritis refractory to anti-TNF therapy (SIRROUND-T): a randomised, double-blind, placebo-controlled, parallel-group, multinational, phase 3 study. *Lancet* 2017;389:1206–17.
- Tanaka Y, Harigai M, Takeuchi T, et al. Golimumab in combination with methotrexate in Japanese patients with active rheumatoid arthritis: results of the GO-FORTH study. *Ann Rheum Dis* 2012;71:817–24.
- Takahashi C, Kaneko Y, Okano Y, et al. Association of erythrocyte methotrexate-polyglutamate levels with the efficacy and

- hepatotoxicity of methotrexate in patients with rheumatoid arthritis: a 76-week prospective study. *RMD Open* 2017;3:e000363.
18. Porter CJ, Charman SA. Lymphatic transport of proteins after subcutaneous administration. *J Pharm Sci* 2000;89:297–310.
  19. McLennan DN, Porter CJ, Charman SA. Subcutaneous drug delivery and the role of the lymphatics. *Drug Discov Today Technol* 2005;2:89–96.
  20. Tibbitts J, Canter D, Graff R, et al. Key factors influencing ADME properties of therapeutic proteins: a need for ADME characterization in drug discovery and development [review]. *MAbs* 2016;8:229–45.
  21. Wesolowski J, Alzogaray V, Reyelt J, et al. Single domain antibodies: promising experimental and therapeutic tools in infection and immunity. *Med Microbiol Immunol* 2009;198:157–74.
  22. Mir MA, Mehraj U, Sheikh BA, et al. Nanobodies: the "magic bullets" in therapeutics, drug delivery and diagnostics. *Hum Antibodies* 2020;28:29–51.
  23. Jovčevska I, Muyldermans S. The therapeutic potential of nanobodies. *BioDrugs* 2020;34:11–26.
  24. Bao G, Tang M, Zhao J, et al. Nanobody: a promising toolkit for molecular imaging and disease therapy. *EJNMMI Res* 2021;11:6.
  25. Levick JR. Permeability of rheumatoid and normal human synovium to specific plasma proteins. *Arthritis Rheum* 1981;24:1550–60.
  26. Wunder A, Muller-Ladner U, Stelzer EH, et al. Albumin-based drug delivery as novel therapeutic approach for rheumatoid arthritis. *J Immunol* 2003;170:4793–801.
  27. Larsen MT, Kuhlmann M, Hvam ML, et al. Albumin-based drug delivery: harnessing nature to cure disease. *Mol Cell Ther* 2016;4:3.
  28. Rahman MU, Buchanan J, Doyle MK, et al. Changes in patient characteristics in anti-tumour necrosis factor clinical trials for rheumatoid arthritis: results of an analysis of the literature over the past 16 years. *Ann Rheum Dis* 2011;70:1631–40.
  29. Van der Heijde D, Landewé R. Should radiographic progression still be used as outcome in RA? *Clin Immunol* 2018;186:79–81.
  30. Matsubara T, Inoue H, Nakajima T, et al. Abatacept in combination with methotrexate in Japanese biologic-naive patients with active rheumatoid arthritis: a randomised placebo-controlled phase IV study. *RMD Open* 2018;4:e000813.
  31. Takeuchi T, Yamanaka H, Ishiguro N, et al. Adalimumab, a human anti-TNF monoclonal antibody, outcome study for the prevention of joint damage in Japanese patients with early rheumatoid arthritis: the HOPEFUL 1 study. *Ann Rheum Dis* 2014;73:536–43.
  32. Takeuchi T, Tatsuki Y, Nogami Y, et al. Postmarketing surveillance of the safety profile of infliximab in 5000 Japanese patients with rheumatoid arthritis. *Ann Rheum Dis* 2008;67:189–94.
  33. Koike T, Harigai M, Inokuma S, et al. Postmarketing surveillance of safety and effectiveness of etanercept in Japanese patients with rheumatoid arthritis. *Mod Rheumatol* 2011;21:343–51.
  34. Koike T, Harigai M, Ishiguro N, et al. Safety and effectiveness of adalimumab in Japanese rheumatoid arthritis patients: postmarketing surveillance report of 7740 patients. *Mod Rheumatol* 2014;24:390–8.
  35. Kanbori M, Suzuka H, Yajima T, et al. Postmarketing surveillance evaluating the safety and effectiveness of golimumab in Japanese patients with rheumatoid arthritis. *Mod Rheumatol* 2018;28:66–75.
  36. Takeuchi T, Kameda H. The Japanese experience with biologic therapies for rheumatoid arthritis [review]. *Nat Rev Rheumatol* 2010;6:644–52.

# Characterization of Blood Mucosal-Associated Invariant T Cells in Patients With Axial Spondyloarthritis and of Resident Mucosal-Associated Invariant T Cells From the Axial Enteses of Non-Axial Spondyloarthritis Control Patients

Nicolas Rosine,<sup>1</sup>  Hannah Rowe,<sup>2</sup> Surya Koturan,<sup>1</sup> Hanane Yahia-Cherbal,<sup>1</sup> Claire Leloup,<sup>1</sup> Abdulla Watad,<sup>2</sup> Francis Berenbaum,<sup>3</sup> Jeremie Sellam,<sup>3</sup> Maxime Dougados,<sup>4</sup> Vishukumar Amanianda,<sup>5</sup> Richard Cuthbert,<sup>2</sup> Charlie Bridgewood,<sup>2</sup> Darren Newton,<sup>6</sup> Elisabetta Bianchi,<sup>7</sup> Lars Rogge,<sup>7</sup> Dennis McGonagle,<sup>2</sup> and Corinne Miceli-Richard<sup>8</sup>

**Objective.** The importance of interleukin-17A (IL-17A) in the pathogenesis of axial spondyloarthritis (SpA) has been demonstrated by the success of IL-17A blockade. However, the nature of the cell populations that produce this important proinflammatory cytokine remains poorly defined. We undertook this study to characterize the major IL-17A-producing blood cell populations in the peripheral blood of patients with axial SpA, with a focus on mucosal-associated invariant T (MAIT) cells, a population known to be capable of producing IL-17.

**Methods.** We evaluated IL-17A production from 5 sorted peripheral blood cell populations, namely, MAIT cells,  $\gamma\delta$  T cells, CD4+ T cells, CD8+ T cells, and neutrophils, before and after stimulation with phorbol myristate acetate, the calcium ionophore A23187, and  $\beta$ -1,3-glucan. Expression of IL-17A transcripts and protein were determined using nCounter and ultra-sensitive Simoa technology, respectively. MAIT cells from the axial enteses of non-axial SpA control patients ( $n = 5$ ) were further characterized using flow cytometric immunophenotyping and quantitative polymerase chain reaction, and the production of IL-17 was assessed following stimulation.

**Results.** On a per-cell basis, MAIT cells from peripheral blood produced the most IL-17A compared to CD4+ T cells ( $P < 0.01$ ), CD8+ T cells ( $P < 0.0001$ ), and  $\gamma\delta$  T cells ( $P < 0.0001$ ). IL-17A was not produced by neutrophils. Gene expression analysis also revealed significantly higher expression of *IL17A* and *IL23R* in MAIT cells. Stimulation of peripheral blood MAIT cells with anti-CD3/CD28 and IL-7 and/or IL-18 induced strong expression of *IL17F*. MAIT cells were present in the normal, unaffected enteses of control patients who did not have axial SpA and showed elevated *AHR*, *JAK1*, *STAT4*, and *TGFB1* transcript expression with inducible IL-17A protein. IL-18 protein expression was evident in spinal entesis digests.

**Conclusion.** Both peripheral blood MAIT cells and resident MAIT cells in normal axial enteses contribute to the production of IL-17 and may play important roles in the pathogenesis of axial SpA.

## INTRODUCTION

Within the last 15 years, a clear role of the interleukin-23 (IL-23)/IL-17 axis underpinning the pathophysiology of axial

spondyloarthritis (SpA) has emerged (1) as many of the genetic variants associated with ankylosing spondylitis (AS) susceptibility have been identified through genome-wide association studies. Among the genes found to be associated with AS are those in the IL-23/IL-

Supported by grants from MSDAVENIR (Project iCARE-SpA), by a Sanofi Innovation award Europe, by the FOREUM Foundation for Research in Rheumatology, and by the Société Française de Rhumatologie. Dr. Rosine's work was supported by a Poste d'Accueil de l'AP-HP and by a grant from the Société Française de Rhumatologie. Ms. Rowe's work was supported by investigator-initiated nonclinical research funding from Novartis UK. Dr. Watad's work was supported by the PARTNER fellowship program. Dr. Cuthbert's work was supported by an investigator-initiated research grant from Pfizer. Dr. Bridgewood's work was supported by investigator-initiated nonclinical research funding from Novartis UK. Dr. McGonagle's work was supported by the Leeds NIHR Biomedical Research Centre.

Dr. Rosine, Ms. Rowe, and Dr. Koturan contributed equally to this work. Drs. Rogge, McGonagle, and Miceli-Richard contributed equally to this work.

<sup>1</sup>Nicolas Rosine, MD, PhD, Surya Koturan, MD, PhD, Hanane Yahia-Cherbal, MD, PhD, Claire Leloup, MSc: Institut Pasteur, Université de Paris, Immunoregulation Unit, Department of Immunology, Paris, France; <sup>2</sup>Hannah Rowe, BSc, Abdulla Watad, MD, Richard Cuthbert, BSc, PhD, Charlie Bridgewood, PhD, Dennis McGonagle, PhD: University of Leeds Institute of Rheumatic and Musculoskeletal Medicine, Leeds, UK; <sup>3</sup>Francis Berenbaum, MD, PhD, Jeremie Sellam, MD, PhD: Sorbonne Université, Service de Rhumatologie, Hôpital Saint-Antoine, AP-HP, and Centre de Recherche Saint-Antoine, INSERM UMR 938, Paris, France; <sup>4</sup>Maxime Dougados, MD, PhD: INSERM Unité 1153, Clinical epidemiology and biostatistics, PRES Université Sorbonne Paris Cité, Université de Paris, Service de Rhumatologie, Hôpital Cochin Port Royal, AP-HP, and Unité Mixte AP-HP/Institut Pasteur, Institut Pasteur, Immunoregulation Unit, Paris, France; <sup>5</sup>Vishukumar Amanianda, PhD: Institut Pasteur, Molecular Mycology Unit, CNRS UMR 2000, Paris, France; <sup>6</sup>Darren Newton, PhD: University of

17 pathway, including *IL23R*, *IL12B*, *IL6R*, *JAK2*, and *TYK2* (2). As IL-17 is the terminal cytokine of this pathophysiologic pathway, the development of new treatments initially focused on blocking this cytokine (3,4). In support of this hypothesis and beyond the findings of genetic association studies, an increased prevalence of IL-17-producing T helper (Th17) cells have been reported in the peripheral blood of axial SpA patients (5) and in the normal entheses of individuals who do not have axial SpA (6). Mucosal-associated invariant T (MAIT) cells and  $\gamma\delta$  T cells have been further described as alternative sources of IL-17A in the blood of patients with axial SpA (7,8). Appel et al also suggested that neutrophils might be the main producers of IL-17A in the facet joints of patients with AS (9).

IL-23 plays a crucial role in maintaining the differentiation state of Th17 cells. Nevertheless, recent studies have identified alternative pathways, independent of IL-23, that can stimulate IL-17 production, including T cell receptor (TCR) signaling through the engagement of major histocompatibility complex class I-related proteins by MAIT cells (10), IL-7 signaling in group 3 innate lymphoid cells (ILCs) (11), transforming growth factor  $\beta$  (TGF $\beta$ ) and IL-1 $\beta$  signaling in invariant natural killer T (iNKT) cells (12,13) and  $\gamma\delta$  T cells (specifically the V $\delta$ 1 T cell subset) (14), and, recently, the combination of IL-12 and IL-18 together with anti-CD3/CD28 triggering in MAIT cells (10). Such observations have substantial translational relevance, given that antagonism of IL-23 has thus far shown no efficacy in the treatment of AS (15,16).

Considering that the growing body of evidence suggests a role for IL-17 in the pathogenesis of SpA, we wished to study the capability of MAIT cells, CD4+ T cells, CD8+ T cells, and  $\gamma\delta$  T cells to express IL-17 in patients with axial SpA. We first analyzed the cell type-specific expression patterns of AS-associated genes in those cells, with a particular focus on genes belonging to the IL-23/IL-17 pathway. We further compared the respective IL-17 production capacity of these different cell subsets from the adaptive and innate immune systems and identified MAIT cells as potent IL-17-secreting cells in patients with axial SpA. MAIT cells from healthy individuals have been reported to express high levels of IL-7 receptor (IL-7R) and IL-18R (17). In this study, we found that MAIT cells can produce IL-17 with combined TCR triggering and stimulation by IL-7 and IL-18, and independently of IL-23 stimulation. Additionally, we identified resident MAIT cells in the axial entheses of normal, healthy individuals, a site at which the unaffected tissue is targeted in the inflammatory process that leads to severe axial inflammation and later spinal fusion in patients with axial SpA. Taken together, our data highlight the crucial role of MAIT cells in the pathophysiology of axial SpA.

Leeds Institute of Rheumatic and Musculoskeletal Medicine, Leeds Institute of Medical Research at St James's, and St James's University Hospital, Leeds, UK; <sup>2</sup>Elisabetta Bianchi, MD, PhD, Lars Rogge, PhD: Institut Pasteur, Université de Paris, Immunoregulation Unit, Department of Immunology, and Unité Mixte AP-HP/Institut Pasteur, Institut Pasteur, Immunoregulation Unit, Paris, France; <sup>3</sup>Corinne Miceli-Richard, MD, PhD: Université de Paris, Service de Rhumatologie, Hôpital Cochin Port Royal, AP-HP, and Unité Mixte AP-HP/Institut Pasteur, Institut Pasteur, Immunoregulation Unit, Paris, France.

## PATIENTS AND METHODS

**Patients and samples.** *Axial SpA.* Blood samples from 18 patients naive to treatment with synthetic medications and biologics and with a clinical diagnosis of axial SpA who fulfilled the Assessment of SpondyloArthritis international Society criteria (18) were included in the study.

*Entheses tissue and peripheral blood samples from controls.* As controls, human interspinous processes and matched peripheral blood samples were obtained from 5 non-axial SpA patients who underwent elective spinal surgery for either decompression or scoliosis correction using methods previously reported (19).

Before enrollment in the study, all patients provided written informed consent as approved by the French Ethics Committee and the North West–Greater Manchester West Research Ethics Committee. The clinical characteristics of the axial SpA patients and of the non-axial SpA control patients who underwent spinal surgery are summarized in Supplementary Table 1, available on the *Arthritis & Rheumatology* website at <http://onlinelibrary.wiley.com/doi/10.1002/art.42090>.

**Cell sorting and stimulation.** The isolation of cell populations from peripheral blood samples and entheses samples was undertaken as previously described (8,20) and is further described in the Supplementary Materials (<http://onlinelibrary.wiley.com/doi/10.1002/art.42090>).

**Gene expression analysis.** Gene expression profiles from the sorted cells of axial SpA patients were assessed using the nCounter Autoimmune Discovery panel (NanoString Technologies), and samples from the normal entheses of non-axial SpA patients were assessed using a focused gene card. Profiling of the transcription factors of entheses and blood MAIT cells (CD3+, CD45+, CD161+, and TCRV $\alpha$ 7.2+) was performed using the entheses and peripheral blood samples from non-axial SpA patients. The basal transcript expression of cytokines, chemokines, growth factors, signaling molecules, and tissue residency markers were assessed using a focused gene card. A description of the RNA preparation and gene expression analysis is available in the Supplementary Materials (<http://onlinelibrary.wiley.com/doi/10.1002/art.42090>).

**Protein expression analyses.** The concentrations of IL-17A (expressed in fg/ml) in cell culture supernatants from axial SpA patients were determined using the Quanterix Simoa IL-17A Advantage Kit and HD-1 platform. Stimulated cells from

Author disclosures are available at <https://onlinelibrary.wiley.com/action/downloadSupplement?doi=10.1002%2Fart.42090&file=art42090-sup-0001-Disclosureform.pdf>.

Address correspondence via email to Corinne Miceli-Richard, MD, PhD, at [corinne.miceli@aphp.fr](mailto:corinne.miceli@aphp.fr); or to Dennis McGonagle, PhD, at [d.g.mcgonagle@leeds.ac.uk](mailto:d.g.mcgonagle@leeds.ac.uk).

Submitted for publication June 29, 2021; accepted in revised form January 21, 2022.

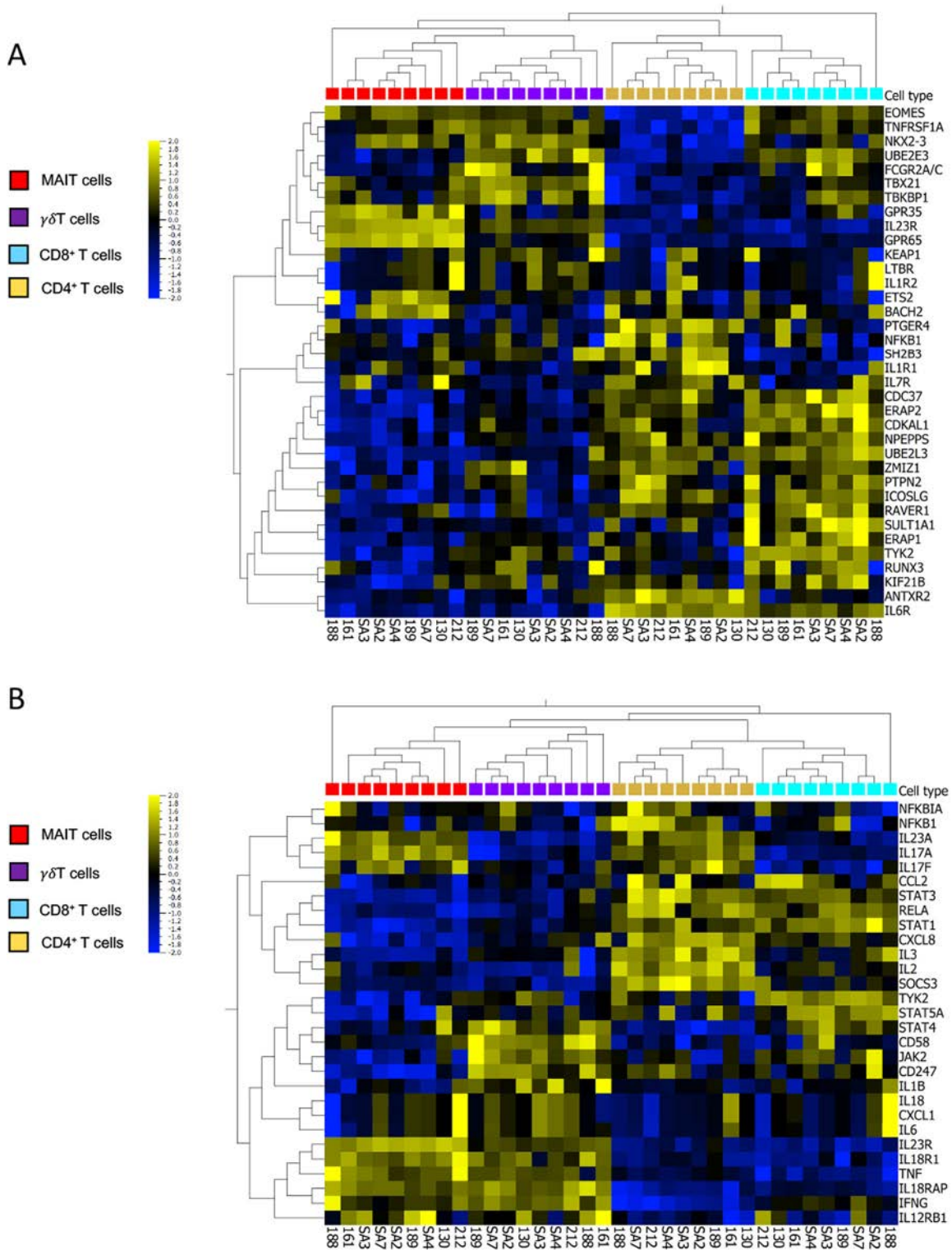


**Figure 1.** Heatmaps showing the expression patterns of genes associated with ankylosing spondylitis (AS) and of genes of the interleukin-23 (IL-23)/IL-17 pathway in T cell subpopulations isolated from the peripheral blood of patients with axial spondyloarthritis (SpA). **A**, Expression levels of 36 genes associated with AS susceptibility in T cells from axial SpA patients. **B**, Messenger RNA expression levels of 29 genes associated with the IL-23/IL-17 pathway, selected from the Molecular Signatures Database. T cells were stimulated for 2 hours with phorbol myristate acetate (50 ng/ml), calcium ionophore A23187 (5  $\mu$ M), and  $\beta$ -1,3-glucan (50  $\mu$ g/ml). Heatmaps show hierarchical clustering of genes among T cell populations from individual patient samples ( $n = 9$ ). Gene expression data are  $\log_2$  transformed, centered to a mean value of 0, and scaled to unit variance. The color key on the left denotes the scale of gene expression, ranging from lower levels (blue) to higher levels (yellow).

perientheseal bone entheseal mononuclear cells (EMCs) were intracellularly stained for tumor necrosis factor (TNF) and IL-17 and analyzed using a flow cytometry gating system, as described previously (8,20). Following 24-hour stimulation with lipopolysaccharides (100 ng/ml), IL-18 protein was analyzed in the supernatant using BioLegend LEGENDplex Human Inflammation Panel 1 and the Beckman Coulter CytoFLEX LX Flow Cytometer, according to the manufacturer's instructions (Supplementary Figure 5, <http://onlinelibrary.wiley.com/doi/10.1002/art.42090>). Serum levels of IL-17A, IL-17F, IL-7, and IL-18 were quantified using the Olink Proximity Extension Assay (Supplementary Materials, <http://onlinelibrary.wiley.com/doi/10.1002/art.42090>).

**Statistical analyses.** GraphPad Prism software was used for statistical analyses. Detailed information regarding methods and statistical analyses is provided in the Supplementary Materials (<http://onlinelibrary.wiley.com/doi/10.1002/art.42090>).

## RESULTS

### Differential expression of genes associated with AS susceptibility in innate and adaptive T cell populations isolated from peripheral blood of axial SpA patients.

Following stimulation with phorbol myristate acetate, the calcium ionophore A23187, and  $\beta$ -1,3-glucan, the expression of 36 genes from a panel of 45 genes associated with AS was analyzed in 4 T cell populations (MAIT cells, CD8+ T cells, CD4+ T cells, and  $\gamma\delta$  T cells) isolated from 9 axial SpA patients. The expression pattern observed after hierarchical clustering showed a clear distinction between the innate and adaptive T cell groups, as shown in the Figure 1A heatmap. Gene clusters consisting of members of

the pathway network for major histocompatibility complex class I-mediated antigen processing and presentation (*NPEPPS* and *UBE2L3*) were up-regulated in CD4+ and CD8+ T cells. We observed that genes were expressed at relatively high levels in specific cell types, such as *PTGER4* in CD4+ T cells and *TYK2* in CD8+ T cells.

MAIT cells expressed high levels of *IL23R* and the G protein-coupled receptors *GPR35* and *GPR65*. We also noted cell type-specific expression of several IL-23/IL-17 pathway genes (Figure 1B). *IL17F* was expressed at higher levels (~1 log-fold difference in expression) in CD4+ T cells and MAIT cells compared to the other T cell populations, while *IL23R* expression was higher (2 log-fold difference) in MAIT cells and  $\gamma\delta$  T cell expression was higher (1 log-fold difference) than that in CD4+ and CD8+ T cells. *NFKB1*, *RELA*, and *NFKBIA* were preferentially expressed in CD4+ T cells, while several genes encoding cytokines and their receptors (*IL23A*, *IL23R*, *IL12RB1*, *IL18R1*, *IL18RAP*, *TNF*, and *IFNG*) were expressed at higher levels in innate-like MAIT cells and  $\gamma\delta$  T cells when compared to adaptive CD4+ and CD8+ T cells. *IL1R1*, *TYK2*, and *RUNX3* were expressed at high levels in CD8+ T cells. Nevertheless, many other genes not belonging to the IL-23/IL-17 pathway participated in cell clustering, suggesting that those different cell types were involved in AS susceptibility beyond their relative role in the IL-23/IL-17 pathway.

### High potential for IL-17A and IL-17F secretion in peripheral blood-derived MAIT cells.

To better define the relative role of MAIT cells, CD4+ T cells, CD8+ T cells, and  $\gamma\delta$  T cells in IL-17 expression, we further sorted these cell types together with neutrophils, whose secretion of IL-17A is still controversial (21). Cell sorting was performed on samples from

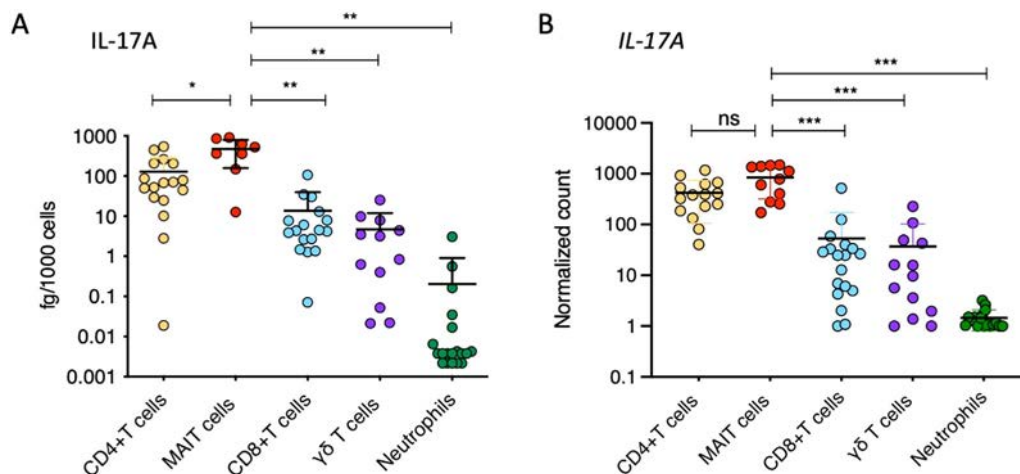


**Figure 2.** IL-17A protein production after 18 hours of stimulation (A) and *IL17A* transcript levels (normalized expression) after 2 hours of stimulation (B) were assessed in sorted CD4+ T cells, mucosal-associated invariant T (MAIT) cells, CD8+ T cells,  $\gamma\delta$  T cells, and neutrophils from the peripheral blood of axial SpA patients. Cells were stimulated with phorbol myristate acetate (50 ng/ml), calcium ionophore A23187 (5  $\mu$ M), and  $\beta$ -1,3-glucan (50  $\mu$ g/ml). Symbols represent individual samples. Bars show the mean  $\pm$  SEM. \* =  $P < 0.05$ ; \*\* =  $P < 0.01$ , by Mann-Whitney test. \*\*\* =  $P < 0.001$ , by Wilcoxon-Mann-Whitney test. ns = not significant (see Figure 1 for other definitions).



18 axial SpA patients (see Supplementary Figure 1 for the gating strategy, available at <http://onlinelibrary.wiley.com/doi/10.1002/art.42090>). The production of IL-17A by MAIT cells was significantly higher than that of CD4+ T cells ( $P < 0.05$ ),  $\gamma\delta$  T cells ( $P < 0.01$ ), CD8+ T cells ( $P < 0.01$ ), and neutrophils ( $P < 0.01$ ). Although lower than in MAIT cells (mean 478.60 fg/1,000 cells), IL-17A production by CD4+ T cells was significant (mean 128.65 fg/1000 cells), while  $\gamma\delta$  T cells produced a smaller amount of IL-17A (mean 13.71 fg/1,000 cells), albeit in the same range as IL-17A production by CD8+ T cells (mean 4.66 fg/1,000 cells).

The main component of *Aspergillus fumigatus* hyphae,  $\beta$ -glucan, has been demonstrated to have a potential effect on the production of IL-17A by human neutrophils (22). Despite strong  $\beta$ -glucan-associated stimulation, the expression of IL-17A by most neutrophils in the axial SpA patients did not exceed the detection limit (Figure 2A).

Gene expression analysis confirmed the findings of the IL-17A protein analysis, with MAIT cells and CD4+ T cells displaying the highest levels of *IL17A* expression (no significant difference between *IL17A* expression in MAIT cells and CD4+ T cells). A low

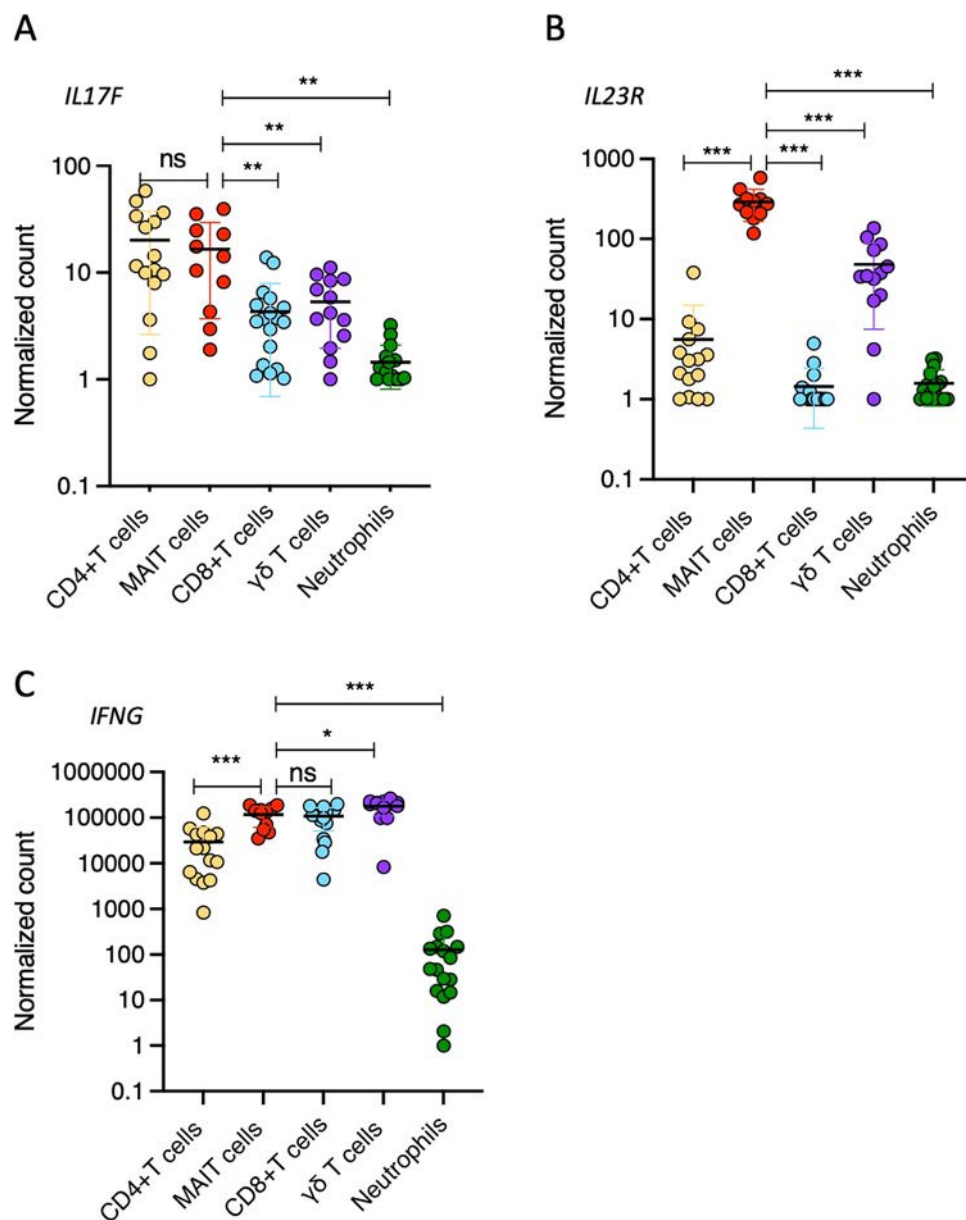


**Figure 3.** Sorted CD4+ T cells, MAIT cells, CD8+ T cells,  $\gamma\delta$  T cells, and neutrophils from the peripheral blood of axial SpA patients were analyzed for gene expression of *IL17F* (A), *IL23R* (B), and *IFNG* (C). Results are presented as normalized transcript levels. Cells were stimulated with phorbol myristate acetate (50 ng/ml), calcium ionophore A23187 (5  $\mu$ M), and  $\beta$ -1,3-glucan (50  $\mu$ g/ml). Symbols represent individual samples. Bars show the mean  $\pm$  SEM. \* =  $P < 0.05$ ; \*\* =  $P < 0.01$ ; \*\*\* =  $P < 0.001$ , by Wilcoxon-Mann-Whitney test. See Figure 2 for definitions.

level of *IL17A* expression was observed in  $\gamma\delta$  T cells and CD8+ T cells. In neutrophils, expression of *IL17A* was undetectable, which was consistent with the findings of the IL-17A protein analysis (Figure 2B).

Next, we expanded our analysis to include the expression of *IL17F*, *IL23R*, and *IFNG*. We observed that the 5 cell populations were similarly ranked in their expression levels of *IL17F* as they were in their expression levels of *IL17A* (Figure 3A), but there was no significant difference in the expression levels of *IL17F* between CD4+ T cells and MAIT cells. We also observed a 10-fold lower level of expression of *IL17F* compared to that of *IL17A* in all cell subsets. Regarding *IL23R* (Figure 3B), MAIT cells had the highest level of expression, followed by  $\gamma\delta$  T cells and CD4+ T cells, while CD8+ T cells and neutrophils did not express significant levels of *IL23R*. In contrast to *IL17A* and *IL17F* expression, *IFNG* was highly expressed in all T cell populations (Figure 3C), suggesting cell-specific expression profiles for *IL17A* and *IL17F*. Collectively, these data indicate that MAIT cells are the major producers of IL-17A on a per-cell level and express high levels of both *IL17F* and *IL23R* compared to other IL-17A-producing cells in patients with axial SpA.

#### Enhancement of *IL17F* expression by IL-7 and IL-18 in peripheral blood-derived MAIT cells.

We further assessed which stimulation conditions induced IL-17A and IL-17F protein expression by MAIT cells. Sorted MAIT cells (see Supplementary Figure 2 for the gating strategy, available at <http://onlinelibrary.wiley.com/doi/10.1002/art.42090>) were stimulated for 36 hours with anti-CD3/anti-CD28, anti-CD3/anti-CD28 in combination with either IL-7 or IL-18, and anti-CD3/anti-CD28 combined with both IL-7 and IL-18. We used CD4+CCR6+ T cells (“Th17-like” T cells) as controls (Figure 4). We observed that stimulation with anti-CD3/anti-CD28 combined with IL-7 or IL-18 induced high expression levels of *IL17F* but not *IL17A* in MAIT cells (Figures 4A and B). Furthermore, we identified increased *IL18R1* expression (Figure 1B) by MAIT cells, which supports the finding that IL-18 induces *IL17F* production. The combination of both IL-7 and IL-18 with anti-CD3/anti-CD28 further increased *IL17F* expression. Expression levels of *IFNG* were also remarkably high after MAIT cells were stimulated with anti-CD3/anti-CD28 and either IL-7 or IL-18 and when they were stimulated with anti-CD3/anti-CD28 and both IL-7 and IL-18 combined (Figure 4C).

Basal levels of IL-18 expression were demonstrated in MAIT cells isolated from the normal entheses of patients who did not

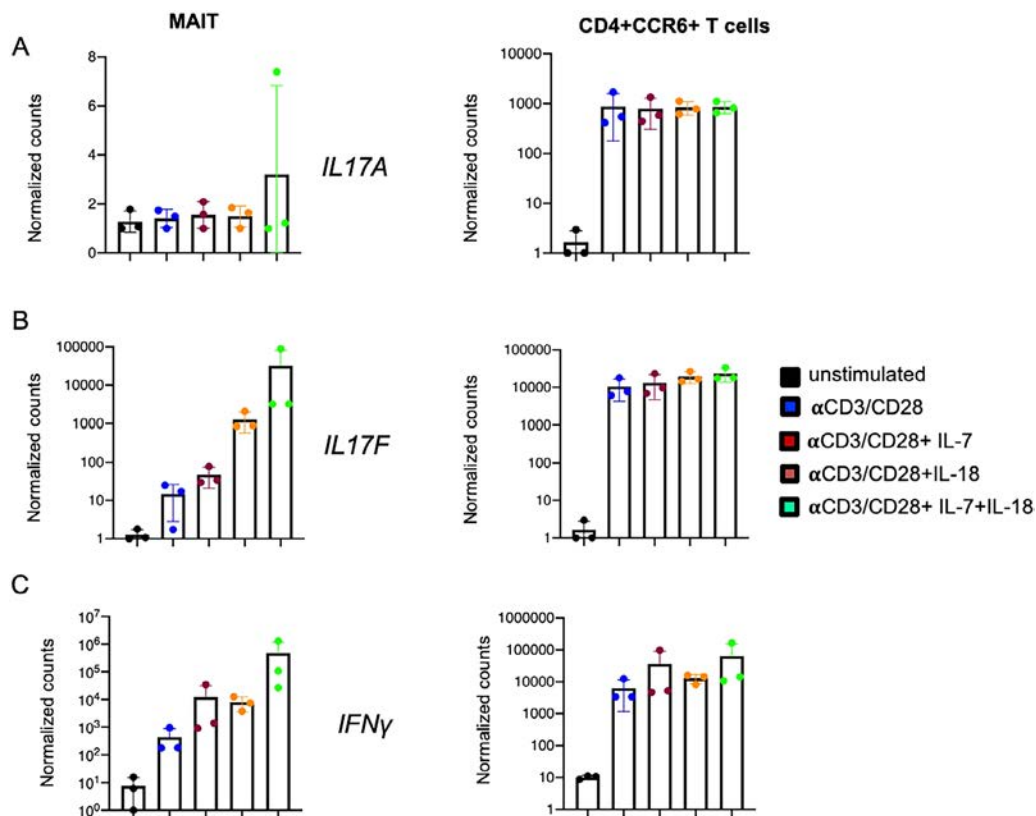


**Figure 4.** Gene expression of *IL17A* (A), *IL17F* (B), and *IFNG* (C) in sorted mucosal-associated invariant T (MAIT) cells and CD4+CCR6+ T cells from non-axial SpA patients (n = 3) after 36 hours of stimulation in 6 different conditions, including unstimulated, stimulation with anti-CD3/anti-CD28, stimulation with anti-CD3/anti-CD28 and interleukin-7 (IL-7) (20 ng/ml), stimulation with anti-CD3/anti-CD28 and IL-18 (50 ng/ml), and stimulation with anti-CD3/anti-CD28 and both IL-7 (20 ng/ml) and IL-18 (50 ng/ml). Results are presented as the mean  $\pm$  SEM normalized transcript levels. Symbols represent individual samples.

have axial SpA (Supplementary Figure 5, <http://onlinelibrary.wiley.com/doi/10.1002/art.42090>), which arguably supports the importance of IL-18 in MAIT cell modulation. In peripheral blood samples, the comparison between axial SpA patients and non-axial SpA control patients did not reveal a significant difference in the serum production of IL-17A and IL-18, but a trend toward increased expression of *IL17F* and *IL7* in axial SpA patients was observed ( $P = 0.0508$  and  $P = 0.06$ , respectively) (Supplementary Figure 6, <http://onlinelibrary.wiley.com/doi/10.1002/art.42090>). In MAIT cells, no significant difference in IL-17A secretion or *IL17A* gene expression was observed (Supplementary Figures 7 and 8, <http://onlinelibrary.wiley.com/doi/10.1002/art.42090>).

**Presence of MAIT cells in entheses unaffected by axial SpA.** Considering that the hallmark of axial SpA

pathogenesis is enthesal inflammation, we investigated and confirmed the presence of MAIT cells in the axial entheses of individuals who did not have axial SpA (Figure 5A). Within both enthesal soft tissue and perienthesal bone, MAIT cells mainly expressed the resident memory marker CD69, while MAIT cells from the peripheral blood mainly expressed CD45RA, which corresponds to a naive/circulating phenotype (Figure 5A).

**Transcriptional profiling of enthesal MAIT cells compared to peripheral blood-derived MAIT cells.** The

comparison of peripheral blood-derived and entheses-derived (from both perienthesal bone and enthesal soft tissue) MAIT cell transcription factors (TCR $\alpha$ 7.2+ and CD161+) showed that enthesal soft tissue MAIT cells had a phenotype characterized by higher *AHR*, *JAK1*, *STAT4*, and *TGF $\beta$ 1* transcript expression

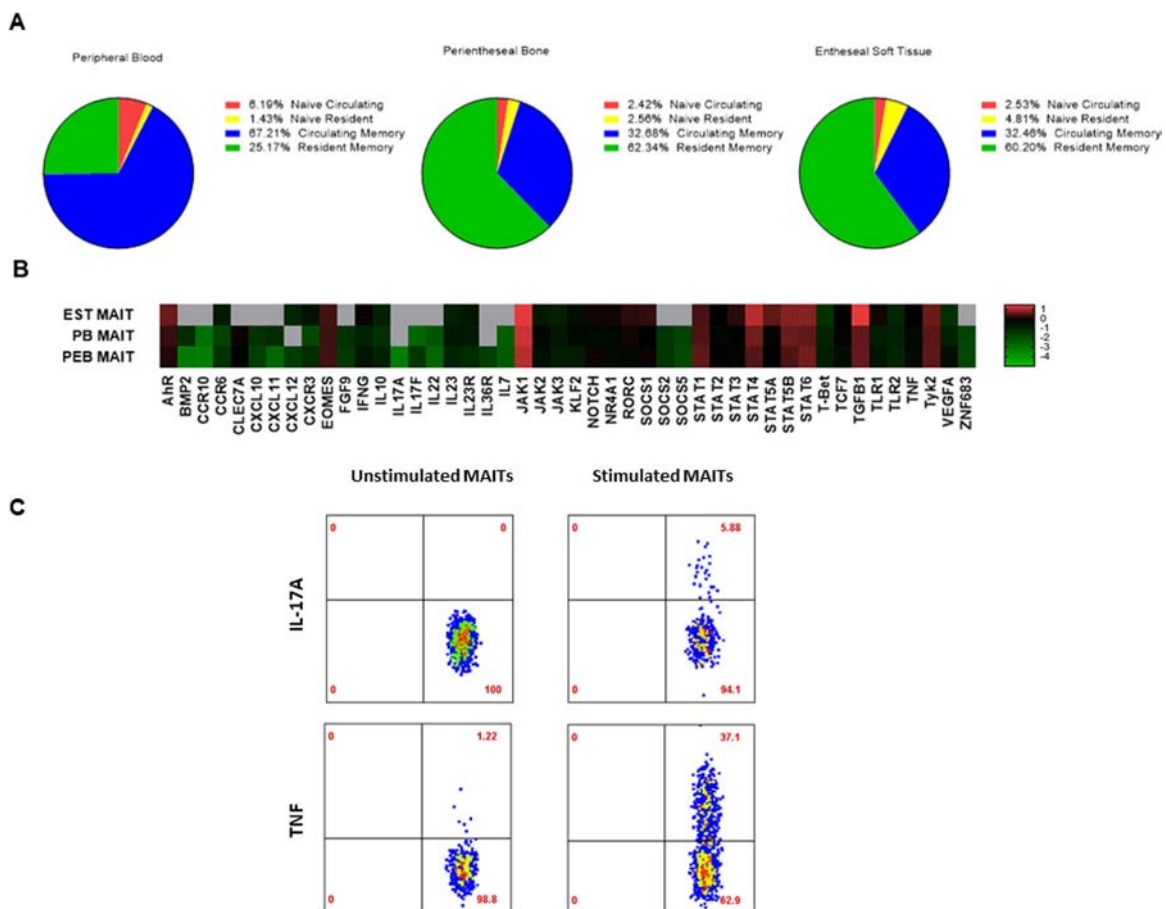


**Figure 5.** Transcriptional profiling of enthesal mucosal-associated invariant T (MAIT) cells and proinflammatory cytokine induction. **A**, Stratification of MAIT cell subsets based on their expression of T cell receptor  $\alpha$ 7.2 and CD161 in enthesal soft tissue (EST), perienthesal bone (PEB), and peripheral blood (PB) from non-axial spondyloarthritis patients. MAIT cells expressing tissue resident/memory markers were identified by CD69 expression, and naive/circulating MAIT cells were identified by CD45RA expression. Results are shown as the mean percentage ( $n = 5$ ). **B**, Basal expression of cytokines, chemokines, growth factors, signaling molecules, and tissue residency markers. Expression values are the  $\log_{10}$  change in threshold cycle relative to the values for hypoxanthine guanine phosphoribosyltransferase ( $n = 7$ ). The color key denotes differential gene expression, in which values  $<-1$  indicate lower relative expression and values  $>1$  indicate higher relative expression. Gray indicates absence of expression.  $P = 0.038$  by 2-tailed  $t$ -test for independent samples for the difference in expression of *CCR6* by MAIT cells from peripheral blood and MAIT cells from perienthesal bone. **C**, Intracellular tumor necrosis factor (TNF) and interleukin-17 (IL-17) cytokine expression in conditions with or without stimulation with phorbol myristate acetate (50 ng/ml) and ionomycin (1  $\mu$ g/ml) for 3 hours in the presence of BD GolgiPlug protein transport inhibitor in perienthesal bone-derived MAIT cells ( $n = 2$ ).

(Figure 5B). Furthermore, transcription factors indicative of circulating T cells, such as *KLF2* and *TBX21*, showed higher expression in peripheral blood-derived MAIT cells (Figure 5B). Enthesis-derived MAIT cells also showed higher expression of growth factors and molecules associated with tissue repair and homeostasis, such as *VEGFA* and *IL10*, when compared to matched peripheral blood-derived MAIT cells (Figure 5B).

In comparison to blood-derived MAIT cells, entheses-derived MAIT cells showed higher *CXCR3* and *CCR6* expression. These findings suggest that entheses-derived MAIT cells are better equipped to mediate proinflammatory signals and tissue migration.

**Induction of TNF and IL-17 expression in enthesal MAIT cells.** Following on previous findings that blood-derived MAIT cells produced IL-17, we next investigated whether enthesal MAIT cells also had the ability to produce this cytokine. Following stimulation with phorbol myristate acetate and ionomycin, MAIT cells showed elevated expression of TNF and IL-17A through intracellular flow (Figure 5C). Overall, 3.2% of stimulated MAIT cells expressed IL-17A and 17.9% of stimulated MAIT cells expressed TNF ( $n = 2$  independent samples with MAIT cells). Given that IL-18 was shown to enhance IL-17 production, we also investigated the expression of IL-18. Our results confirmed that IL-18 was expressed at basal levels in the normal entheses (Supplementary Figure 5, <http://onlinelibrary.wiley.com/doi/10.1002/art.42090>).

## DISCUSSION

The findings presented herein suggest a potentially important role for MAIT cells in the setting of axial SpA. Gene expression profiles based on gene polymorphisms associated with AS showed substantial clustering in MAIT cells. Furthermore, MAIT cells had at least as much IL-17A production capacity as CD4+ T cells. In addition, MAIT cells were able to produce *IL17A* and *IL17F* under conditions of combined stimulation with IL-7 and IL-18 together with TCR triggering. Finally, MAIT cells were present in the spinal entheses of healthy controls, where they were mainly of the resident memory cell phenotype with inducible IL-17A protein production. Collectively, these findings substantially add to the body of evidence incriminating innate-like lymphocytes in the pathogenesis of axial SpA.

We first analyzed the gene expression profiles of 45 genes whose polymorphisms were significantly associated with the predisposition to AS in 4 T cell populations: CD4+ T cells, CD8+ T cells,  $\gamma\delta$  T cells, and MAIT cells. Eighty percent of these genes were expressed among these 4 cell types, with differential expression from one cell population to another leading to cell subset clustering. We observed higher expression levels of prostaglandin receptor EP<sub>4</sub> (*PTGER4*) in CD4+ T cells, through which prostaglandin E<sub>2</sub> regulates Th17 cell differentiation and functioning (23).

This up-regulation of the receptor EP<sub>4</sub> in axial SpA patients could promote CD4 differentiation toward the Th17 pathway, as has been previously reported (23). *TYK2* was expressed at higher levels in adaptive CD8+ T cells, followed by innate-like  $\gamma\delta$  T cells. Tyk2 is a crucial type 3 immunity mediator in SpA, and its inhibition can prevent disease progression by reducing the expansion of Th17 cells in murine models of SpA (24). Inhibition of Tyk2 also showed promising results in a phase II trial in psoriasis (25).

We observed an up-regulation of *IL18R1* and *IL18RAP* in MAIT cells, in accordance with the sensitivity of MAIT cells to IL-18 stimulation for the induction of IL-17. High expression of IL-18R and IL-12R by MAIT cells has been shown to facilitate their activation in a TCR-independent manner, such as during viral infections (26). The relatively high expression of the AS-associated G protein-coupled receptor genes *GPR35* and *GPR65* in MAIT cells could indicate their pathogenic role in the setting of axial SpA, as increased expression of *GPR65* in granulocyte-macrophage colony-stimulating factor-positive CD4+ T cells has been associated with “pathogenic” Th17 cells in SpA patients (27). These results could help us to design functional analyses specifically for MAIT cells.

To better decipher the relative contribution of MAIT cells to IL-17A/IL-17F expression in comparison to CD4+ T cells, we assessed the secretion of IL-17A in cell culture supernatants after stimulation. Generally, MAIT cell frequency is relatively low compared to CD4+ T cells and CD8+ T cells. However, on a per-cell basis, MAIT cells were the major producers of IL-17A in axial SpA patients when compared to CD4+ T cells, CD8+ T cells, and  $\gamma\delta$  T cells. Analysis on a per-cell basis allowed us to precisely characterize the production capacity of each cell type, which is generally challenging for small cell subsets.

MAIT cells strongly expressed *IL23R*, but our work shows that cytokines other than IL-23, such as IL-7/IL-18 alone or in combination, can induce strong expression of *IL17F* messenger RNA. We found particularly high levels of *IL18R1* and *IL18RAP* expression in MAIT cells, suggesting that IL-18 is an important cytokine in the modulation of their function. Furthermore, we found IL-18 production at the basal level in unstimulated MAIT cells derived from the perienthesal bone of non-axial SpA patients, which demonstrates the importance of IL-18 in MAIT cell regulation. IL-18, which is associated with IL-12 and IL-15, induces IFN $\gamma$  secretion by Th1 cells (28) and has been shown to synergize with IL-12 to promote the production of IL-17A/IL-17F by MAIT cells independently of IL-23 (10).

Here we show that another cytokine combination (IL-7 and IL-18) particularly potentiates the production of IL-17F by MAIT cells. To our knowledge, this is the first time that a combination of cytokines has been shown to induce the expression of *IL17F* by MAIT cells in the setting of axial SpA. IL-7 is a key cytokine of the adaptive immune system not only for the development of T cells and dendritic cells, but also for the expansion and survival of immature B cells. While stromal and epithelial cells are known

to be the main producers of IL-7, a study by Ciccia et al demonstrated that intestinal Paneth cells could also produce IL-7 (29). IL-7 is constitutively produced at low levels, but elevated levels of IL-7 have been observed in the sacroiliac joint fluid of patients with SpA (30). Recently, IL-17F has gained interest with the approval of bimekizumab for the treatment of psoriasis (31), and bimekizumab has also shown promising results in patients with axial SpA (32). In the present study, we did not focus on the role of *IL23R* in the pathogenesis of axial SpA. Additional studies with specific approaches to better deciphering the complexity of the interactions in the different IL-17-producing cells are needed.

In this work, the contribution of  $\gamma\delta$  T cells and CD8+ T cells from peripheral blood to the production of IL-17A was minimal, but it is possible that tissue-specific expression of IL-17A is much higher at sites targeted during the inflammatory process in axial SpA. While neutrophils have previously been described as IL-17-producing cells (22), our work with 2 robust techniques (nCounter and Simoa technology) did not confirm this, even when strong stimulation combining phorbol myristate acetate, the calcium ionophore A23187, and  $\beta$ -1,3-glucan was used. This supports the previous finding that neutrophils do not substantially contribute to the production of IL-17 (21).

Several reports have suggested that in the peripheral form of axial SpA, MAIT cells are not the only cells which produce IL-17. Both iNKT and  $\gamma\delta$  T cells are increased in the synovial fluid of patients with SpA and contribute to IL-17 expression, but they contribute through an IL-23-dependent mechanism (13). This may be in part due to the shared transcription factor promyelocytic leukaemia zinc-finger (PLZF; encoded by *ZBTB16*), which is present in MAIT cells, iNKTs, and  $\gamma\delta$  T cells (33). Kenna et al observed high expression of IL-23R on the surface of  $\gamma\delta$  T cells (6), but this cell population did not appear to be the main source of IL-17 production in the axial form of SpA. Group 3 innate lymphoid cells are also capable of producing IL-17A, but Blijdorp et al (34) recently demonstrated that these cells produced IL-22 rather than IL-17A in the joints of patients with peripheral SpA.

This study had some limitations which can be addressed in future research, such as the assessment of local production of IL-7 and IL-18 within the enthesal tissues of axial SpA patients. It would be ideal to use matched MAIT cells from the blood and entheses of patients with axial SpA, but enthesal tissue samples from axial SpA patients are difficult to access.

In this study, we used data from genome-wide association studies to examine transcript expression in cells relevant to the pathogenesis of axial SpA, and given the recent and unexpected developments in translational therapeutics for the treatment of SpA where IL-17 inhibition rather than IL-23 inhibition was effective, we focused our research on the IL-23/IL-17 pathway. Our findings support the hypothesis of major involvement of conventional T cell subsets and innate-like lymphocytes in the pathogenesis of SpA. However, MAIT cells from peripheral blood were shown to be the main producers of IL-17A in axial SpA patients

when compared to CD4+ T cells, CD8+ T cells, and  $\gamma\delta$  T cells. Moreover, the stimulation of MAIT cells with combined IL-7 and IL-18 was able to strongly induce *IL-17F* expression. A trend toward increased expression of IL-17F and IL-7 was also observed in the serum of axial SpA patients compared to control patients. The importance of MAIT cells was highlighted by their identification within enthesal tissues where basal IL-18 protein expression was also found. Further studies are needed to assess whether similar findings hold true in the enthesal tissues from axial SpA patients and to what extent the in situ production of IL-7 and IL-18 induces IL-17F expression.

## ACKNOWLEDGMENT

We thank the members of Cytometry and Biomarkers UTechS from the Institut Pasteur for their technical assistance.

## AUTHOR CONTRIBUTIONS

All authors were involved in drafting the article or revising it critically for important intellectual content, and all authors approved the final version to be published. Dr. Miceli-Richard had full access to all of the data in the study and takes responsibility for the integrity of the data and the accuracy of the data analysis.

**Study conception and design.** Rosine, Rowe, Koturan, Yahia-Cherbal, Leloup, Watad, Berenbaum, Sellam, Dougados, Aimaniananda, Cuthbert, Bridgewood, Newton, Bianchi, Rogge, McGonagle, Miceli-Richard.

**Acquisition of data.** Rosine, Rowe, Koturan, Yahia-Cherbal, Leloup.


**Analysis and interpretation of data.** Rosine, Rowe, Koturan, Cuthbert, Bridgewood, Newton, Bianchi, Rogge, McGonagle, Miceli-Richard.

## REFERENCES

- Smith JA, Colbert RA. The interleukin-23/interleukin-17 axis in spondyloarthritis pathogenesis: Th17 and beyond. *Arthritis Rheumatol* 2014;66:231–41.
- Ellinghaus D, Jostins L, Spain SL, et al. Analysis of five chronic inflammatory diseases identifies 27 new associations and highlights disease-specific patterns at shared loci. *Nat Genet* 2016;48:510–8.
- Baeten D, Baraliakos X, Braun J, et al. Anti-interleukin-17A monoclonal antibody secukinumab in treatment of ankylosing spondylitis: a randomised, double-blind, placebo-controlled trial. *Lancet* 2013;382:1705–13.
- Van der Heijde D, Wei JC, Dougados M, et al. Ixekizumab, an interleukin-17A antagonist in the treatment of ankylosing spondylitis or radiographic axial spondyloarthritis in patients previously untreated with biological disease-modifying anti-rheumatic drugs (COAST-V): 16-week results of a phase 3 randomised, double-blind, active-controlled and placebo-controlled trial. *Lancet* 2018;398:2441–51.
- Jandus C, Bioley G, Rivals JP, et al. Increased numbers of circulating polyfunctional Th17 memory cells in patients with seronegative spondylarthritides. *Arthritis Rheum* 2008;58:2307–17.
- Kenna TJ, Davidson SI, Duan R, et al. Enrichment of circulating interleukin-17-secreting interleukin-23 receptor-positive  $\gamma\delta$  T cells in patients with active ankylosing spondylitis. *Arthritis Rheum* 2012;64:1420–9.
- Gracey E, Qaiyum Z, Almaghlouth I, et al. IL-7 primes IL-17 in mucosal-associated invariant T (MAIT) cells, which contribute to the Th17-axis in ankylosing spondylitis. *Ann Rheum Dis* 2016;75:2124–32.

8. Watad A, Rowe H, Russell T, et al. Normal human entheses harbours conventional CD4+ and CD8+ T cells with regulatory features and inducible IL-17A and TNF expression. *Ann Rheum Dis* 2020;79:1044–54.
9. Appel H, Maier R, Wu P, et al. Analysis of IL-17(+) cells in facet joints of patients with spondyloarthritis suggests that the innate immune pathway might be of greater relevance than the Th17-mediated adaptive immune response. *Arthritis Res Ther* 2011;13:R95.
10. Cole S, Murray J, Simpson C, et al. Interleukin (IL)-12 and IL-18 synergize to promote MAIT Cell IL-17A and IL-17F production independently of IL-23 signaling. *Front Immunol* 2020;11:585134.
11. Spits H, Artis D, Colonna M, et al. Innate lymphoid cells—a proposal for uniform nomenclature [review]. *Nat Rev Immunol* 2013;13:145–9.
12. Monteiro M, Almeida CF, Agua-Doce A, et al. Induced IL-17-producing invariant NKT cells require activation in presence of TGF- $\beta$  and IL-1 $\beta$ . *J Immunol* 2013;190:805–11.
13. Venken K, Jacques P, Mortier C, et al. ROR $\gamma$ t inhibition selectively targets IL-17 producing iNKT and  $\gamma\delta$ -T cells enriched in Spondyloarthritis patients. *Nat Commun* 2019;10:9.
14. Cuthbert RJ, Bridgwood C, Watad A, et al. Evidence that tissue resident human entheses  $\gamma\delta$ T-cells can produce IL-17A independently of IL-23R transcript expression. *Ann Rheum Dis* 2019;78:1559–65.
15. Baeten D, Østergaard M, Wei JC, et al. Risankizumab, an IL-23 inhibitor, for ankylosing spondylitis: results of a randomised, double-blind, placebo-controlled, proof-of-concept, dose-finding phase 2 study. *Ann Rheum Dis* 2018;77:1295–302.
16. Wendling D, Prati C, Chouk M, et al. Effects of anti-IL-23 and anti-IL-17: the hidden side of spondyloarthritis polymorphism? [editorial]. *Joint Bone Spine* 2020;87:5–7.
17. Tang XZ, Jo J, Tan AT, et al. IL-7 licenses activation of human liver intrasinusoidal mucosal-associated invariant T cells. *J Immunol* 2013;190:3142–52.
18. Rudwaleit M, van der Heijde D, Landewé R, et al. The development of Assessment of SpondyloArthritis international Society classification criteria for axial spondyloarthritis (part II): validation and final selection. *Ann Rheum Dis* 2009;68:777–83.
19. Bridgwood C, Russell T, Weedon H, et al. The novel cytokine Metrn-1/IL-41 is elevated in psoriatic arthritis synovium and inducible from both entheses and synovial fibroblasts. *Clin Immunol* 2019;208:108253.
20. Menegatti S, Guillemot V, Latis E, et al. Immune response profiling of patients with spondyloarthritis reveals signalling networks mediating TNF-blocker function in vivo. *Ann Rheum Dis* 2020;80:475–86.
21. Tamassia N, Arruda-Silva F, Calzetti F, et al. A reappraisal on the potential ability of human neutrophils to express and produce IL-17 family members in vitro: failure to reproducibly detect it. *Front Immunol* 2018;9:795.
22. Taylor PR, Roy S, Leal SM, et al. Activation of neutrophils by autocrine IL-17A-IL-17RC interactions during fungal infection is regulated by IL-6, IL-23, ROR $\gamma$ t and dectin-2. *Nat Immunol* 2014;15:143–51.
23. Klasen C, Meyer A, Wittekind PS, et al. Prostaglandin receptor EP4 expression by Th17 cells is associated with high disease activity in ankylosing spondylitis. *Arthritis Res Ther* 2019;21:159.
24. Gracey E, Hromadová D, Lim M, et al. TYK2 inhibition reduces type 3 immunity and modifies disease progression in murine spondyloarthritis. *J Clin Invest* 2020;130:1863–78.
25. Papp K, Gordon K, Thaçi D, et al. Phase 2 trial of selective tyrosine kinase 2 inhibition in psoriasis. *N Engl J Med* 2018;379:1313–21.
26. Ussher JE, Willberg CB, Klenerman P. MAIT cells and viruses. *Immunol Cell Biol* 2018;96:630–41.
27. Al-Mossawi MH, Chen L, Fang H, et al. Unique transcriptome signatures and GM-CSF expression in lymphocytes from patients with spondyloarthritis. *Nat Commun* 2017;8:1510.
28. Leng T, Akther HD, Hackstein CP, et al. TCR and inflammatory signals tune human MAIT cells to exert specific tissue repair and effector functions. *Cell Reports* 2019;28:3077–91.
29. Ciccio F, Guggino G, Rizzo A, et al. Type 3 innate lymphoid cells producing IL-17 and IL-22 are expanded in the gut, in the peripheral blood, synovial fluid and bone marrow of patients with ankylosing spondylitis. *Ann Rheum Dis* 2015;74:1739–47.
30. Rihl M, Kellner H, Kellner W, et al. Identification of interleukin-7 as a candidate disease mediator in spondylarthritis. *Arthritis Rheum* 2008;58:3430–5.
31. Papp KA, Merola JF, Gottlieb AB, et al. Dual neutralization of both interleukin 17A and interleukin 17F with bimekizumab in patients with psoriasis: results from BE ABLE 1, a 12-week randomized, double-blinded, placebo-controlled phase 2b trial. *J Am Acad Dermatol* 2018;79:277–86.
32. Van der Heijde D, Gensler LS, Deodhar A, et al. Dual neutralisation of interleukin-17A and interleukin-17F with bimekizumab in patients with active ankylosing spondylitis: results from a 48-week phase IIb, randomised, double-blind, placebo-controlled, dose-ranging study. *Ann Rheum Dis* 2020;79:595–604.
33. Zhang S, Laouar A, Denzin LK, et al. Zbtb16 (PLZF) is stably suppressed and not inducible in non-innate T cells via T cell receptor-mediated signaling. *Sci Rep* 2015;5:12113.
34. Blijdorp IC, Menegatti S, Mens LJ, et al. Expansion of interleukin-22- and granulocyte-macrophage colony-stimulating factor-expressing, but not interleukin-17A-expressing, group 3 innate lymphoid cells in the inflamed joints of patients with spondyloarthritis. *Arthritis Rheumatol* 2019;71:392–402.

# Choroid Plexus–Infiltrating T Cells as Drivers of Murine Neuropsychiatric Lupus

Erica Moore,<sup>1</sup> Michelle W. Huang,<sup>1</sup> Cara A. Reynolds,<sup>2</sup> Fernando Macian,<sup>2</sup> and Chaim Putterman<sup>3</sup> 

**Objective.** T cells are critical in the pathogenesis of systemic lupus erythematosus (SLE) in that they secrete inflammatory cytokines, help autoantibody production, and form autoreactive memory T cells. Although the contribution of T cells to several forms of organ-mediated damage in SLE has been previously demonstrated, the role of T cells in neuropsychiatric SLE (NPSLE), which involves diffuse central nervous system manifestations and is observed in 20–40% of SLE patients, is not known. Therefore, we conducted this study to evaluate how behavioral deficits are altered after depletion or transfer of T cells, to directly assess the role of T cells in NPSLE.

**Methods.** MRL/lpr mice, an NPSLE mouse model, were either systemically depleted of CD4+ T cells or intracerebroventricularly injected with choroid plexus (CP)–infiltrating T cells and subsequently evaluated for alterations in neuropsychiatric manifestations. Our study end points included evaluation of systemic disease and assessment of central nervous system changes.

**Results.** Systemic depletion of CD4+ T cells ameliorated systemic disease and cognitive deficits. Intracerebroventricular injection of CP–infiltrating T cells exacerbated depressive-like behavior and worsened cognition in recipient mice compared with mice who received injection of splenic lupus T cells or phosphate buffered saline. Moreover, we observed enhanced activation in CP–infiltrating T cells when cocultured with brain lysate–pulsed dendritic cells in comparison to the activation levels observed in cocultures with splenic T cells.

**Conclusion.** T cells, and more specifically CP–infiltrating antigen-specific T cells, contributed to the pathogenesis of NPSLE in mice, indicating that, in the development of more targeted treatments for NPSLE, modulation of T cells may represent a potential therapeutic strategy.

## INTRODUCTION

T cells are integral in the pathogenesis of systemic lupus erythematosus (SLE), a complex, systemic autoimmune disease that primarily affects women (1,2). As a result of aberrant activation and defects in peripheral tolerance, SLE T cells promote chronic inflammation by secreting inflammatory cytokines, helping autoantibody production, and forming autoreactive memory T cells. Furthermore, the infiltration of SLE T cells into nonlymphoid target organs, such as the skin, kidneys, and the brain, perpetuates localized damage (2).

The pathogenicity of SLE T cells has been extensively established in studies that used monoclonal antibodies (3–5), fusion proteins (6,7), and gene-targeted deletion (8,9) involving both

specific T cell subsets and costimulatory pathways. In addition to their role in the increased expression of the major histocompatibility complex (10) and the oligoclonality present in lupus nephritis (11), kidney-specific SLE CD4+ T cell clones have been shown to accelerate kidney damage without increasing anti-double-stranded DNA (anti-dsDNA) antibodies (12). This suggests that organ-infiltrating T cells are autospecific for tissue-dependent antigens.

Neuropsychiatric systemic lupus erythematosus (NPSLE) affects ~20–40% of patients with SLE and encompasses a wide spectrum of clinical symptoms, including those related to mood and cognitive disorders (13). The issue of appropriate attribution of symptoms to disease or therapeutic side effects further complicates the clinical care of patients with NPSLE. Despite their

Dr. Moore's work was supported by the Gina M. Finzi Memorial Student Summer Fellowship Program and the Medical Scientist Training Program (award T32-GM007288).

<sup>1</sup>Erica Moore, MS, Michelle W. Huang, PhD: Department of Microbiology and Immunology, Division of Rheumatology, Albert Einstein College of Medicine, New York; <sup>2</sup>Cara A. Reynolds, MS, Fernando Macian, MD, PhD: Department of Pathology, Albert Einstein College of Medicine, New York; <sup>3</sup>Chaim Putterman, MD: Azrieli Faculty of Medicine of Bar-Ilan University, Safed, Israel, Galilee Research Institute, Nahariya, Israel, and Department of

Microbiology and Immunology, Division of Rheumatology, Albert Einstein College of Medicine, New York.

Author disclosures are available at <https://onlinelibrary.wiley.com/action/downloadSupplement?doi=10.1002%2Fart.42252&file=art42252-sup-0001-Disclosureform.pdf>.

Address correspondence via email to Chaim Putterman, MD, at [chaim.putterman@einsteinmed.edu](mailto:chaim.putterman@einsteinmed.edu).

Submitted for publication March 6, 2022; accepted in revised form May 24, 2022.

established contribution to systemic disease and organ-mediated damage, T cells have not been shown to play a role in the underlying mechanisms responsible for the central nervous system (CNS) manifestations in SLE patients (14,15).

In some NPSLE patients and NPSLE mouse models, a leukocytic infiltrate has been noted in the choroid plexus (CP) (16–19). The CP forms the blood–cerebrospinal fluid barrier and is increasingly considered to be a neuroimmune interface (20). Furthermore, resolution of the CP infiltrate was associated with improvement in behavior (21,22). In particular, the CP in the MRL/lpr strain, a widely used NPSLE mouse model that develops cognitive and affective behavioral deficits similar to neuropsychiatric manifestations in human lupus, becomes heavily infiltrated with T cells while the brain parenchyma is mostly unaffected (16,19,23). O’Sullivan et al have previously described amelioration of the CP infiltrate with CD4+ T cell depletion but did not detail whether behavioral deficits were similarly improved (24). Furthermore, our recent findings of unique T cell receptor (TCR) clonality in the CP compared with other affected tissue sites in MRL/lpr mice suggest that brain-infiltrating T cells may be locally contributing to NPSLE and may have specific reactivity to brain-specific antigens (25).

Using a mouse model of lupus, we investigated the potential contribution of T cells to the pathogenesis of NPSLE by performing systemic depletion of CD4+ T cells or by locally injecting CP-infiltrating T cells intracerebroventricularly (ICV) in mice to evaluate whether neuropsychiatric disease was attenuated or promoted, respectively. We conducted further evaluations to understand the mechanisms by which T cells may be contributing to NPSLE. As T cell therapies are currently being evaluated in the treatment of lupus, our study examines brain-infiltrating T cells as specific contributors to NPSLE.

## METHODS

**Mice.** Female MRL/MpJ-Fas<sup>lpr/lpr</sup> (MRL/lpr) mice were either purchased from The Jackson Laboratory at ~5–6 weeks of age or bred at the Albert Einstein College of Medicine animal facilities. We used only female MRL/lpr mice for experiments, since, similar to human lupus, the disease phenotype is more penetrant and severe in females. We used baseline serum anti-dsDNA indices to normalize and assign mice into treatment groups. Mice were housed at 21–23°C on a 12-hour light/dark cycle. All animal protocols were approved by the Albert Einstein College of Medicine Animal Care and Use Committee.

**Stimulation and expansion of T cells.** We generated pooled (nonsorted) single-cell suspensions from phosphate buffered saline (PBS)–perfused spleen or CP tissue excised from donor 16- to 18-week-old female MRL/lpr mice (7–10 mice), as previously described (17). Cells were initially stimulated and expanded on plates precoated with 0.5 µg/ml of anti-CD3

antibodies (BD Pharmingen) and with 0.5 µg/ml of anti-CD28 antibodies (BD Pharmingen) added to RPMI 1640 medium supplemented with 10% fetal bovine serum (17). We then added 10 units of murine interleukin-2 (IL-2) (R&D Systems) every other day to further stimulate T cell proliferation for 7 days, after which cells were prepared for phenotyping and/or injection.

**Systemic depletion of CD4+ T cells.** Female MRL/lpr mice were systemically depleted of CD4+ T cells as previously described (24). In brief, the 2 cohorts of 6-week-old female mice (~7 mice per group) were intraperitoneally (IP) injected with a bolus of 2 mg of either anti-CD4 (Clone GK1.5; Bioxcell) or anti-keyhole limpet hemocyanin IgG2b isotype (Clone LTF-2; Bioxcell) as control, with the initial injection subsequently followed by weekly 1-mg IP injections. At 14 weeks of age, mice were assessed for cognitive and affective deficits. For postmortem assessments of mice at end of study, 1 mouse cohort was used for histologic analyses and the other for transcriptome analyses. Only one isotype-treated mouse was excluded from behavioral results because of insufficient exploration.

**ICV adoptive transfer.** We administered a single ICV injection of CP T cells, splenic T cells, or PBS into 6-week-old MRL/lpr female mice (4 cohorts of 4–8 mice per group because of technical considerations related to the surgery) (26). In brief, we implanted a single-guide syringe (Hamilton) into the right lateral ventricle at the following coordinates: 0.34 mm anteroposterior, 1.00 mm mediolateral, and 2 mm dorsal ventricular. The T cells, which underwent 3 washes in PBS, were injected at a rate of 0.35 µl/minute for a total count of 200,000 cells and a volume of 2 µl; PBS alone was used as a control. We performed the surgeries during daytime hours and provided postsurgical care to the mice in accordance with the approved animal protocol. After 4 weeks, injected mice underwent behavioral testing. After testing, we conducted postmortem histology, transcriptome, and flow cytometry assessments.

**Carboxyfluorescein succinimidyl ester (CFSE) labeling and in vivo tracking.** After stimulation and expansion of cells for 7 days, we prepared the CP and splenic T cells into pellets and discarded the supernatant. We resuspended the T cells in CFSE staining solution (Invitrogen) and incubated the cells at 37°C for 20 minutes. Stained cells were quenched with the addition of medium and further incubated at 37°C for 5 additional minutes. Cells were robustly washed and resuspended in sterile PBS. We then intravenously injected the recipient 6- to 7-week-old MRL/lpr female mice with 500,000 cells; mice were killed 2 or 4 days after injection to evaluate CFSE-labeled T cell infiltration in various organs by flow cytometry.

**Isolation and coculture of pulsed dendritic cells with T cells.** Single-cell suspensions of MRL/lpr splenocytes



were generated, and CD11c+ dendritic cells were subsequently isolated from the splenocytes using CD11c+ microbeads (Miltenyi Biotec) (27). MRL/*lpr* splenocytes or CD11c+ dendritic cells were pulsed for 24 hours with lysates containing either 200 µg/ml brain tissue from MRL/*lpr* or MRL/MpJ mice or 200 µg/ml liver tissue from MRL/*lpr* mice. After 1–2 hours of incubation, we added 100 ng/ml of lipopolysaccharide to activate and mature the dendritic cells. We added CFSE-labeled splenic or CP T cells retrieved from the 16- to 18-week-old MRL/*lpr* mice at a ratio of ~1:1 and cocultured the cells with the pulsed dendritic cells for 28 hours. After we added cell activation cocktail with brexfieldin A (Biolegend) for the final 6 hours of incubation, we evaluated T cell proliferation and activation markers by flow cytometry.

**Behavioral tests.** *Object placement (OP) and object recognition (OR) tests.* We used OP and OR tests to evaluate spatial memory and recognition memory, respectively. The mice were subjected to 2 trials; these “training periods” were meant to initially expose the mice to 2 identical objects in fixed positions. After a retention interval, we placed the mice back into the same field but with one of the objects moved (OP test) or replaced (OR test). Interactions of mice with either the “novel” object or the “old” object were manually recorded. Experimenters were blinded to the experimental assignment of tested mice. Due to a mouse’s innate preference to explore novel objects in their environment, the OP and OR tests were evaluated categorically as a “pass” (>55% novel object preference) or a “fail” (<55% novel object preference); this robust cutoff was previously determined for this behavioral test in the MRL/*lpr* strain (28). We calculated the OP or OR preference score as follows: exploration time of novel object/total interaction time with either object × 100 (expressed as a percentage). We excluded mice if they insufficiently explored the field and objects (<3 seconds in either trial).

*Porsolt swim test.* Mice underwent the Porsolt swim test to assess depressive-like behavior, with assessments based on a mouse’s immobility when swimming. In brief, we placed each mouse into a transparent cylindrical tank with water at 27°C. Animals were allowed to initially adjust to the environment for 1 minute, after which we scored the mice over three 3-minute intervals. The immobility percentage was calculated as the amount of time a mouse was immobile/total time evaluated. Mice that failed to meet prespecified inclusion criteria were excluded from the behavioral test analyses.

**Flow cytometry.** Cells were stained for flow cytometry as previously described (17). In brief, we generated single-cell suspensions after the final PBS perfusion using a 0.25% trypsin-EDTA digestion buffer (Gibco) for the CP or a mechanical dissociation method for the spleen. After lysis of red blood cells (Thermo Fisher Scientific), cells were washed and then Fc blocked with anti-CD16 (BD Pharmingen) in 3% fetal bovine serum–PBS for 15–30 minutes on ice. Multiple panels were used to stain cells,

including phenotyping of activated/proliferating T cells and phenotyping of the CP infiltrate for lymphoid and myeloid cells.

**Enzyme-linked immunosorbent assays (ELISAs).** We measured IgG anti-dsDNA antibodies, IgG anti-chromatin antibodies, and total immunoglobulins by ELISA in serum samples obtained at baseline and/or at study end as previously described (29–31). We conducted blood urea nitrogen ELISAs according to the manufacturer’s instructions (BioAssay Systems).

**Histology and immunofluorescence staining.** Staff at the Albert Einstein Histopathology and Comparative Pathology Core conducted hematoxylin and eosin (H&E) staining. For immunofluorescence staining, brain and kidney sections were deparaffinized and rehydrated, followed by antigen retrieval in citrate buffer (pH 6) at 90–95°C for 10 minutes. Slides were subsequently washed in PBS and blocked in 20% horse serum–2% Triton in PBS for 1 hour at room temperature. Slides were incubated with antibodies against either CD3 (1:200; Invitrogen), B220 (1:200; Becton Dickinson, now known simply as BD), CD4 (1:200; eBioscience), CD8a (1:200; eBioscience), ionized calcium-binding adapter molecule 1 (IBA-1) (1:200; Fujifilm Wako), glial fibrillary acidic protein (GFAP) (1:200; Invitrogen), or C3 (1:200; MP Biomedicals) for 2 days, with the first day at room temperature and the second day at 4°C. Slides were washed in PBS and incubated with either donkey anti-rat or donkey anti-rabbit secondary antibodies (1:200; JacksonImmuno Research). For final steps, slides were washed, stained with DAPI, and mounted using Fluoromount-G (Southern Biotech). Sections were imaged using the EVOS Fl Auto 2 and quantified with either ImageJ or Volocity software.

**RNA isolation, complementary DNA (cDNA) synthesis, and polymerase chain reaction (PCR) arrays.**

Retrieved tissue was flash frozen in liquid nitrogen. RNA was homogenized and isolated from tissue using TRIzol and either the Zymo Mini kit or the Micro-prep kit, according to the manufacturer’s instructions. We synthesized cDNA from 400 ng of RNA using the Qiagen RT<sup>2</sup> First-Strand kit. We used the Qiagen RT<sup>2</sup> Profiler PCR array according to the manufacturer’s instructions, with arrays run on the real-time quantitative PCR ViiA 7 system (Thermo Fisher Scientific). We normalized and analyzed data using the manufacturer’s provided online tool. We identified the top differentially expressed genes based on either >2-fold change in expression level or significant difference in expression based on a threshold of  $P < 0.05$  (determined by Student’s *t*-test).

**Statistical analysis.** We used GraphPad Prism 9 software for all data analyses. For each experiment, we included multiple replications or mouse cohorts. When comparing groups, we first tested data for normality and then performed either a Student’s *t*-test or one-way analysis of variance. For the OP and OR

behavioral tests, we performed chi-square tests. We used Tukey's or Dunn's tests for multiple comparisons based on normality results. Throughout the results,  $P$  values less than 0.05 were considered significant.

## RESULTS

**Control of systemic disease in MRL/lpr mice by systemic depletion of CD4+ T cells.** To confirm the successful depletion of CD4+ T cells, we performed flow cytometry on blood samples from mice after they had undergone several weeks of IP injection of anti-CD4 antibodies or isotype control. Blood samples from mice that received anti-CD4 antibody treatment were significantly depleted of CD4+ T cells compared with the isotype control group, whereas the percentage of CD8+ T cells was not

significantly different between the anti-CD4-treated and control groups (Figure 1A). Postmortem assessments of the treated mice indicated that splenomegaly and anti-dsDNA autoantibodies were significantly decreased in the CD4+ T cell-depleted mice versus the isotype control group (Figures 1B and C, respectively). Furthermore, kidney disease was similarly significantly attenuated (Figure 1D). These results confirm that depletion of CD4+ T cells ameliorated systemic and kidney disease in MRL/lpr mice.

**Amelioration of neuropsychiatric manifestations by systemic depletion of CD4+ T cells.** Our evaluation of cognitive deficits and affective behavior in MRL/lpr mice systemically depleted of CD4+ T cells showed that, compared with mice in the isotype control group without CD4+ T cell depletion, the CD4+ T cell-depleted mice demonstrated significantly improved

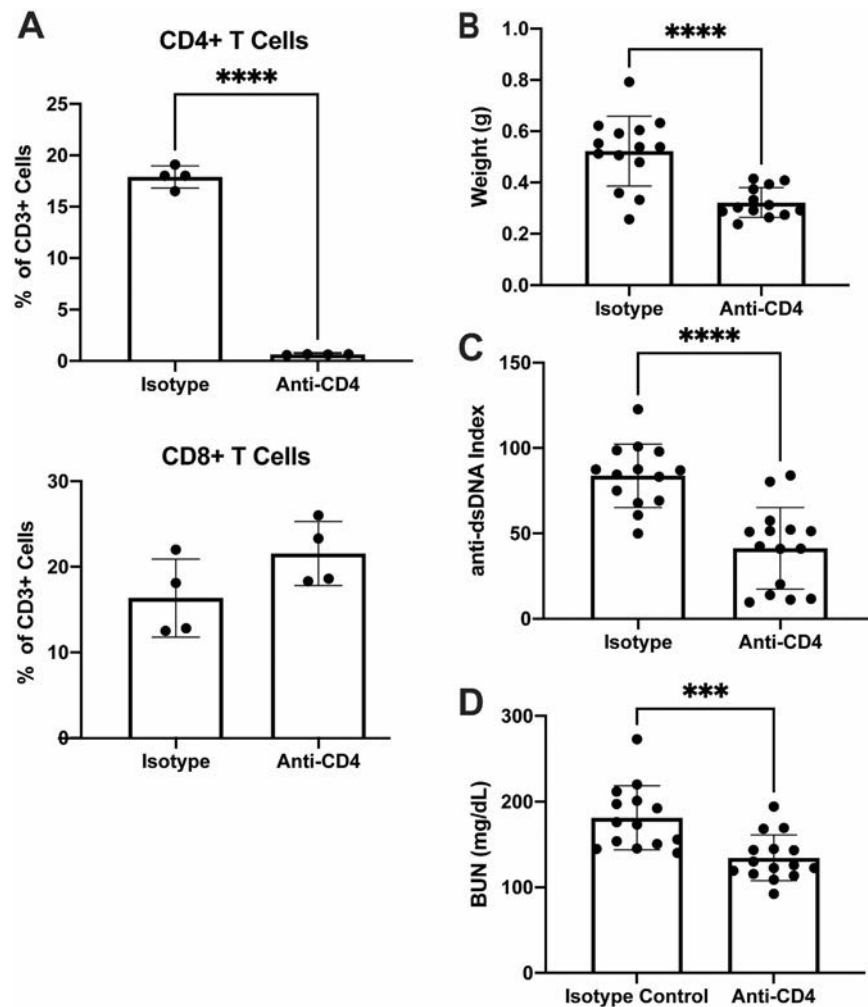


**Figure 1.** Attenuation of systemic disease in MRL/lpr mice after depletion of CD4+ T cells. **A**, Percentage of CD4+ and CD8+ T cells among peripheral blood mononuclear cells in blood samples obtained from mice 4 weeks after treatment with anti-CD4 or isotype control. **B**, Weight of spleens obtained postmortem from mice to assess presence of splenomegaly. **C**, Assessment of postmortem titer levels of serum anti-double-stranded DNA (anti-dsDNA) autoantibodies in mice. **D**, Measurement of blood urea nitrogen (BUN) in postmortem serum samples from mice to assess lupus nephritis. In **A–D**, solid symbols show individual mice; bars show the mean  $\pm$  SD. The treatment groups were compared using Student's  $t$ -test. \*\*\* =  $P < 0.001$ ; \*\*\*\* =  $P < 0.0001$ .

spatial and recognition memory (Figures 2A and B). Furthermore, we observed a modest improvement in depressive-like behavior according to the Porsolt swim test in CD4+ T cell-depleted mice (Supplementary Figure 1, available on the *Arthritis & Rheumatology* website at <https://onlinelibrary.wiley.com/doi/10.1002/art.42252>). Overall, these results suggested that CD4+ T cells do contribute, whether

directly or indirectly, to the neuropsychiatric manifestations in MRL/lpr mice.

Systemic CD4+ T cell depletion significantly attenuated the CP infiltrate present in MRL/lpr mice. H&E staining of brain tissue from CD4+ T cell-depleted mice showed that very few lymphocytes were present in the CP (Figure 2C). Concordantly, immunofluorescence staining indicated that CD4+ T cells were absent

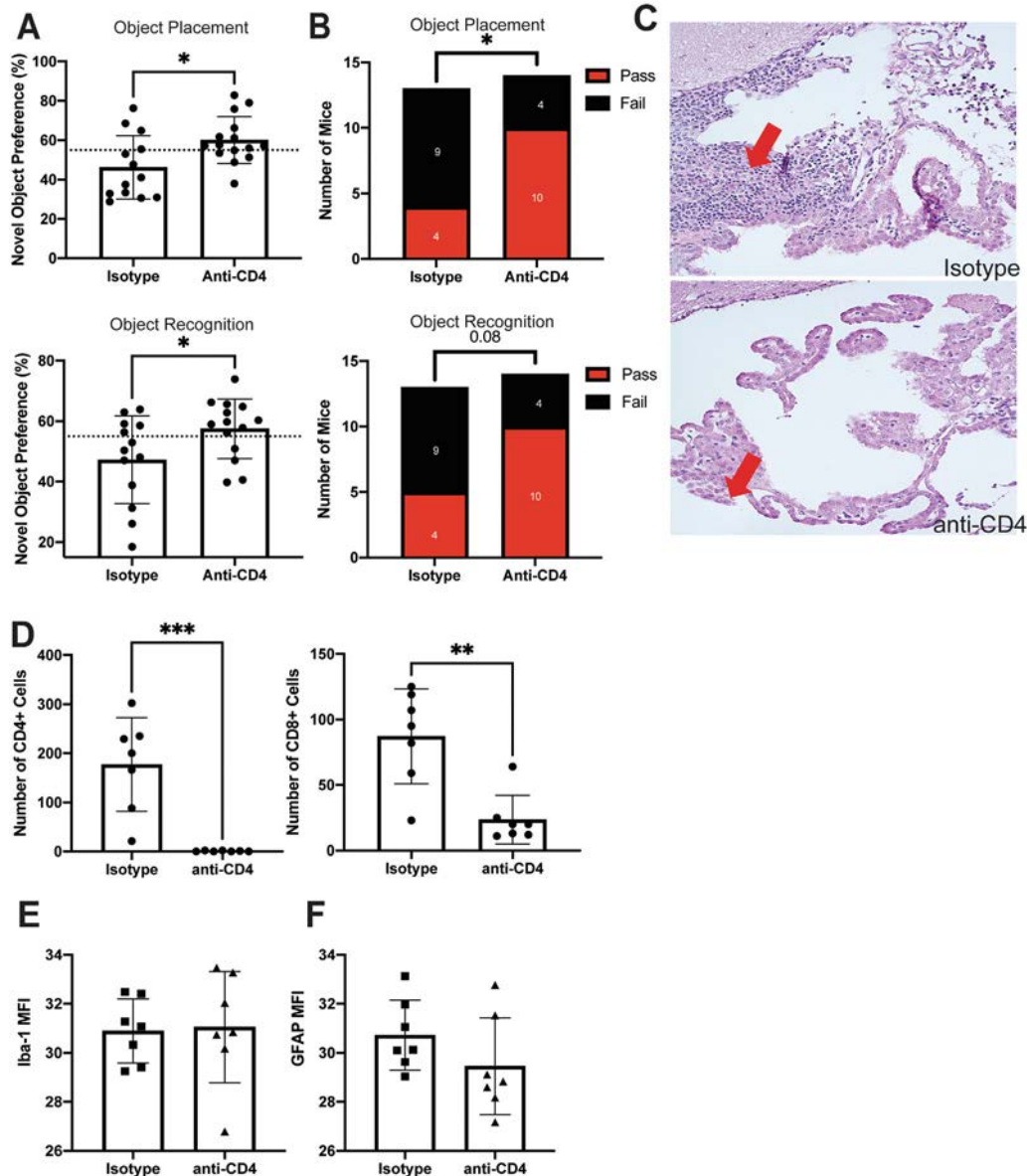


**Figure 2.** Improved cognition in MRL/lpr mice after systemic depletion of CD4+ T cells. **A**, Percentage of mice exhibiting novel object preference in assessments of spatial memory (object placement test) and recognition memory (object recognition test). Dashed line indicates a cutoff level of 55% for pass/fail, where those above the line had a passing score (i.e., showed novel object preference). **B**, Number of mice with a passing or failing score, based on 55% cutoff, during novel object preference tests for either spatial memory ( $n = 13$  mice) (top) or recognition memory ( $n = 14$  mice) (bottom). **C**, Representative images of hematoxylin and eosin–stained brain tissue from mice treated with isotype control or anti-CD4, with **arrows** indicating the choroid plexus (CP) infiltrate. **D–F**, Immunofluorescence staining (expressed as mean fluorescence intensity [MFI]) of CD4+ and CD8+ in T cells in the CP (**D**), of ionized calcium–binding adapter molecule 1 (IBA-1) in the hippocampus to assess microglial activation ( $n = 7$  mice) (**E**), and of glial fibrillary acidic protein (GFAP) in the hippocampus to assess astrocyte activation (**F**). In **A** and **D–F**, solid symbols show individual mice; bars show the mean  $\pm$  SD. The treatment groups were compared using Student's *t*-test or chi-square test. \* =  $P < 0.05$ ; \*\* =  $P < 0.01$ ; \*\*\* =  $P < 0.001$ . Color figure can be viewed in the online issue, which is available at <http://onlinelibrary.wiley.com/doi/10.1002/art.42252/abstract>.

and the number of CD8+ T cells was significantly decreased in the CP (Figure 2D). Hippocampal tissue was stained for IBA-1 and GFAP as markers of microglial and astrocyte activation, respectively. We found no significant differences in the mean fluorescence intensity results for IBA-1 or GFAP (Figures 2E and F, respectively) between the groups. Thus, CD4+ T cell-depleted MRL/lpr mice had attenuated systemic and neuropsychiatric disease with significant resolution of the CP infiltrate.

**Accelerated neuropsychiatric disease by local adoptive transfer of CP-infiltrating T cells.** To demonstrate

the local and specific effects of brain-infiltrating T cells on neuropsychiatric disease, we cultured CP T cells or splenic T cells from older MRL/lpr mice (14 weeks of age) and then injected the cells by ICV into prediseased, younger MRL/lpr mice (6 weeks of age). At 4 weeks after adoptive transfer surgery, young MRL/lpr mice underwent behavioral assessments to evaluate whether neuropsychiatric disease was accelerated. The cultured T cells injected into these mice were phenotyped, with the results indicating that, compared with the phenotype of expanded splenic T cells, expanded CP T cells were mostly double negative (Figure 3A). Mice that received CP T cells had significantly worse spatial memory than mice injected with PBS and significantly worse

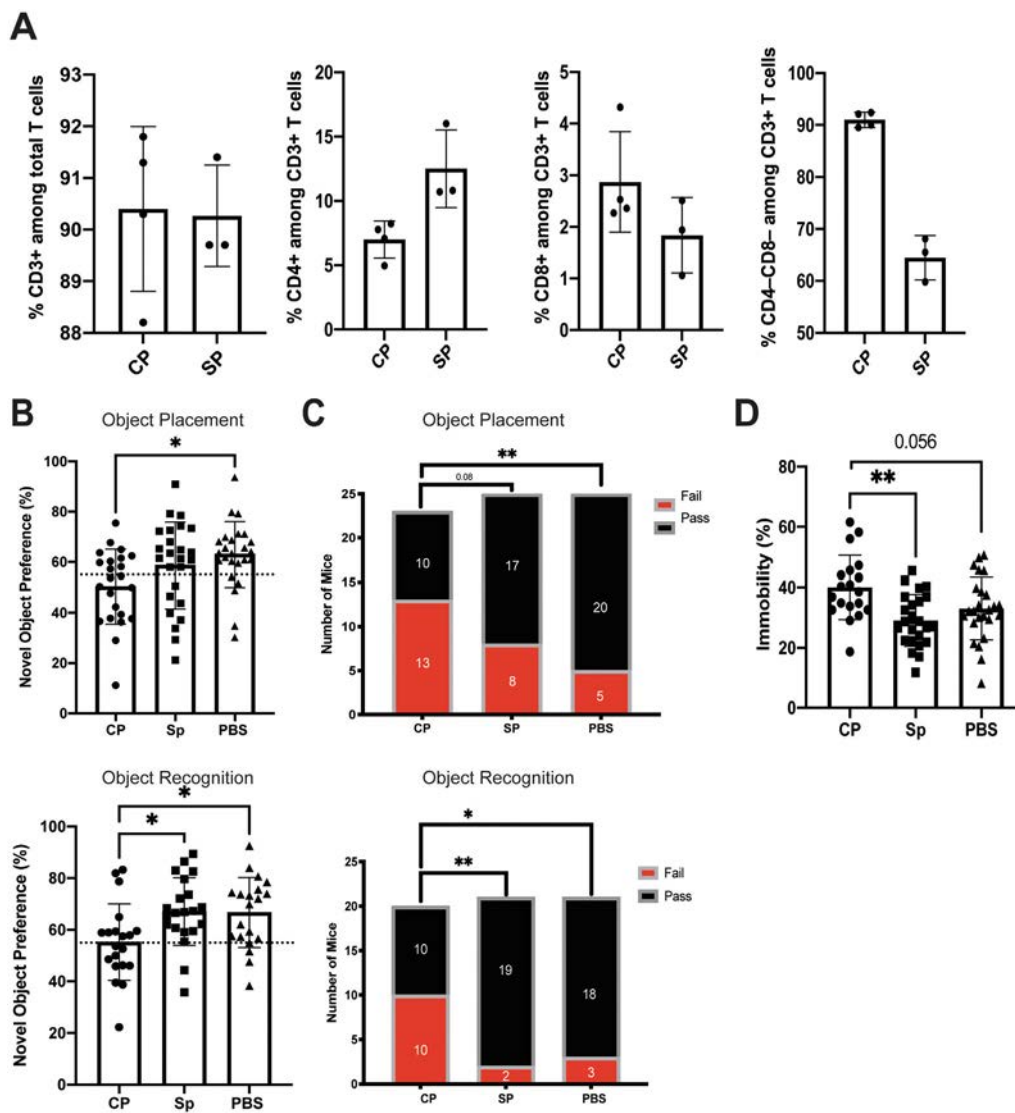


**Figure 3.** Accelerated neuropsychiatric disease in MRL/lpr mice that received local adoptive transfer of cultured choroid plexus (CP)-infiltrating T cells or splenic (SP) T cells obtained from older MRL/lpr mice or that received phosphate buffered saline (PBS) as control. **A**, Phenotypes of the cultured CP or splenic T cells injected into prediseased, younger MRL/lpr mice. **B** and **C**, Results of assessments of spatial memory (object placement test) and recognition memory (objection recognition test) showing percentages of mice exhibiting novel object preference based on the 55% pass/fail cutoff (dashed line) (**B**) and numbers of mice with a passing or failing score based on the 55% cutoff (**C**). **D**, Assessments of depressive-like behavior with the Porsolt swim test, showing percentage of time that a mouse spent immobile. In **A**, **B**, and **D**, solid symbols show individual mice; bars show the mean ± SD. Groups were compared using one-way analysis of variance or chi-square test. \* =  $P < 0.05$ ; \*\* =  $P < 0.01$ . Color figure can be viewed in the online issue, which is available at <http://onlinelibrary.wiley.com/doi/10.1002/art.42252/abstract>.

recognition memory than both the PBS-injected mice and splenic T cell recipient mice (Figures 3B and C). In addition, mice that received CP T cells had worse depressive-like behavior than the other 2 mouse groups (Figure 3D).

Saccharin preference was also decreased in the CP T cell recipient mouse group compared with mice that received splenic T cells (Supplementary Figure 2A, available on the *Arthritis & Rheumatology* website at <https://onlinelibrary.wiley.com/doi/10.1002/art.42252>). This latter finding points to anhedonia, a feature of murine depressive-like behavior. Importantly, no significant behavioral differences were observed between the PBS-injected group and the mice that did not undergo surgical manipulation (Supplementary Figures 2B and C). Thus, we found that local adoptive transfer of CP-infiltrating T cells but not splenic T cells

exacerbated the cognitive deficits and worsened the affective behavior of MRL/*lpr* mice injected with these cells, a finding that is consistent with the neuropsychiatric phenotype in this mouse model.

#### No effect from ICV T cell delivery on systemic disease markers.

A potential advantage to the experimental ICV delivery of T cells is the ability to directly affect the CNS without significantly altering systemic disease. Across the treatment groups, there was no difference in splenomegaly, a hallmark of the mouse model (Supplementary Figure 3A, available on the *Arthritis & Rheumatology* website at <https://onlinelibrary.wiley.com/doi/10.1002/art.42252>). Furthermore, spleens from mice that received either CP T cells or splenic T cells showed no

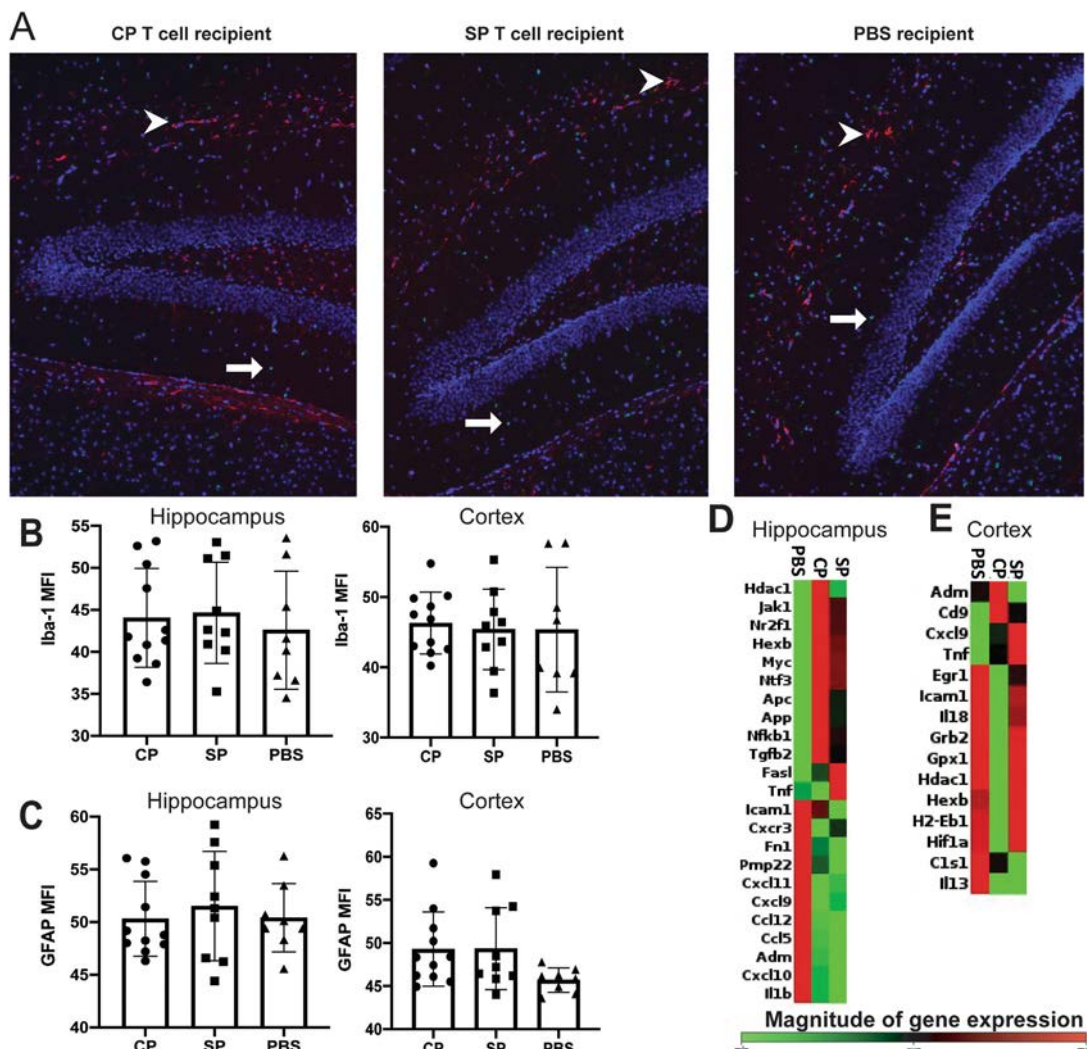


**Figure 4.** Identification of differential gene expression in MRL/*lpr* mice that received intracerebroventricular (ICV) injection of choroid plexus-infiltrating T cells (CP), splenic T cells (SP), or phosphate buffered saline (PBS). **A**, Staining of the hippocampus for IBA-1 and GFAP in a representative CP T cell recipient mouse, SP T cell recipient mouse, and PBS recipient mouse. Microglia are shown in green (IBA-1+) (arrows), astrocytes in red (GFAP+) (arrowheads), and nuclear areas in blue (DAPI+). **B** and **C**, Immunofluorescence staining of the hippocampus and cortex for IBA-1 (**B**) and for GFAP (**C**) in recipient mice. **D** and **E**, Heatmaps of genes up-regulated in the hippocampus (**D**) and in the cortex (**E**) of mice after ICV treatment (CP, SP, or PBS). In **B** and **C**, solid symbols show individual mice; bars show the mean  $\pm$  SD. See Figure 2 for other definitions. Color figure can be viewed in the online issue, which is available at <http://onlinelibrary.wiley.com/doi/10.1002/art.42252/abstract>.

differences in the composition of either innate or adaptive immune cells compared with spleens from mice that received PBS (Supplementary Figure 3B). Interestingly, there was a significant decrease in titers of anti-dsDNA antibodies in mice that received CP T cells compared with the other 2 treatment groups (Supplementary Figure 3C). However, this finding does not align with titer results for other antinuclear antibodies as there were no changes in titer levels of antichromatin antibodies in postmortem samples (Supplementary Figure 3D) and total IgG antibodies (Supplementary Figure 3E). Finally, the severity of nephritis was not significantly different among the treatment groups (Supplementary Figure 3F). Therefore, although neuropsychiatric disease was accelerated in the CP T cell recipient mice, systemic disease was generally unaffected.

**Exacerbation of select markers of neuroinflammation in ICV CP T cell recipient mice.** Because we found robust differences in behavior among the 3 ICV recipient groups, which

was consistent with and complementary to the results shown in the CD4+ T cell depletion studies, we next evaluated markers of neuroinflammation in response to different treatments, as there may be a correlation between modulation of these markers and T cell-induced neurobehavioral deficits. IBA-1 and GFAP staining of the hippocampus and the cortex revealed no significant differences in astrocyte and microglial activation levels between the groups (Figures 4A–C). Further evaluation of the hippocampus and the cortex revealed several differentially expressed genes across the ICV recipient groups. In hippocampal tissue, we observed up-regulation of *NFKB1*, *TGFB2*, and *JAK1* genes in mice that received ICV injection of T cells compared with mice that received ICV injection of PBS (Figure 4D). In the cortex, the top up-regulated genes of CP T cell recipient mice were *ADM* and *CD9*, which are involved in vasorelaxation and cell adhesion, respectively (Figure 4E). After hierarchical clustering of the genes to identify potentially significant general pathways, we found that the T cell recipient groups were more closely aligned in their gene expression profiles compared with the PBS and nonsurgical control groups

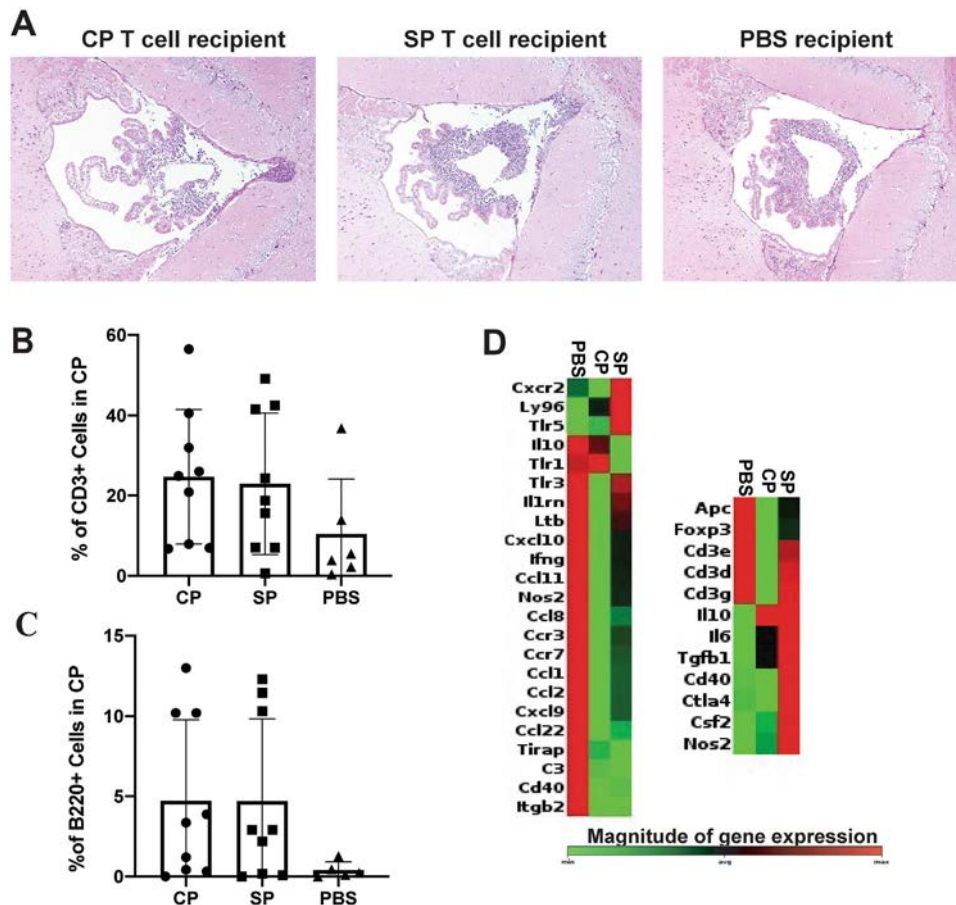


**Figure 5.** Similarity in the characteristics of the choroid plexus (CP) infiltrate across the MRL/*lpr* mouse treatment groups that received intracerebroventricular (ICV) injection of CP-infiltrating T cells, splenic (SP) T cells, or phosphate buffered saline (PBS). **A**, Representative images of hematoxylin and eosin-stained brain tissue samples showing composition of CP in the 3 treatment groups. **B** and **C**, Percentage of CD3+ cells (**B**) and B220+ cells (**C**) among total cells by immunofluorescence staining in the CP of mice by treatment group. **D**, Heatmap of chemokine and receptor gene expression down-regulated in the CP of mice after ICV treatment (CP, SP, PBS). In **B** and **C**, solid symbols show individual mice; bars show the mean  $\pm$  SD. Color figure can be viewed in the online issue, which is available at <http://onlinelibrary.wiley.com/doi/10.1002/art.42252/abstract>.

(Supplementary Figure 4, available on the *Arthritis & Rheumatology* website at <https://onlinelibrary.wiley.com/doi/10.1002/art.42252>).

**No difference in composition of CP across ICV-injected mouse groups.** We next evaluated the effects of local injection of T cells on the CP of recipient mice. Initial histologic scoring of the H&E-stained brain tissue revealed no apparent differences between the 3 treatment groups (Figure 5A). Further quantification of T and B cells with CD3 and B220 immunofluorescence staining revealed no differences in the percentage of CD3+ T cells and B220+ B cells in the 2 T cell recipient groups (Figures 5B and C). We performed flow cytometry in one recipient mouse cohort to further characterize both the lymphoid and myeloid populations present. Similarly, no significant differences were observed in percentages of these populations, including CD4, CD8, or double-negative T cells, between the 3 experimental groups (Supplementary Figure 5, available on the *Arthritis & Rheumatology* website at <https://onlinelibrary.wiley.com/doi/10.1002/art.42252>).

To evaluate gene expression, we conducted PCR array analyses on CP from ICV-injected mice. Interestingly, when we compared the spleens of mice that received T cells versus mice that received PBS, we found down-regulation of many chemokines, cytokines, and their respective receptors in the CP T cell recipient group (Figure 5D). With regard to genes related to T and B cell activation, *Foxp3* expression was significantly decreased in the CP T cell recipient mice, suggesting potential regulatory T cell dysfunction; however *IL10* expression levels were significantly elevated, indicating their potential production by other immune cells (i.e., macrophages).

**Enhanced CP T cell activation upon major histocompatibility complex presentation of brain lysate, supporting brain-specific antigenicity.** We previously demonstrated that the CP in MRL/lpr mice has enhanced clonality of the TCR $\beta$  third complementary-determining region, skewed V gene usage, and increased sequence homology compared with

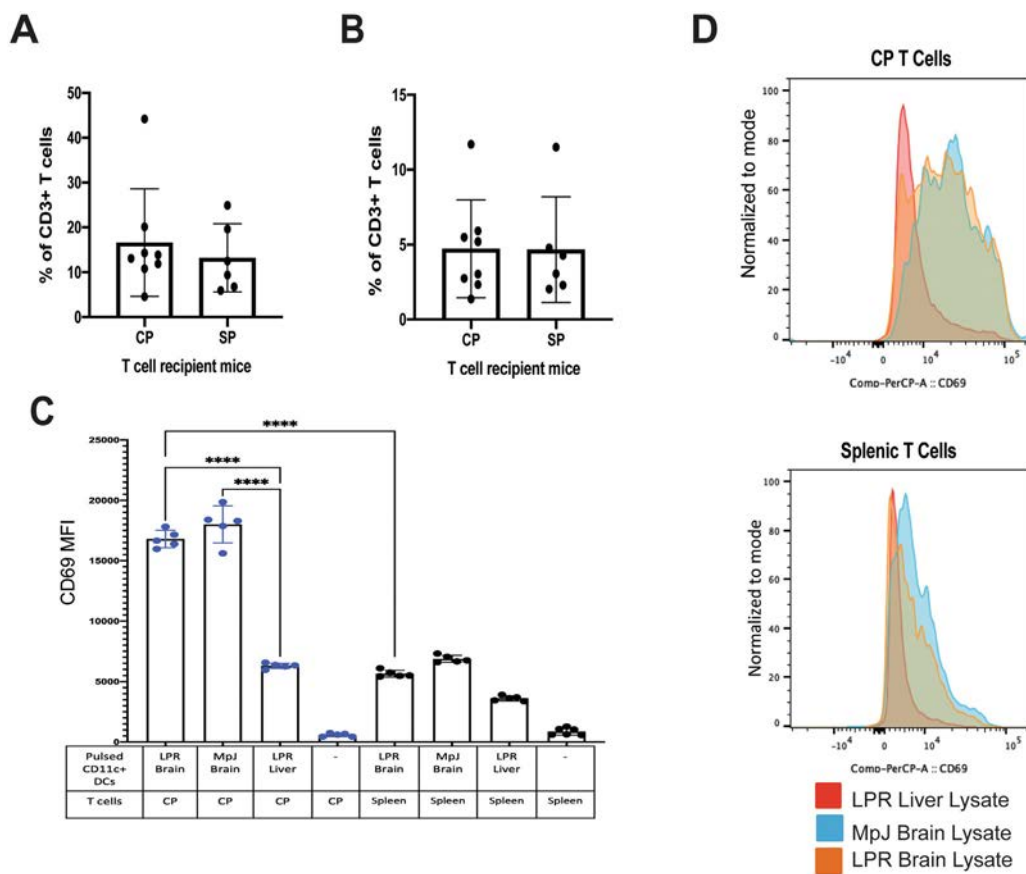


**Figure 6.** Enhanced activation of choroid plexus (CP)-infiltrating T cells in brain tissue from MRL/lpr mice that received intracerebroventricular injection of CP-infiltrating T cells (CP) or splenic T cells (SP). **A**, Percentage of carboxyfluorescein succinimidyl ester (CFSE)-labeled CP or SP T cells in the CP (**A**) and in spleens (**B**) of recipient mice. No differences in the infiltration of T cells are shown. **C**, Mean fluorescence intensity (MFI) of CD69 expression in T cells cocultured with pulsed dendritic cells. CP T cells are labeled in blue and splenic T cells in black. **D**, Overlays showing expression of CD69 by CP T cells or SP T cells incubated with CD11c+ dendritic cells pulsed with either LPR mouse liver lysates, MpJ mouse brain lysates, or LPR mouse brain lysates. Solid symbols show individual mice (**A**, **B**) or pooled samples from 2 or 3 mice each (**C**); bars show the mean  $\pm$  SD. Groups were compared using one-way analysis of variance or Student's *t*-test. \*\*\*\* =  $P < 0.0001$ . Color figure can be viewed in the online issue, which is available at <http://onlinelibrary.wiley.com/doi/10.1002/art.42252/abstract>.

other tissue sites in MRL/lpr mice, suggesting that the CP T cells may be preferentially infiltrating and/or proliferating in CP tissue (25). We hypothesized that T cells were selectively infiltrating the CP and proliferating in mice with neuropsychiatric lupus because of specific autoreactivity to brain-specific antigens. In our evaluation of the presence of CFSE-labeled T cells in CP or spleen tissue of recipient mice that were intravenously injected with either CP- or spleen-derived T cells 2 days earlier, we observed no differences in the percentage of CFSE-labeled T cells in the CP of mice that received either CP T cells or splenic T cells (Figures 6A and B). These results suggest that there may not be a difference between CP and splenic T cells in migration into the CP.

To evaluate the antigen reactivity of CP-infiltrating T cells, pooled CFSE-labeled CP T cells were cocultured with brain lysate-pulsed or liver lysate-pulsed CD11c+ dendritic cells, enriched from the splenocytes of MRL/lpr mice. Compared with expression levels at baseline, expression levels of CD69, an early T cell activation marker, had significantly increased in cocultured CP T cells in the presence of brain lysate-loaded dendritic cells (Figures 6C and D). Specifically, CP T cells cocultured with either MRL/lpr or MRL/MpJ mouse brain lysate demonstrated significantly enhanced expression of CD69 compared with CP T cells cocultured with liver lysate. Furthermore, the CP T cell group had increased CD69 expression compared with the respective T cell splenocyte group in the presence of dendritic cells primed with brain lysates (Figures 6C and D). Similar findings were observed when T cells were cocultured with lysate-primed splenocytes (Supplementary Figure 6, available on the *Arthritis & Rheumatology* website at <https://onlinelibrary.wiley.com/doi/10.1002/art.42252>). These findings suggest that the potential mechanism for contribution of CP T cells to NPSLE is through their autoreactivity to brain-specific antigens.

## DISCUSSION

T cells are integral to SLE but have not been previously implicated in playing a role in the pathogenesis of NPSLE. Our results showed that systemic depletion of CD4+ T cells significantly normalized both systemic disease and neurobehavioral deficits in a mouse model. Given this effect on systemic disease, the adoptive transfer method was then chosen to specifically address the contribution of brain-infiltrating T cells to NPSLE. Mice that underwent ICV injection of brain-infiltrating T cells demonstrated exacerbated behavior deficits compared with mice that received ICV injection of other autoreactive T cells, suggesting that CP T cells uniquely contribute to neuropsychiatric disease. However, although NPSLE manifestations were affected, we observed no changes in systemic disease in mice that received T cell ICV injection versus PBS. No differences between the groups were seen in the histologic characteristics or composition of the infiltrate. Nevertheless, although the results did not demonstrate a greater infiltration of the CP with CFSE-labeled CP T cells when compared with

splenic T cells, we did observe enhanced activation of CP T cells when cocultured with dendritic cells primed with whole brain lysate, suggesting brain-specific reactivity.

Our results showed that cognitive deficits were attenuated or worsened upon depletion or transfer of T cells, respectively. Remarkably, although the lack of a significant improvement in depressive-like behavior with systemic anti-CD4 antibody treatment might lead to a conclusion that T cells are not relevant in affective aspects of neuropsychiatric lupus, depressive-like behavior in mice was worse upon adoptive transfer of CP T cells. These seemingly discordant results in studying the effects of T cells on depressive-like behavior may simply be reflective of the different methods used for systemic depletion versus direct ICV injection of T cells. Alternatively, different mechanisms may underlie distinct neuropsychiatric manifestations (32), and thus additional studies are necessary to further elucidate the contribution of T cells to depressive-like behavior.

Interestingly, despite some variability in the representation of T cell subsets in injected cell pools depending on their original source (CP versus spleen), no significant differences were observed regarding the composition of infiltrating cells present in the CP or in the migration capacity of CP- versus spleen-derived T cells. Therefore, we surmise that the enhanced pathogenicity of CP T cells, compared with splenic T cells, was attributable to the differential autoreactivity that we had demonstrated with brain antigens.

The identification of the antigens involved, specifically in target organs, continues to interest SLE researchers. Recent studies have reported vimentin-reactive T cells in the urine of patients with lupus nephritis and demonstrated that kidney-infiltrating T cells can initiate lupus nephritis after their adoptive transfer to mice (12,33). Previously, our group described increased clonality and sequence homology present in the CP of NPSLE mice, suggesting that the TCR repertoire is being specifically shaped (25). Results of our experiments with brain lysate-pulsed dendritic cells suggested that CP T cells respond with enhanced activation to whole brain lysate, from both healthy and inflamed brains. Therefore, in combination with the behavioral results, NPSLE appears to be driven by antigen-specific T cells in the CP. Accumulation of CP T cells does not therefore reflect nonspecific lymphoproliferation or infiltration.

In human NPSLE, the role of T cells has not been elucidated or robustly evaluated. In many clinical trials that used T cell therapies, primary outcomes were related to general disease activity (e.g., the SLE Disease Activity Index) or lupus nephritis specifically and not to NPSLE (34). This omission may be because of the challenges with including appropriate attribution of neuropsychiatric manifestations, variability of symptoms and their onset, and the lack of standardized diagnostic or prognostic tools for NPSLE (35). Nevertheless, despite limited studies, there is some evidence to support the use of T cell-modulating therapies such as azathioprine and cyclosporine, alone or in combination, in NPSLE



(28,36–38). These studies further support the possibility that targeting T cells might be a more specific, yet insufficiently explored, approach to treatment of NPSLE.

Our analysis into the specific contribution and autoreactivity of brain-infiltrating T cells in NPSLE has several limitations. Although the MRL/*lpr* mouse model is the mostly widely accepted and utilized mouse model to evaluate SLE and NPSLE pathogenesis, it does not recapitulate the entire diverse neuropsychiatric presentations of NPSLE or focal disease caused by antiphospholipid syndrome (39–41). We considered locally depleting T cells with osmotic pumps; however, in this study, we implemented the adoptive transfer method in mice by a single ICV injection to demonstrate the specific contribution of CP-infiltrating T cells. Because of the limited number of cells that could be retrieved from a single donor mouse's CP, the pooling and stimulating expansion of CP T cells and splenic T cells were necessary to yield enough cells to inject into recipient mice. A regimen of anti-CD3/anti-CD28 antibody stimulation and IL-2 was utilized to selectively stimulate the expansion of T cells alone. Despite differences in the phenotype of stimulated cells versus the composition of the T cell infiltrate in situ in the CP of MRL/*lpr* mice (17,25), the differential expansion of CD4+, CD8+, and double-negative T cells upon stimulation as well as loss of marker expression (i.e., CD4 or CD8) upon activation can explain the increased percentage of double-negative T cells in culture (42,43).

Our initial studies suggested that it is CD4+ T cells that drive neuropsychiatric disease, but the subsequent ICV experiments would also be consistent with the double-negative (CD4–CD8–) T cell subset as a prominent contributor to NPSLE. We had previously described a population of double-negative T cells in the CP of MRL/*lpr* mice (17,25), and this subset was prominent in the ICV-injected T cells in our present study. In the periphery, double-negative T cells in SLE have been shown to be clonal and to secrete IL-17 and interferon- $\gamma$  (44). Furthermore, double-negative T cells can promote immunoglobulin and anti-dsDNA antibody production (45). In the CNS, double-negative T cells are increased in postischemic mouse brains and shown to enhance neuroinflammation responses (46). Whether these cells contribute to neuropsychiatric disease and how they might do so are so far unknown. Another interesting point is that, after systemic anti-CD4 depletion, CD8+ and CD4+ T cells were decreased in the CP. We believe that the depletion of CD4 T cells reasonably decreased not only their number but also their inflammatory contribution to the local brain environment, thus indirectly affecting the infiltration of CD8+ T cells. Therefore, future studies (to include, for example, having subsets of cultured T cells before ICV injection) are needed to continue to parse the specific subset contribution of CP-infiltrating CD4+, CD8+, and particularly double-negative T cells in NPSLE.

In conclusion, we have demonstrated that T cells, specifically CP-infiltrating T cells, contribute and drive NPSLE in the MRL/*lpr* mouse model. Several additional studies are warranted to further

elucidate the specific mechanisms by which these cells affect the CNS parenchyma and subsequent clinical symptoms, as well as to evaluate how T cell modulation affects NPSLE in human disease.

## ACKNOWLEDGMENTS

We acknowledge Noelle Cayla and Dr. Kamran Khodakhah for their expertise and use of their stereotaxic instruments to perform the ICV injections.

## AUTHOR CONTRIBUTIONS

All authors were involved in drafting the article or revising it critically for important intellectual content, and all authors approved the final version to be published. Dr. Putterman had full access to all of the data in the study and takes responsibility for the integrity of the data and the accuracy of the data analysis.

**Study conception and design.** Moore, Huang, Macian, Putterman.

**Acquisition of data.** Moore, Huang, Reynolds.

**Analysis and interpretation of data.** Moore, Huang, Reynolds, Macian, Putterman.

## REFERENCES

1. Tsokos GC. Systemic lupus erythematosus. *N Engl J Med* 2011;365:2110–21.
2. Comte D, Karampetsou MP, Tsokos GC. T cells as a therapeutic target in SLE. *Lupus* 2015;24:351–63.
3. Merino R, Fossati L, Iwamoto M, et al. Effect of long-term anti-CD4 or anti-CD8 treatment on the development of *lpr* CD4–CD8– double negative T cells and of the autoimmune syndrome in MRL-*lpr/lpr* mice. *J Autoimmun* 1995;8:33–45.
4. Jabs DA, Burek CL, Hu Q, et al. Anti-CD4 monoclonal antibody therapy suppresses autoimmune disease in MRL/Mp-*lpr/lpr* mice. *Cell Immunol* 1992;141:496–507.
5. Early GS, Zhao W, Burns CM. Anti-CD40 ligand antibody treatment prevents the development of lupus-like nephritis in a subset of New Zealand black x New Zealand white mice. Response correlates with the absence of an anti-antibody response. *J Immunol* 1996;157:3159–64.
6. Furie R, Nicholls K, Cheng TT, et al. Efficacy and safety of abatacept in lupus nephritis: a twelve-month, randomized, double-blind study. *Arthritis Rheumatol* 2014;66:379–89.
7. Merrill JT, Burgos-Vargas R, Westhovens R, et al. The efficacy and safety of abatacept in patients with non-life-threatening manifestations of systemic lupus erythematosus: results of a twelve-month, multicenter, exploratory, phase IIb, randomized, double-blind, placebo-controlled trial. *Arthritis Rheum* 2010;62:3077–87.
8. Bubier JA, Sproule TJ, Foreman O, et al. A critical role for IL-21 receptor signaling in the pathogenesis of systemic lupus erythematosus in BXSB-Yaa mice. *Proc Natl Acad Sci U S A* 2009;106:1518–23.
9. Kytaris VC, Zhang Z, Kuchroo VK, et al. Cutting edge: IL-23 receptor deficiency prevents the development of lupus nephritis in C57BL/6-*lpr/lpr* mice. *J Immunol* 2010;184:4605–9.
10. Cheah PL, Looi LM, Chua CT, et al. Enhanced major histocompatibility complex (MHC) class II antigen expression in lupus nephritis. *Malays J Pathol* 1997;19:115–20.
11. Massengill SF, Goodenow MM, Sleasman JW. SLE nephritis is associated with an oligoclonal expansion of intrarenal T cells. *Am J Kidney Dis* 1998;31:418–26.

12. Okamoto A, Fujio K, Tsuno NH, et al. Kidney-infiltrating CD4+ T-cell clones promote nephritis in lupus-prone mice. *Kidney Int* 2012;82:969–79.
13. Schwartz N, Stock AD, Putterman C. Neuropsychiatric lupus: new mechanistic insights and future treatment directions. *Nat Rev Rheumatol* 2019;15:137–52.
14. Govoni M, Hanly JG. The management of neuropsychiatric lupus in the 21<sup>st</sup> century: still so many unmet needs? *Rheumatology (Oxford)* 2020;59 Suppl:v52–62.
15. Bendorius M, Po C, Muller S, et al. From systemic inflammation to neuroinflammation: the case of neurolupus. *Int J Mol Sci* 2018;19:3588.
16. Stock AD, Der E, Gelb S, et al. Tertiary lymphoid structures in the choroid plexus in neuropsychiatric lupus. *JCI Insight* 2019;4:e124203.
17. Jain S, Stock A, Macian F, et al. A distinct T follicular helper cell subset infiltrates the brain in murine neuropsychiatric lupus. *Front Immunol* 2018;9:487.
18. James WG, Hutchinson P, Bullard DC, et al. Cerebral leucocyte infiltration in lupus-prone MRL/MpJ-fas lpr mice—roles of intercellular adhesion molecule-1 and P-selectin. *Clin Exp Immunol* 2006;144:299–308.
19. Ma X, Foster J, Sakic B. Distribution and prevalence of leukocyte phenotypes in brains of lupus-prone mice. *J Neuroimmunol* 2006;179:26–36.
20. Meeker RB, Williams K, Killebrew DA, et al. Cell trafficking through the choroid plexus. *Cell Adh Migr* 2012;6:390–6.
21. Duprez T, Nzeusseu A, Peeters A, et al. Selective involvement of the choroid plexus on cerebral magnetic resonance images: a new radiological sign in patients with systemic lupus erythematosus with neurological symptoms. *J Rheumatol* 2001;28:387–91.
22. Atkins CJ, Kondon J, Quismorio F, et al. The choroid plexus in systemic lupus erythematosus. *Ann Rheum Dis* 1971;30:333.
23. Ariel DS, Sivan G, Ofer P, et al. The blood brain barrier and neuropsychiatric lupus. *Autoimmun Rev* 2017;16:612–9.
24. O'Sullivan FX, Vogelweid CM, Besch-Williford CL, et al. Differential effects of CD4+T cell depletion on inflammatory central nervous system disease, arthritis and sialadenitis in MRL/lpr mice. *J Autoimmun* 1995;8:163–75.
25. Moore E, Huang MW, Jain S, et al. The T cell receptor repertoire in neuropsychiatric systemic lupus erythematosus. *Front Immunol* 2020;11:1476.
26. Wen J, Chen CH, Stock A, et al. Intracerebroventricular administration of TNF-like weak inducer of apoptosis induces depression-like behavior and cognitive dysfunction in non-autoimmune mice. *Brain Behav Immun* 2016;54:27–37.
27. Mukherjee G, Geliebter A, Abad J, et al. DEC-205-mediated antigen targeting to steady-state dendritic cells induces deletion of diabetogenic CD8+ T cells independently of PD-1 and PD-L1. *Int Immunol* 2013;25:651–60.
28. Papachristos DA, Oon S, Hanly JG, et al. Management of inflammatory neurologic and psychiatric manifestations of systemic lupus erythematosus: a systematic review. *Semin Arthritis Rheum* 2021;51:49–71.
29. Chalmers SA, Wen J, Shum J, et al. CSF-1R inhibition attenuates renal and neuropsychiatric disease in murine lupus. *Clin Immunol* 2017;185:100–8.
30. Mike EV, Makinde HM, Gulinello M, et al. Lipocalin-2 is a pathogenic determinant and biomarker of neuropsychiatric lupus. *J Autoimmun* 2019;96:59–73.
31. Putterman C, Diamond B. Immunization with a peptide surrogate for double-stranded DNA (dsDNA) induces autoantibody production and renal immunoglobulin deposition. *J Exp Med* 1998;188:29–38.
32. Gao HX, Campbell SR, Cui MH, et al. Depression is an early disease manifestation in lupus-prone MRL/lpr mice. *J Neuroimmunol* 2009;207:45–56.
33. Tesch S, Abdirama D, Grießbach AS, et al. Identification and characterization of antigen-specific CD4+ T cells targeting renally expressed antigens in human lupus nephritis with two independent methods. *Sci Rep* 2020;10:21312.
34. Nandkumar P, Furie R. T-cell-directed therapies in systemic lupus erythematosus. *Lupus* 2016;25:1080–5.
35. Moore E, Huang MW, Putterman C. Advances in the diagnosis, pathogenesis and treatment of neuropsychiatric systemic lupus erythematosus. *Curr Opin Rheumatol* 2020;32:152–8.
36. Germano V, Diamanti AP, Ferlito C, et al. Cyclosporine A in the long-term management of systemic lupus erythematosus. *J Biol Regul Homeost Agents* 2011;25:397–403.
37. Fargetti S, Ugolini-Lopes MR, Pasoto SG, et al. Short- and long-term outcome of systemic lupus erythematosus peripheral neuropathy: bimodal pattern of onset and treatment response. *J Clin Rheumatol* 2021;27:S212.
38. Magro-Checa C, Zirkzee EJ, Huizinga TW, et al. Management of neuropsychiatric systemic lupus erythematosus: current approaches and future perspectives. *Drugs* 2016;76:459–83.
39. Gulinello M, Putterman C. The MRL/lpr mouse strain as a model for neuropsychiatric systemic lupus erythematosus. *J Biomed Biotech* 2011;2011:1–15.
40. Jeltsch-David H, Muller S. Neuropsychiatric systemic lupus erythematosus and cognitive dysfunction: the MRL-lpr mouse strain as a model. *Autoimmun Rev* 2014;13:963–73.
41. Moore E, Putterman C. Are lupus animal models useful for understanding and developing new therapies for human SLE? *J Autoimmun* 2020;112:102490.
42. Bristeau-Leprince A, Mateo V, Lim A, et al. Human TCR  $\alpha/\beta$ +CD4-CD8- double-negative T cells in patients with autoimmune lymphoproliferative syndrome express restricted V $\beta$  TCR diversity and are clonally related to CD8+ T cells. *J Immunol* 2008;181:440–8.
43. Ford MS, Zhang ZX, Chen W, Zhang L. Double-negative T regulatory cells can develop outside the thymus and do not mature from CD8+ T cell precursors. *J Immunol* 2006;177:2803–9.
44. Crispin JC, Oukka M, Bayliss G, et al. Expanded double negative T cells in patients with systemic lupus erythematosus produce IL-17 and infiltrate the kidneys. *J Immunol* 2008;181:8761–6.
45. Shivakumar S, Tsokos GC, Datta SK. T cell receptor  $\alpha/\beta$  expressing double-negative (CD4-/CD8-) and CD4+ T helper cells in humans augment the production of pathogenic anti-DNA autoantibodies associated with lupus nephritis. *J Immunol* 1989;143:103–12.
46. Meng H, Zhao H, Cao X, et al. Double-negative T cells remarkably promote neuroinflammation after ischemic stroke. *Proc Natl Acad Sci U S A* 2019;116:5558–63.

# Longitudinal Immune Cell Profiling in Patients With Early Systemic Lupus Erythematosus

Takanori Sasaki,<sup>1</sup> Sabrina Bracero,<sup>1</sup> Joshua Keegan,<sup>1</sup> Lin Chen,<sup>1</sup> Ye Cao,<sup>1</sup> Emma Stevens,<sup>1</sup> Yujie Qu,<sup>2</sup> Guoxing Wang,<sup>2</sup> Jennifer Nguyen,<sup>1</sup> Jeffrey A. Sparks,<sup>1</sup> V. Michael Holers,<sup>3</sup> Stephen E. Alves,<sup>2</sup> James A. Lederer,<sup>1</sup> Karen H. Costenbader,<sup>1</sup> and Deepak A. Rao<sup>1</sup>

**Objectives.** To investigate the immune cell profiles of patients with systemic lupus erythematosus (SLE), and to identify longitudinal changes in those profiles over time.

**Methods.** We employed mass cytometry with 3 different panels of 38–39 markers (an immunophenotyping panel, a T cell/monocyte panel, and a B cell panel) in cryopreserved peripheral blood mononuclear cells (PBMCs) from 9 patients with early SLE, 15 patients with established SLE, and 14 controls without autoimmune disease. We used machine learning–driven clustering, flow self-organizing maps, and dimensional reduction with t-distributed stochastic neighbor embedding to identify unique cell populations in early SLE and established SLE. We used mass cytometry data of PBMCs from 19 patients with early rheumatoid arthritis (RA) and 23 controls to compare levels of specific cell populations in early RA and SLE. For the 9 patients with early SLE, longitudinal mass cytometry analysis was applied to PBMCs at enrollment, 6 months after enrollment, and 1 year after enrollment. Serum samples were also assayed for 65 cytokines using Luminex multiplex assay, and associations between cell types and cytokines/chemokines were assessed.

**Results.** Levels of peripheral helper T cells, follicular helper T (T<sub>fh</sub>) cells, and several Ki-67+ proliferating subsets (ICOS+Ki-67+ CD8 T cells, Ki-67+ regulatory T cells, CD19<sup>intermediate</sup>Ki-67<sup>high</sup> plasmablasts, and PU.1<sup>high</sup>Ki-67<sup>high</sup> monocytes) were increased in patients with early SLE, with more prominent alterations than were seen in patients with early RA. Longitudinal mass cytometry and multiplex serum cytokine assays of samples from patients with early SLE revealed that levels of T<sub>fh</sub> cells and CXCL10 had decreased 1 year after enrollment. Levels of CXCL13 were positively correlated with levels of several of the expanded cell populations in early SLE.

**Conclusion.** Two major helper T cell subsets and unique Ki-67+ proliferating immune cell subsets were expanded in patients in the early phase of SLE, and the immunologic features characteristic of early SLE evolved over time.

## INTRODUCTION

Systemic lupus erythematosus (SLE) is a prototypical autoimmune disease that affects multiple vital organs. Untreated activation of inflammation pathways in SLE patients can lead to tissue inflammation and irreversible organ damage; thus, rapid recognition of lupus disease activity is an important goal in the care of patients with SLE. Delays in treatment initiation are associated with poorer treatment responses and worse outcomes (1–3).

Despite the importance of early recognition and intervention, diagnosis of early SLE is often difficult because initial manifestations of the disease frequently include relatively nonspecific symptoms. Fever, autoantibody production, hypocomplementemia, and leukopenia are relatively common in patients with early SLE (4), indicating that systemic immunologic features are already altered in the early phase of the disease. We hypothesize that defining the alterations in immune cell populations that occur in the early phase of the disease course will provide critical insights into the early evolution of

Supported in part by funding from Merck Sharp & Dohme, and by the Lupus Research Alliance, Burroughs Wellcome Fund Career Award in Medical Sciences, Doris Duke Charitable Foundation Clinical Scientist Development Award. This work was also supported by the National Institute of Arthritis and Musculoskeletal and Skin Diseases, NIH (grant P30-AR-070253 to Drs. Lederer and Rao, grant K24-AR-066109 to Dr. Costenbader, and grant K08-AR-072791 to Dr. Rao).

<sup>1</sup>Takanori Sasaki, MD, PhD, Sabrina Bracero, BS, Joshua Keegan, BS, Lin Chen, BA, Ye Cao, PhD, Emma Stevens, BA, Jennifer Nguyen, BS, Jeffrey A. Sparks, MD, MMSc, James A. Lederer, PhD, Karen H. Costenbader, MD, MPH, Deepak A. Rao, MD, PhD: Brigham and Women's Hospital and Harvard

Medical School, Boston, Massachusetts; <sup>2</sup>Yujie Qu, MD, Guoxing Wang, MD, PhD, Stephen E. Alves, PhD: Merck Sharp & Dohme, Kenilworth, New Jersey; <sup>3</sup>V. Michael Holers: Division of Rheumatology, University of Colorado School of Medicine, Aurora, Colorado.

Author disclosures are available at <https://onlinelibrary.wiley.com/action/downloadSupplement?doi=10.1002%2Fart.42248&file=art42248-sup-0001-Disclosureform.pdf>.

Address correspondence via email to Deepak A. Rao, MD, PhD, at [darao@bwh.harvard.edu](mailto:darao@bwh.harvard.edu).

Submitted for publication November 12, 2021; accepted in revised form May 24, 2022.

pathologic activation of immune cells in patients with SLE and may yield key metrics for the diagnosis of SLE in the early phase.

A series of single-cell RNA sequencing studies of inflamed tissues recently identified aberrant expansion of immune cells and cytokine/chemokine-mediated cellular networks within the affected organs of patients with SLE (5,6). These unbiased analyses provided broad and robust information on the composition of the immune cell infiltrates in the setting of lupus nephritis. However, since it is difficult to perform multiple biopsies in most cases and most of the tissue samples used in these previous studies were obtained from patients with established SLE, there is limited information on the immunologic features of early SLE and the changes in inflammatory features over time. From this perspective, blood samples are easier to access and analyze longitudinally; yet, to our knowledge, few longitudinal studies on the associations between immunophenotypes and the clinical features of patients with SLE over time have been completed (7,8).

Mass cytometry (or cytometry by time-of-flight mass spectrometry) is a powerful tool to broadly assess the surface markers as well as the intracellular proteins of immune cells. Dimensional reduction with t-distributed stochastic neighbor embedding (t-SNE) (9) combined with machine learning-driven clustering, such as with flow self-organizing maps (FlowSOM) (10), allow for the discrimination of distinct immune cell clusters in an unbiased way. Previously, the increase of PD-1<sup>high</sup>CXCR5-CCR2+ CD4 T cells (peripheral helper T [T<sub>ph</sub>] cells) in the peripheral blood of patients with SLE was identified by this method (11). In 2 recently published studies, mass cytometry was used to examine blood samples from patients with established SLE (12,13), but longitudinal changes in the immune cell compositions and clinical features of SLE patients have not yet been studied.

Here we report broad mass cytometry data analyses of 3 different panels of 38–39 markers in blood cells from patients who received a new diagnosis of SLE. We first identified several unique immune cell populations in patients with early SLE through unsupervised clustering. We further investigated the levels of immune cells and serum cytokines in patients with early SLE over time. These longitudinal analyses indicated that several unique Ki-67+ proliferating immune cell subsets are expanded even in the early phase of SLE and remain consistently elevated over time. In contrast, follicular helper T (T<sub>fh</sub>) cells decreased over time. Serum cytokine profiling identified increased CXCL10, CD40L, interleukin-20 (IL-20), and TWEAK expression in patients with early SLE, but among those patients, CXCL10 expression decreased longitudinally. Our data provide a detailed assessment of the immunologic features characteristic of patients with early SLE as well as the changes in those features over time.

## PATIENTS AND METHODS

A detailed description of the methods used in this study are available in the Supplementary Materials and Methods on the

*Arthritis & Rheumatology* website at <http://onlinelibrary.wiley.com/doi/10.1002/art.42248>. All SLE patients met the 1997 American College of Rheumatology (ACR) classification criteria for SLE (14), as well as the 2012 Systemic Lupus International Collaborating Clinics (SLICC) criteria for SLE and the 2019 European Alliance of Associations for Rheumatology (EULAR)/ACR classification criteria for SLE (15,16). For the early SLE cohort, 9 SLE patients who were within 6 months of disease diagnosis and who were not receiving major immunosuppressive therapies (treatment with prednisone doses of  $\leq 10$  mg and hydroxychloroquine were permitted) were included. For the SLE cohort, 14 controls without autoimmune disease and 15 patients with established SLE were also included. In the validation cohort, 7 patients with established SLE and 5 controls without autoimmune disease who were not included in the SLE cohort were enrolled. In the early rheumatoid arthritis (RA) cohort, 19 patients who had received a diagnosis of early anti-citrullinated peptide antibody+ RA within 1 year of enrollment and 23 matched controls were included. RA patients fulfilled the 2010 ACR/EULAR classification criteria for RA (17). For serum analyses, the same 9 patients with early SLE were evaluated along with 9 controls without autoimmune disease (not the same controls included in the cross-sectional study).

## RESULTS

**An unsupervised cell clustering view of the immune cell landscape in SLE.** To investigate immunologic and longitudinal changes in the setting of SLE, we evaluated cross-sectional and longitudinal analyses of peripheral blood mononuclear cells (PBMCs) by mass cytometry using 3 different panels (a broad immunophenotype panel, a T cell/monocyte-focused panel, and a B cell-focused panel), along with profiling data of 65-analyte serum cytokines (Supplementary Figure 1A and Supplementary Tables 1–3, <http://onlinelibrary.wiley.com/doi/10.1002/art.42248>). As an overview of our approach, we first applied unsupervised cell clustering using FlowSOM and dimensionality reduction using t-SNE to the cross-sectional mass cytometry data from 9 patients with early SLE, 15 patients with established SLE, and 14 controls without autoimmune disease. Patients with early SLE were younger than those with established SLE (21.6 versus 36.5 years old;  $P < 0.001$ ), and a lower proportion of patients with early SLE received treatment with glucocorticoids compared to patients with established SLE (33.3% versus 93.3%;  $P = 0.03$ ). The doses of glucocorticoids received by patients with early SLE were also lower compared to the doses received by patients with established SLE (2.5 mg/day versus 14.5 mg/day;  $P = 0.01$ ). Systemic Lupus Erythematosus Disease Activity Index 2000 (SLEDAI-2K) (18) scores were comparable between patients with early SLE and patients with established SLE (5.8 points versus 5.1 points, respectively;  $P = 0.80$ ) (Supplementary Tables 4 and 5, <http://onlinelibrary.wiley.com/doi/10.1002/art.42248>).

We then investigated the longitudinal changes in the distinct immune cell populations and the levels of 65 cytokines of the 9 patients with early SLE (Supplementary Figure 1B, <http://onlinelibrary.wiley.com/doi/10.1002/art.42248>).

For an initial, high-level view of the circulating immune cell populations, we first performed t-SNE clustering of immunophenotype panel mass cytometry data from the cross-sectional cohorts (Supplementary Figure 1C, <http://onlinelibrary.wiley.com/doi/10.1002/art.42248>).

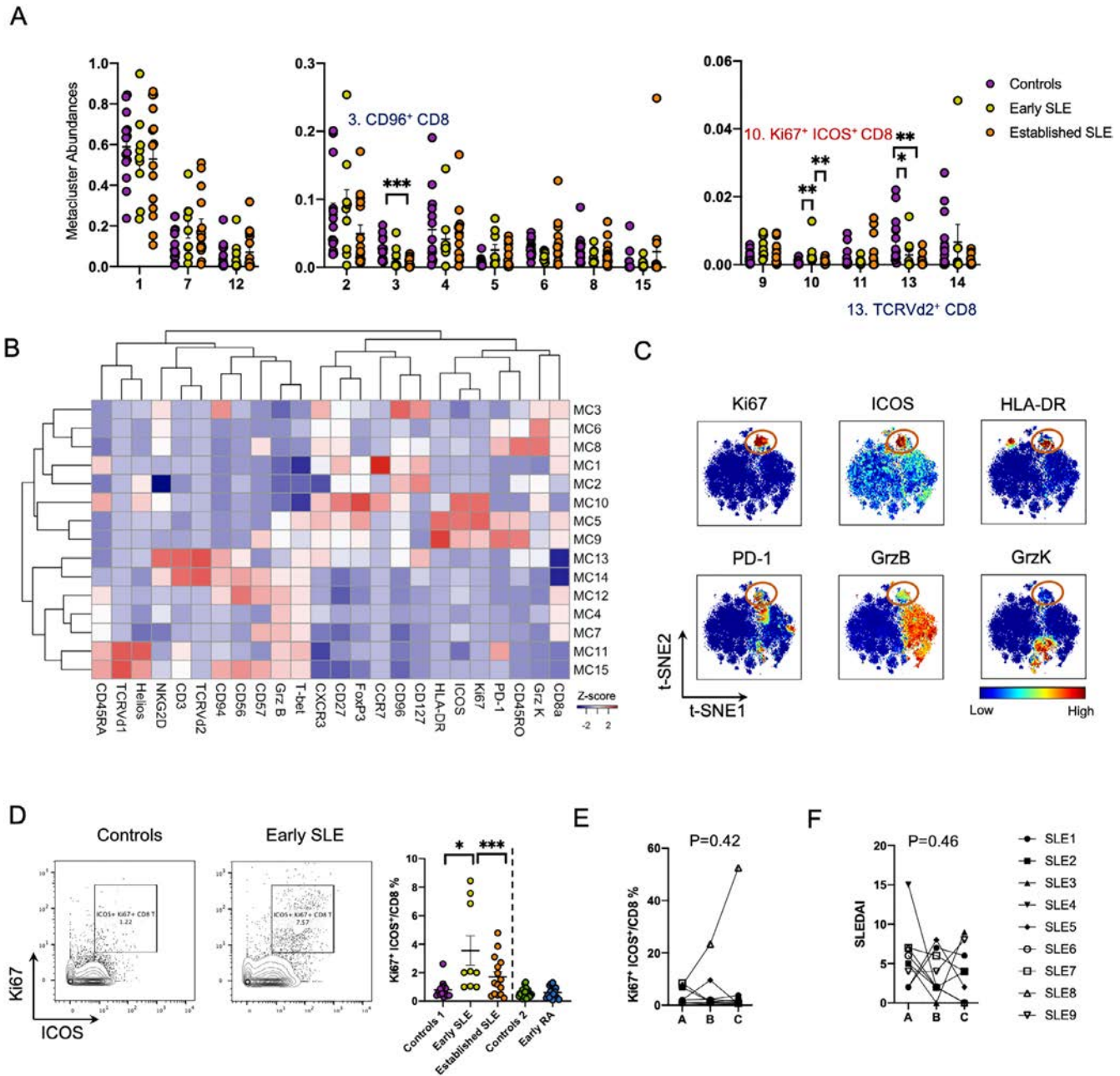


**Figure 1.** Characterization of Ki-67+ICOS+ CD8 T cell populations in 9 patients with early systemic lupus erythematosus (SLE), 15 patients with established SLE, and 14 controls without autoimmunity (controls 1), as well as in 19 early rheumatoid arthritis (RA) patients and 23 controls without autoimmunity (controls 2). **A**, Abundance of FlowSOM metaclusters of CD8+ T cells (% of total CD8+ T cells). **B**, Heatmap of normalized expression of mass cytometry markers with average medians of >0.2 in metaclusters (MCs) 1–15. **C**, Visualization of CD8+ T cells (t-distributed stochastic neighbor embedding [t-SNE] plots) in early SLE patients (Ki-67+ICOS+ CD8 T cells indicated by orange circles). **D**, Representative gating for Ki-67+ICOS+ CD8 T cell populations in CD3+CD14–CD4–CD8+ cells and comparison of their proportions in each patient and control group. **E** and **F**, Longitudinal changes in proportions of Ki-67+ICOS+ CD8 T cells (**E**) and longitudinal changes in disease activity assessed by Systemic Lupus Erythematosus Disease Activity Index (SLEDAI) (**F**) in early SLE patients at enrollment (time A), 6 months (time B), and 12 months (time C). \* =  $P < 0.05$ ; \*\* =  $P < 0.01$ ; \*\*\* =  $P < 0.001$ , by Kruskal-Wallis test and Dunn's multiple comparison test in **A** and **D**, and by Wilcoxon log-rank test in **E** and **F**. Bars show the mean  $\pm$  SEM. Symbols represent individual participants unless otherwise indicated. TCR = T cell receptor; PD-1 = programmed death 1; GrzB = granzyme B; GrzK = granzyme K.

[com/doi/10.1002/art.42248](https://doi.org/10.1002/art.42248)). The t-SNE allowed clear visualization of distinct immune cell clusters, including 3 major CD3+ T cell populations, CD3–CD56+ natural killer (NK) cells, CD19+ B cells, CD14+ monocytes, and CD14–CD11c+ myeloid dendritic cells. Two of the CD3+ clusters that were visualized included CD3+CD4+ T cells and CD3+CD8+ T cells. A third cluster (CD3+CD4–CD8– T cells) expressed  $\gamma\delta$  T cell receptor (TCR $\gamma\delta$ ), identifying this population as  $\gamma\delta$  T cells. The proportions of CD3+CD8+ T cells were increased and the proportions of CD3+CD4+ T cells were decreased in patients with established SLE compared to controls, but none of these cell populations were present in higher proportions in patients with early SLE compared to controls.

**Expanded Ki-67+ activated CD8 T cell populations in SLE patients.** To identify cell populations that differ between controls without autoimmunity and SLE patients, we next used FlowSOM to cluster CD8 T cells based on the 39-marker, T cell–focused immunophenotyping panel. We compared the abundances of the clusters between SLE patients and controls and identified metacluster 10 as significantly increased in patients with early SLE (Figure 1A). Heatmap expression analysis revealed that metacluster 10 contained cells with increased expression of Ki-67 and ICOS (Figure 1B). The t-SNE visualization of merged data from patients with early SLE confirmed that the Ki-67+ proliferative population expressed ICOS (Figure 1C). This population also expressed PD-1 and HLA-DR. Interestingly, the Ki-67+CD8 T cells did not highly express granzyme B and granzyme K. Biaxial plots demonstrated that proportions of Ki-67+ICOS+CD8 T cells were significantly increased in patients with early SLE compared to controls (0.8% versus 3.5%), but not in patients with early RA (Figure 1D and Supplementary Table 6, <http://onlinelibrary.wiley.com/doi/10.1002/art.42248>).

In longitudinal analyses, proportions of Ki-67+ICOS+CD8 T cells remained persistently elevated over time. Disease activity in the early SLE patient cohort remained similarly active during this time frame (Figures 1E and F). We also determined that metacluster 13, which contained T cells with elevated expression of CD94, CD56, and TCRV $\delta$ 2, was significantly decreased in patients with early SLE and patients with established SLE (Figures 1A and B). Metacluster 3, which contained CD96+CD8 T cells, was reduced in patients with established SLE but not in patients with early SLE (Figures 1A and B).

**Decrease of Tfh cells but not Tph cells over time in early SLE patients.** We next applied FlowSOM to CD4 T cells in controls without autoimmune disease and SLE patients, and identified metaclusters 6, 13, 14, and 15 as significantly increased in patients with early SLE at the time of diagnosis (Figure 2A). Metacluster 6 and metacluster 13 highly expressed PD-1, ICOS, and CD40L, but did not express CXCR5, suggesting that these 2 metaclusters contained Tph cells (Figure 2B). Interestingly,

these 2 clusters were quite different in their expression of CXCR3 and T-bet, with low expression levels in metacluster 6 and high expression levels in metacluster 13. Metacluster 14 could be classified as Tfh cells based on the increased expression of PD-1, ICOS, and CXCR5 found in the cells of that cluster. Metacluster 15 demonstrated a proliferating Treg cell phenotype with high levels of Ki-67, FoxP3, CTLA-4, Helios, CD25, and CD39 expression, and low levels of CD127 expression (Figure 2B). Visualization with t-SNE revealed distinct clusters of PD-1 in either CXCR5+ or CXCR5– regions and Ki-67+ Treg cells in patients with early SLE (Figure 2C).

Quantification by biaxial gating confirmed that proportions of CXCR5–PD-1<sup>high</sup> Tph cells, CXCR5+PD-1<sup>high</sup> Tfh cells, and Ki-67+FoxP3+ Treg cells were increased in patients with early SLE and patients with established SLE (Figures 2D and E). In contrast, in patients with early RA, proportions of CXCR5–PD-1<sup>high</sup> Tph cells and CXCR5+PD-1<sup>high</sup> Tfh cells were comparable with controls. Establishing the cutoff for high PD-1 expression used to define Tph and Tfh cells can vary between studies (11,19) and may explain the difference between this finding and those presented in a prior report indicating an increased frequency of Tph cells in patients with early RA (20). Consistent with this possibility, using a higher PD-1 cutoff to define Tph and Tfh cells (PD-1<sup>very high</sup> Tph and Tfh cells) identified a significant increase in PD-1<sup>very high</sup> Tph and Tfh cells in patients with early RA compared to controls (Supplementary Figure 2, <http://onlinelibrary.wiley.com/doi/10.1002/art.42248>).

We also found that proportions of Tph cells and Ki-67+ Treg cells were consistently elevated at 1 year, whereas proportions of Tfh cells decreased over time (Figure 2F). Proportions of Tfh cells did not correlate with glucocorticoid dose and were not significantly different between patients who were treated with prednisone doses of >10 mg or mycophenolate mofetil (MMF) and those who were not, suggesting that the decrease in proportions of Tfh cells occurred independent of immunosuppressive treatment (Figures 2G and H). We discovered that the numbers of metaclusters 1 and 3 were significantly decreased in patients with established SLE (Figure 2A). These metaclusters highly expressed CD127 and CD40L, but the differences in expression of CXCR5 were quite distinct between metacluster 1 (CXCR5–) and metacluster 3 (CXCR5+) (Figure 2B).

**Increased CD19<sup>intermediate</sup>Ki-67<sup>high</sup> plasmablasts in early SLE.** We next applied the same clustering approach to CD19+ B cells using the B cell–focused mass cytometry panel (Supplementary Table 1, <http://onlinelibrary.wiley.com/doi/10.1002/art.42248>). We found that metacluster 4 was increased in patients with early SLE, metaclusters 11, 12, 13, and 15 were increased in patients with established SLE, and metacluster 14 was increased in both patients with early SLE and patients with established SLE (Figure 3A). Heatmap expression analysis indicated that metacluster 4 contained a CD19<sup>intermediate</sup>Ki-67<sup>high</sup>

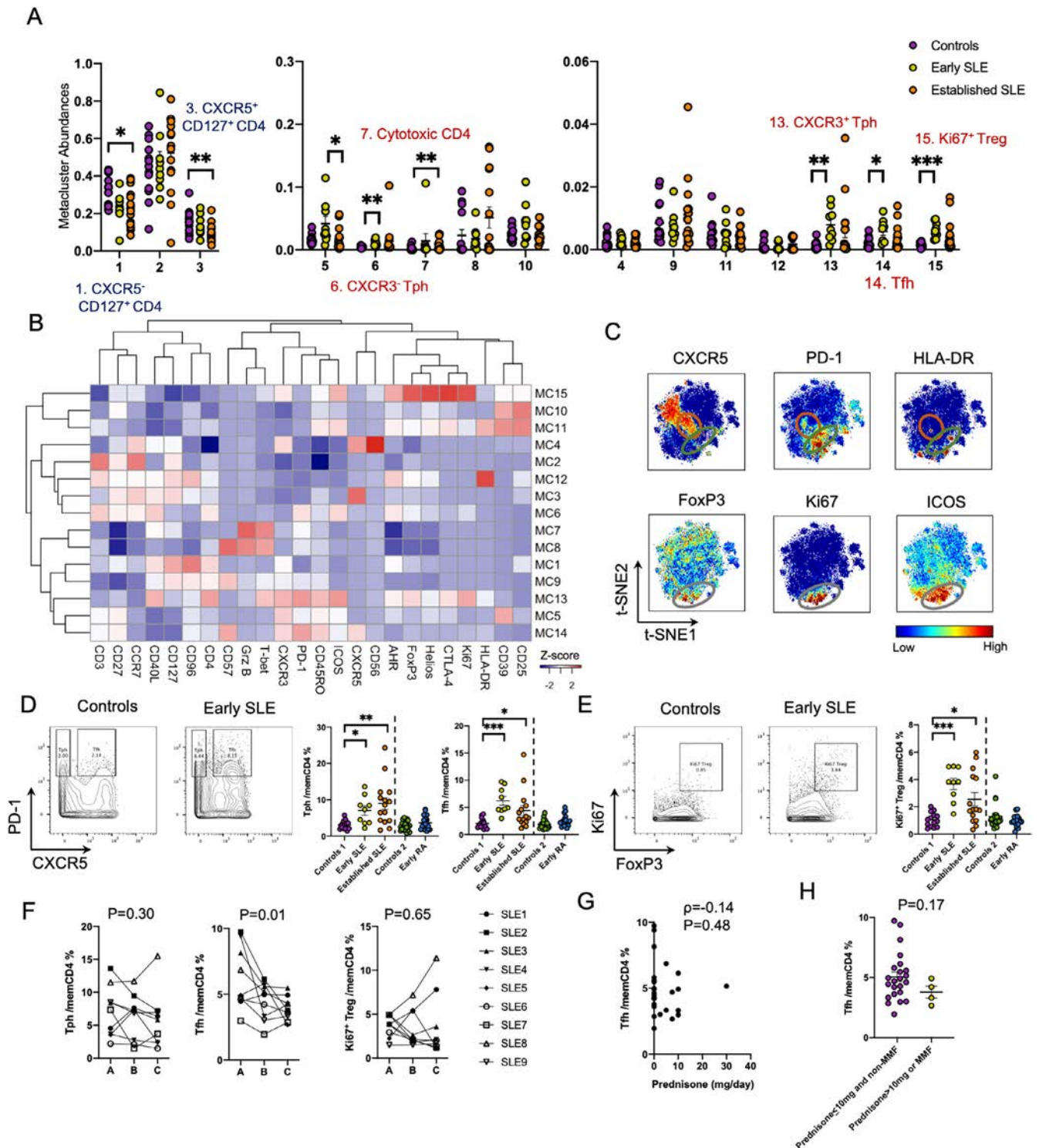


**Figure 2.** Characterization of peripheral helper T (Tph) cells and follicular helper T (Tfh) cells in 9 patients with early SLE, 15 patients with established SLE, and 14 controls without autoimmunity (controls 1), and in 19 early RA patients and 23 controls (controls 2). **A**, Abundance of FlowSOM metaclusters of CD4<sup>+</sup> T cells. **B**, Heatmap of normalized expression of mass cytometry markers in metaclusters with average medians of >0.2. **C**, Visualization of CD4 T cells by t-SNE in early SLE patients, showing Tfh cells (orange circle), Tph cells (green circle), and Ki-67<sup>high</sup> Treg cells (grey circle). **D** and **E**, Representative gating for Tph cells, Tfh cells, and Ki-67<sup>high</sup> Treg cells in CD3<sup>+</sup>CD14<sup>-</sup>CD4<sup>+</sup>CD8<sup>-</sup>CD45RO<sup>+</sup> memory CD4 T cells and comparison of their proportions in each patient and control group. **F**, Longitudinal changes in proportions of Tph cells, Tfh cells, and Ki-67<sup>+</sup> Treg cells in early SLE patients at enrollment (time A), 6 months (time B), and 12 months (time C). **G**, Correlation between prednisone dose and Tfh cell frequency in 27 data points (9 early SLE patients at 3 different timepoints). **H**, Tfh frequency in early SLE patients receiving >10 mg of prednisone or mycophenolate mofetil (MMF) and those receiving ≤10 mg prednisone and no MMF. \* =  $P < 0.05$ ; \*\* =  $P < 0.01$ , \*\*\* =  $P < 0.001$ . Bars show the mean ± SEM. Symbols represent individual participants unless indicated otherwise. See Figure 1 for other definitions.

plasmablast population with elevated expression of CD27 and CD38, indicating proliferating plasmablasts (Figure 3B). We also identified the following 5 metaclusters consistent with CD11c+ T-bet+CD21<sup>low</sup>CXCR5- age-associated B cells (ABCs): HLA-DR+CD38-immunoglobulin G (IgG)+ ABCs (metacluster 11), HLA-DR++CD38+Ki-67+IgG+ ABCs (metacluster 12), CD1c+IgM+ ABCs (metacluster 13), IgM+IgD+ ABCs (metacluster 14), and CD11c<sup>high</sup>T-bet<sup>high</sup> ABCs (metacluster 15).

Visualization with t-SNE demonstrated distinct marker expression of CD19<sup>intermediate</sup>Ki-67<sup>high</sup> plasmablasts and CD11c+T-bet+CD21<sup>low</sup>CXCR5- ABCs in patients with early SLE (Figure 3C). Biaxial plots confirmed that the CD19<sup>intermediate</sup>Ki-67<sup>high</sup> population contained CD27+CD38+ plasmablasts, but the CD19<sup>high</sup>Ki-67<sup>low</sup> population did not (Figure 3D). Proportions of CD19<sup>intermediate</sup>Ki-67<sup>high</sup>CD27+CD38+ plasmablasts were significantly increased in patients with early SLE (0.88%) compared to patients with established SLE (0.18%) and controls (0.07%), while proportions of CD11c+CD21<sup>low</sup> ABCs were increased in patients with established SLE (14.8%) compared to patients with early SLE (7.6%) and controls (3.8%) (Figures 3D and E). Proportions of CD19<sup>intermediate</sup>Ki-67<sup>high</sup>CD27+CD38+ plasmablasts were significantly lower in patients with established SLE compared to patients with early SLE, but were also significantly lower in SLE patients who were treated with prednisone doses of >10 mg or MMF compared to patients who were treated with prednisone doses of ≤10 mg and additional medications other than MMF (Supplementary Figure 3, <http://onlinelibrary.wiley.com/doi/10.1002/art.42248>). These findings suggest that treatment with immunosuppressive drugs may affect the abundance of plasmablasts.

Consistent with the finding that there was an increased abundance of metacluster 14 in patients with early SLE, proportions of IgM+IgD+ ABCs were significantly higher in patients with early SLE compared to controls (Figure 3F). In contrast, proportions of CD11c+CD21<sup>low</sup> ABCs, CD19<sup>intermediate</sup>Ki-67<sup>high</sup>CD27+CD38+ plasmablasts, and IgM+IgD+ ABCs were not increased in patients with early RA (Figures 2D–F). In other subclasses, almost 40% of CD19<sup>intermediate</sup>Ki-67<sup>high</sup>CD27+CD38+ plasmablasts expressed IgA, and IgG expression was rare, while IgG was more frequently expressed (20%) in CD11c+CD21<sup>low</sup> ABCs (Figure 3G). In longitudinal analyses, levels of CD19<sup>intermediate</sup>Ki-67<sup>high</sup> plasmablasts and ABCs and levels of IgG or IgA class-switched CD19<sup>intermediate</sup>Ki-67<sup>high</sup> plasmablasts and ABCs remained high at 1 year after study enrollment (Figure 3H and Supplementary Figure 4, <http://onlinelibrary.wiley.com/doi/10.1002/art.42248>). We also determined that metacluster 6, which contained IgA+IgD-CD27+ memory B cells, was relatively decreased in patients with early SLE.

#### Increased PU.1<sup>high</sup>Ki-67<sup>high</sup> monocytes in early SLE.

In the CD14+ monocyte FlowSOM analysis which used the T cell/monocyte panel, metacluster 8 was found to be decreased and

metacluster 13 was found to be increased in patients with early SLE and patients with established SLE, as compared to controls (Figure 4A). Heatmap analysis indicated that metacluster 13 contained HLA-DR-PU.1<sup>high</sup>Ki-67<sup>high</sup> monocytes (Figure 4B). Visualization with t-SNE confirmed that Ki-67<sup>high</sup> monocytes highly expressed PU.1 but not HLA-DR (Figure 4C). Biaxial plots revealed that metacluster 13 was strongly correlated with both HLA-DR-Ki-67<sup>high</sup> monocytes and PU.1<sup>high</sup>Ki-67<sup>high</sup> monocytes but was more strongly correlated with PU.1<sup>high</sup>Ki-67<sup>high</sup> monocytes (Figure 4D). Consistent with the findings of FlowSOM analysis, proportions of PU.1<sup>high</sup>Ki-67<sup>high</sup> monocytes were increased in patients with early SLE (29.6%), with proportions that were comparable to those in patients with established SLE (29.7%) (7.6% for controls) (Figure 4E). Proportions of PU.1<sup>high</sup>Ki-67<sup>high</sup> monocytes were also increased in patients with early RA compared to controls. PU.1<sup>high</sup>Ki-67<sup>high</sup> monocytes expressed higher levels of CCR2 compared to PU.1<sup>low</sup>Ki-67<sup>low</sup> monocytes ( $P < 0.001$ ) (Figure 4F). Proportions of PU.1<sup>high</sup>Ki-67<sup>high</sup> monocytes did not change significantly over time in patients with early SLE (Figure 4G).

#### Validation of cellular changes in an independent

**SLE cohort.** To validate these cellular changes in a separate SLE cohort, we utilized an independent mass cytometry dataset, interrogating PBMCs from 7 SLE patients and 5 controls that were generated using a distinct but overlapping antibody panel. In this validation cohort, the mean age of SLE patients was 35 years, and the mean SLEDAI-2K disease activity score was 9.4. Of the SLE patients included in the cohort, 86% were treated with prednisone, with a mean dosage of 18 mg/day (Supplementary Table 7, <http://onlinelibrary.wiley.com/doi/10.1002/art.42248>). By biaxial gating, we found that proportions of Ki-67+ICOS+CD8 T cells, Ki-67+ Treg cells, PD-1<sup>high</sup>CD4 T cells (including CXCR5-PD-1<sup>high</sup> Tph cells and CXCR5+PD-1<sup>high</sup> Tfh cells), and CD19<sup>intermediate</sup>CD27+CD38+ plasmablasts were also increased in this validation cohort, consistent with findings from the early and established SLE patient cohorts described above (Supplementary Figure 5, <http://onlinelibrary.wiley.com/doi/10.1002/art.42248>).

#### Associations between expanded immune cell populations in SLE.

Since the analyses across multiple mass cytometry panels revealed that several Ki-67+ proliferating cell populations were expanded in patients with SLE, we hypothesized that proportions of Ki-67+ NK cells would also be increased in patients with SLE. As expected, biaxial plots indicated that proportions of NKG2D+Ki-67+CD3-CD56+ NK cells were highly increased in patients with SLE, with levels remaining stable over time in patients with early SLE (Figures 5A and B). The Ki-67+ cell population did not express PD-1, HLA-DR, and ICOS, unlike Ki-67+ CD4 or CD8 T cells (Figure 5C).

Next, we applied a hierarchical clustering analysis using the frequencies of Ki-67+ICOS+ CD8 T cells, Tph cells, Tfh cells,



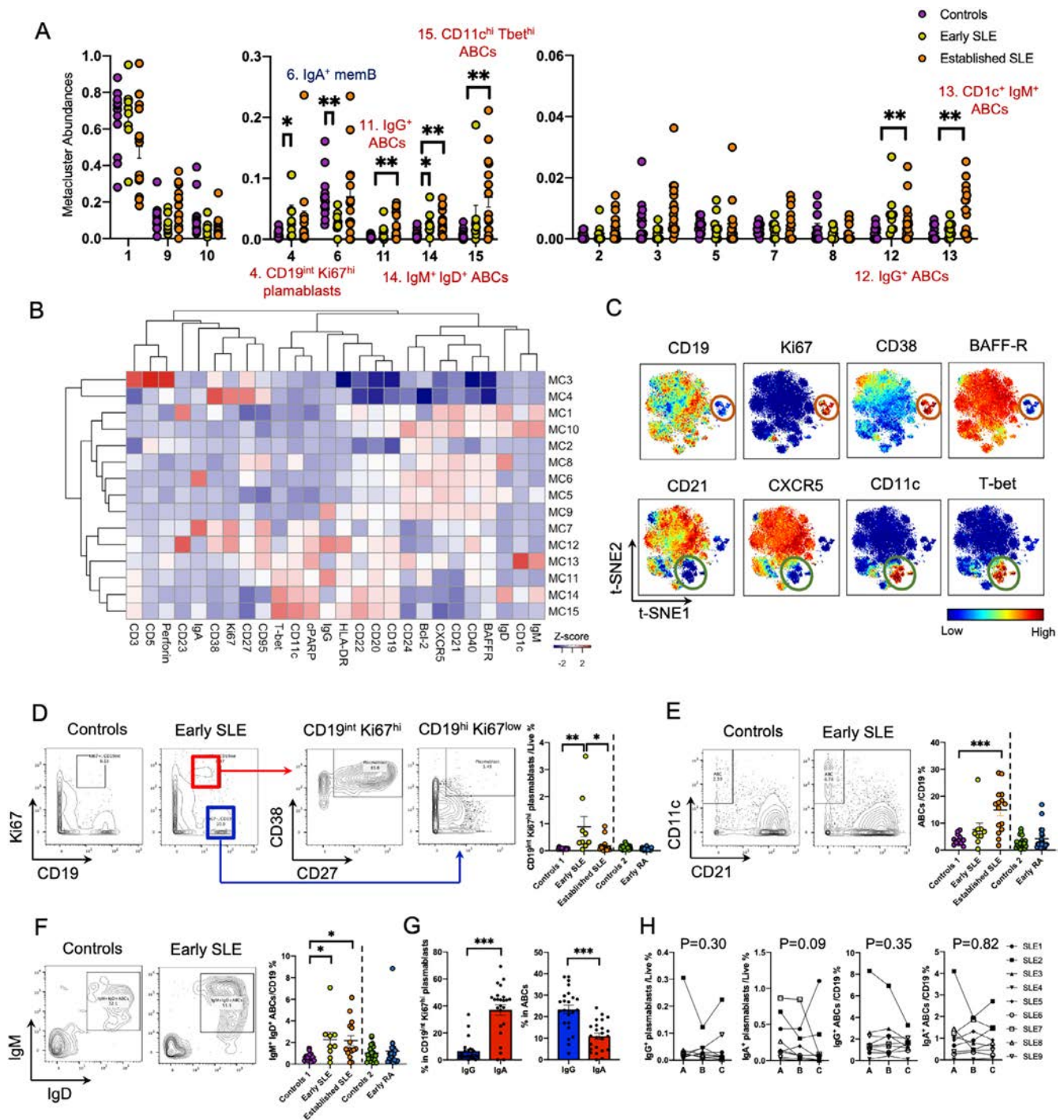


**Figure 3.** Characterization of age-associated B cell (ABC) and plasmablast populations in 9 early SLE patients, 15 established SLE patients, and 14 controls without autoimmunity (controls 1), and in 19 early RA patients and 23 controls (controls 2). **A**, Abundance of flow self-organizing map metaclusters of B cells (% of total B cells). **B**, Heatmap of normalized expression of mass cytometry markers in metaclusters with average medians of >0.2. **C**, Visualization by t-SNE of CD19<sup>+</sup> B cells in early SLE patients (CD19<sup>intermediate</sup>Ki-67<sup>high</sup> plasmablasts indicated by orange circles and ABCs indicated by green circles). **D–F**, Representative gating for CD19<sup>intermediate</sup>Ki-67<sup>high</sup> plasmablasts, ABCs, and IgM<sup>+</sup>IgD<sup>+</sup> ABCs in CD19<sup>+</sup>CD14<sup>–</sup> B cells and comparison of their proportions in each patient and control group. **G**, Proportions of IgG<sup>+</sup> and IgA<sup>+</sup> cells in CD19<sup>intermediate</sup>Ki-67<sup>high</sup> plasmablasts and ABCs in early SLE and established SLE patients. **H**, Longitudinal changes in proportions of IgG<sup>+</sup>CD19<sup>intermediate</sup>Ki-67<sup>high</sup> plasmablasts, IgA<sup>+</sup>CD19<sup>intermediate</sup>Ki-67<sup>high</sup> plasmablasts, IgG<sup>+</sup> ABCs, and IgA<sup>+</sup> ABCs in early SLE patients at enrollment (time A), 6 months after enrollment (time B), and 12 months after enrollment (time C). \* =  $P < 0.05$ ; \*\* =  $P < 0.01$ ; \*\*\* =  $P < 0.001$ , by Kruskal-Wallis test and Dunn's multiple comparison test in **A**, **D**, **E**, and **F**, and by Wilcoxon log-rank test in **G** and **H**. Bars show the mean  $\pm$  SEM. See Figure 1 for other definitions.

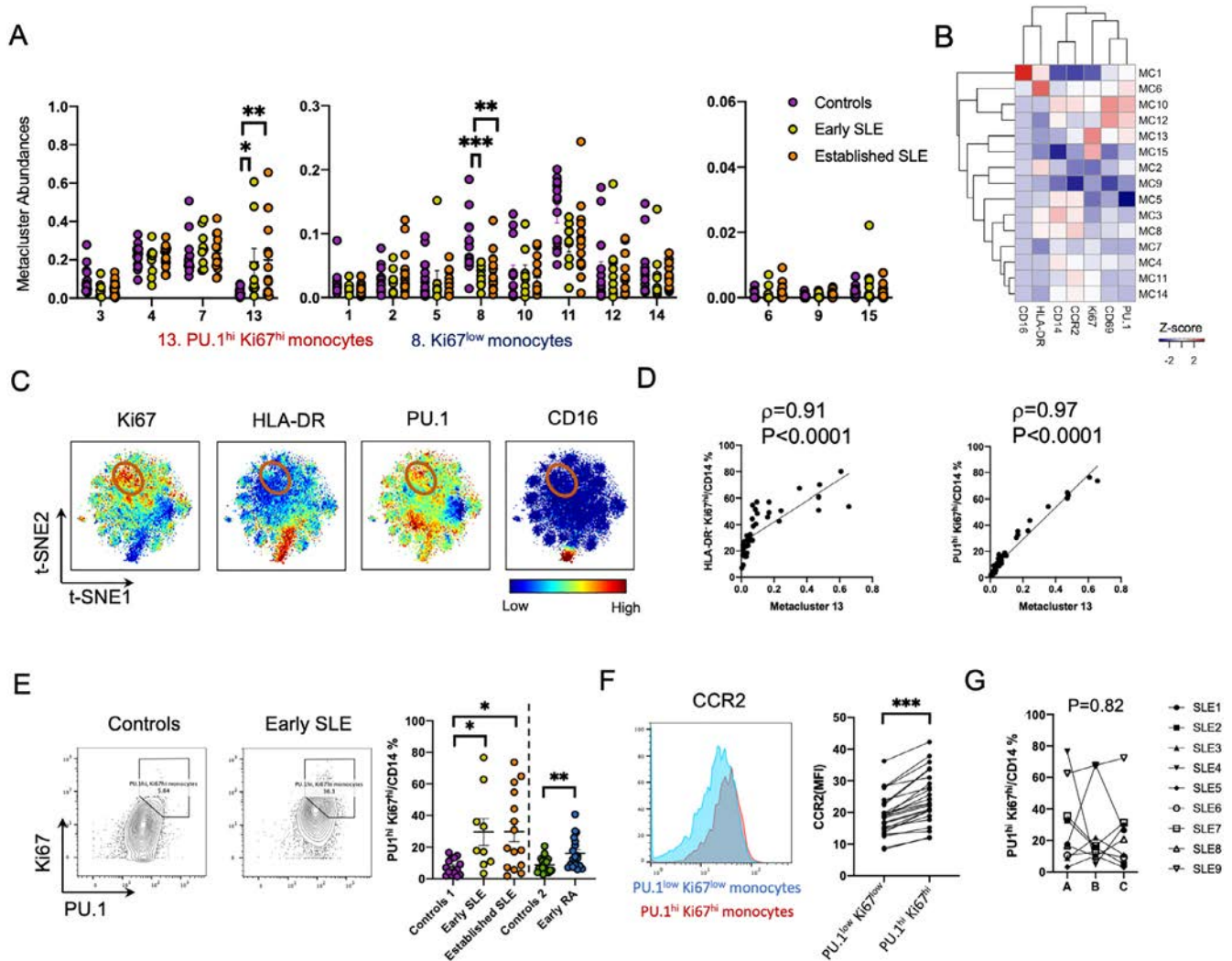


**Figure 4.** Characterization of PU.1<sup>high</sup>Ki-67<sup>high</sup> monocyte populations in 9 patients with early SLE, 15 patients with established SLE, and 14 controls without autoimmunity (controls 1), and in 19 early RA patients and 23 controls without autoimmunity (controls 2). **A**, Abundance of flow self-organizing map metaclusters of monocytes (% of total monocytes). **B**, Heatmap of normalized expression levels of PU.1, CD69, Ki-67, CCR2, CD14, HLA-DR, and CD16 in 14 metaclusters. **C**, Visualization by t-SNE of CD14 monocytes in early SLE patients (PU.1<sup>high</sup>Ki-67<sup>high</sup> monocytes indicated by orange circles). **D**, Correlation of metacluster 13 with HLA-DR-Ki-67<sup>high</sup> monocytes and PU.1<sup>high</sup>Ki-67<sup>high</sup> monocytes by Spearman’s rho. Solid line represents line of best fit. **E**, Representative gating for PU.1<sup>high</sup>Ki-67<sup>high</sup> monocytes and comparison of their proportions in each patient and control group. **F**, CCR2 expression in PU.1<sup>high</sup>Ki-67<sup>high</sup> monocytes and PU.1<sup>low</sup>Ki-67<sup>low</sup> monocytes in early SLE and established SLE patients. **G**, Longitudinal changes in proportions of PU.1<sup>high</sup>Ki-67<sup>high</sup> monocytes in early SLE patients at enrollment (time A), 6 months (time B), and 12 months. \* = *P* < 0.05; \*\* = *P* < 0.01; \*\*\* = *P* < 0.001, Kruskal-Wallis test and Dunn’s multiple comparison test in **A** and **E**, by Spearman’s correlation coefficient in **D**, and by Wilcoxon log-rank test in **F** and **G**. Bars show the mean ± SEM. See Figure 1 for definitions.

IgG+CD19<sup>intermediate</sup>Ki-67<sup>high</sup> plasmablasts, IgA+CD19<sup>intermediate</sup>Ki-67<sup>high</sup> plasmablasts, IgG+ ABCs, IgA+ ABCs, PU.1<sup>high</sup>Ki-67<sup>high</sup> monocytes, and NKG2D+Ki-67+ NK cells. This analysis stratified cell populations into clusters with distinct patterns, including one cluster of PU.1<sup>high</sup>Ki-67<sup>high</sup> monocytes and NKG2D+Ki-67+ NK cells (innate immunity cluster), one cluster of Ki-67+ICOS+ CD8 T cells, Tph cells, and Tfh cells (T cell cluster), and one larger cluster of IgG+CD19<sup>intermediate</sup>Ki-67<sup>high</sup> plasmablasts, IgA+CD19<sup>intermediate</sup>Ki-67<sup>high</sup> plasmablasts, IgG+ ABCs, and IgA+ ABCs (B cell cluster) (Figure 5D). Notably, Tph cells correlated with ABCs

(*r* = 0.51, *P* = 0.006) and CD19<sup>intermediate</sup>Ki-67<sup>high</sup> plasmablast (*r* = 0.43, *P* = 0.01), whereas Tfh cells did not (Figure 5E).

**Longitudinal cytokine and chemokine profiles in patients with early SLE.** We next measured levels of 65 cytokines and chemokines in serum from 9 controls and 9 patients with early SLE, with the early SLE patients again assessed at 3 different timepoints as in the cytometry analyses. Among the 65 cytokines/chemokines we selected a priori to be potentially important in the pathogenesis of early SLE, 33 cytokines were

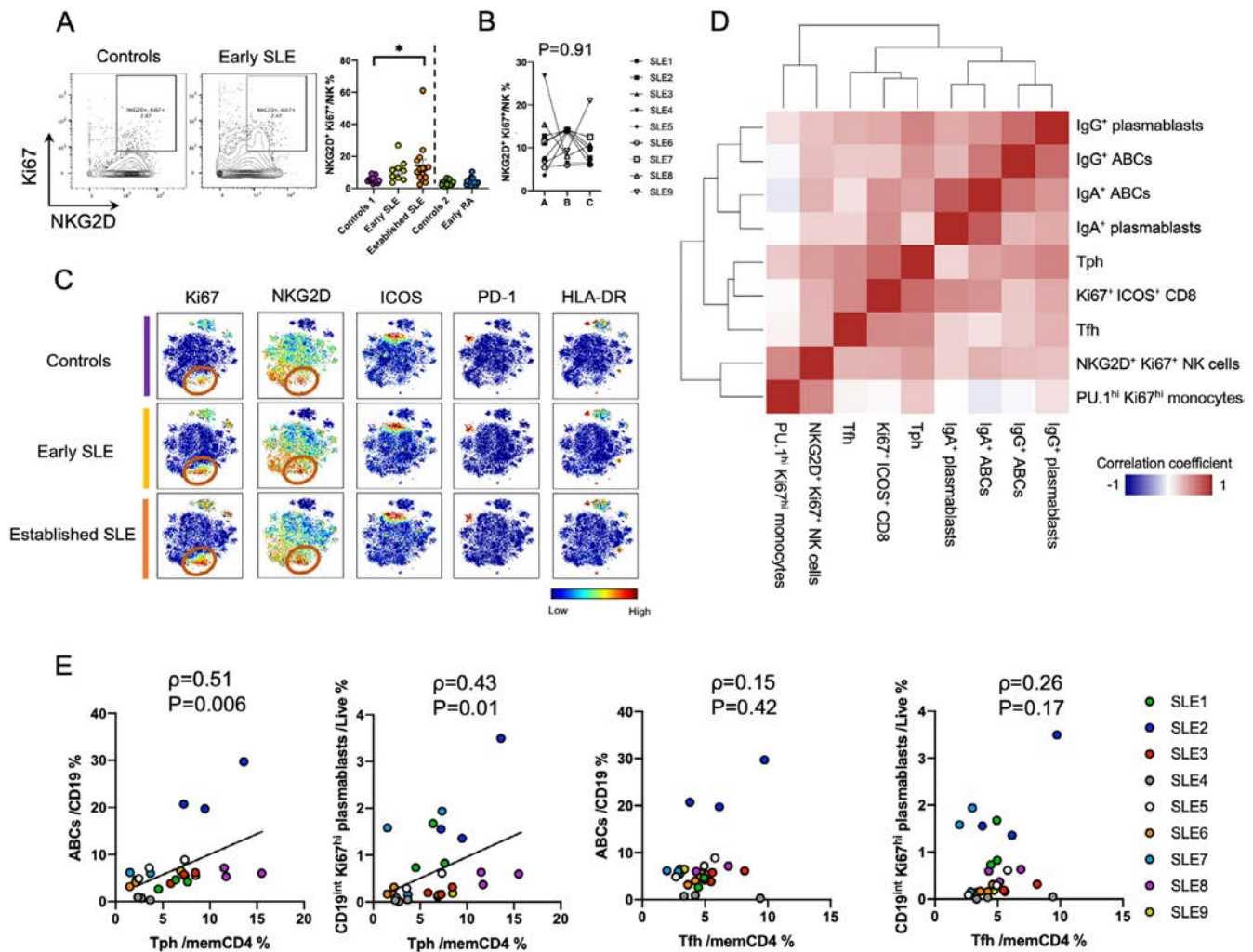


**Figure 5.** Characterization of peripheral helper T (Tph) cells, follicular helper T (Tfh) cells, and Ki-67 proliferative immune cells in 9 early SLE patients, 15 established SLE patients, and 14 controls without autoimmunity (controls 1), and in 19 early RA patients and 23 without autoimmunity (controls 2). **A**, Representative gating for NKG2D+Ki67+ natural killer (NK) cells and comparison of their proportions in each patient and control group. **B**, Longitudinal changes in proportions of NKG2D+Ki67+ NK cells in 9 early SLE patients at enrollment (time A), 6 months (time B), and 12 months (time C). **C**, Visualization by t-SNE of NKG2D+Ki67+ NK cells (orange circle). **D**, Hierarchical clustering heatmap of expanded immune cell types in early SLE patients in 27 data points (9 patients at 3 different time points). Correlation coefficients were calculated by Spearman's test. **E**, Correlation by Spearman's rho between Tph cells, Tfh cells, ABCs, and CD19<sup>int</sup>Ki67<sup>int</sup> plasmablasts; solid line represents line of best fit. \* =  $P < 0.05$ ; \*\* =  $P < 0.01$ ; \*\*\* =  $P < 0.001$ , by Kruskal-Wallis test and Dunn's multiple comparison test. Bars show the mean  $\pm$  SEM. ABC = age-associated B cells (see Figure 1 for other definitions).

detected in serum samples. Interestingly, these cytokines positively correlated with each other, suggesting the presence of a coordinately regulated underlying cytokine network in patients with early SLE (Figure 6A). Most cytokines, with the exception of IL-16, were present at higher levels in early SLE patient samples, and expression levels of IL-2R, CXCL10, CXCL13, IL-12p70, IL-17A, TSLP, CCL8, CCL24, tumor necrosis factor receptor type II, IL-2, IL-20, CD40L, CCL3, CD30, and TWEAK were significantly increased in early SLE patients, with CXCL10, CD40L, IL-20, and TWEAK remaining significantly higher even after Bonferroni correction to adjust for multiple testing (Figure 6B and Supplementary Figures 6 and 7, <http://onlinelibrary.wiley.com/>

[doi/10.1002/art.42248](http://doi.org/10.1002/art.42248)). Among these 4 cytokines, CXCL10 expression was significantly decreased at 1 year ( $P = 0.03$ ), but expression levels of CD40L, IL-20, and TWEAK remained high. (Figure 6C and Supplementary Figure 8, <http://onlinelibrary.wiley.com/doi/10.1002/art.42248>).

Next, we investigated correlations between immune cell levels and serum chemokine levels in early SLE patients. Notably, CXCL13 expression was broadly and strongly correlated with expanded lymphocyte subsets (Tph cells, Tfh cells, Ki-67<sup>high</sup>ICOS<sup>+</sup> CD8 T cells, ABCs, and plasmablasts) in samples from patients with early SLE (Figure 6D). In contrast, CCL2 expression was strongly correlated with levels of PU.1<sup>high</sup>Ki-67<sup>high</sup>

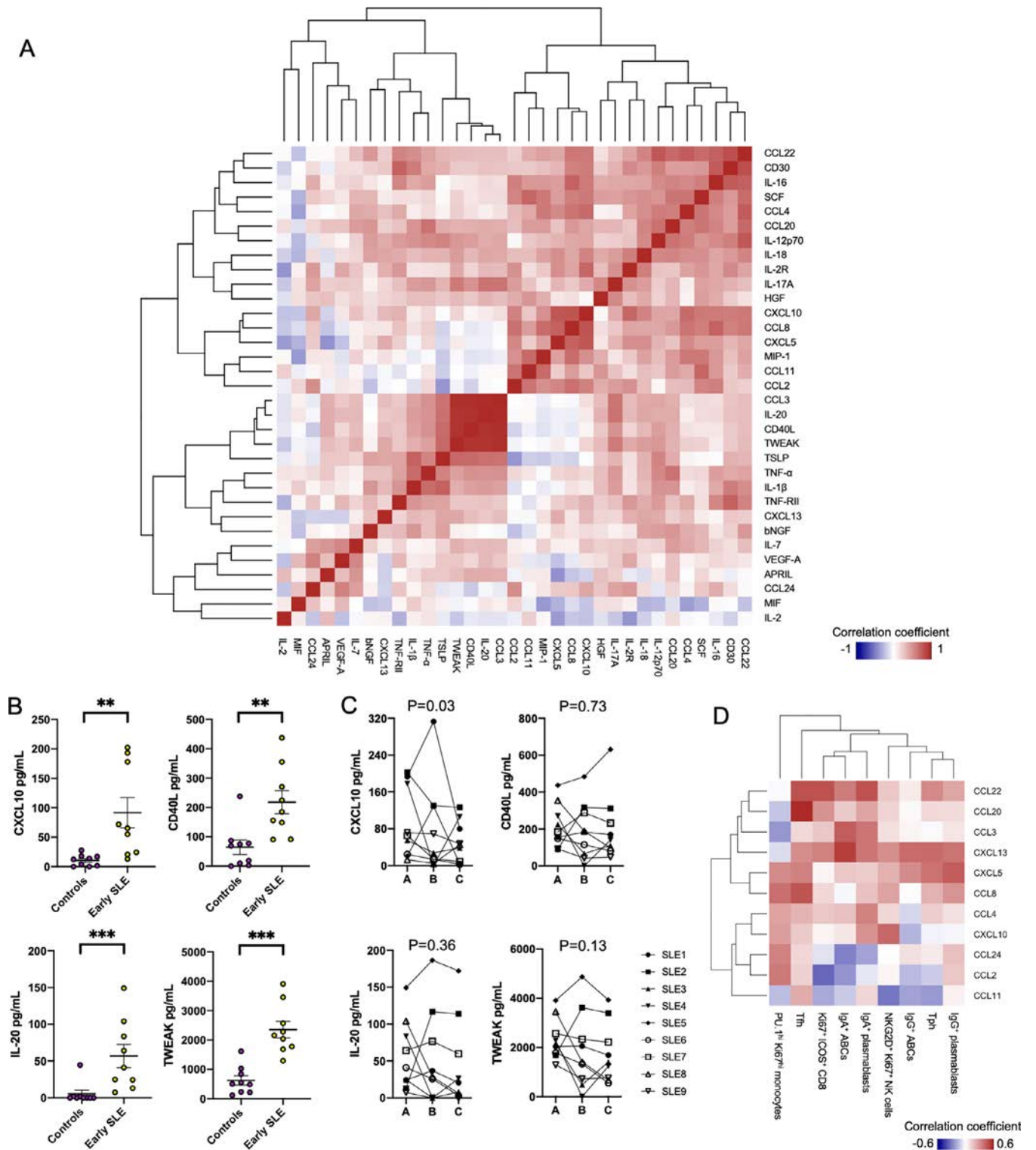


**Figure 6.** Dysregulated cytokine and chemokine networks in early SLE patients. **A**, Hierarchical clustering heatmap of 33 serum cytokines and chemokines detected by Luminex assay (65 total assessed) in early SLE patients (9 patients assessed at 3 different time points). **B**, Comparisons of serum cytokine levels between 9 controls without autoimmunity and 9 early SLE patients at time A, demonstrating significant differences in 15 cytokines between the 2 groups. **C**, Longitudinal changes in levels of CXCL10, CD40L, IL-20, and TWEAK in 9 early SLE patients at enrollment (time A), 6 months after enrollment (time B), and 12 months after enrollment (time C). **D**, Hierarchical clustering heatmap of expanded immune cell types and chemokines in early SLE patients (9 patients assessed at 3 different time points). Correlation coefficients calculated by Spearman’s correlation test in **A** and **D**. \* =  $P < 0.05$ ; \*\* =  $P < 0.01$ ; \*\*\* =  $P < 0.001$ , by Wilcoxon log-rank test in **A** and **C**, and by Mann-Whitney U test in **B**. Bars show the mean  $\pm$  SEM. See Figure 1 for definitions.

monocytes (the subset which highly expressed CCR2), suggesting the involvement of the CCL2–CCR2 axis in the migration of PU.1<sup>high</sup>Ki-67<sup>high</sup> monocytes to inflamed sites. These results suggest that different coregulated pathways, which link cell types to related circulating factors, are active in early SLE patients.

## DISCUSSION

By broad and longitudinal cellular immunophenotyping and serum cytokine/chemokine profiling, we identified multiple expanded immune cell populations in patients with early SLE and evaluated their changes in the first year of disease and their relationships with serum cytokines/chemokines. We found that several lymphocyte populations expanded in early SLE share the common feature of Ki-67 expression, a well-established marker of lymphocyte proliferation. This shared cytometric feature may capture the broad, active immune response occurring in early SLE. These Ki-67+ lymphocyte populations, as well as Tph cells and ABCs, remain consistently elevated over the first year of disease and are similarly elevated in established SLE patients, suggesting that these pathways are activated early and continue to characterize the pathologic immune response in patients with SLE.

Our results are consistent with those of prior studies demonstrating elevations in levels of ABCs (11,21), plasmablasts (22,23), Tph cells, and Tfh cells in patients with established SLE (11,24,25). We have extended these observations to demonstrate that these cell populations are already altered in the early phase of SLE, prior to the initiation of immunosuppressive therapy. Further, we demonstrated that additional populations, including Ki-67+ICOS+CD8, Ki-67+ Treg cells, PU.1<sup>high</sup>Ki-67<sup>high</sup> monocytes, and NKG2D+Ki-67+ NK cells (4 proliferating immune cell subsets) were also increased in the SLE patients included in this study. While patients in the early SLE cohort were younger than the patients in the established SLE cohort, similar cellular alterations were observed in both cohorts. Our longitudinal analyses identified specific features of the immune response that change over time in early SLE patients. Although Tfh cells and some of their inducing factors, such as IL-12, have been considered therapeutic targets in the treatment of SLE (26,27), a phase III study of ustekinumab, a monoclonal antibody targeting IL-12 and IL-23, was discontinued due to lack of efficacy (the LOTUS study) (28). Since Tfh cells expanded initially but decreased longitudinally, this target may have a therapeutic window of opportunity. Moreover, expression levels of CD40L, IL-20, and TWEAK remained persistently elevated, while CXCL10 expression decreased over time. These data suggest that immune profiles change in each phase of SLE (Supplementary Figure 9, <http://onlinelibrary.wiley.com/doi/10.1002/art.42248>), such that quantification of some features of the immune response in SLE need to be adjusted based on disease duration.

Diagnosing early SLE is challenging because the initial clinical manifestations are often nonspecific. Our study revealed that both antibody-secreting plasmablasts and helper T cells, including Tfh cells and Tph cells, were activated in the early phase and could be markers for early SLE. Since autoantibodies are increased several years prior to SLE onset (29,30), the disease is thought to emerge from preclinical lupus. Genetic factors (31–33) and environmental factors (34,35) contribute to the risk of developing SLE, but no robust methods for predicting the development of clinical SLE from preclinical SLE have been established. Thus, it will be of major interest to determine whether alterations in circulating activated B cells and helper T cells can serve as specific hallmarks to predict the risk of developing clinically evident SLE and to guide decisions regarding the initiation of immunosuppressive therapy.

Although we envision alterations in these cell phenotypes as potential metrics for identifying immune activation in patients being evaluated for a diagnosis of SLE, increases in levels of Tph cells, Tfh cells, ABCs, and plasmablasts have been observed in the setting of several diseases, such as RA, Sjögren's syndrome, and systemic sclerosis (35–39). While cellular changes are particularly pronounced in SLE, it seems unlikely that an increase in the levels of these cell populations will provide a specific diagnostic test for SLE; rather, the levels of these cell populations may provide a measurement of disease activity—reflecting the typical changes seen in active SLE—even though these changes may also occur in other diseases. This is conceptually similar to the way serum levels of C-reactive protein are used to help evaluate patients with RA. We propose that the marked expansion of these cell types in SLE patients makes SLE a particularly appealing disease in which to pursue such cellular biomarkers.

Both Tph cells and Tfh cells contribute to B cell responses through the production of IL-21, CD40L, and CXCL13 (40,41). Strikingly, Tph cell levels remained high during the first year after study enrollment, whereas levels of Tfh cells decreased longitudinally, suggesting distinct roles for Tph cells and Tfh cells over the course of SLE. One major difference between Tph cells and Tfh cells is their chemokine receptor expression. Tph cells migrate into local inflammatory sites through receptors such as CCR2 and CCR5, while Tfh cells accumulate in B cell follicles within secondary lymphoid organs through a CXCR5–CXCL13 axis (42). Our data imply that Tfh cell–B cell interactions in secondary lymphoid organs may be particularly important at the initial onset of SLE, but the importance may shift to Tph cell–B cell interactions at local inflammatory sites over time.

In the B cell analysis, the dominant subclasses differed in ABCs and CD19<sup>intermediate</sup>Ki-67<sup>high</sup> plasmablasts. Recent broad B cell receptor analysis of 6 different autoimmune diseases indicated that plasmablasts expressed more IgA1/IgA2 than IgG1/IgG2, whereas IgD–CD27– B cells, which contain much of the ABC population, expressed more IgG1/IgG2 (43). Among these

6 autoimmune diseases, the frequency with which IgA1/IgA2 was expressed in PBMC B cells was greater in patients with SLE, patients with IgA vasculitis, patients with Crohn's disease, and patients with Behçet's disease compared to healthy controls. Considering that mucosa-associated lymphoid tissues and gut-associated lymphoid tissues are the main source of IgA+ plasmablasts (44), intestinal dysbiosis might be involved in the increase of plasmablasts in patients with SLE.

We found that an expanded monocyte population in patients with SLE expressed elevated levels of PU.1, a transcription factor implicated in macrophage development and function (45). The findings of previous single-cell, RNA sequencing analyses of kidney biopsy samples suggest that inflammatory monocytes differentiate into phagocytic and M2-like macrophages in lupus nephritis (5). As PU.1<sup>high</sup>Ki-67<sup>high</sup> monocytes expressed CCR2 and correlated strongly with serum levels of CCL2, this monocyte population in the blood may be a precursor of inflammatory monocytes that infiltrate tissues.

Overall, we found elevated levels of specific cytokines and immune cell populations in SLE patients; however, the cytokine levels and the frequencies with which the immune cells were present varied among patients, indicating heterogeneity of these immune features. Previously, Kubo et al classified SLE patients into a T cell-independent group, a Tfh cell-dominant group, and a Treg cell-dominant group based on flow cytometric features (23), and others have stratified SLE patients based on transcriptomic signatures (7,46). Since several drugs in ongoing clinical trials are molecularly targeted, stratifying SLE patients into subsets based on immune features may be important to enable a personalized approach.

A hierarchical clustering of immune cell subsets revealed distinct clusters of subsets with correlated abundance patterns, including clusters reflective of innate immunity, T cell activation, and B cell activation. Of note, Tph cells and Ki-67+ICOS+CD8 T cells were strongly correlated, suggesting that these 2 subsets may be regulated through a common inducing factor. In this context, type I interferon (IFN) may play an important role in the regulation. A series of RNA sequencing analyses revealed that IFN signatures were highly enriched in the Tph cells of patients with SLE (11) and in Ki-67<sup>high</sup>CD8 T cells in patients with immune checkpoint inhibitor-associated arthritis (47). In addition, type I IFN has negative regulatory effects on the expression of CXCR5 (48,49). As Tph cells and Ki-67+ICOS+CD8 T cells may be pathogenic drivers of SLE, anifrolumab (a fully human monoclonal antibody against the type I IFN receptor) may act to ameliorate disease activity in part through the regulation of Tph cells and Ki-67+ICOS+CD8 T cells (50).

Our study had several limitations. The relatively small number of patients followed up in the early SLE cohort limited our ability to identify cocorrelated immune features and precluded evaluation of clinical correlates of the cellular features identified. The early SLE patients included in this study had relatively mild disease activity through the first year of disease, yet still had

clearly demonstrable immune alterations. In future studies, it will be of interest to determine whether phenotypes of circulating immune cells differ in patients who initially present with more severe disease and what effects specific immunosuppressive therapies have. Two of the 9 patients in the early SLE cohort were lymphopenic at enrollment, and 1 patient developed lupus nephritis during follow up; however, the cohort was underpowered for the purpose of assessing cellular correlates of these clinical features. Additional study will also be required to evaluate whether the same cellular patterns are observed in other SLE cohorts, including cohorts with a larger representation of Black patients, in order to better understand the generalizability of the results. In addition, our study focuses only on blood samples and does not contain parallel tissue studies. Nevertheless, the substantial alterations demonstrated in the circulating immune cells of lupus patients in this study support the idea that clinically relevant signals are detectable in blood samples.

In conclusion, this study highlighted persistent activation of Tph cells, ABCs, and Ki-67+ proliferating immune cell populations in the blood in early SLE patients. Our findings underscore the value of using broad, longitudinal immunophenotyping to define patterns of immune cell activity in the setting of SLE, which may help refine potential biomarkers and prioritize therapeutic targets in early and established phases of SLE.

## AUTHOR CONTRIBUTIONS

All authors were involved in drafting the article or revising it critically for important intellectual content, and all authors approved the final version to be published. Dr. Rao had full access to all of the data in the study and takes responsibility for the integrity of the data and the accuracy of the data analysis.

**Study conception and design.** Sasaki, Sparks, Holers, Alves, Lederer, Costenbader, Rao.

**Acquisition of data.** Sasaki, Keegan, Stevens, Qu, Wang, Nguyen, Sparks, Holers, Alves, Lederer, Costenbader, Rao.

**Analysis and interpretation of data.** Sasaki, Bracero, Chen, Cao, Sparks, Holers, Alves, Lederer, Costenbader, Rao.

## ROLE OF THE STUDY SPONSOR

Merck Sharp & Dohme was involved in the study design, acquisition of data, and interpretation of data. Publication of this article was not contingent upon approval by Merck Sharp & Dohme.

## ADDITIONAL DISCLOSURES

Authors Qu, Wang, and Alves are employees of Merck Sharp & Dohme.

## REFERENCES

1. Choi MY, Barber MR, Barber CE, Clarke AE, Fritzler MJ. Preventing the development of SLE: identifying risk factors and proposing pathways for clinical care. *Lupus* 2016;25:838–49.

2. Amsden LB, Davidson PT, Fevrier HB, Goldfien R, Herrinton LJ. Improving the quality of care and patient experience of care during the diagnosis of lupus: a qualitative study of primary care. *Lupus* 2018;27:1088–99.
3. Kernder A, Richter JG, Fischer-Betz R, Winkler-Rohlfing B, Brinks R, Aringer M, et al. Delayed diagnosis adversely affects outcome in systemic lupus erythematosus: cross sectional analysis of the LuLa cohort. *Lupus* 2021;30:431–8.
4. Mosca M, Costenbader KH, Johnson SR, Lorenzoni V, Sebastiani GD, Hoyer BF, et al. How Do patients with newly diagnosed systemic lupus erythematosus present? A multicenter cohort of early systemic lupus erythematosus to inform the development of new classification criteria. *Arthritis Rheumatol* 2019;71:91–8.
5. Arazi A, Rao DA, Berthier CC, Davidson A, Liu Y, Hoover PJ, et al. *Nat Immunol* 2019;20:902–14.
6. Der E, Suryawanshi H, Morozov P, Kustagi M, Goilav B, Ranabothu S, et al. Tubular cell and keratinocyte single-cell transcriptomics applied to lupus nephritis reveal type I IFN and fibrosis relevant pathways. *Nat Immunol* 2019;20:915–27.
7. Banchereau R, Hong S, Cantarel B, Baldwin N, Baisch J, Edens M, et al. Personalized immunomonitoring uncovers molecular networks that stratify lupus patients. *Cell* 2016;165:551–65.
8. Hong S, Banchereau R, Maslow BL, Guerra MM, Cardenas J, Baisch J, et al. Longitudinal profiling of human blood transcriptome in healthy and lupus pregnancy. *J Exp Med* 2019;216:1154–69.
9. Amir el-AD, Davis KL, Tadmor MD, Simonds EF, Levine JH, Bendall SC, et al. viSNE enables visualization of high dimensional single-cell data and reveals phenotypic heterogeneity of leukemia. *Nat Biotechnol* 2013;31:545–52.
10. Van Gassen S, Callebaut B, Van Helden MJ, Lambrecht BN, Demeester P, Dhaene T, et al. FlowSOM: using self-organizing maps for visualization and interpretation of cytometry data. *Cytometry A* 2015;87:636–45.
11. Bocharnikov AV, Keegan J, Wacleche VS, Cao Y, Fonseka CY, Wang G, et al. PD-1hiCXCR5- T peripheral helper cells promote B cell responses in lupus via MAF and IL-21. *JCI Insight* 2019;4:e130062.
12. O’Gorman WE, Kong DS, Balboni IM, Rudra P, Bolen CR, Ghosh D, et al. Mass cytometry identifies a distinct monocyte cytokine signature shared by clinically heterogeneous pediatric SLE patients. *J Autoimmun* 2017:S0896-8411:30412–7. E-pub ahead of print.
13. Van der Kroef M, van den Hoogen LL, Mertens JS, Blokland SL, Haskett S, Devaprasad A, et al. Cytometry by time of flight identifies distinct signatures in patients with systemic sclerosis, systemic lupus erythematosus and Sjögrens syndrome. *Eur J Immunol* 2020;50:119–29.
14. Hochberg MC. Updating the American College of Rheumatology revised criteria for the classification of systemic lupus erythematosus [letter]. *Arthritis Rheum* 1997;40:1725.
15. Petri M, Orbai AM, Alarcón GS, Gordon C, Merrill JT, Fortin PR, et al. Derivation and validation of the Systemic Lupus International Collaborating Clinics classification criteria for systemic lupus erythematosus. *Arthritis Rheum* 2012;64:2677–86.
16. Aringer M, Costenbader K, Daikh D, Brinks R, Mosca M, Ramsey-Goldman R, et al. 2019 European League Against Rheumatism/American College of Rheumatology classification criteria for systemic lupus erythematosus. *Arthritis Rheumatol* 2019;71:1400–12.
17. Aletaha D, Neogi T, Silman AJ, Funovits J, Felson DT, Bingham CO III, et al. 2010 Rheumatoid arthritis classification criteria: an American College of Rheumatology/European League Against Rheumatism collaborative initiative. *Arthritis Rheum* 2010;62:2569–81.
18. Gladman DD, Ibanez D, Urowitz MB. Systemic Lupus Erythematosus Disease Activity Index 2000. *J Rheumatol* 2002;29:288–91.
19. Wacleche VS, Wang R, Rao DA. Identification of T peripheral helper (Tph) cells. *Methods Mol Biol* 2022;2380:59–76.
20. Fortea-Gordo P, Nuño L, Villalba A, Peiteado D, Monjo I, Sánchez-Mateos P, et al. Two populations of circulating PD-1hiCD4 T cells with distinct B cell helping capacity are elevated in early rheumatoid arthritis. *Rheumatology (Oxford)* 2019;58:1662–73.
21. Jenks SA, Cashman KS, Zumaquero E, Marigorta UM, Patel AV, Wang X, et al. Distinct effector B cells induced by unregulated toll-like receptor 7 contribute to pathogenic responses in systemic lupus erythematosus. *Immunity* 2018;49:725–39.
22. Mei HE, Hahne S, Redlin A, Hoyer BF, Wu K, Baganz L, et al. Plasmablasts with a mucosal phenotype contribute to plasmacytosis in systemic lupus erythematosus. *Arthritis Rheumatol* 2017;69:2018–28.
23. Kubo S, Nakayamada S, Yoshikawa M, Miyazaki Y, Sakata K, Nakano K, et al. Peripheral immunophenotyping identifies three subgroups based on T cell heterogeneity in lupus patients. *Arthritis Rheumatol* 2017;69:2029–37.
24. Makiyama A, Chiba A, Noto D, Murayama G, Yamaji K, Tamura N, et al. Expanded circulating peripheral helper T cells in systemic lupus erythematosus: association with disease activity and B cell differentiation. *Rheumatology (Oxford)* 2019;58:1861–9.
25. Lin J, Yu Y, Ma J, Ren C, Chen W. PD-1+CXCR5-CD4+T cells are correlated with the severity of systemic lupus erythematosus. *Rheumatology (Oxford)* 2019;58:2188–92.
26. Blanco P, Ueno H, Schmitt N. T follicular helper (Tfh) cells in lupus: activation and involvement in SLE pathogenesis. *Eur J Immunol* 2016;46:281–90.
27. Van Vollenhoven RF, Hahn BH, Tsokos GC, Wagner CL, Lipsky P, Touma Z, et al. Efficacy and safety of ustekinumab, an IL-12 and IL-23 inhibitor, in patients with active systemic lupus erythematosus: results of a multicentre, double-blind, phase 2, randomised, controlled study. *Lancet* 2018;392:1330–9.
28. Janssen Research & Development, sponsor. A study of ustekinumab in participants with active systemic lupus erythematosus. *ClinicalTrials.gov* identifier: NCT03517722; 2018.
29. Arbuckle MR, McClain MT, Rubertone MV, Scofield RH, Dennis GJ, James JA, et al. Development of autoantibodies before the clinical onset of systemic lupus erythematosus. *N Engl J Med* 2003;349:1526–33.
30. Eriksson C, Kokkonen H, Johansson M, Hallmans G, Wadell G, Rantapää-Dahlqvist S. Autoantibodies predate the onset of systemic lupus erythematosus in northern Sweden. *Arthritis Res Ther* 2011;13:R30.
31. Cui Y, Sheng Y, Zhang X. Genetic susceptibility to SLE: recent progress from GWAS. *J Autoimmun* 2013;41:25–33.
32. Morris DL, Sheng Y, Zhang Y, Wang YF, Zhu Z, Tomblinson P. Genome-wide association meta-analysis in Chinese and European individuals identifies ten new loci associated with systemic lupus erythematosus. *Nat Genet* 2016;48:940–6.
33. Wang YF, Zhang Y, Lin Z, Zhang H, Wang TY, Cao Y, et al. Identification of 38 novel loci for systemic lupus erythematosus and genetic heterogeneity between ancestral groups. *Nat Commun* 2021;12:772.
34. Shapira Y, Agmon-Levin N, Shoenfeld Y. Geoepidemiology of autoimmune rheumatic diseases [review]. *Nat Rev Rheumatol* 2010;6:468–76.
35. Bengtsson AA, Rylander L, Hagmar L, Nived O, Sturfelt G. Risk factors for developing systemic lupus erythematosus: a case-control study in southern Sweden. *Rheumatology (Oxford)* 2002;41:563–71.
36. Verstappen GM, Meiners PM, Cometh OB, Visser A, Arends S, Abdulhad WH, et al. Attenuation of follicular helper T cell-dependent B cell hyperactivity by abatacept treatment in primary Sjögren’s Syndrome. *Arthritis Rheumatol* 2017;69:1850–61.

37. Ricard L, Jachiet V, Malard F, Ye Y, Stocker N, Rivière S, et al. Circulating follicular helper T cells are increased in systemic sclerosis and promote plasmablast differentiation through the IL-21 pathway which can be inhibited by ruxolitinib. *Ann Rheum Dis* 2019;78:539–50.
38. Pontarini E, Murray-Brown WJ, Croia C, Lucchesi D, Conway J, Rivellese F, et al. Unique expansion of IL-21+ Tfh and Tph cells under control of ICOS identifies Sjögren's syndrome with ectopic germinal centres and MALT lymphoma. *Ann Rheum Dis* 2020;79:1588–99.
39. Marks KE, Rao DA. T peripheral helper cells in autoimmune diseases. *Immunol Rev* 2022;307:191–202.
40. Rao DA, Gurish MF, Marshall JL, Slowikowski K, Fonseka CY, Liu Y, et al. Pathologically expanded peripheral T helper cell subset drives B cells in rheumatoid arthritis. *Nature* 2017;542:110–4.
41. Yoshitomi H, Ueno H. Shared and distinct roles of T peripheral helper and T follicular helper cells in human diseases. *Cell Mol Immunol* 2021;18:523–7.
42. Rao DA. T cells that help B cells in chronically inflamed tissues. *Front Immunol* 2018;9:1924.
43. Bashford-Rogers RJ, Bergamaschi L, McKinney EF, Pombal DC, Mescia F, Lee JC, et al. Analysis of the B cell receptor repertoire in six immune-mediated diseases. *Nature* 2019;574:122–6.
44. Lycke NY, Bernmark M. The regulation of gut mucosal IgA B-cell responses: recent developments. *Mucosal Immunol* 2017;10:1361–74.
45. Klemsz MJ, McKercher SR, Celada A, Van Beveren C, Maki RA. The macrophage and B cell-specific transcription factor PU.1 is related to the ets oncogene. *Cell* 1990;61:113–24.
46. Andreoletti G, Lanata CM, Trupin L, Paranjpe I, Jain TS, Nititham J, et al. Transcriptomic analysis of immune cells in a multi-ethnic cohort of systemic lupus erythematosus patients identifies ethnicity- and disease-specific expression signatures. *Commun Biol* 2021;4:488.
47. Wang R, Singaraju A, Marks KE, Shakib L, Dunlap G, Cunningham-Bussel A, et al. Clonally expanded CD38hi cytotoxic CD8 T cells define the T cell infiltrate in checkpoint inhibitor-associated arthritis. *BioRxiv* 20211020 [preprint]. doi: <https://doi.org/10.1101/2021.10.19.464961>.
48. Schmitt N, Liu Y, Bentebibel SE, Munagala I, Bourdery L, Venuprasad K, et al. The cytokine TGF- $\beta$  co-opts signaling via STAT3-STAT4 to promote the differentiation of human TFH cells. *Nat Immunol* 2014;15:856–65.
49. Locci M, Wu JE, Arumemi F, Mikulski Z, Dahlberg C, Miller AT, et al. Activin A programs the differentiation of human TFH cells. *Nat Immunol* 2016;17:976–84.
50. Morand EF, Furie R, Tanaka Y, Bruce IN, Askanase AD, Richez C, et al. Trial of Anifrolumab in active systemic lupus erythematosus. *N Engl J Med* 2020;382:211–21.



# Two Distinct Immune Cell Signatures Predict the Clinical Outcomes in Patients With Amyopathic Dermatomyositis With Interstitial Lung Disease

Yan Ye,<sup>1</sup> Xueliang Zhang,<sup>1</sup> Teng Li,<sup>2</sup> Jiaqiang Ma,<sup>2</sup> Ran Wang,<sup>1</sup>  Chunmei Wu,<sup>1</sup> Runci Wang,<sup>1</sup>  Chunde Bao,<sup>1</sup>   
Shuang Ye,<sup>1</sup> Nan Shen,<sup>1</sup>  Qiang Guo,<sup>1</sup> Qiong Fu,<sup>1</sup>  and Xiaoming Zhang<sup>3</sup>

**Objective.** Amyopathic dermatomyositis (ADM) is a heterogeneous and life-threatening autoimmune disease with a high mortality rate. In particular, anti-melanoma differentiation-associated protein 5 antibody-positive patients are at a high risk of developing rapidly progressive interstitial lung disease (RPILD). This study was undertaken to identify immunologic signatures among patients who have ADM with ILD (ADM-ILD) and to discover the biomarkers predicting prognosis.

**Methods.** The landscape of 42 immune cell phenotypes in the peripheral blood of 82 ADM-ILD patients and 82 age- and sex-matched healthy donors was assessed by multicolor flow cytometry. Patients were stratified using an unsupervised machine learning method (hierarchical clustering analysis) by immune cell subsets. Multiple Wilcoxon's signed rank tests and supervised machine learning methods were performed to identify important immune cell subsets. Kaplan-Meier survival analysis with log rank tests was used to create survival curves.

**Results.** We identified 2 distinct clusters correlating with different disease activities and clinical outcomes in ADM-ILD. Cluster 1 was enriched in the activated CD45RA+HLA-DR+CD8+ T cells with decreased CD56<sup>dim</sup> natural killer cell proportions and showed a higher prevalence of RPILD and higher mortality. In contrast, the other subgroup, cluster 2 (the nonactivated T cell-dominant cluster), displayed favorable clinical outcomes with high survival rates. Our data also revealed that immunophenotype was an independent risk factor associated with 1-year survival.

**Conclusion.** Peripheral immunologic features may have the potential to stratify patients with ADM-ILD according to different disease severity and clinical outcomes, which may have implications for outcome prediction, pathogenesis study, and therapy selection.

## INTRODUCTION

Amyopathic dermatomyositis (ADM) is a unique subtype of classic dermatomyositis (DM) that can affect the skin, lungs, and joints, but without muscle involvement (1,2). It is estimated that 50–100% of patients with ADM develop interstitial lung disease (ILD), and 38–71% of patients with ILD develop rapidly progressive ILD (RPILD) (3–7). More than 50% of affected patients

have an inadequate response or no response to aggressive immunosuppressive treatments and die of respiratory failure within 1 year (6–9). In contrast, ADM patients with chronic or stable ILD usually have favorable outcomes. For such patients, intensive immunosuppressive regimens may not improve outcomes and may increase the risk of opportunistic infection, which is also a critical cause of death (1,10,11). Therefore, there is an urgent clinical need to identify biomarkers in ADM patients

Supported by the National Key Research and Development Program of China (award 2021YFE0200600), the National Natural Science Foundation of China (awards 81771733 and 81771737), the Shanghai Municipal Science and Technology Major Project (awards 2019SHZDZX02 and HS2021SHZX001), the Shanghai Municipal Science and Technology Fund (award 21ZR438800), the Shanghai Jiaotong University “Star of Jiaotong University” Medical Engineering Cross Research Fund (award YG2022QN018), and the Pujiang Rheumatism Young Doctor Training Program (award SPORG2108).

Drs. Y. Ye and Xueliang Zhang contributed equally to this article.

<sup>1</sup>Yan Ye, MD, PhD, Xueliang Zhang, MD, Ran Wang, MD, Chunmei Wu, MD, PhD, Runci Wang, MD, PhD, Chunde Bao, MD, Shuang Ye, MD, PhD, Nan Shen, MD, PhD, Qiang Guo, MD, PhD, Qiong Fu, MD, PhD: Department of Rheumatology, Renji Hospital, Shanghai Jiaotong University School of Medicine, Shanghai, China; <sup>2</sup>Teng Li, PhD, Jiaqiang Ma, PhD: The Center for Microbes, Development and Health, Key Laboratory of Molecular

Virology & Immunology, Institut Pasteur of Shanghai, Chinese Academy of Sciences/University of Chinese Academy of Sciences, Shanghai, China; <sup>3</sup>Xiaoming Zhang, PhD: The Center for Microbes, Development and Health, Key Laboratory of Molecular Virology & Immunology, Institut Pasteur of Shanghai, Chinese Academy of Sciences/University of Chinese Academy of Sciences, and Shanghai Huashen Institute of Microbes and Infections, Shanghai, China.

Author disclosures are available at <https://onlinelibrary.wiley.com/action/downloadSupplement?doi=10.1002%2Fart.42264&file=art42264-sup-0001-Dislosureform.pdf>.

Address correspondence via email to Xiaoming Zhang, PhD at [xmzhang@ips.ac.cn](mailto:xmzhang@ips.ac.cn), to Qiong Fu, MD, PhD at [fuqiong5@163.com](mailto:fuqiong5@163.com), or to Qiang Guo, MD, PhD at [bluedescent@126.com](mailto:bluedescent@126.com).

Submitted for publication November 3, 2021; accepted in revised form June 9, 2022.

for effective risk stratification, outcome prediction, and treatment optimization.

Efforts have been made to stratify patients according to clinical manifestations, serum biomarkers, and pulmonary function (3,12,13). Anti-melanoma differentiation-associated protein 5 antibody (anti-MDA-5) is a risk factor for poor prognosis and is closely associated with RPILD (14,15); however, there is a lack of specificity regarding mortality prediction. In our prior cohort study, we generated a FLAIR score, which incorporated 5 independent risk factors: ferritin level, lactate dehydrogenase (LDH) level, semi-quantitative anti-MDA-5 antibody level, high-resolution computed tomography (HRCT) imaging score, and the presence of RPILD/non-RPILD (3). The FLAIR score successfully stratifies patients who have ADM with ILD (ADM-ILD) into low-, medium-, and high-risk groups and requires external validation in other cohorts. In another multicenter Japanese cohort, initial concentrations of C-reactive protein (CRP), Krebs von den Lungen 6 (KL-6), and anti-MDA-5 antibodies were used to establish a predictive model for mortality in patients with DM/polymyositis (PM)-associated ILD (13). However, it is intriguing to explore whether immunologic features could act as potential biomarkers to stratify ADM-ILD patients as well as to provide clues for disease pathogenesis.

In the present study, we investigated the peripheral blood immunologic profiles of ADM-ILD patients. We aimed to predict clinical outcomes by identifying novel immune cell phenotypes to provide deeper recognition of the pathogenesis and guide more precise individualized therapy.

## PATIENTS AND METHODS

**Study subjects.** Peripheral blood samples were collected from 82 ADM-ILD patients who were admitted to the Department of Rheumatology at Renji Hospital and 82 age- and sex-matched healthy donors from the Renji Hospital Biobank. Written informed consent was obtained from each patient and healthy donor. The study was approved by the Ethics Committee of Renji Hospital (identification no. 2013-126) in Shanghai, China. Patients with ADM were eligible to be included in the study if they fulfilled the modified Sontheimer's definitions (16), based on classic cutaneous manifestations of DM and with no myositis. All patients met the ILD criteria; among them, 21 patients developed RPILD. Patients with underlying malignancy, concomitant infections, and other autoimmune rheumatic diseases were excluded. Demographic data, laboratory data, clinical manifestations, and treatment data were collected from participants' medical records. The workflow chart of the study appears in Supplementary Figure 1, available on the *Arthritis & Rheumatology* website at <https://onlinelibrary.wiley.com/doi/10.1002/art.42264>.

**Diagnosis and assessment of ILD and RPILD.** The ILD criteria comprised respiratory manifestations, pulmonary function tests, and radiologic findings. RPILD was defined as rapid deterioration of dyspnea secondary to ILD within 1 month of the

diagnosis of ILD (17). The HRCT score represents the severity of the ILD imaging, as previously described (3). Details of HRCT score calculation are presented in the Supplementary Materials (<https://onlinelibrary.wiley.com/doi/10.1002/art.42264>).

**Flow cytometry.** There are 2 flow cytometry panels in our study: 1 lineage panel for whole blood and 1 lymphocyte panel for peripheral blood mononuclear cell (PBMCs). Whole blood or PBMCs from patients were stained with fluorochrome-conjugated antibodies, and data were collected using a flow cytometry analyzer (BD LSR Fortessa; BD Biosciences). Data were analyzed by FlowJo software, version 9.3.2. Antibodies used for staining and detailed gating strategies are described in Supplementary Tables 1 and 2 and Supplementary Figures 2A–C (<https://onlinelibrary.wiley.com/doi/10.1002/art.42264>).

**Machine learning approaches.** We used supervised machine learning approaches for immunologic feature selection. One machine learning approach was the sparse partial least-squares discriminant analysis (PLS-DA) and the other was the balanced random forest (BRF) algorithm. Patients were stratified using an unsupervised machine learning method (hierarchical clustering), and then important immune subsets were selected using the top 10 variables as calculated by the Gini impurity index in the BRF model, and the top 10 weighting variables in sparse PLS-DA analysis. To avoid overfitting, 10-fold cross-validation with 50 repetitions was used to validate the performance of sparse PLS-DA and BRF models. A detailed description of the machine learning models and data analysis platforms is provided in the Supplementary Materials (<https://onlinelibrary.wiley.com/doi/10.1002/art.42264>).

**Statistical analysis.** Data are expressed as the mean  $\pm$  SD or as the median and interquartile range (IQR), depending on data distribution. Statistical analysis was performed using R software, version 4.0.3, and GraphPad Prism, version 6.0. Comparisons were analyzed using Student's *t*-test, Wilcoxon's signed rank test, analysis of variance, or chi-square test, as appropriate. Data were corrected for multiple testing using a false discovery rate of 5% (Benjamini-Hochberg algorithm). Youden's index was used to set the optimal cutoff. Univariate and multivariate analyses using the Cox proportional hazards model were performed to identify prognostic risk factors. Kaplan-Meier curves were estimated using the log rank test. Two-sided *P* values less than 0.05 were considered statistically significant.

## RESULTS

**Different immune cell subtypes in patients with ADM-ILD and healthy donors.** In the study groups, the female:male ratio was almost 3:1 (59:23 in the ADM-ILD group; 66:16 in the healthy donor group), and the mean  $\pm$  SD age

was similar ( $48.76 \pm 9.6$  years in the ADM-ILD group;  $47.61 \pm 10.75$  years in the healthy donor group).

To explore an overview of the immunophenotypes in the ADM-ILD patients, we measured 42 immunologic parameters by flow cytometry. We found remarkable differences in peripheral immune cell compositions between ADM-ILD patients and healthy donors (Figure 1A). Interestingly, T cell subsets, as important components of adaptive immunity, were activated in ADM-ILD patients, particularly represented by the remarkable enrichment of CD8+ T cell subsets. In B cells, the proportions of plasma and naive B cells were increased in ADM-ILD patients, while the proportions of transitional and isotype-switched B cells were decreased, suggesting that abnormal B cell differentiation might play a role in the pathogenesis of ADM-ILD. According to the results of sparse PLS-DA analysis,

ADM-ILD patients and healthy donors showed a clear separation in immune cell types (Figure 1B).

ADM-ILD patients appeared to have a skewed active adaptive immune response. Comparing ADM-ILD patients to healthy donors, respectively, the proportions of CD45RA+HLA-DR+CD8+ T cells (mean  $\pm$  SD  $13.96 \pm 15.49\%$  versus  $4.79 \pm 5.22\%$ ) and plasma B cells (mean  $\pm$  SD  $12.39 \pm 13.99\%$  versus  $1.70\% \pm 2.10\%$ ) were significantly elevated in ADM-ILD, while innate immune cell subsets, such as basophils (mean  $\pm$  SD  $0.12 \pm 0.20\%$  versus  $0.61 \pm 0.37\%$ ), eosinophils (mean  $\pm$  SD  $0.39 \pm 0.78\%$  versus  $2.35 \pm 2.40\%$ ), plasmacytoid dendritic cells (DCs) (mean  $\pm$  SD  $0.03 \pm 0.05\%$  versus  $0.10 \pm 0.06\%$ ), and blood dendritic cell antigen 1-positive (BDCA1+) myeloid DCs (mean  $\pm$  SD  $0.03 \pm 0.06\%$  versus  $0.17 \pm 0.09\%$ ) were decreased in ADM-ILD, with slightly

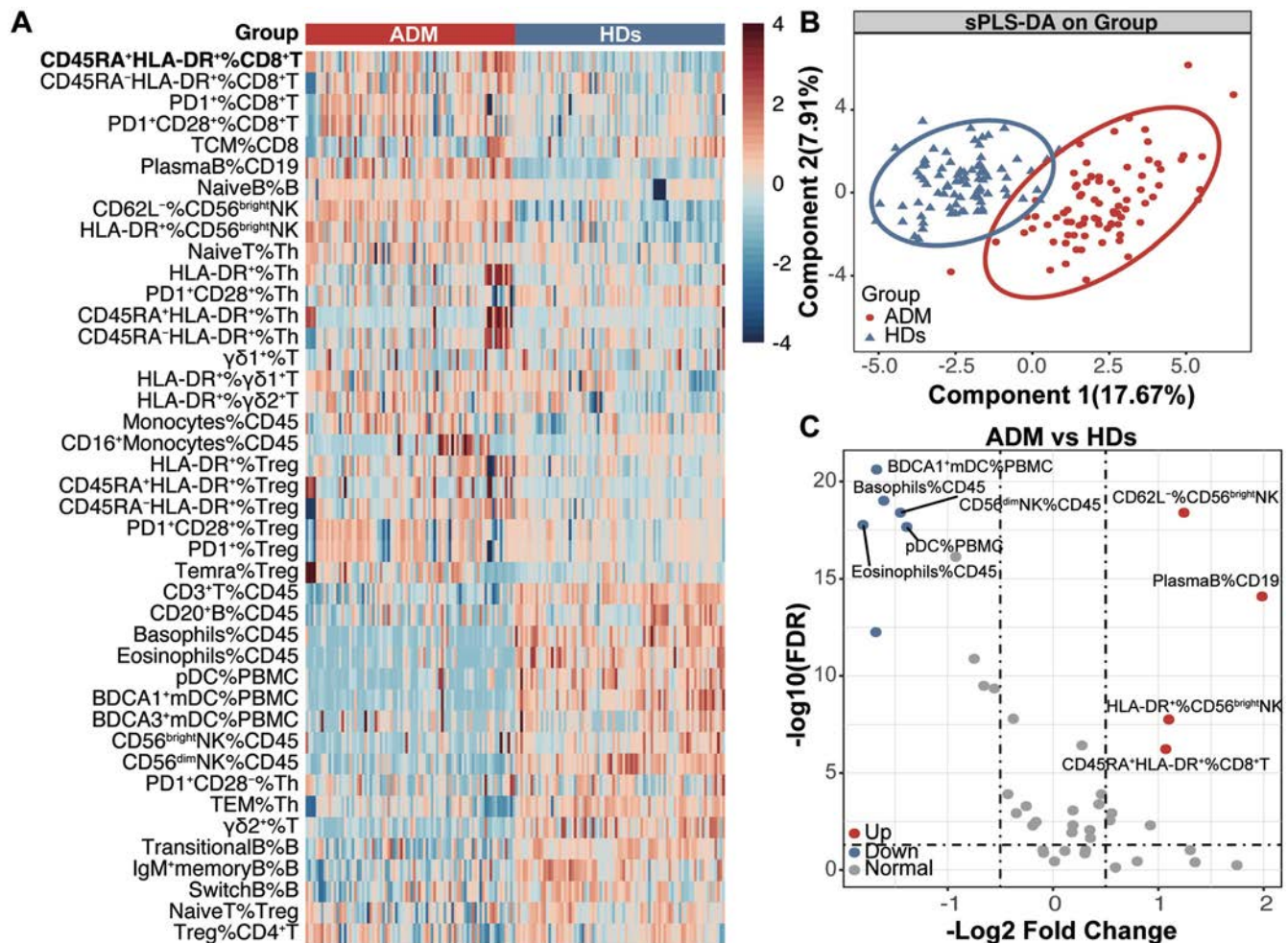


**Figure 1.** Immunologic profile between patients with amyopathic dermatomyositis with interstitial lung disease (ADM-ILD) and healthy donors (HDs). **A**, Heatmap showing the overall immunogram patterns from 42 immunologic signatures in ADM-ILD patients and healthy donors. **B**, Sparse partial least-squares discriminant analysis (sPLS-DA) performed with 42 immune subsets. Individual distribution points and confidence ellipses for ADM-ILD and healthy donors are plotted in red and blue, respectively. **C**, Volcano plot displaying significant differences in cell subset expression (fold change values) between ADM-ILD patients and healthy donors. *P* values were calculated using Wilcoxon's unpaired signed rank tests. The horizontal dashed line represents the  $\log_{10}$ -adjusted *P* value following a 5% false discovery rate (FDR) adjustment for multiple comparisons. The vertical dashed lines represent  $\pm \log_2$  fold change in expression in the ADM-ILD group relative to the healthy donor group. PD-1 = programmed death 1; TCM = central memory T; NK = natural killer; PBMC = peripheral blood mononuclear cell; BDCA = blood dendritic cell antigen; mDC = myeloid dendritic cell; pDC = plasmacytoid dendritic cells; TEM = effector memory T cells. Color figure can be viewed in the online issue, which is available at <http://onlinelibrary.wiley.com/doi/10.1002/art.42264/abstract>.

increased monocytes (mean  $\pm$  SD  $5.11 \pm 3.60\%$  versus  $3.59 \pm 2.02\%$ ) (Figure 2). The proportions of CD56<sup>bright</sup> cells (mean  $\pm$  SD  $0.07 \pm 0.12\%$  versus  $0.12 \pm 0.07\%$ ) and CD56<sup>dim</sup> natural killer (NK) cells (mean  $\pm$  SD  $1.21 \pm 1.23\%$  versus  $5.14 \pm 3.7\%$ ) in ADM-ILD patients were significantly lower than in healthy donors, while the percentage of CD62L<sup>-</sup> and HLA-DR<sup>+</sup> cells among CD56<sup>bright</sup> NK cells showed an increasing trend (Figure 1C and Figure 2), indicating low yet activated NK cell populations in patients with ADM-ILD.

**Immunophenotype-based stratification of patients with ADM-ILD using machine learning.** We next explored whether the peripheral immune cell subsets could be used to stratify ADM-ILD patients with different clinical features and outcomes. We used hierarchical clustering, an unsupervised machine learning algorithm, and found that patients could be divided into 2 clusters (cluster 1,  $n = 34$ ; cluster 2,  $n = 48$ ) (Figure 3A and Supplementary Figure 3, <https://onlinelibrary.wiley.com/doi/10.1002/art.42264>). We then compared the immunophenotypes between cluster 1 and cluster 2. Patients in cluster 1 showed a predominant active T cell signature with a remarkable elevation in HLA-DR<sup>+</sup> T cell subsets, represented by significantly higher proportions of CD45RA+HLA-DR+CD8<sup>+</sup> T cells, CD45RA+HLA-DR<sup>+</sup> Th cells, and HLA-DR<sup>+</sup> Th cells (Figure 3B). In contrast, patients in cluster 2 showed lower proportions of these highly activated HLA-DR<sup>+</sup>

T cell subsets despite higher proportions of total CD3<sup>+</sup> T cells. In cluster 2, the proportion of translational B cells was up-regulated. There were no differences in other late-stage B cell subsets. In addition, patients in cluster 2 had higher proportions of BDCA3<sup>+</sup> myeloid DC cells and eosinophils. Compared to that in cluster 1, the proportion of CD56<sup>dim</sup> NK cells was significantly higher in cluster 2 (Figure 3B). A decreased peripheral CD56<sup>dim</sup> NK cell population has been associated with an active immune system (18). With these considerations, patients in cluster 1 demonstrated a prominent activated immune profile compared to patients in cluster 2.

We next used sparse PLS-DA and BRF models to further distinguish and validate the hierarchical clustered groups. As shown in Figure 3C, sparse PLS-DA analysis revealed a clear separation between the 2 patient groups and identified the dominant distinguishing immune cell subsets, which were similar to the above-mentioned subsets, namely CD45RA+HLA-DR+CD8<sup>+</sup> T cells for cluster 1 and CD56<sup>dim</sup> NK cells for cluster 2 (Figure 3D).

Subsequently, we used the BRF model to weight the immunologic parameters. After optimizing the model, the mean decrease in the Gini index was calculated and ranked to show the importance of the immune signatures. The percentage of CD45RA+HLA-DR+CD8<sup>+</sup> T cells and CD56<sup>dim</sup> NK cells strongly contributed to the differences in the clusters (Figure 3E). The area under the receiver operating characteristic curve (AUC) of the univariate BRF models ranged from 0.8567 to

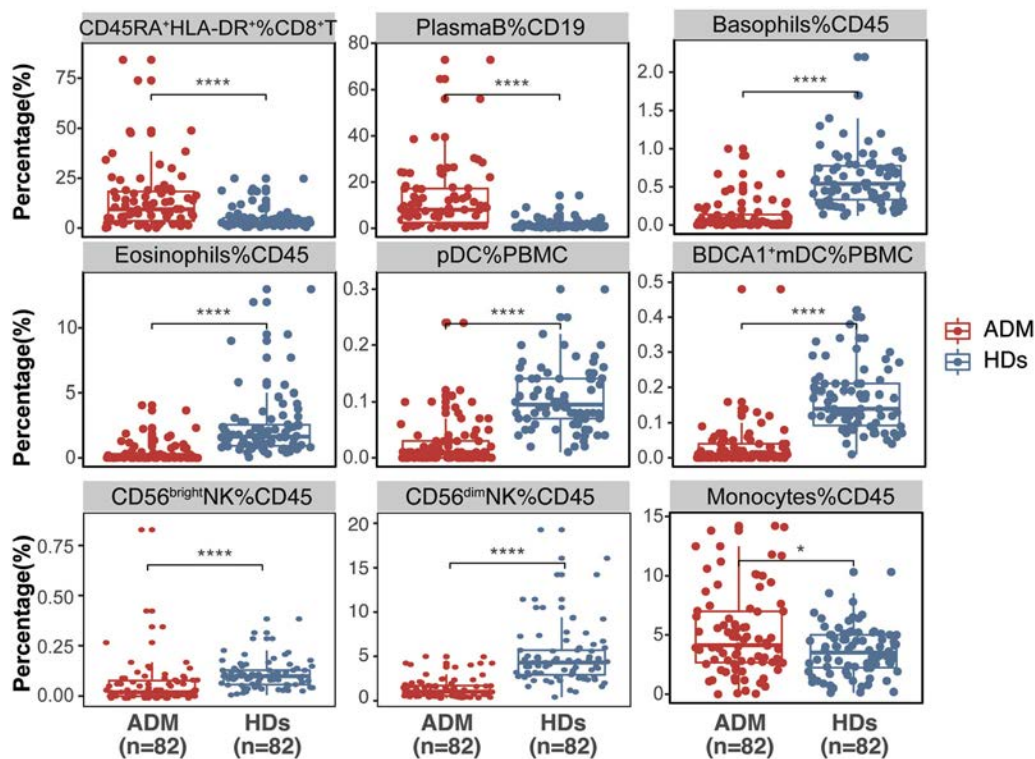


**Figure 2.** Altered immunologic architecture in ADM-ILD patients. Box plots show the immune cell subsets that were significantly different between ADM-ILD patients and healthy donors. Each box represents the range of values. Lines inside the boxes represent the mean. Lines outside the boxes represent the minimum and maximum. Adjusted  $P$  values are shown. \* =  $P < 0.05$ ; \*\*\*\* =  $P < 0.0001$ , by Wilcoxon's unpaired signed rank test. See Figure 1 for definitions. Color figure can be viewed in the online issue, which is available at <http://onlinelibrary.wiley.com/doi/10.1002/art.42264/abstract>.

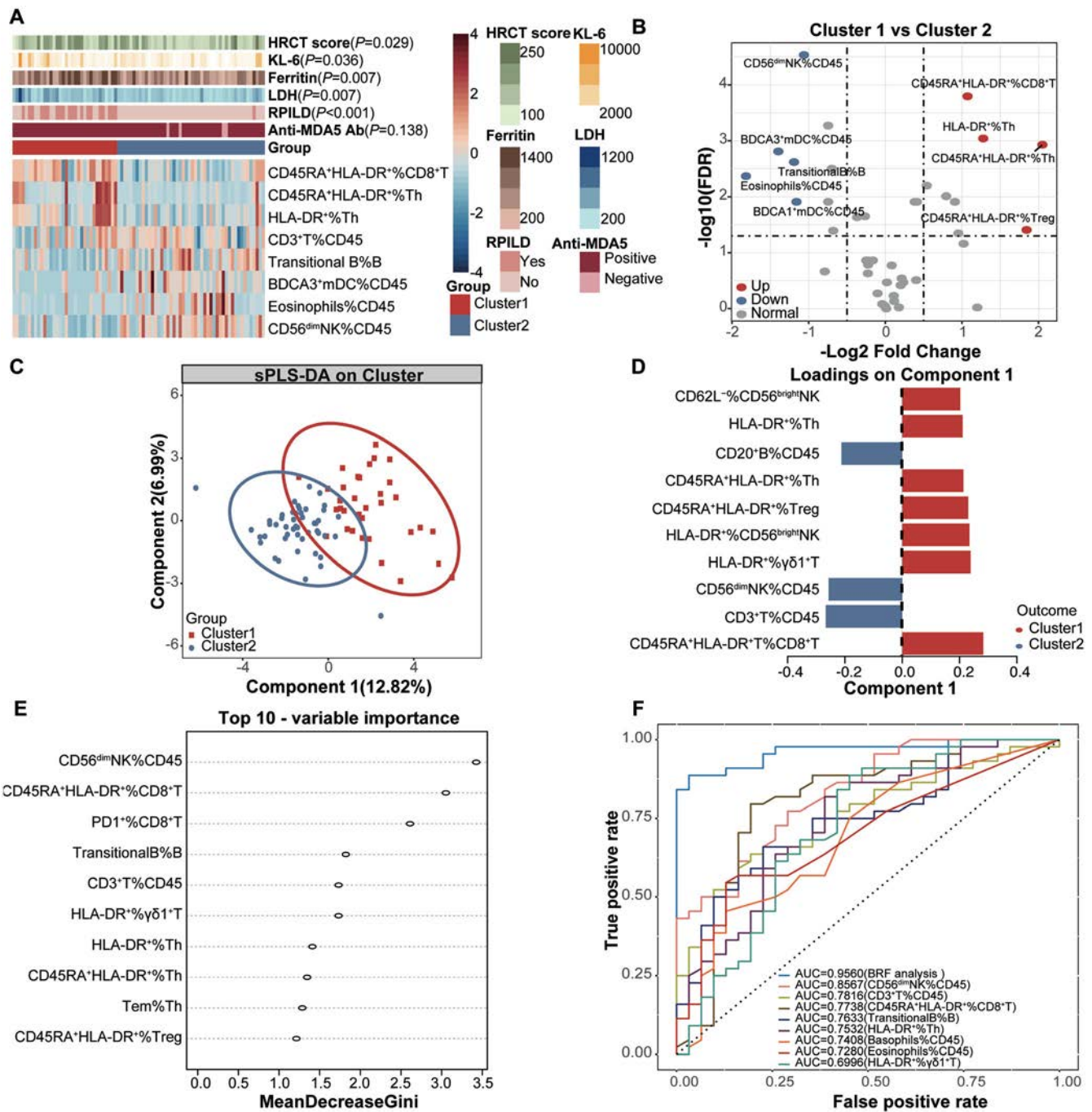


**Figure 3.** Hierarchical clusters of patients with ADM-ILD according to the immunologic parameters. **A**, Heatmap shows the most significant differences in the clinical parameters and the frequency of immune cell subpopulations between cluster 1 and cluster 2. **B**, Volcano plot displays the significant differences in cell subset expression (fold change values) between the 2 clusters.  $P$  values were calculated using Wilcoxon's unpaired signed rank tests. The horizontal dashed line represents the  $\log_{10}$ -adjusted  $P$  value following a 5% FDR adjustment for multiple comparisons. The vertical dashed lines represent the  $\pm 2 \log_2$  fold change in expression between clusters. **C**, Sparse PLS-DA plot analysis was performed to validate the top 10 hits from the predictive model. Individual distribution points and confidence ellipses for clusters 1 and 2 are plotted in red and blue, respectively. **D**, Factor-loading weights in component 1 for the top 10 ranked immunologic parameters are shown. Colors indicate the class with maximal mean value. **E**, A balanced random forest (BRF) model using all 42 immunologic subsets was used, and the top 10 variables contributing to the model are shown. The Gini index of the optimized BRF model was calculated and ranked by each score. **F**, Receiver operating characteristic curve analysis was performed with the multivariate BRF model and univariate models in the 10-fold cross-validation. HRCT = high-resolution computed tomography; KL-6 = Krebs von den Lungen 6; LHD = lactate dehydrogenase; RPILD = rapidly progressive ILD; anti-MDA-5 Ab = anti-melanoma differentiation-associated protein 5 antibody; AUC = area under the receiver operating characteristic curve (see Figure 1 for other definitions). Color figure can be viewed in the online issue, which is available at <http://onlinelibrary.wiley.com/doi/10.1002/art.42264/abstract>.

0.6996, with the best performance in the proportion of CD56<sup>dim</sup> NK cells followed by the CD45RA+HLA-DR+CD8+ T cell model (AUC 0.7738) and CD3+ T cell model (AUC 0.7816), showing that the multivariate BRF model (AUC 95.6%; accuracy 86.6%) outperformed the univariate models in the 10-fold cross-validation analysis (Figure 3F). Therefore, ADM-ILD patients could be stratified into 2 clusters according to their peripheral immunophenotypes using multiple machine learning approaches.

**Correlation of distinct clusters with different disease activities and clinical outcomes.** To further evaluate the clinical significance of immunologic profiles, differences in demographic data, clinical features, laboratory findings, and treatments were compared between cluster 1 and cluster 2. The results showed that cluster 1 distinguished ADM-ILD patients with more severe disease activity and worse clinical prognosis (Table 1). Patients in cluster 1 had a higher prevalence of RPILD,

**Table 1.** Demographic and clinical characteristics of the ADM-ILD patients\*

	Total (n = 82)	Cluster 1 (n = 34)	Cluster 2 (n = 48)	P
<b>Demographics</b>				
Sex, no. (%)				1.00
Female	59 (72)	24 (71)	35 (73)	
Male	23 (28)	10 (29)	13 (27)	
Age, mean ± SD years	48.76 ± 9.60	49.59 ± 9.07	48.17 ± 10.01	0.505
<b>Laboratory findings</b>				
Anti-MDA-5, no. (%)	78 (95)	34 (100)	44 (92)	0.138
RPILD, no. (%)	21 (26)	20 (59)	1 (2)	<0.001
CK, units/liter	46 (25–86)	51 (26.25–113)	41 (25–70.75)	0.344
LDH, units/liter	282 (226–379.50)	343.50 (272–530.25)	269.50 (223.75–317.25)	0.007
Ferritin, ng/ml	594.25 (234.45–959.98)	731.6 (427.62–1,500)	400.3 (172.12–890.55)	0.007
KL-6, units/ml	889.5 (603–1,642.25)	1,014 (782.50–1,896.75)	754 (576.50–1,413.25)	0.036
ALT, units/liter	57 (24–95.75)	62 (26.75–105.50)	54.5 (23–92.25)	0.437
AST, units/liter	40 (25–75)	41.5 (29.50–80)	36.5 (24.50–75)	0.224
CRP, mg/liter	3.48 (3.28–9.26)	4.36 (3.28–20.10)	3.48 (3.28–5.25)	0.388
ESR, mm/hour	27 (15.25–45)	26 (17–44.75)	27.5 (12–45.25)	0.575
Hemoglobin, mean ± SD gm/liter	127.94 ± 19.09	125.03 ± 20.50	130 ± 17.97	0.259
Platelets, ×10 <sup>9</sup> /liter	190.5 (157.50–254.25)	183.5 (136.5–240.5)	194 (169.75–261.75)	0.128
HRCT score, %	139 (121.17–188.33)	167.25 (124.63–217)	130.83 (119.75–179)	0.029
<b>Pulmonary function tests</b>				
FVC%	68.1 (59.72–76.05)	67.55 (61.22–75.45)	68.1 (59.40–77.15)	0.958
DLco%	59 (46–85)	54 (44.95–75.38)	63.6 (54–85.50)	0.030
Unable to perform test, no. (%)	14 (17)	13 (38)	1 (2)	<0.001
WBC, ×10 <sup>9</sup> /liter	6.73 (5.56–8.95)	6.24 (5.58–8.57)	7.72 (5.53–9)	0.519
Neutrophils, ×10 <sup>9</sup> /liter	5.22 (4.26–6.56)	5.12 (4.52–8)	5.32 (4.11–6.21)	0.292
Lymphocytes, ×10 <sup>9</sup> /liter	0.92 (0.59–1.6)	0.79 (0.54–1.18)	1.21 (0.66–1.86)	0.035
Monocytes, ×10 <sup>9</sup> /liter	0.47 (0.31–0.72)	0.49 (0.31–0.73)	0.44 (0.31–0.69)	0.836
Neutrophil:lymphocyte ratio	5.3 (3.41–8.14)	7.53 (4.73–10.15)	3.94 (2.67–5.95)	<0.001
ANA (≥1:80), no. (%)	28 (34)	10 (29)	18 (38)	0.600
<b>Clinical features, no. (%)</b>				
Heliotrope rash	69 (84)	27 (79)	42 (88)	0.496
Gotttron's papules	21 (26)	10 (29)	11 (23)	0.684
Skin ulceration	46 (56)	17 (50)	29 (60)	0.477
Periungual erythema	35 (43)	14 (41)	21 (44)	0.996
<b>Treatment</b>				
GC dose, mg	50 (50–95)	75 (50–95)	50 (30–85)	0.026
GC alone, no. (%)	4 (5)	2 (6)	2 (4)	1
GC and CSA, no. (%)	17 (21)	5 (15)	12 (25)	0.392
GC and TAC, no. (%)	13 (16)	8 (24)	5 (10)	0.195
GC and CYC, no. (%)	1 (1)	0 (0)	1 (2)	1
GC and MMF, no. (%)	1 (1)	0 (0)	1 (2)	1
GC, CSA, and another agent, no. (%)	37 (45)	15 (44)	22 (46)	1
IVIG, no. (%)	8 (10)	3 (9)	5 (10)	1
No treatment, no. (%)	9 (11)	4 (11)	5 (10)	1

\* Except where indicated otherwise, values are the median (interquartile range). Differences between amyopathic dermatomyositis with interstitial lung disease (ADM-ILD) clusters were analyzed using *t*-tests, Wilcoxon's unpaired signed rank tests, or analysis of variance. *P* values less than 0.05 were considered statistically significant. Anti-MDA-5 = anti-melanoma differentiation-associated protein 5; RPILD = rapidly progressive interstitial lung disease; CK = creatine kinase; LDH = lactate dehydrogenase; KL-6 = Krebs von den Lungen 6; ALT = alanine transaminase; AST = aspartate transaminase; CRP = C-reactive protein; ESR = erythrocyte sedimentation rate; FVC% = forced vital capacity percent predicted; DLco% = diffusing capacity of lung carbon monoxide percent predicted; WBC = white blood cell count; ANA = antinuclear antibody; GC = glucocorticoid; CSA = cyclosporin A; TAC = tacrolimus; CYC = cyclophosphamide; MMF = mycophenolate mofetil; IVIG = intravenous immunoglobulin.

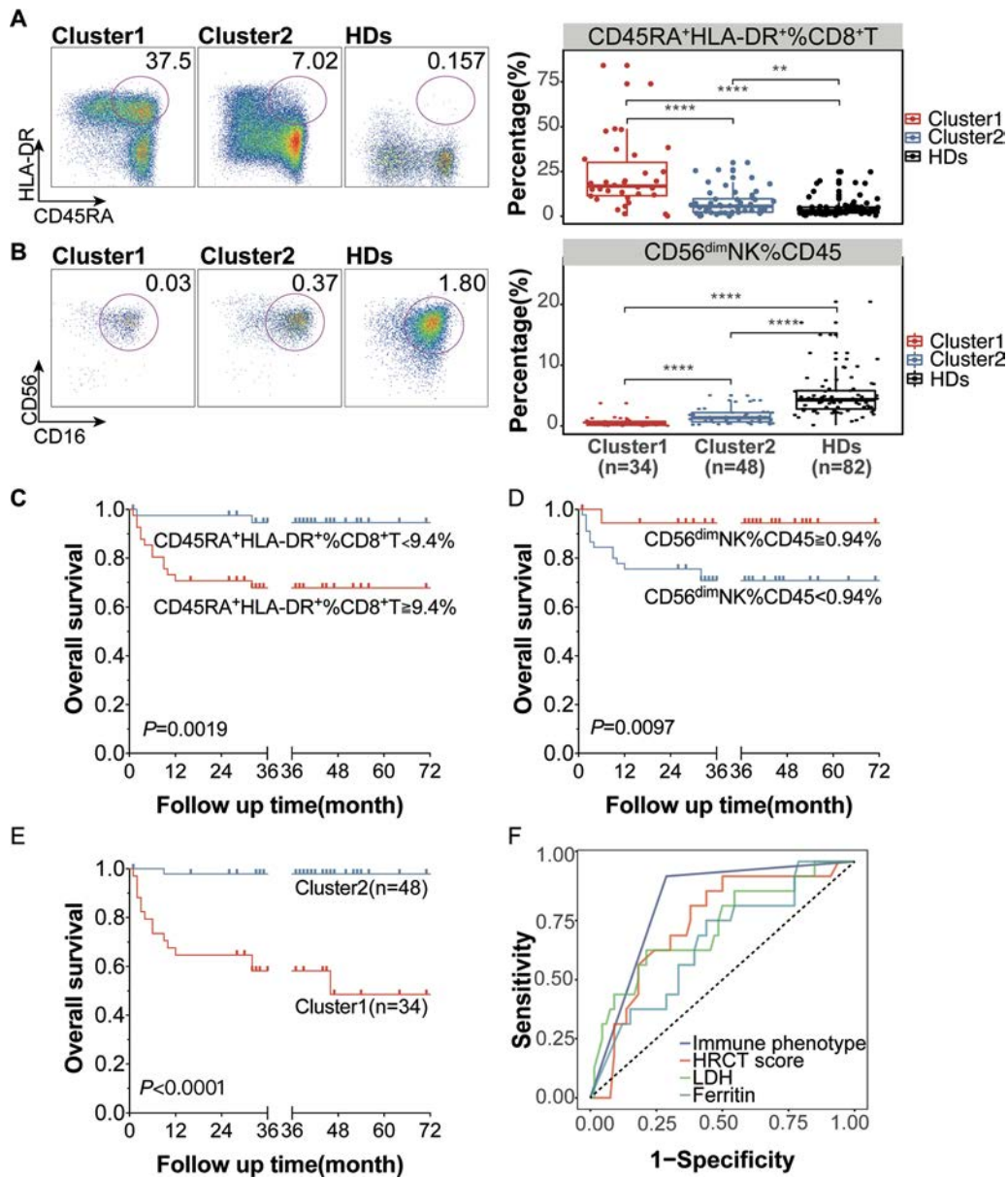


**Figure 4.** Distinct prominent immune subsets might affect the prognosis of ADM-ILD patients. **A** and **B**, Flow cytometric analysis of CD45RA+HLA-DR+CD8+ T cells and CD56<sup>dim</sup> NK cells from cluster 1 and cluster 2 ADM-ILD patients and healthy donors, and the percentage of the indicated cell populations. Statistical analysis was performed using Wilcoxon's unpaired signed rank tests. Data are shown as box plots. Each box represents the range of values. Lines inside the boxes represent the mean. Lines outside the boxes represent the minimum and maximum. \*\* =  $P < 0.01$ ; \*\*\*\* =  $P < 0.0001$ . **C–E**, Prognostic significance of the subsets of CD45RA+HLA-DR+CD8+ T cells (**C**) and CD56<sup>dim</sup> NK cells (**D**) per cluster, as well as both cell subsets combined in cluster 1 and cluster 2 (**E**), in predicting the risk of mortality in ADM-ILD patients. Kaplan-Meier analysis of overall survival was estimated using the log rank test. Patients were classified into 2 groups according to Youden's index to achieve the optimal cutoffs. **F**, Receiver operating characteristics curve analysis with area under the curves determined in univariate Cox proportional hazards regression models for the sensitivity and specificity of immunophenotyping and different clinical parameters. HRCT = high-resolution computed tomography; LDH = lactate dehydrogenase (see Figure 1 for other definitions). Color figure can be viewed in the online issue, which is available at <http://onlinelibrary.wiley.com/doi/10.1002/art.42264/abstract>.

a higher neutrophil:lymphocyte ratio, higher levels of serum LDH, ferritin, and KL-6, and a higher HRCT score, all of which were associated with unfavorable clinical outcomes in ADM-ILD patients (3,19,20). As shown in Table 1, there were no significant differences in sex, age, clinical features, and other laboratory findings between the 2 clusters. Regarding pulmonary function testing (PFT), 13 patients in cluster 1 were unable to perform

the PFT due to poor respiratory condition, while only 1 patient in cluster 2 could not perform it. In those who had PFT data, patients in cluster 1 had significantly lower diffusing capacity of lung carbon monoxide percent predicted compared to those in cluster 2 (median 54% [IQR 44.95–75.38%] versus 63.6% [IQR 54–85.5%];  $P = 0.03$ ), while there was no significant difference in forced vital capacity percent predicted between the 2 groups

**Table 2.** Univariate and multivariate analysis of the risk of mortality according to immunophenotypes and per-unit change in clinical parameters using Cox proportional hazards regression models\*

Characteristic	Per unit for HR	Univariate analysis		Multivariate analysis	
		HR (95% CI)	<i>P</i>	HR (95% CI)	<i>P</i>
Immunophenotype	Cluster 1	26.815 (3.535–203.401)	0.002	19.222 (2.350–156.900)	0.006
HRCT score	5	1.017 (1.006–1.028)	0.003	1.011 (0.999–1.023)	0.082
LDH	1 unit/liter	1.002 (1.001–1.004)	0.011	1.001 (0.999–1.003)	0.460
Ferritin	1 ng/ml	1.000 (1.000–1.002)	0.039	1.000 (0.999–1.001)	0.900
KL-6	1 unit/ml	1.000 (1.000–1.000)	0.054	–	–
CRP	1 mg/liter	1.041 (0.999–1.085)	0.057	–	–
ANA positivity	≥1:80	0.392 (0.111–1.377)	0.140	–	–
Age	1 year	1.038 (0.984–1.094)	0.170	–	–
Sex	Male	0.555 (0.158–1.951)	0.360	–	–
ALT	1 unit/liter	1.003 (0.997–1.008)	0.400	–	–
AST	1 unit/liter	1.002 (0.997–1.008)	0.500	–	–
Neutrophil:lymphocyte ratio	1 liter	1.018 (0.965–1.074)	0.510	–	–
ESR	1 mm/hour	1.005 (0.984–1.027)	0.630	–	–
CK	1 unit/liter	1.000 (0.999–1.000)	0.800	–	–

\* HR = hazard ratio; 95% CI = 95% confidence interval (see Table 1 for other definitions).

(median 67.55% [IQR 61.22–75.45%]) versus 68.1% [IQR 59.4–77.15%]; *P* = 0.958).

Of the 34 patients in cluster 1, 15 patients died. Most of them (*n* = 12; 80%) died within 1 year after diagnosis due to respiratory failure. The other 3 patients died after 1 year because of opportunistic infections and other reasons. To further explore the factors that were associated with survival in cluster 1, we compared various clinical features in survivors and nonsurvivors. There were no significant differences in terms of rashes, laboratory findings including levels of LDH, ferritin, KL-6, erythrocyte sedimentation rate, CRP, or neutrophil:lymphocyte ratio, or treatment regimens. As RPILD is closely associated with mortality, all nonsurvivors had RPILD and only 26% of survivors had RPILD (Supplementary Table 3, <https://onlinelibrary.wiley.com/doi/10.1002/art.42264>).

No obvious differences were observed between the clusters except for the maximum dose of glucocorticoids (GCs). The GC dose in cluster 1 was higher than in cluster 2 (median 75 mg/day [range 50–95 mg/day] in cluster 1; median 50 mg/day [range 30–85 mg/day] in cluster 2; *P* = 0.026), suggesting that the patients in cluster 1 had more severe disease requiring higher doses of GCs. Nine patients in our cohort were treatment-naïve. We then compared these naïve patients to healthy donors and to treated patients and found that there were obvious differences between treatment-naïve ADM patients and healthy donors, but we observed a similar trend between treatment-naïve ADM patients and treated ADM patients (Supplementary Figures 4A and B, <https://onlinelibrary.wiley.com/doi/10.1002/art.42264>). Further, according to subgroup dimensionality reduction, we observed little difference between untreated patients and treated patients (Supplementary Figure 4C).

**Using immunophenotypes to predict 1-year survival in ADM-ILD patients.** The frequencies of CD45RA+HLA-DR+CD8+ T cells and CD56<sup>dim</sup>NK cells were

significantly different between cluster 1 and cluster 2. The percentage of CD45RA+HLA-DR+CD8+ T cells in cluster 1 was obviously higher than that in cluster 2 and in healthy donors (mean ± SD 22.70 ± 19.48% in cluster 1; 7.766 ± 7.27% in cluster 2; 4.785 ± 5.22% in healthy donors) (Figure 4A). Moreover, we used flow cytometry to identify CD45RA+HLA-DR+CD8+ T cells, for which the typical immunophenotype was CCR7–CD27–CD45RA+CD127<sup>lo</sup>. Therefore, we defined this CD8+ T cell subpopulation as terminal effector memory T (TEMRA) cells (Supplementary Figure 5, <https://onlinelibrary.wiley.com/doi/10.1002/art.42264>). Correspondingly, the percentage of CD56<sup>dim</sup> NK cells in cluster 2 was higher than in cluster 1, but lower than in healthy donors (mean ± SD 0.57 ± 0.71% in cluster 1; 1.66 ± 1.33% in cluster 2; 5.75 ± 6.13% in healthy donors) (Figure 4B).

The optimal cutoff values for the frequency of CD45RA+HLA-DR+CD8+ T cells and CD56<sup>dim</sup> NK cells were 9.4% and 0.94%, respectively. We found that patients with a higher proportion (≥9.4%) of CD45RA+HLA-DR+CD8+ T cells had significantly worse prognosis, in terms of 1-year mortality, than those with a lower proportion (<9.4%) (*P* = 0.0019 by log rank test) (Figure 4C). Patients with a higher proportion (≥0.94%) of CD56<sup>dim</sup> NK cells had better outcomes compared with patients with a lower proportion (<0.94%) (*P* = 0.0097 by log rank test) (Figure 4D). Considering all these factors, cluster 1 identified a subgroup of ADM-ILD patients with a poorer prognosis than patients in cluster 2 regarding 1-year survival (58.82% versus 97.92%; *P* < 0.0001 by log rank test) (Figure 4E).

To verify the clinical utility of immunophenotypes in predicting prognosis, we performed a multivariable analysis, which revealed that the immunophenotype for cluster 1 was the most relevant factor associated with mortality (HR 9.636, *P* = 0.03644), when comparing current clinical parameters (Table 2). The receiver operating characteristic curve analysis showed that the AUC for immunophenotype (AUC 0.8248) was better than HRCT score



(AUC 0.7363), LDH level (AUC 0.7206), and ferritin level (AUC 0.6558) (Figure 4F).

## DISCUSSION

To our knowledge, this is the first study to identify the peripheral immunologic signatures in patients with ADM-ILD. Using machine learning approaches, ADM-ILD patients could be stratified into 2 clusters. Of note, cluster 1, which was the activated T cell–dominant cluster, showed a higher prevalence of RPILD and a lower 1-year survival rate (58.82%). In contrast, cluster 2, the nonactivated T cell–dominant cluster, displayed better clinical outcomes, with a 97.92% 1-year survival rate. These findings improve our understanding of ADM-ILD immunopathology and suggest that immune cell profiles can potentially predict the clinical outcome and guide future treatment. The current immunophenotyping performed better than existing clinical parameters to predict a patient's prognosis. Although the anti-MDA-5 antibody is considered closely associated with RPILD, our data showed that the presence of this antibody did not fully predict the prognosis. In our cohort, 95% of the patients had positive anti-MDA-5 antibody test results, yet the patients were divided into 2 groups with opposite clinical outcomes.

Cluster 1 had higher serum levels of ferritin, LDH, and KL-6 and higher HRCT scores than cluster 2, which heralded worse clinical outcomes. In our prior cohort study, we generated a FLAIR score to stratify ADM-ILD patients into low-, medium-, and high-risk groups (3). We found that most patients in cluster 1 (85.2%) fell into high- or medium-risk groups stratified by FLAIR scores, and these subgroups of patients (cluster 1 plus high- or medium-risk group according to FLAIR score) were at particular risk of poor outcomes in the follow-up period (Supplementary Figure 6, <https://onlinelibrary.wiley.com/doi/10.1002/art.42264>). We believe that combination of immunologic biomarkers with existing clinical parameters could enhance the clinical utility of immunophenotyping and improve individualized treatment. Patients with the cluster 1 immune signature require more intense monitoring and active treatment, whereas, in patients with the cluster 2 immune signature, overtreatment must be avoided.

The roles of CD4+ T lymphocytes in DM have been widely studied and are well recognized. Emerging evidence also suggests that CD8+ T cells play a critical role in the induction, progression, and pathogenesis of autoimmune diseases (21). Among cluster 1 patients, we observed predominant active T cell immune signatures with a remarkable elevated frequency of CD45RA+HLA-DR+CD8+ T cells, CD45RA+HLA-DR+ Th cells, and HLA-DR+ Th cells. In particular, the frequency of CD45RA+HLA-DR+CD8+ T cells, identified as active TEMRA CD8+T cells exhibiting the CD45RA+CCR7- phenotype, were increased the most and were closely related to a poor prognosis. This CD8+ T cell subset has long been considered a hallmark of immune senescence and is associated with aging and patients

with chronic viral infections, specifically, cytomegalovirus (22,23). Recently, Houtman et al confirmed that CD8+ T cells represent a major divergence between PM and DM patients (MDA-5+ DM included) compared with CD4+ T cells by T cell transcriptomics, emphasizing the role of CD8+ T cells in DM (24).

There are several hypotheses for the correlation between activated TEMRA CD8+ T cells and disease severity or RPILD in ADM. First, similar immunophenotypes are seen in COVID-19 with activation of adaptive immune cells and elevated frequencies of CD8+ T cells (25), including effector TEMRA cells, suggesting that COVID-19 and ADM might share some similar immunologic signatures. Consistent with this hypothesis, a common pathogenic link may underlie the remarkable similarities between anti-MDA-5-associated RPILD and lung disease in COVID-19 (26). These findings may suggest that certain viruses trigger terminal effector differentiation and TEMRA cell formation in ADM-RPILD. Second, expansion of TEMRA CD8+ T cells has been documented in patients with lupus, Sjögren's syndrome, and antineutrophil cytoplasmic antibody-associated vasculitis (27–30). This cell subset has a high cytotoxic potential, reflected in the strong expression of perforin and granzyme B, which may be implicated in tissue damage that manifests clinically as RPILD (29,31).

Third, most patients in this study received treatments targeting T cells, such as calcineurin inhibitors, cyclosporin A, and tacrolimus. Broad T cell depletion may be followed by immune system reconstitution that paradoxically expands the highly differentiated pathogenic TEMRA cell populations after preferential depletion of naive and central memory T cells (32,33). This means that, for some patients, current conventional immunosuppressive drugs fail to prevent an increase in TEMRA CD8+T cells (29,31). The lack of TEMRA CD8+ T cell-specific target therapeutics could partially explain why patients are resistant to current treatments. In addition to CD45RA+HLA-DR+CD8+ T cells, our data showed that the percentage of CD56<sup>dim</sup> NK cells also contributed strongly to differentiating the clusters. There was a negative association between CD56<sup>dim</sup> NK cell percentage and disease activity (34). NK cells are innate effector lymphocytes that are typically divided into cytokine-producing CD56<sup>bright</sup> NK cells and cytotoxic CD56<sup>dim</sup> NK cells (35). Consistent with our findings, Thom et al reported decreased NK cell percentages in the blood of juvenile DM patients, and NK cells trended toward normalization with the cessation of active disease (34). The loss of circulating CD56<sup>dim</sup> NK cells was also reported in SLE, which can be attributed to activation-induced cell death mediated by interferon- $\alpha$  and chemotaxis to inflamed tissue (36,37). Therefore, we hypothesize that CD56<sup>dim</sup> NK cell loss in ADM-ILD, especially in cluster 1, could be due to apoptosis or the migration from peripheral blood to local tissue causing lung injury, indicating the possibility that NK cells play an immunoregulatory role in ADM-ILD.

There were 4 anti-MDA-5–negative patients in the study. We compared the clinical features as well as immune cell subsets between ADM patients positive for and those negative for

anti-MDA-5 in the same cluster and found very few differences between the 2 groups. If we removed the 4 anti-MDA-5-negative patients, the current results and conclusion remained similar. Even though the number is low, the anti-MDA-5-negative ADM samples may represent a neglected but important small patient population that warrants further study. After all, ADM is a well-accepted subtype of idiopathic inflammatory myopathy in the classification criteria at this point (2) and is still widely used in clinical settings, especially in places that lack easy and timely access to myositis autoantibody examinations. Therefore, this early finding could provide valuable information for clinicians to manage patients with severe ADM-ILD.

There are limitations to our study. First, despite the fact that immunophenotyping performed well in our study, external validation in large samples is still needed to confirm our findings. We hope that external validation can further define the boundary value of the most relevant single indicator with reliability and repeatability, making the data robust. Second, it is challenging to recruit treatment-naive ADM patients because of disease rarity. The current results might be influenced by the preexisting treatment. Third, the roles of TEMRA CD8+ T cells and CD56<sup>dim</sup> NK cells in ADM-ILD have not been explored extensively. Future studies should focus on the functions of these cell subsets and clarify their contribution to the disease.

In summary, our results showed that peripheral immune cell subsets have the potential to stratify ADM-ILD patients with different outcomes beyond clinical manifestations into immunologic clusters, which may have implications for clinical monitoring, individualized therapy, and pathogenesis investigation. Further studies are needed to explore the previously ignored role of the TEMRA CD8+ T cell and CD56<sup>dim</sup> NK cell subsets in the pathogenesis of ADM-ILD.

## AUTHOR CONTRIBUTIONS

All authors were involved in drafting the article or revising it critically for important intellectual content, and all authors approved the final version to be published. Dr. Xiaoming Zhang had full access to all of the data in the study and takes responsibility for the integrity of the data and the accuracy of the data analysis.

**Study conception and design.** Y. Ye, Ma, Bao, S. Ye, Guo, Fu, Xiaoming Zhang.

**Acquisition of data.** Y. Ye, Li, Ran Wang, Wu, Shen, Fu, Xiaoming Zhang.

**Analysis and interpretation of data.** Y. Ye, Xueliang Zhang, Runci Wang, Fu, Xiaoming Zhang.

## REFERENCES

- Selva-O'Callaghan A, Pinal-Fernandez I, Trallero-Araguás E, et al. Classification and management of adult inflammatory myopathies. *Lancet Neurol* 2018;17:816–28.
- Lundberg IE, Tjärnlund A, Bottai M, et al. 2017 European League Against Rheumatism/American College of Rheumatology classification criteria for adult and juvenile idiopathic inflammatory myopathies and their major subgroups. *Arthritis Rheumatol* 2017;69:2271–82.
- Lian X, Zou J, Guo Q, et al. Mortality risk prediction in amyopathic dermatomyositis associated with interstitial lung disease: the FLAIR model. *Chest* 2020;158:1535–45.
- Moghadam-Kia S, Oddis CV, Sato S, et al. Anti-melanoma differentiation-associated gene 5 is associated with rapidly progressive lung disease and poor survival in US patients with amyopathic and myopathic dermatomyositis. *Arthritis Care Res (Hoboken)* 2016; 68:689–94.
- Motegi SI, Sekiguchi A, Toki S, et al. Clinical features and poor prognostic factors of anti-melanoma differentiation-associated gene 5 antibody-positive dermatomyositis with rapid progressive interstitial lung disease. *Eur J Dermatol* 2019;29:511–7.
- Koga T, Fujikawa K, Horai Y, et al. The diagnostic utility of anti-melanoma differentiation-associated gene 5 antibody testing for predicting the prognosis of Japanese patients with DM. *Rheumatology (Oxford)* 2012;51:1278–84.
- Sato S, Hoshino K, Satoh T, et al. RNA helicase encoded by melanoma differentiation-associated gene 5 is a major autoantigen in patients with clinically amyopathic dermatomyositis: association with rapidly progressive interstitial lung disease. *Arthritis Rheum* 2009;60: 2193–200.
- Ye S, Chen XX, Lu XY, et al. Adult clinically amyopathic dermatomyositis with rapid progressive interstitial lung disease: a retrospective cohort study. *Clin Rheumatol* 2007;26:1647–54.
- Mukae H, Ishimoto H, Sakamoto N, et al. Clinical differences between interstitial lung disease associated with clinically amyopathic dermatomyositis and classic dermatomyositis. *Chest* 2009;136:1341–7.
- Huang K, Vinik O, Shojania K, et al. Clinical spectrum and therapeutics in Canadian patients with anti-melanoma differentiation-associated gene 5 (MDA5)-positive dermatomyositis: a case-based review. *Rheumatol Int* 2019;39:1971–81.
- Hsu CY, Ko CH, Wang JL, et al. Comparing the burdens of opportunistic infections among patients with systemic rheumatic diseases: a nationally representative cohort study. *Arthritis Res Ther* 2019; 21:211.
- Wu W, Xu W, Sun W, et al. Forced vital capacity predicts the survival of interstitial lung disease in anti-MDA5 positive dermatomyositis: a multi-centre cohort study. *Rheumatology (Oxford)* 2021;61:230–9.
- Gono T, Masui K, Nishina N, et al. Risk prediction modeling based on a combination of initial serum biomarker levels in polymyositis/dermatomyositis-associated interstitial lung disease. *Arthritis Rheumatol* 2021;73:677–86.
- Nakashima R, Imura Y, Kobayashi S, et al. The RIG-I-like receptor IFIH1/MDA5 is a dermatomyositis-specific autoantigen identified by the anti-CADM-140 antibody. *Rheumatology (Oxford)* 2010;49: 433–40.
- Mimori T, Nakashima R, Hosono Y. Interstitial lung disease in myositis: clinical subsets, biomarkers, and treatment. *Curr Rheumatol Rep* 2012;14:264–74.
- Sontheimer RD. Would a new name hasten the acceptance of amyopathic dermatomyositis (dermatomyositis sine myositis) as a distinctive subset within the idiopathic inflammatory dermatomyopathies spectrum of clinical illness? *J Am Acad Dermatol* 2002;46:626–36.
- Sato S, Hirakata M, Kuwana M, et al. Autoantibodies to a 140-kd polypeptide, CADM-140, in Japanese patients with clinically amyopathic dermatomyositis. *Arthritis Rheum* 2005;52:1571–6.
- Liu M, Liu J, Zhang X, et al. Activation status of CD56(dim) natural killer cells is associated with disease activity of patients with systemic lupus erythematosus. *Clin Rheumatol* 2021;40:1103–12.
- Ye Y, Fu Q, Wang R, et al. Serum KL-6 level is a prognostic marker in patients with anti-MDA5 antibody-positive dermatomyositis associated with interstitial lung disease. *J Clin Lab Anal* 2019;33:e22978.

20. Zou J, Guo Q, Chi J, et al. HRCT score and serum ferritin level are factors associated to the 1-year mortality of acute interstitial lung disease in clinically amyopathic dermatomyositis patients. *Clin Rheumatol* 2015;34:707–14.
21. Gravano DM, Hoyer KK. Promotion and prevention of autoimmune disease by CD8+ T cells. *J Autoimmun* 2013;45:68–79.
22. Kumar BV, Connors TJ, Farber DL. Human T cell development, localization, and function throughout life. *Immunity* 2018;48:202–13.
23. Wertheimer AM, Bennett MS, Park B, et al. Aging and cytomegalovirus infection differentially and jointly affect distinct circulating T cell subsets in humans. *J Immunol* 2014;192:2143–55.
24. Houtman M, Ekholm L, Hesselberg E, et al. T-cell transcriptomics from peripheral blood highlights differences between polymyositis and dermatomyositis patients. *Arthritis Res Ther* 2018;20:188.
25. Mann ER, Menon M, Knight SB, et al. Longitudinal immune profiling reveals key myeloid signatures associated with COVID-19. *Sci Immunol* 2020;5:eabd6197.
26. Saud A, Naveen R, Aggarwal R, et al. COVID-19 and myositis: what we know so far. *Curr Rheumatol Rep* 2021;23:63.
27. McKinney EF, Lee JC, Jayne DR, et al. T-cell exhaustion, co-stimulation and clinical outcome in autoimmunity and infection. *Nature* 2015;523:612–6.
28. McKinney EF, Lyons PA, Carr EJ, et al. A CD8+ T cell transcription signature predicts prognosis in autoimmune disease. *Nat Med* 2010;16:586–91.
29. Néel A, Bucchia M, Néel M, et al. Dampening of CD8+ T cell response by B cell depletion therapy in antineutrophil cytoplasmic antibody-associated vasculitis. *Arthritis Rheumatol* 2019;71:641–50.
30. Tasaki S, Suzuki K, Nishikawa A, et al. Multiomic disease signatures converge to cytotoxic CD8 T cells in primary Sjogren's syndrome. *Ann Rheum Dis* 2017;76:1458–66.
31. Jacquemont L, Tilly G, Yap M, et al. Terminally differentiated effector memory CD8(+) T cells identify kidney transplant recipients at high risk of graft failure. *J Am Soc Nephrol* 2020;31:876–91.
32. Greenberg SA, Pinkus JL, Kong SW, et al. Highly differentiated cytotoxic T cells in inclusion body myositis. *Brain* 2019;142:2590–604.
33. Wu Z, Bensinger SJ, Zhang J, et al. Homeostatic proliferation is a barrier to transplantation tolerance. *Nat Med* 2004;10:87–92.
34. Throm AA, Alinger JB, Pingel JT, et al. Dysregulated NK cell PLCγ2 signaling and activity in juvenile dermatomyositis. *JCI Insight* 2018;3:e123236.
35. Vivier E, Tomasello E, Baratin M, et al. Functions of natural killer cells. *Nat Immunol* 2008;9:503–10.
36. Liu M, Liang S, Zhang C. NK cells in autoimmune diseases: protective or pathogenic? *Front Immunol* 2021;12:624687.
37. Huang Z, Fu B, Zheng SG, et al. Involvement of CD226+ NK cells in immunopathogenesis of systemic lupus erythematosus. *J Immunol* 2011;186:3421–31.

# Recombinant Zoster Vaccine Uptake and Risk of Flares Among Older Adults With Immune-Mediated Inflammatory Diseases in the US

Jessica Leung,<sup>1</sup>  Tara C. Anderson,<sup>1</sup> Kathleen Dooling,<sup>1</sup> Fenglong Xie,<sup>2</sup> and Jeffrey R. Curtis<sup>2</sup> 

**Objective.** Persons with immune-mediated inflammatory diseases (IMIDs) are at an increased risk of herpes zoster (HZ). In 2018, the Centers for Disease Control and Prevention recommended a highly efficacious vaccine, recombinant zoster vaccine (RZV), for prevention of HZ in immunocompetent patients  $\geq 50$  years of age. This study was undertaken to estimate RZV vaccination among adults ages  $\geq 50$  years with IMIDs during 2018–2019 and to examine possible vaccine-related flares following RZV.

**Methods.** We identified a cohort of IMID patients using medical claims data from the IBM MarketScan (ages 50–64 years) and Centers for Medicare and Medicaid Services Medicare (ages  $\geq 65$  years) databases. Presumed flares were defined as hospitalization/emergency department visit for their respective IMIDs, or steroid treatment with a short-acting oral glucocorticoid or parenteral glucocorticoid injection. We conducted a self-controlled case series (SCCS) analysis to examine a temporal association between RZV and flares.

**Results.** Among enrollees with IMIDs, 14.8% of 55,654 MarketScan enrollees and 43.2% of 160,545 Medicare enrollees received  $\geq 1$  dose of RZV in 2018–2019. Two-dose series completion rates were 76.6% in MarketScan enrollees and 85.4% in Medicare enrollees. In the SCCS analysis, 10% and 13% developed flares in the control window, compared to 9% and 11–12% in the risk window following 1 or 2 doses of RZV among MarketScan and Medicare enrollees, respectively. We found no statistically significant increase in flares following RZV administration for any IMID in either age group following RZV dose 1 or dose 2.

**Conclusion.** We did not find an increase in presumed flares following RZV vaccination. Among adults ages  $\geq 50$  years with IMIDs, a substantial proportion received RZV compared to general zoster coverage estimates, and series completion rates were high.

## INTRODUCTION

Herpes zoster (HZ) causes a significant public health burden, and an estimated 1 million cases occurred in the US annually during the prevaccine era (1). Since October 2017, recombinant zoster vaccine (RZV; Shingrix) has been licensed in the US for prevention of HZ for adults ages  $\geq 50$  years by the US Food and Drug Administration and recommended for immunocompetent adults ages  $\geq 50$  years by the Advisory Committee on Immunization Practices (ACIP). RZV is recommended as a 2-dose vaccine series separated by 2–6 months (2). Zoster vaccine uptake in

the general US population has grown appreciably over time. In 2018, coverage with either zoster vaccine live (ZVL) or RZV was 24.1% among adults ages  $\geq 50$  years and 2.4% with self-reported RZV vaccination (3). Coverage with ZVL or RZV reached 41% in 2019 (4). In October 2021, the ACIP recommended RZV for the prevention of HZ and related complications in adults ages  $\geq 19$  years who are or will be immunodeficient or immunosuppressed because of disease or therapy (5).

Increasing age and immunocompromised status are known risk factors for HZ. Persons with immune-mediated inflammatory diseases (IMIDs) are at increased risk of HZ and related

---

The findings and conclusions in this report are those of the authors and do not necessarily represent the official position of the Centers for Disease Control and Prevention and the US Department of Health and Human Services.

Dr. Curtis's work was supported by the NIH (award P30-AR-072583).

<sup>1</sup>Jessica Leung, MPH, Tara C. Anderson, DVM, MPH, PhD, Kathleen Dooling, MD, MPH: Division of Viral Diseases, National Center for Immunization and Respiratory Diseases, Centers for Disease Control and Prevention, Atlanta, Georgia; <sup>2</sup>Fenglong Xie, PhD, Jeffrey R. Curtis, MD, MS, MPH: Division

of Clinical Immunology and Rheumatology, University of Alabama at Birmingham.

Author disclosures are available at <https://onlinelibrary.wiley.com/action/downloadSupplement?doi=10.1002%2Fart.42261&file=art42261-sup-0001-Disclosureform.pdf>.

Address correspondence via email to Jessica Leung, MPH at [jleung@cdc.gov](mailto:jleung@cdc.gov).

Submitted for publication January 24, 2022; accepted in revised form June 2, 2022.

complications, including postherpetic neuralgia (6–12). One study showed that the age-specific incidence rate of HZ in patients with rheumatoid arthritis (RA) and systemic lupus erythematosus (SLE) in those ages  $\geq 40$  years was  $\sim 2$  times more than older (age 61–70 years) healthy adults (11). Additionally, immunosuppressive treatments may contribute to the increased risk and are highly variable in the HZ risk they confer (13). For example, JAK inhibitors approximately double HZ risk, and glucocorticoids may further double that risk (13,14). HZ vaccination has been recommended for certain groups of patients with RA, inflammatory bowel disease (IBD), and psoriasis (PsO) by professional organizations including the American College of Rheumatology, the American College of Gastroenterology, and the Medical Board of the National Psoriasis Foundation for persons  $\geq 50$  years of age and also those  $< 50$  years of age for select groups with PsO (15–17).

RZV contains a novel adjuvant (AS01<sub>B</sub>) and causes substantial systemic immune activation, and thus there is a theoretical risk that RZV may lead to a flare of a person's IMID in this population of vaccine recipients. Vaccine uptake is largely unknown in IMID populations, but concern for disease flare may prove an impediment to effective vaccination strategies for patients with these conditions. Due to this evidence gap, we evaluated vaccine uptake using 2 national US data sources and then conducted a self-controlled case series analysis (SCCS), a commonly used study design in vaccine evaluation studies, to investigate whether a temporal association exists between RZV administration and disease flares in older adults with IMIDs.

## MATERIALS AND METHODS

**Study design.** We used a retrospective cohort design to estimate RZV coverage among persons ages  $\geq 50$  years during 2018–2019. We described characteristics of those who were vaccinated, prescriber information, place of vaccination, and whether they received pneumococcal or influenza vaccination at the same visit. Among subjects who received only 1 dose of RZV, we examined whether there may have been missed opportunities for the second dose of RZV by examining whether they received another common adult vaccine (pneumococcal or influenza vaccine) but not their second dose of RZV.

We used a self-controlled risk interval study design, a subtype of the SCCS method, to evaluate the risk of flares following RZV vaccination in patients with IMID conditions (18–20). This method relies on studying the within-person temporal associations of the outcome (flares) among individuals with both the selected IMID and the exposure of interest (RZV). This study design utilizes prespecified risk and control windows within individuals to eliminate effects of time-invariant confounders. We compared the risk of flares during a 42-day risk window (1–42 days after RZV vaccination) versus a 42-day control window (98–140 days prior to RZV vaccination). We selected a control window further from RZV, as patients tend to be

healthier and less likely to have flares in the period right before vaccination. This study design includes only patients who had IMIDs and received RZV during the study.

**Data sources and study population.** We analyzed health claims from 2 sources, including the 2017–2019 IBM MarketScan commercial databases and the 2017–2020 Centers for Medicare and Medicaid Services (CMS) Medicare databases. From the MarketScan databases, we included all persons who were 50–64 years of age during the study period for whom outpatient pharmaceutical claims data were available (patients covered by employer-sponsored insurance each year from all US states). From the CMS Medicare database, we included all persons ages  $\geq 65$  years during the study period with enrollment in Medicare Parts A (hospital insurance), B (outpatient medical insurance), and D (prescription drug coverage). Beneficiaries were not eligible for the study if they were enrolled in Medicare Part C (managed care plan), as all claims data may not be available for this population. Individuals included in the analysis had to be enrolled from 5 months (20 weeks) before RZV through 42 days after RZV. We excluded persons with a history of malignancy, HIV, or organ transplant in the 0–20 weeks before RZV vaccination. This study was deemed by the Centers for Disease Control and Prevention (CDC) not to be human subject research, and the study did not require CDC Institutional Review Board approval.

**Study definitions.** *IMIDs.* The following populations with IMIDs were included in the analysis: RA, ankylosing spondylitis (AS), axial spondyloarthritis (axSpA), psoriatic arthritis (PsA), PsO, IBD, Crohn's disease (CD), ulcerative colitis (UC), and SLE. IMIDs were defined as fulfilling all 3 of the following criteria: 1)  $\geq 2$  outpatient visits for their respective conditions within 365 days and separated by  $> 7$  days; 2)  $\geq 1$  claim for disease-specific medications within 365 days of the first visit for the condition detected during the study period; and 3)  $\geq 1$  visit to a relevant specialist (rheumatologist for RA, AS, axSpA, PsA, SLE; gastroenterologist for IBD, CD, UC; dermatologist for PsO) for their IMID condition. Participants may have been included in multiple IMID condition populations. Diagnostic codes, specialty codes, and disease-specific medications used to define conditions are shown in Supplementary Table 1, available on the *Arthritis & Rheumatology* website at <https://onlinelibrary.wiley.com/doi/10.1002/art.42261>.

*Vaccinations and flares.* Since vaccinations are reimbursable health care procedures, RZV, pneumococcal, and influenza vaccination were defined using the National Drug Code (NDC) and Current Procedural Terminology codes (Supplementary Table 1). Information on prescribers and pharmacies were available for RZV vaccinations identified using NDC codes. Presumed flares were defined as any the following: 1) hospitalization or emergency department (ED) visit for the IMID condition, with the IMID diagnosis coded in the primary position of the hospital or ED claim; 2) treatment with a short-acting oral glucocorticoid (e.g., methylprednisolone 6-day dosing pack); or

**Table 1.** RZV 1- and 2-dose vaccination in persons with IMIDs in 2018–2019\*

IMID	MarketScan (ages 50–64 years; n = 55,654)			CMS Medicare (ages ≥65 years; n = 160,545)		
	Total no.	≥1 dose, no. (%)	2-dose completion (%)†	Total no.	≥1 dose, no. (%)	2-dose completion (%)†
RA	22,631	3,898 (17.2)	76.0	89,498	43,730 (48.9)	85.1
AS	1,049	182 (17.3)	74.4	106	67 (63.2)	84.1
AxSpA	1,305	239 (18.3)	74.0	129	54 (63.6)	83.3
PsA	6,991	1,144 (16.4)	76.8	15,845	6,448 (40.7)	85.5
PsO	10,323	1,198 (11.6)	75.7	23,495	5,907 (25.1)	85.0
IBD	13,013	1,693 (13.0)	78.8	31,097	12,012 (38.6)	87.3
CD	5,322	682 (12.8)	77.4	13,086	5,094 (38.9)	86.8
UC	7,764	1,045 (13.5)	80.3	18,321	7,024 (38.3)	87.7
SLE	4,482	576 (12.9)	75.4	8,746	4,022 (46.0)	84.3
Any	55,654	8,251 (14.8)	76.6	160,545	69,345 (43.2)	85.4

\* Data sources included the 2017–2019 IBM MarketScan commercial databases and the 2017–2019 Centers for Medicare and Medicaid Services (CMS) Medicare databases. IMIDs = immune-mediated inflammatory diseases; RA = rheumatoid arthritis; AS = ankylosing spondylitis; axSpA = axial spondyloarthritis; PsA = psoriatic arthritis; PsO = psoriasis; IBD = inflammatory bowel disease; CD = Crohn’s disease; UC = ulcerative colitis; SLE = systemic lupus erythematosus.

† Recombinant zoster vaccine (RZV) 2-dose series completion within 6 months of receipt of their first dose among 5,048 persons ages 50–64 years and 44,253 persons ages ≥65 years who received their first dose before July 1, 2019.

3) any parenteral glucocorticoid injection. If any of these 3 criteria were fulfilled, then this was considered a presumed flare.

**Statistical analysis.** We used SCCS methods to compare the rates of flares in the 6 weeks after each administered dose of RZV (risk window, 1–42 days following vaccination) as compared to a 6-week period (control window, 98–140 days prior to RZV vaccination) within individuals. We used conditional Poisson regression to compare rates and proportion of visits in

risk versus control periods. Data were analyzed using SAS 9.4 statistical software. The Genmod procedure was used to calculate relative incidence, 95% confidence intervals, and *P* values. Chi-square tests were used to compare whether there was a possible association between a flare after the first dose and second dose of RZV among participants who received their first dose of RZV with ≥6 months follow-up time. We also evaluated whether a flare had any impact on the likelihood to receive the second RZV dose.

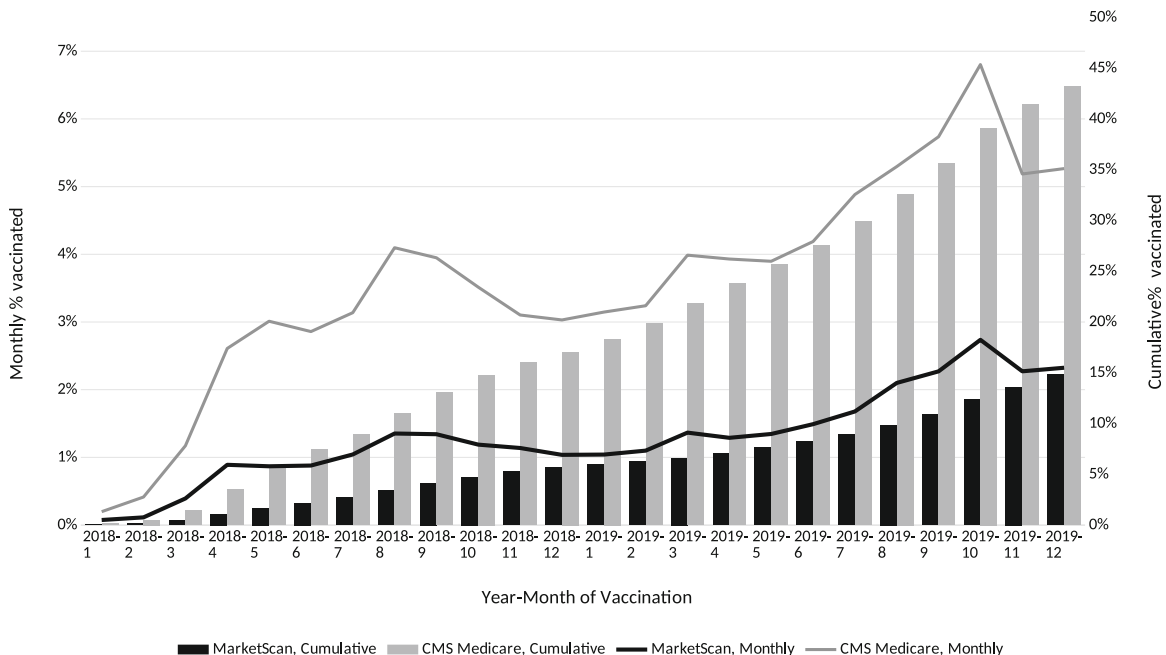


**Figure 1.** Monthly and cumulative frequencies of vaccination with the recombinant zoster vaccine by month and year of vaccination among persons with immune-mediated inflammatory diseases in the IBM MarketScan database (50–64 years of age) and the Centers for Medicare and Medicaid Services (CMS) database (≥65 years of age) in 2018–2019.

**Table 2.** Characteristics of the IMiD patients ages ≥50 years who received ≥1 dose of RZV\*

	Any IMiD	RA	AS	AXSpA	PSA	PSO	IBD	CD	UC	SLE
MarketScan patients (ages 50–64 years)										
No. of patients	7,207	3,415	166	216	992	1,039	1,477	594	916	507
Age, median (IQR) years	59 (55–62)	59 (56–62)	58 (55–62)	58 (55–61)	59 (55–62)	59 (56–62)	59 (55–61)	58 (55–61)	59 (55–61)	58 (54–61)
Sex										
Male	31	21	60	56	42	42	45	43	46	8
Female	69	79	40	44	58	58	55	57	54	92
RZV										
≥1 dose, no.	7,207	3,415	166	216	992	1,039	1,477	594	916	507
≥2 doses, no. (% among patients who received ≥1 dose)	4,687 (65)	2,025 (59)	85 (51)	109 (50)	600 (60)	613 (59)	896 (61)	349 (59)	571 (62)	292 (58)
Interval between doses, median (IQR) days	91 (69–132)	89 (69–125)	90 (70–119)	88 (67–116)	85 (68–118)	91 (68–131)	87 (69–122)	85 (68–125)	88 (70–120)	91 (69–135)
Change in IMiD treatment†	4	5	0	0	6	3	2	2	2	6
Flare										
Control window (98–140 days before RZV)	10	13	11	13	10	7	7	8	7	10
Dose 1 risk window (1–42 days after dose 1)	9	11	10	11	12	8	7	9	7	9
Dose 2 risk window (1–42 days after dose 2)	9	11	8	8	10	9	8	8	7	10
CMS Medicare patients (ages ≥65 years)										
No. of patients	72,468	45,851	72	86	6,678	5,993	12,679	5,384	7,416	4,205
Age, median (IQR) years	73 (70–78)	74 (70–79)	73 (70–76)	73 (70–76)	72 (69–76)	73 (69–77)	73 (70–77)	73 (70–77)	73 (70–78)	72 (69–77)
Sex										
Male	30	25	68	62	40	43	44	42	45	12
Female	70	75	32	38	60	57	56	58	55	88
RZV										
≥1 dose, no.	72,468	45,851	72	86	6,678	5,993	12,679	5,384	7,416	4,205
≥2 doses, no. (% among patients who received ≥1 dose)	62,094 (86)	35,981 (78)	60 (83)	70 (81)	5,409 (81)	4,737 (79)	10,279 (81)	4,231 (80)	6,045 (82)	3,222 (77)
Interval between doses, median (IQR) days	96 (71–137)	96 (71–138)	94 (70–162)	110 (70–168)	96 (71–136)	95 (70–134)	95 (70–135)	96 (71–137)	94 (70–133)	97 (71–138)
Change in IMiD treatment†	4	4	0	1	3	1	3	2	3	12
Flare										
Control window (98–140 days before RZV)	13	14	10	13	13	10	9	11	9	11
Dose 1 risk window (1–42 days after dose 1)	12	13	11	12	13	10	9	10	9	11
Dose 2 risk window (1–42 days after dose 2)	11	13	13	14	12	9	9	11	8	12

\* Data sources included the 2017–2019 IBM MarketScan commercial databases and the 2017–2019 CMS Medicare databases. Except where indicated otherwise, values are the percentage. IQR = interquartile range (see Table 1 for other definitions).

† Proportion of patients who changed their treatment in the 6-month period after RZV from the treatment they were given in the 6-month period before receiving RZV.

**Table 3.** Self-controlled case series analysis of the risk of flares among the IMID patients ages  $\geq 50$  years after dose 1 or dose 2 of RZV\*

Group	Control window, no. of flares 98–140 days before RZV	Risk window, no. of flares 1–42 days after RZV	Risk ratio (95% CI)
MarketScan patients (ages 50–64 years)			
RA dose 1	448	364	0.8 (0.7–0.9)
RA dose 2	253	219	0.9 (0.7–1.0)
AS dose 1	18	17	0.9 (0.5–1.8)
AS dose 2	10	7	0.7 (0.3–1.8)
AxSpA dose 1	27	24	0.9 (0.5–1.5)
AxSpA dose 2	13	9	0.6 (0.3–1.6)
PsA dose 1	102	116	1.1 (0.9–1.5)
PsA dose 2	60	56	0.9 (0.6–1.3)
PsO dose 1	71	87	1.2 (0.9–1.7)
PsO dose 2	43	52	1.2 (0.8–1.8)
IBD dose 1	108	110	1.0 (0.8–1.3)
IBD dose 2	67	66	1.0 (0.7–1.4)
CD dose 1	50	53	1.1 (0.7–1.6)
CD dose 2	28	27	1.0 (0.6–1.6)
UC dose 1	60	62	1.0 (0.7–1.5)
UC dose 2	39	38	1.0 (0.6–1.5)
SLE dose 1	52	48	0.9 (0.6–1.4)
SLE dose 2	31	27	0.9 (0.5–1.5)
Any IMID dose 1	746	683	0.9 (0.8–1.0)
Any IMID dose 2	432	397	0.9 (0.8–1.1)
CMS Medicare patients (ages $\geq 65$ years)			
RA dose 1	6,362	6,020	0.9 (0.9–1.0)
RA dose 2	4,879	4,491	0.9 (0.9–1.0)
AS dose 1	<11	<11	1.1 (0.4–3.2)
AS dose 2	<11	<11	2.0 (0.6–6.6)
AxSpA dose 1	11	<11	0.9 (0.4–2.1)
AxSpA dose 2	<11	<11	1.7 (0.6–4.6)
PsA dose 1	881	836	0.9 (0.9–1.0)
PsA dose 2	714	629	0.9 (0.8–1.0)
PsO dose 1	618	585	0.9 (0.8–1.1)
PsO dose 2	483	432	0.9 (0.8–1.0)
IBD dose 1	1,198	1,157	1.0 (0.9–1.0)
IBD dose 2	968	928	1.0 (0.9–1.1)
CD dose 1	585	540	0.9 (0.8–1.0)
CD dose 2	463	458	1.0 (0.9–1.1)
UC dose 1	635	633	1.0 (0.9–1.1)
UC dose 2	521	475	0.9 (0.8–1.1)
SLE dose 1	474	470	1.0 (0.9–1.1)
SLE dose 2	354	363	1.0 (0.9–1.2)
Any IMID dose 1	9,077	8,598	0.9 (0.9–1.0)
Any IMID dose 2	7,030	6,506	0.9 (0.9–1.0)

\* Data sources included the 2017–2019 IBM MarketScan commercial databases and the 2017–2020 CMS Medicare databases. 95% CI = 95% confidence interval (see Table 1 for other definitions).

## RESULTS

Among the 55,654 MarketScan enrollees ages 50–64 years with IMIDs, 14.8% received  $\geq 1$  dose of RZV, ranging from 11.6% to 18.3% depending on the IMID (Table 1). There were 160,545 Medicare enrollees ages  $\geq 65$  years with IMIDs, among whom 43.2% had received  $\geq 1$  dose of RZV, ranging from 25.1% to 63.6% depending on condition. Cumulative RZV vaccination and the frequency of persons vaccinated monthly steadily increased during 2018–2019 (Figure 1). Among patients who initiated RZV vaccination and received  $\geq 1$  dose, the rate of 2-dose series completion within 6 months was 76.6% in 50–64-year-olds and 85.4% in those  $\geq 65$  years of age; 2-dose series completion

rates were similar between sexes, although some variation by sex was noted for some IMID conditions (Supplementary Table 2, <https://onlinelibrary.wiley.com/doi/10.1002/art.42261>). Among individuals who received 2 vaccine doses, the median interval between doses was 100 days (interquartile range [IQR] 73–147 days) for 50–64-year-olds and 98 days (IQR 73–139 days) for those  $\geq 65$  years of age.

Pneumococcal or influenza vaccination was administered on the same day as RZV vaccination in 17.3% of 50–64-year-olds and 9.9% of  $\geq 65$ -year-olds. In those who received only 1 dose of RZV, 19.8% of 50–64-year-olds and 28.2% of  $\geq 65$ -year-olds received pneumococcal or influenza vaccination within 28–180 days of their first dose of RZV. When the specialty of the provider prescribing



vaccination was known from outpatient drug claims (92% of vaccine doses) for  $\geq 65$ -year-olds, it was most frequently prescribed by physicians in family practice or internal medicine (50.9%) or pharmacists (14.4%), and uncommonly by rheumatologists (2.4%), gastroenterologists (0.6%), or dermatologists (0.1%). The places of service for almost all RZV doses from the outpatient drug claims for  $\geq 65$ -year-olds were community/retail pharmacies (96.9%), followed by other pharmacy types (2.6%), and long-term care pharmacies (0.5%).

In the subgroup analysis using SCCS to evaluate the risk of flare, 7,207 50–64-year-olds and 72,468  $\geq 65$ -year-olds with IMIDs were included in the analysis, among whom 65% and 86% received  $\geq 2$  doses of RZV, respectively (Table 2). Among 50–64-year-olds, 10% developed flares during the control window (before vaccination), compared to 9% who developed flares in the risk window following the first or second doses of RZV. Among  $\geq 65$ -year-olds, 13% developed flares during the control window, and 11–12% developed flares in the risk window following the first or second doses of RZV. We did not find a statistically significant increase in flares following RZV vaccination for any specific IMID condition in either age group following either the first or second RZV dose (Table 3). We did find that a higher proportion of women developed flares compared to men (~1–2-fold higher in women), but the proportion who developed flares following either the first or second dose of RZV was not increased in women or men (Supplementary Table 2, <https://onlinelibrary.wiley.com/doi/10.1002/art.42261>). Two-dose series completion rates were similar in those without and those with flares in the 1–42-day window following the first dose of RZV: 79% versus 77% ( $P = 0.293$ ) in 50–64-year-olds, and 87% versus 85% ( $P < 0.001$ ) in  $\geq 65$ -year-olds, respectively.

## DISCUSSION

We found that a substantial proportion of US adults ages  $\geq 50$  years with IMIDs have received RZV vaccination, reaching almost 15% in adults 50–64 years of age and 43% in adults  $\geq 65$  years of age, with a little over half of vaccinations prescribed by family practice and internal medicine physicians. Most who received the first dose of RZV completed the 2-dose series (77% of 50–64-year-olds and 86% of  $\geq 65$ -year-olds). The risk of IMID flare or disease worsening following vaccination was not increased compared to the 6-week control window (9–12% following vaccination versus 10–13% in the control window). This finding was consistent across both age groups and all IMIDs.

Among IMID patients in our analysis, the proportions vaccinated with RZV were higher than currently available general zoster vaccine coverage estimates (3,4). In addition, second-dose completion rates within 6 months were higher in older age groups compared to younger age groups for all IMID subpopulations (85% in  $\geq 65$ -year-olds versus 77% in 50–64-year-olds) and somewhat higher than those in the general population (78% in  $\geq 65$ -year-olds and 65–70% in  $\geq 50$ -year-olds) (21–23).

These findings suggest there may be excellent provider and patient acceptability of this vaccine to prevent HZ and related complications. Although there are limited data, a survey of primary care providers conducted in 2020, before there was an ACIP recommendation for use of RZV in immunocompromised adults ages  $\geq 19$  years, found that 42–67% of surveyed physicians already recommended RZV for patients ages  $\geq 50$  years with various immunocompromising conditions.

There is theoretical concern that vaccine adjuvants may trigger a disease flare in persons with IMIDs, as adjuvants are immune stimulants. Based on the preliminary definition of flares that we used, we did not observe an increase in flares after RZV vaccination in any of the selected IMID groups, nor did the occurrence of flares have a substantial impact on receiving the second dose of RZV. In the present study, 9% of patients with IMID experienced flares following the first dose of RZV. Of note, grade 3 systemic reactions (severe enough to prevent normal activities) following vaccination were reported by 11% of individuals who received RZV in clinical trials of immunocompetent adults ages  $\geq 50$  years—not all of which may result in medical visits (2,24).

The prior literature examining IMID patient cohorts and vaccination ranged in size from 67 to 1,943 patients and have shown highly variable rates of flares, ranging from 1.5% to 16.4%. For example, in the safety analyses of persons with preexisting potential immune-mediated diseases (pIMDs) from the pooled RZV clinical trials, 2.8% in the RZV group reported a possible exacerbation of their preexisting pIMDs or onset of a different pIMD (25). One study that examined 359 IMID patients found that 16% developed flares in the 12 weeks following vaccination: 34 after the first dose and 17 after the second dose (median 31 and 45 days after the respective doses). Among the subset of 88 RA patients, 24% developed flares (26). In another study that included 403 patients with RA and other systemic rheumatic diseases, 6.7% of patients had flares in the 84 days following RZV, all of which were mild (27). A smaller study that examined flares in 67 IBD patients identified only 1 patient (1.5%) who experienced a flare following RZV vaccination (28). Differences in study findings were likely due to varying flare definitions, methods of case ascertainment (i.e., prospective assessment versus retrospective review), whether patients were receiving treatment and types of treatment, and methods for identifying IMID patients.

In October 2021, the ACIP recommended RZV for adults ages  $\geq 19$  years who are or will be immunodeficient or immunosuppressed because of disease or therapy (5). Prior to this recommendation, some IMID groups, including adults with RA and those anticipating immunosuppression were recommended to receive RZV (2). Other countries have varying RZV recommendations for IMID populations (29). However, no clinical trials of RZV specific to IMID patients have been initiated. A post hoc analysis of data from the RZV clinical trial data (ZOE-50/ZOE-70) examined the efficacy and safety of RZV in participants with preexisting pIMDs and not receiving immunosuppressive therapies at

enrollment, including patients with RA, IBD, PsO, and spondyloarthropathy, and found an overall efficacy of 90.5%, with serious adverse events reported in 14.6% of RZV recipients (30). However, these patients may not have had active disease at the time of vaccination, and the absence of systemic therapy may reduce generalizability of these results to typical IMID patients (30).

A cohort study of participants ages  $\geq 65$  years found vaccine effectiveness to be similar in individuals with IMIDs (based only on diagnostic codes) compared to the overall population (21). A large study of  $\sim 33,000$  patients ages  $\geq 50$  years with IBD, using data from the national Veterans Affairs Healthcare System, demonstrated a lower risk of HZ in RZV recipients as compared to those who were unvaccinated (31). Laboratory-based studies in immunocompromised populations ages  $\geq 18$  years have found that RZV vaccination induced both humoral and cellular immunity after RZV, with an acceptable safety profile (32–34). A challenge in interpreting these vaccine studies is knowing how well studies generalize across diseases and immunomodulatory treatments. For example, certain immunomodulatory therapies (e.g., JAK inhibitors, B cell-depleting therapies such as rituximab, T cell costimulation blockade, and mycophenolate) have mechanisms of action that may uniquely attenuate the effectiveness of RZV vaccination, as has been suggested for vaccination against SARS-CoV-2 in IMID populations (35).

Similar to other studies, we found that most RZV vaccinations in the US are now administered to IMID patients in the pharmacy setting and not in primary care or specialists' offices (23,24). Among individuals who received only 1 dose,  $\sim 20$ – $30\%$  received a vaccine for pneumococcal and influenza within 28–180 days after the first RZV dose. This potential opportunity for coadministration of recommended vaccines reflects a missed opportunity to receive the second dose of RZV. Automated reminders for providers, pharmacies, and patients may help to increase RZV coverage and second dose completion rates. Coadministration with other recommended adult vaccines such as influenza, pneumococcal, and recommended doses for COVID-19 vaccines may help to increase RZV coverage (36,37).

This study has several limitations. Administrative data may include errors in coding; we did not have access to medical records to confirm the diagnosis of IMIDs or the occurrence of flares. However, we attempted to use a very specific definition for each of the IMIDs, using methods in past validation studies with high positive predictive values (PPVs) (38–40). For example, a systematic review of validated methods for identifying RA patients showed that having  $\geq 2$  codes for RA combined with RA medication and a diagnosis by a rheumatologist yielded high PPVs; adding the requirement of treatment increased the PPV from 66% to 97% (39). It may be challenging to distinguish vaccine-induced flares from systemic reactogenicity or disease worsening, at least in the short term. However, based on the RZV clinical trials where reactogenicity of all types typically ensued within 1–3 days after vaccination and resolved within a few days,

persistent IMID disease activity lasting 1 week following vaccination may warrant medical attention, as this time course exceeds that expected from vaccine reactogenicity.

Patients may have had multiple IMID conditions, and due to the small sample size, we were unable to examine those exclusively with only 1 IMID condition. More work is needed to validate the definition of presumed flares used in this study, which intentionally favored specificity by requiring health care intervention (e.g., hospitalization, ED visit, short-term glucocorticoid use) but may have missed mild flares for which medical attention was not sought. We may also have missed flares if prescriptions were paid for in cash, if steroids from a previous prescription were used to manage a new flare, or if parenteral steroids were given for reasons unrelated to a flare (e.g., to treat a respiratory illness or for preexposure prophylaxis to an intravenous infusion medication to reduce immunogenicity). Finally, we restricted the MarketScan analysis to individuals ages 50–64 years. Flare rates may be higher in younger individuals who may mount a more vigorous immune response to vaccine adjuvants; however, uptake in 2017–2019 in individuals younger than 50 years was anticipated to be trivial given the lack of a recommendation for RZV at that time, precluding analysis in younger patients.

In conclusion, this observational study provides new data on the safety of RZV vaccination in adults ages  $\geq 50$  years with selected IMIDs. Within the limitations of administrative data and our presumed flare definition, we did not find an increase in flares after receiving an RZV dose. Additional treatment specific data on efficacy and safety of RZV vaccination in this population are needed. We found that a substantial proportion of adults ages  $\geq 50$  years with IMIDs had received RZV compared to currently available general zoster vaccine coverage estimates. The recent recommendation for use of RZV in immunocompromised adults ages  $\geq 19$  years may help to further increase RZV vaccination rates in this population. Based on clinical trial data on RZV, providers should counsel patients that systemic symptoms are common following RZV and typically resolve within the first week postvaccination.

## AUTHOR CONTRIBUTIONS

All authors were involved in drafting the article or revising it critically for important intellectual content, and all authors approved the final version to be published. Ms. Leung had full access to all of the data in the study and takes responsibility for the integrity of the data and the accuracy of the data analysis.

**Study conception and design.** Leung, Anderson, Dooling, Xie, Curtis.

**Acquisition of data.** Leung.

**Analysis and interpretation of data.** Leung, Anderson, Dooling, Xie, Curtis.

## REFERENCES

1. Harpaz R, Ortega-Sanchez IR, Seward JF. Prevention of herpes zoster: recommendations of the Advisory Committee on Immunization Practices (ACIP). *MMWR Recomm Rep* 2008;57:1–30.

2. Dooling KL, Guo A, Patel M, Lee GM, Moore K, Belongia EA, et al. Recommendations of the Advisory Committee on Immunization Practices for Use of Herpes Zoster Vaccines. *MMWR Morb Mortal Wkly Rep* 2018;67:103–8.
3. Lu PJ, Hung MC, Srivastav A, Grohskopf LA, Kobayashi M, Harris AM, et al. Surveillance of vaccination coverage among adult populations—United States, 2018. *MMWR Surveill Summ* 2021;70:1–26.
4. Kawai K, Kawai AT. Racial/ethnic and socioeconomic disparities in adult vaccination coverage. *Am J Prev Med* 2021;61:465–73.
5. Anderson TC, Masters NB, Guo A, Shepersky L, Leidner AJ, Lee GM, et al. Use of recombinant zoster vaccine in immunocompromised adults aged  $\geq 19$  years: recommendations of the advisory committee on immunization practices—United States, 2022. *MMWR Morb Mortal Wkly Rep* 2022;71:80–4.
6. Chakravarty EF, Michaud K, Katz R, Wolfe F. Increased incidence of herpes zoster among patients with systemic lupus erythematosus. *Lupus* 2013;22:238–44.
7. Forbes HJ, Thomas SL, Smeeth L, Clayton T, Farmer R, Bhaskaran K, et al. A systematic review and meta-analysis of risk factors for post-herpetic neuralgia. *Pain* 2016;157:30–54.
8. Kawai K, Yawn BP. Risk Factors for herpes zoster: a systematic review and meta-analysis. *Mayo Clin Proc* 2017;92:1806–21.
9. Mareque M, Oyagüez I, Morano R, Casado MA. Systematic review of the evidence on the epidemiology of herpes zoster: incidence in the general population and specific subpopulations in Spain. *Public Health* 2019;167:136–46.
10. Pego-Reigosa JM, Nicholson L, Pooley N, Langham S, Embleton N, Marjenberg Z, et al. The risk of infections in adult patients with systemic lupus erythematosus: systematic review and meta-analysis. *Rheumatology (Oxford)* 2021;60:60–72.
11. Yun H, Yang S, Chen L, Xie F, Winthrop K, Baddley JW, et al. Risk of herpes zoster in autoimmune and inflammatory diseases: implications for vaccination. *Arthritis Rheumatol* 2016;68:2328–37.
12. Veetil BM, Myasoedova E, Matteson EL, Gabriel SE, Green AB, Crowson CS. Incidence and time trends of herpes zoster in rheumatoid arthritis: a population-based cohort study. *Arthritis Care Res (Hoboken)* 2013;65:854–61.
13. Curtis JR, Xie F, Yun H, Bernatsky S, Winthrop KL. Real-world comparative risks of herpes virus infections in tofacitinib and biologic-treated patients with rheumatoid arthritis. *Ann Rheum Dis* 2016;75:1843–7.
14. Curtis JR, Xie F, Yang S, Bernatsky S, Chen L, Yun H, et al. Risk for herpes zoster in tofacitinib-treated rheumatoid arthritis patients with and without concomitant methotrexate and glucocorticoids. *Arthritis Care Res (Hoboken)* 2019;71:1249–54.
15. Baumrin E, Van Voorhees A, Garg A, Feldman SR, Merola JF. A systematic review of herpes zoster incidence and consensus recommendations on vaccination in adult patients on systemic therapy for psoriasis or psoriatic arthritis: from the medical board of the National Psoriasis Foundation. *J Am Acad Dermatol* 2019;81:102–10.
16. Farraye FA, Melmed GY, Lichtenstein GR, Kane SV. ACG clinical guideline: preventive care in inflammatory bowel disease. *Am J Gastroenterol* 2017;112:241–58.
17. Singh JA, Saag KG, Bridges SL Jr, Akl EA, Bannuru RR, Sullivan MC, et al. 2015 American College of Rheumatology guideline for the treatment of rheumatoid arthritis. *Arthritis Rheumatol* 2016;68:1–26.
18. Li R, Stewart B, Weintraub E. Evaluating efficiency and statistical power of self-controlled case series and self-controlled risk interval designs in vaccine safety. *J Biopharm Stat* 2016;26:686–93.
19. Petersen I, Douglas I, Whitaker H. Self controlled case series methods: an alternative to standard epidemiological study designs. *BMJ* 2016;354:i4515.
20. Weldelessie YG, Whitaker HJ, Farrington CP. Use of the self-controlled case-series method in vaccine safety studies: review and recommendations for best practice. *Epidemiol Infect* 2011;139:1805–17.
21. Izurieta HS, Wu X, Forshee R, Lu Y, Sung HM, Agger PE, et al. Recombinant zoster vaccine (Shingrix) real-world effectiveness in the first two years post-licensure. *Clin Infect Dis* 2021;73:941–8.
22. McGirr A, Bourgoin T, Wortzman M, Millson B, McNeil SA. An early look at the second dose completion of the recombinant zoster vaccine in Canadian adults: a retrospective database study. *Vaccine* 2021;39:3397–403.
23. Patterson BJ, Chen CC, McGuinness CB, Glasser LI, Sun K, Buck PO. Early examination of real-world uptake and second-dose completion of recombinant zoster vaccine in the United States from October 2017 to September 2019. *Hum Vaccin Immunother* 2021;17:2482–7.
24. McGirr A, Widenmaier R, Curran D, Espié E, Mrkvan T, Oostvogels L, et al. The comparative efficacy and safety of herpes zoster vaccines: a network meta-analysis. *Vaccine* 2019;37:2896–909.
25. López-Fauqued M, Campora L, Delannois F, El Idrissi M, Oostvogels L, De Looze FJ, et al. Safety profile of the adjuvanted recombinant zoster vaccine: pooled analysis of two large randomised phase 3 trials. *Vaccine* 2019;37:2482–93.
26. Lenfant T, Jin Y, Kirchner E, Hajj-Ali RA, Calabrese LH, Calabrese C. Safety of recombinant zoster vaccine: a retrospective study of 622 rheumatology patients. *Rheumatology (Oxford)* 2021; 60: 5149–57.
27. Stevens E, Weinblatt ME, Massarotti E, Griffin F, Emani S, Desai S. Safety of the zoster vaccine recombinant adjuvanted in rheumatoid arthritis and other systemic rheumatic disease patients: a single center's experience with 400 patients. *ACR Open Rheumatol* 2020;2:357–61.
28. Satyam VR, Li PH, Reich J, Qazi T, Noronha A, Wasan SK, et al. Safety of recombinant zoster vaccine in patients with inflammatory bowel disease. *Dig Dis Sci* 2020;65:2986–91.
29. Parikh R, Widenmaier R, Lecrenier N. A practitioner's guide to the recombinant zoster vaccine: review of national vaccination recommendations [review]. *Expert Rev Vaccines* 2021;20:1065–75.
30. Dagnew AF, Rausch D, Hervé C, Zahaf T, Levin MJ, Schuind A. Efficacy and serious adverse events profile of the adjuvanted recombinant zoster vaccine in adults with pre-existing potential immune-mediated diseases: a pooled post hoc analysis on two parallel randomized trials. *Rheumatology (Oxford)* 2021;60:1226–33.
31. Khan N, Wang L, Trivedi C, Pernes T, Patel M, Xie D, et al. Efficacy of recombinant zoster vaccine in patients with inflammatory bowel disease. *Clin Gastroenterol Hepatol* 2022;20:1570–8.
32. Dagnew AF, Vink P, Drame M, Willer DO, Salaun B, Schuind AE. Immune responses to the adjuvanted recombinant zoster vaccine in immunocompromised adults: a comprehensive overview [review]. *Hum Vaccin Immunother* 2021;17:4132–43.
33. López-Fauqued M, Co-van der Mee M, Bastidas A, Beukelaers P, Dagnew AF, Fernandez Garcia JJ, et al. Safety profile of the adjuvanted recombinant zoster vaccine in immunocompromised populations: an overview of six trials. *Drug Saf* 2021;44:811–23.
34. Racine É, Gilca V, Amini R, Tunis M, Ismail S, Sauvageau C. A systematic literature review of the recombinant subunit herpes zoster vaccine use in immunocompromised 18–49 year old patients. *Vaccine* 2020;38:6205–14.
35. Curtis JR, Johnson SR, Anthony DD, Arasaratnam RJ, Baden LR, Bass AR, et al. American College of Rheumatology Guidance for COVID-19 vaccination in patients with rheumatic and musculoskeletal diseases: version 3. *Arthritis Rheumatol* 2021;73:e60–75.
36. American College of Rheumatology COVID-19 Vaccine Clinical Guidance Task Force. COVID-19 vaccine clinical guidance summary for patients with rheumatic and musculoskeletal diseases. 2021 URL:

- <https://www.rheumatology.org/Portals/0/Files/COVID-19-Vaccine-Clinical-Guidance-Rheumatic-Diseases-Summary.pdf>.
37. Curtis JR, Johnson SR, Anthony DD, Arasaratnam RJ, Baden LR, Bass AR, et al. American College of Rheumatology Guidance for COVID-19 vaccination in patients with rheumatic and musculoskeletal diseases: version 4. *Arthritis Rheumatol* 2022;74:e21–36.
  38. Booth MJ, Clauw D, Janevic MR, Kobayashi LC, Piette JD. Validation of self-reported rheumatoid arthritis using medicare claims: a nationally representative longitudinal study of older adults. *ACR Open Rheumatol* 2021;3:239–49.
  39. Chung CP, Rohan P, Krishnaswami S, McPheeters ML. A systematic review of validated methods for identifying patients with rheumatoid arthritis using administrative or claims data. *Vaccine* 2013;31 Suppl:K41–61.
  40. Curtis JR, Xie F, Zhou H, Salchert D, Yun H. Use of ICD-10 diagnosis codes to identify seropositive and seronegative rheumatoid arthritis when lab results are not available. *Arthritis Res Ther* 2020;22:242.

# Strong Association of Combined Genetic Deficiencies in the Classical Complement Pathway With Risk of Systemic Lupus Erythematosus and Primary Sjögren's Syndrome

Christian Lundtoft,<sup>1</sup> Christopher Sjöwall,<sup>2</sup> Solbritt Rantapää-Dahlqvist,<sup>3</sup> Anders A. Bengtsson,<sup>4</sup> Andreas Jönsen,<sup>4</sup> Pascal Pucholt,<sup>1</sup> Yee Ling Wu,<sup>5</sup> Emeli Lundström,<sup>6</sup> Majja-Leena Eloranta,<sup>1</sup> Iva Gunnarsson,<sup>6</sup> Eva Baecklund,<sup>1</sup> Roland Jonsson,<sup>7</sup> Daniel Hammenfors,<sup>8</sup> Helena Forsblad-d'Elia,<sup>9</sup> Per Eriksson,<sup>2</sup> Thomas Mandl,<sup>10</sup> Sara Bucher,<sup>11</sup> Katrine B. Norheim,<sup>12</sup> Svein Joar Auglaend Johnsen,<sup>13</sup> Roald Omdal,<sup>14</sup> Marika Kvarnström,<sup>15</sup> Marie Wahren-Herlenius,<sup>16</sup> Lennart Truedsson,<sup>17</sup> Bo Nilsson,<sup>18</sup> Sergey V. Kozyrev,<sup>19</sup> Matteo Bianchi,<sup>19</sup> Kerstin Lindblad-Toh,<sup>20</sup> the DISSECT consortium, the ImmunoArray consortium, Chack-Yung Yu,<sup>21</sup> Gunnel Nordmark,<sup>1</sup> Johanna K. Sandling,<sup>1</sup> Elisabet Svenungsson,<sup>6</sup> Dag Leonard,<sup>1</sup> and Lars Rönnblom<sup>1</sup>

**Objective.** Complete genetic deficiency of the complement component C2 is a strong risk factor for monogenic systemic lupus erythematosus (SLE), but whether heterozygous C2 deficiency adds to the risk of SLE or primary Sjögren's syndrome (SS) has not been studied systematically. This study was undertaken to investigate potential associations of heterozygous C2 deficiency and C4 copy number variation with clinical manifestations in patients with SLE and patients with primary SS.

**Methods.** The presence of the common 28-bp C2 deletion rs9332736 and C4 copy number variation was examined in Scandinavian patients who had received a diagnosis of SLE (n = 958) or primary SS (n = 911) and in 2,262 healthy controls through the use of DNA sequencing. The concentration of complement proteins in plasma and classical complement function were analyzed in a subgroup of SLE patients.

**Results.** Heterozygous C2 deficiency—when present in combination with a low C4A copy number—substantially increased the risk of SLE (odds ratio [OR] 10.2 [95% confidence interval (95% CI) 3.5–37.0]) and the risk of primary SS (OR 13.0 [95% CI 4.5–48.4]) when compared to individuals with 2 C4A copies and normal C2. For patients heterozygous for rs9332736 with 1 C4A copy, the median age at diagnosis was 7 years earlier in patients with SLE and 12 years earlier in patients with primary SS when compared to patients with normal C2. Reduced C2 levels in plasma ( $P = 2 \times 10^{-9}$ ) and impaired function of the classical complement pathway ( $P = 0.03$ ) were detected in SLE patients with heterozygous C2 deficiency. Finally, in a primary SS patient homozygous for C2 deficiency, we observed low levels of anti-Scl-70, which suggests a risk of developing systemic sclerosis or potential overlap between primary SS and other systemic autoimmune diseases.

**Conclusion.** We demonstrate that a genetic pattern involving partial deficiencies of C2 and C4A in the classical complement pathway is a strong risk factor for SLE and for primary SS. Our results emphasize the central role of the complement system in the pathogenesis of both SLE and primary SS.

Supported by the Swedish Research Council for Medicine and Health, the Swedish Rheumatism Association, King Gustaf V's 80-Year Foundation, the Swedish Heart-Lung Foundation, ALF funding from Stockholm County and Region Östergötland, the Swedish Society for Medical Research, the Swedish Society of Medicine, the Ingegerd Johansson donation, and the Gustafsson Family Foundation. Dr. Lindblad-Toh's work was supported by a Wallenberg Scholarship.

<sup>1</sup>Christian Lundtoft, PhD, Pascal Pucholt, PhD (current address: Olink Proteomics), Majja-Leena Eloranta, PhD, Eva Baecklund, MD, PhD, Gunnel Nordmark, MD, PhD, Johanna K. Sandling, PhD, Dag Leonard, MD, PhD, Lars Rönnblom, MD, PhD: Department of Medical Sciences, Rheumatology, Uppsala University, Uppsala, Sweden; <sup>2</sup>Christopher Sjöwall, MD, PhD, Per Eriksson, MD, PhD: Division of Inflammation and Infection, Department of Biomedical and Clinical

Sciences, Linköping University, Linköping, Sweden; <sup>3</sup>Solbritt Rantapää-Dahlqvist, MD, PhD: Department of Public Health and Clinical Medicine/Rheumatology, Umeå University, Umeå, Sweden; <sup>4</sup>Anders A. Bengtsson, MD, PhD, Andreas Jönsen, MD, PhD: Department of Clinical Sciences Lund, Rheumatology, Lund University, and Skåne University Hospital, Lund, Sweden; <sup>5</sup>Yee Ling Wu, PhD: Center for Microbial Pathogenesis, The Research Institute at Nationwide Children's Hospital, Columbus, Ohio, and the Department of Microbiology and Immunology, Loyola University, Chicago, Illinois; <sup>6</sup>Emeli Lundström, PhD, Iva Gunnarsson, MD, PhD, Elisabet Svenungsson, MD, PhD: Division of Rheumatology, Department of Medicine Solna, Karolinska Institutet, Karolinska University Hospital, Stockholm, Sweden; <sup>7</sup>Roland Jonsson, DMD, PhD: Broegelmann Research Laboratory, Department of Clinical Science, University of

## INTRODUCTION

Deficiencies in genes of the early classical complement pathway (i.e., *C1Q*, *C1R*, *C1S*, *C2*, and *C4*) are among the strongest risk factors for monogenic systemic lupus erythematosus (SLE) and lupus-like disease (1,2). While rare, *C1Q* deficiency translates into SLE in ~90% of the described cases, whereas deficiencies of *C1R*, *C1S*, and *C4* have a penetrance in the range of 65–80% (3). In contrast, complete *C2* deficiency is one of the most common complement deficiencies, with an estimated prevalence of 1:20,000 in the Swedish population and a penetrance for SLE of ~25% (4–6).

The predominant cause of complete *C2* deficiency is a 28-bp deletion (rs9332736) in the exon/intron boundary of exon 6. The deletion introduces an early stop codon in the *C2* transcript, thereby leading to the absence of the *C2* protein in plasma (7,8). The minor allele frequency of the 28-bp *C2* deletion is 0.01 in populations of European descent, which means that 1 of 50 individuals are heterozygous carriers of the deleterious variant. Although a few case reports and small studies exist (9–12), heterozygous *C2* deficiency due to rs9332736 and the association with rheumatic disease have not previously been evaluated systematically.

In addition to heterozygous *C2* deficiency, a high level of copy number variation is seen for the paralogous *C4* genes *C4A* and *C4B*. We and others have previously shown that a low copy number of *C4A* is strongly associated with both SLE and primary Sjögren's syndrome (SS) (13–18). In the general population, the copy number of *C4A* ranges between 0 and 5 copies, with ~50% of individuals having 2 copies of *C4A*. For *C4B*, the copy number generally ranges between 0 and 4 copies.

The purpose of the current study was to evaluate the interplay between heterozygous *C2* deficiency and the common copy number variation of *C4* in relation to the risk of SLE and primary SS. Further, we aimed to evaluate the clinical consequences of the partial complement deficiencies in SLE and primary SS.

## PATIENTS AND METHODS

**Study participants.** In the current study, we included patients diagnosed as having SLE or primary SS at Scandinavian rheumatology clinics and healthy blood donors and population controls as previously described (19,20). SLE patients met  $\geq 4$  of the American College of Rheumatology (ACR) 1982 revised criteria for the classification of SLE (21), while primary SS patients fulfilled the American–European Consensus Group criteria for primary SS (22). Patients and controls were analyzed by targeted DNA sequencing as part of the dissecting disease mechanisms in three systemic inflammatory autoimmune diseases with an interferon signature (DISSECT) project, and basic characteristics of the study participants are presented in Supplementary Table 1 (available on the *Arthritis & Rheumatology* website at <http://onlinelibrary.wiley.com/doi/10.1002/art.42270>). The capturing array (23), targeted sequencing, genotyping of single-nucleotide variants, and quality control have been described previously (19,20), and a brief summary of the workflow, including variant- and individual-based quality control, can be found in the Supplementary Information (available at <http://onlinelibrary.wiley.com/doi/10.1002/art.42270>). In addition, we included 1,000 Swedish population controls analyzed by whole-genome sequencing as part of the SweGen project (24), and the workflow is presented in the Supplementary Information.

For the genetic analysis, we combined all population controls from the SweGen project and the 2 targeted sequencing studies previously conducted by our group (19,20), excluding related individuals and genetic population outliers (Supplementary Information). Findings on the prevalence of heterozygous carriers of the *C2* variant rs9332736 in the individual study cohorts of SLE and primary SS patients and healthy controls, as well as the association between the rs9332736 variant and *C4A* copy number, can be found in Supplementary Figure 1 (available at <http://onlinelibrary.wiley.com/doi/10.1002/art.42270>). In order to increase the power of the functional and clinical analysis of SLE and primary SS patients, we included all patients (including population outliers)

Bergen, Bergen, Norway; <sup>8</sup>Daniel Hammenfors, MD: Department of Rheumatology, Haukeland University Hospital, Bergen, Norway; <sup>9</sup>Helena Forsblad-d'Elia, MD, PhD: Department of Rheumatology and Inflammation Research, Sahlgrenska Academy, University of Gothenburg, Gothenburg, Sweden; <sup>10</sup>Thomas Mandl, MD, PhD: Division of Rheumatology, Department of Clinical Sciences Malmö, Lund University, and Novartis, Malmö, Sweden; <sup>11</sup>Sara Bucher, MD: Department of Rheumatology, Faculty of Medicine and Health, Örebro University, Örebro, Sweden; <sup>12</sup>Katrine B. Norheim, MD, PhD: Department of Rheumatology, Stavanger University Hospital, Stavanger, Norway, and the Institute of Clinical Science, University of Bergen, Bergen, Norway; <sup>13</sup>Svein Joar Auglaend Johnsen, MD, PhD: Department of Rheumatology, Stavanger University Hospital, Stavanger, Norway; <sup>14</sup>Roald Omdal, MD, PhD: Broegelmann Research Laboratory, Department of Clinical Science, University of Bergen, Bergen, Norway, and the Department of Rheumatology, Stavanger University Hospital, Stavanger, Norway; <sup>15</sup>Marika Kvarnström, MD, PhD: Division of Rheumatology, Department of Medicine Solna, Karolinska Institutet, Karolinska University Hospital, Stockholm, Sweden, and the Academic Specialist Center, Center for Rheumatology, Stockholm Health Services, Stockholm, Sweden; <sup>16</sup>Marie Wahren-Herlenius, MD, PhD: Division of Rheumatology, Department of Medicine Solna, Karolinska Institutet, Karolinska University Hospital,

Stockholm, Sweden, and Broegelmann Research Laboratory, Department of Clinical Science, University of Bergen, Bergen, Norway; <sup>17</sup>Lennart Truedsson, MD, PhD: Department of Microbiology, Immunology, and Glycobiology, Lund University Hospital, Lund, Sweden; <sup>18</sup>Bo Nilsson, MD, PhD: Department of Immunology, Genetics, and Pathology, Uppsala University, Uppsala, Sweden; <sup>19</sup>Sergey V. Kozyrev, PhD, Matteo Bianchi, PhD: Science for Life Laboratory, Department of Medical Biochemistry and Microbiology, Uppsala University, Uppsala, Sweden; <sup>20</sup>Kerstin Lindblad-Toh, PhD: Science for Life Laboratory, Department of Medical Biochemistry and Microbiology, Uppsala University, Uppsala, Sweden, and Broad Institute of MIT and Harvard, Cambridge, Massachusetts; <sup>21</sup>Chack-Yung Yu, PhD: Center for Microbial Pathogenesis, The Research Institute at Nationwide Children's Hospital, Columbus, Ohio.

Author disclosures are available at <https://onlinelibrary.wiley.com/action/downloadSupplement?doi=10.1002%2Fart.42270&file=art42270-sup-0001-Disclosureform.pdf>.

Address correspondence via email to Lars Rönnblom, MD, PhD, at [lars.ronnblom@medsci.uu.se](mailto:lars.ronnblom@medsci.uu.se).

Submitted for publication March 17, 2022; accepted in revised form June 10, 2022.

who passed the quality filters for genotype calls of the 28-bp C2 deletion and C4 copy number (Supplementary Information, <http://onlinelibrary.wiley.com/doi/10.1002/art.42270>). The individual studies were approved by local ethics committees, and all study participants gave informed consent.

**Genotyping of the 28-bp C2 deletion.** As the previous analyses of genetic variation in the targeted sequencing data by our group comprised single-nucleotide variants only (19,20), a focused reanalysis of the sequencing data was performed in order to genotype the 28-bp deletion rs9332736 in C2 as described in the Supplementary Information, including quality control of the genotype calls. We excluded 1 SLE patient with a heterozygous call for rs9332736 that clustered with homozygous carriers of the C2 deletion (Supplementary Information, <http://onlinelibrary.wiley.com/doi/10.1002/art.42270>).

**Analysis of C4 copy number and HLA alleles from DNA sequencing data.** The complement C4 copy numbers for both targeted sequencing data and whole-genome sequencing data were estimated based on read depth using the GermlineCNVCaller (Genome Analysis Toolkit) as described previously (18), and a brief description can be found in the Supplementary Information. The integer copy number of C4A and C4B was estimated using the relative read depths of 5 single-nucleotide variants in exon 26 specific for C4A and C4B while accounting for the total copy number of C4. Alleles of the 6 HLA genes HLA-A, B, C, DPB1, DQB1, and DRB1 were called from sequencing reads at 2-field (i.e., 4-digit) resolution using xHLA (25) as described previously (18).

**Clinical data, analysis of complement proteins in plasma, and autoantibody status.** Plasma levels of C2 had been analyzed in a subset of SLE patients by electroimmunoassay as previously described (26), with the C2 level being reported relative to the concentration of a reference serum. Measurement of plasma C3 levels and plasma C4 levels in SLE patients (27) and function of the classical complement pathway (28,29) have been described previously. Clinical information including autoantibody status was extracted from medical records.

**Statistical analysis.** R version 4.0.4 (30) was used for statistical analyses that included logistic regression, analysis of variance, and Cox proportional hazards regression. Two-tailed *P* values less than 0.05 were considered significant, and the models and covariates that were included are described in the text or in the figure legends.

**Data availability.** Raw data for individual figures are available in the Supplementary Data (<http://onlinelibrary.wiley.com/doi/10.1002/art.42270>). Genotype data at the individual level are

not publicly available since some of the information could compromise research participant privacy and consent. Scripts for calling C4 copy number in GATK GermlineCNVCaller are available upon request.

## RESULTS

**Heterozygous C2 deficiency in combination with low C4A copy number associated with SLE and primary SS.** Initially, we analyzed the occurrence of a 28-bp deletion in complement C2 (i.e., rs9332736) in our cohort and found that 3.3% of both SLE patients (*n* = 31) and primary SS patients (*n* = 30) were heterozygous for the variant compared to 1.9% of healthy controls (*n* = 43). Further, we identified 3 patients who were homozygous for the deletion. The heterozygous presence of the 28-bp C2 deletion rs9332736 was associated with an increased risk for both SLE and primary SS (odds ratio [OR] 1.75 [95% confidence interval (95% CI) 1.08–2.81] and OR 1.72 [95% CI 1.05–2.81], respectively) (Figure 1A).

A low copy number of C4A is a strong risk factor for both SLE and primary SS (17,18), and since both C4 and C2 are part of the early classical complement pathway, we investigated whether heterozygous C2 deficiency in combination with a low copy number of C4A would impose an even greater disease risk. The copy number of C4A ranged between 0 and 5 copies for patients and healthy controls. However, all individuals heterozygous for rs9332736 carried 1–3 copies of C4A due to linkage disequilibrium between C4 and C2 (both genes are located in the HLA region on chromosome 6). Interestingly, we detected an increased risk of both SLE and primary SS for patients heterozygous for rs9332736 when the deletion was present in combination with a C4A copy number of 1 (Figure 1B). In contrast, heterozygous C2 deficiency was not associated with SLE or primary SS when present with a C4A copy number of 2 or 3, and no association was seen with a low copy number of C4B.

We next evaluated the combined effect of low C4A copy number and heterozygous C2 deficiency in comparison to individuals with 2 C4A copies and normal C2. A C4A copy number of 1 in combination with heterozygous C2 deficiency was associated to an even greater extent with a substantially increased risk of both SLE and primary SS (OR 10.2 and OR 13.0, respectively) (Figure 1C) than was a C4A copy number of 0 (OR 7.5 for SLE and OR 4.9 for primary SS). Further, we noted a tendency toward a significant interaction between heterozygous C2 deficiency and C4A copy number (for SLE and primary SS combined, *P* = 0.06 by logistic regression adjusted for C4B copy number and sex).

Due to C2 being located in the HLA region, we assessed the linkage between the 28-bp C2 deletion rs9332736 and disease-associated HLA alleles. We noted a strong linkage disequilibrium between rs9332736 and multiple single-nucleotide polymorphisms, but the linkage to HLA alleles was limited (Figure 1D), indicating that the effect of 28-bp C2 deletion was not through an

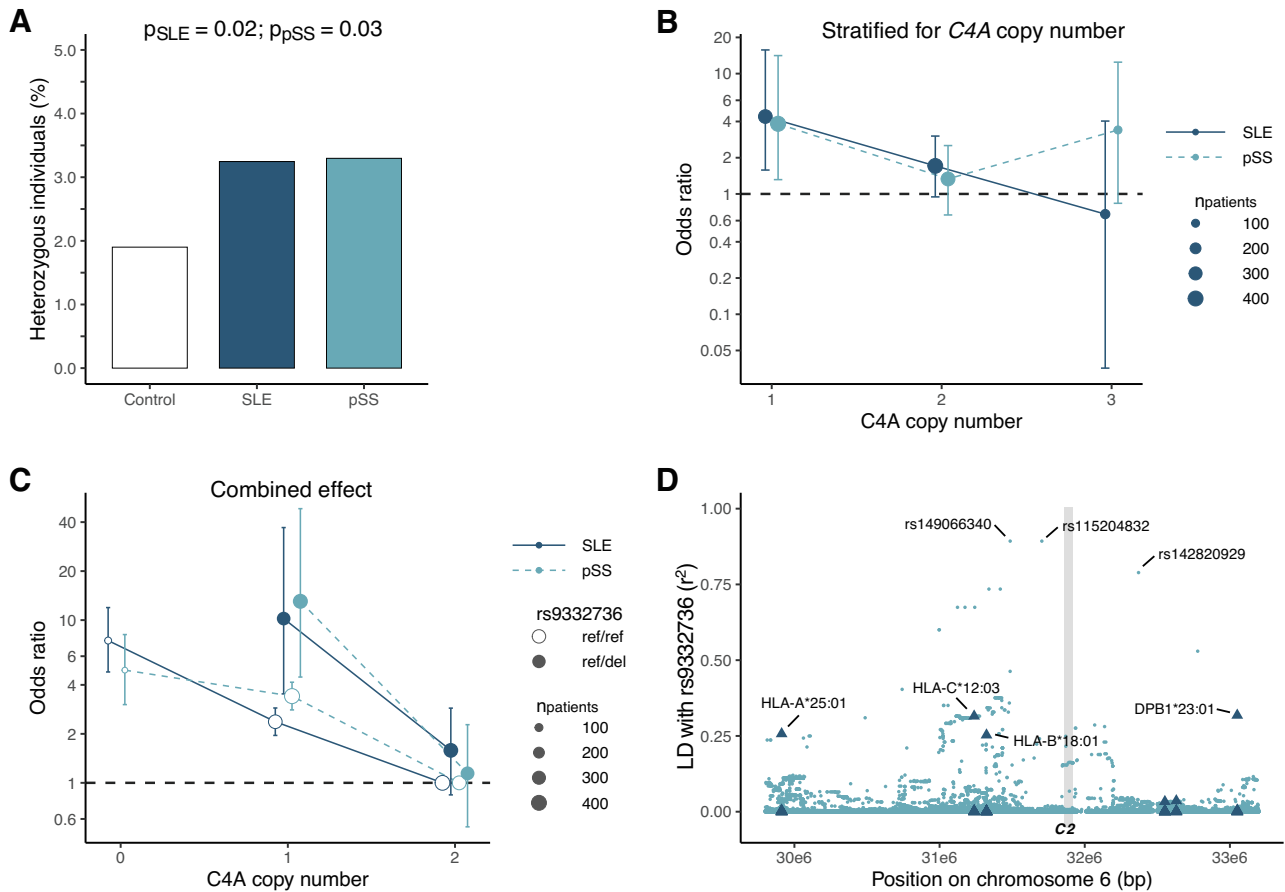


**Figure 1.** Heterozygosity of the 28-bp *C2* deletion rs9332736 in systemic lupus erythematosus (SLE) patients and primary Sjögren's syndrome (SS) patients. **A**, Prevalence of heterozygous carriers of the *C2* loss-of-function variant rs9332736 in SLE patients ( $n = 955$ ), primary SS patients ( $n = 910$ ), and healthy controls ( $n = 2,262$ ). Individuals homozygous for the rs9332736 variant (2 SLE patients and 1 primary SS patient) were excluded. **B**, Risk of association with SLE or primary SS according to number of *C4A* copies in rs9332736, with odds calculated relative to healthy controls. **C**, Risk of association with SLE or primary SS according to the combined effect of *C4A* copy number and rs9332736 heterozygosity (ref/del), with odds calculated relative to a *C4A* copy number of 2 and normal *C2* (ref/ref). Due to rs9332736 segregating with *C4A*, no individuals heterozygous for rs9332736 have 0 *C4A* copies. Data were analyzed using logistic regression and adjusted for sex (**A**, **B**, and **C**) and *C4B* copy number (**B** and **C**). In **B** and **C**, bars show the 95% confidence intervals. **D**, Linkage disequilibrium (LD;  $r^2$ ) between the 28-bp *C2* deletion rs9332736 and *HLA* alleles/biallelic single-nucleotide polymorphisms in the *HLA* region. LD with *HLA* alleles for 6 *HLA* genes are indicated by triangles, including *HLA* alleles *A*, *C*, *B*, *DRB1*, *DQB1*, and *DPB1*. The vertical gray-shaded line indicates the genomic position of *C2*. LD was estimated using SweGen whole-genome sequencing samples ( $n = 1,000$ ). Color figure can be viewed in the online issue, which is available at <http://onlinelibrary.wiley.com/doi/10.1002/art.42270/abstract>.

indirect link to a disease-associated *HLA* allele such as *DRB1\*03:01* or *DRB1\*15:01*.

In summary, we identified heterozygous *C2* deficiency as a risk factor for SLE and primary SS when it occurs in combination with low *C4A* copy number, highlighting the role of the early classical complement pathway in the pathogenesis of SLE and primary SS.

**Decreased classical complement function for rs9332736 carriers.** Having demonstrated a genetic association between the 28-bp *C2* deletion and SLE and primary SS, we continued evaluating the functional consequences of heterozygous *C2* deficiency. Levels of complement proteins were analyzed in a subgroup of SLE patients. As expected, patients heterozygous for the deleterious *C2* variant rs9332736 had lower

plasma *C2* levels when compared to patients without the genetic variant ( $P$  for *C2* =  $2 \times 10^{-9}$ ) (Figure 2A). Further, we detected lower function of the classical complement pathway in patients heterozygous for rs9332736 ( $P = 0.03$ ) (Figure 2B).

Nevertheless, a substantial number of SLE patients without the deleterious rs9332736 variant presented with low levels of plasma *C2* (defined here as  $<80\%$ ) (Figure 2A), and we investigated whether the low concentration could be explained by other, nongenetic effects. Analysis of *C3* and *C4* levels in plasma revealed lower concentration of both proteins for this subgroup of SLE patients, whereas patients heterozygous for rs9332736 had normal levels of *C3* and *C4* (Figures 2C and D). These data suggest that the lower plasma concentration of *C2* in SLE patients without a genetic cause for low *C2* may be due to



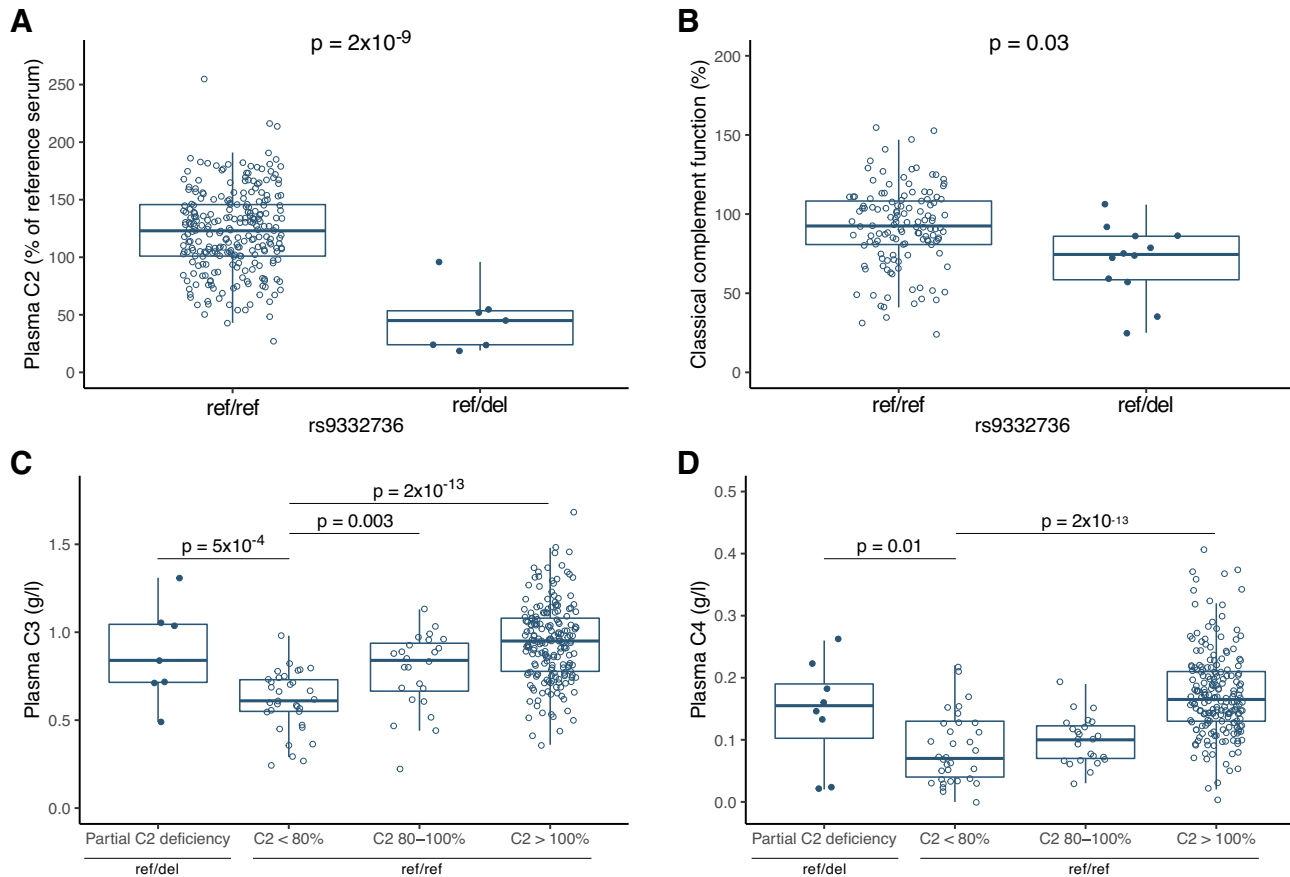


**Figure 2.** Concentration of plasma complement components in systemic lupus erythematosus (SLE) patients with the 28-bp C2 deletion rs9332736 (ref/del) and in SLE patients with normal C2 (ref/ref), including plasma C2 concentration relative to a reference serum ( $n = 261$ ) (A), classical complement function ( $n = 140$ ) (B), plasma C3 (C) and plasma C4 (D) concentration stratified by presence of the 28-bp C2 deletion rs9332736 and plasma C2 concentration ( $n = 258$  for C and D). Data were analyzed by analysis of variance and adjusted for sex and age at sampling (A, C, and D), and for copy number of *C4A* and *C4B* (B). Plasma concentration of C4 was square root transformed. Data are shown as box plots. Each box represents the 25th to 75th percentiles. Lines inside the boxes represent the median, and whiskers extend to 1.5 times the interquartile range. Solid circles represent individual SLE patients heterozygous for rs9332736; open circles represent individual SLE patients with normal C2. Color figure can be viewed in the online issue, which is available at <http://onlinelibrary.wiley.com/doi/10.1002/art.42270/abstract>.

complement activation and consumption of proteins in the complement pathway.

**Lower age at diagnosis in patients with heterozygous C2 deficiency.** Next, we evaluated the association between heterozygous C2 deficiency and clinical manifestations in SLE. However, we did not detect any associations between the 28-bp C2 deletion and the ACR criteria used for clinical classification of SLE patients (Supplementary Figure 2, <http://onlinelibrary.wiley.com/doi/10.1002/art.42270>). The relatively low number of patients carrying the rs9332736 variant likely limited the power in cross-sectional analyses, and we reasoned that time-dependent analyses would be more suitable.

Therefore, we evaluated how the deleterious C2 variant rs9332736 affected the progression of SLE and primary SS. Intriguingly, SLE patients heterozygous for rs9332736 who had a *C4A* copy number of 1 were diagnosed earlier when compared to patients with normal C2 ( $P$  for rs9332736 = 0.002) (Figure 3A),

with the difference in median age at diagnosis being 7 years. In contrast, rs9332736 was not found to have an effect on disease progression in SLE patients with 2 copies of *C4A* ( $P$  for rs9332736 = 0.70) (Figure 3A). A similar pattern was seen for primary SS patients, where patients with heterozygous C2 deficiency and a *C4A* copy number of 1 tended to have lower age at diagnosis ( $P$  for rs9332736 = 0.05) (Figure 3B), the difference in median age at diagnosis being 12 years. Again, rs9332736 was not found to have an effect on disease progression in patients with primary SS with 2 *C4A* copies ( $P$  for rs9332736 = 0.48) (Figure 3B).

We continued by analyzing the association between rs9332736 and age at first event of nephritis in SLE patients and identified a similar pattern. It was found that SLE patients heterozygous for 28-bp C2 deletion who had 1 copy of *C4A* tended to have earlier occurrences of nephritis when compared to SLE patients with normal C2, although the difference was not significant ( $P$  for rs9332736 = 0.17) (Figure 4). No

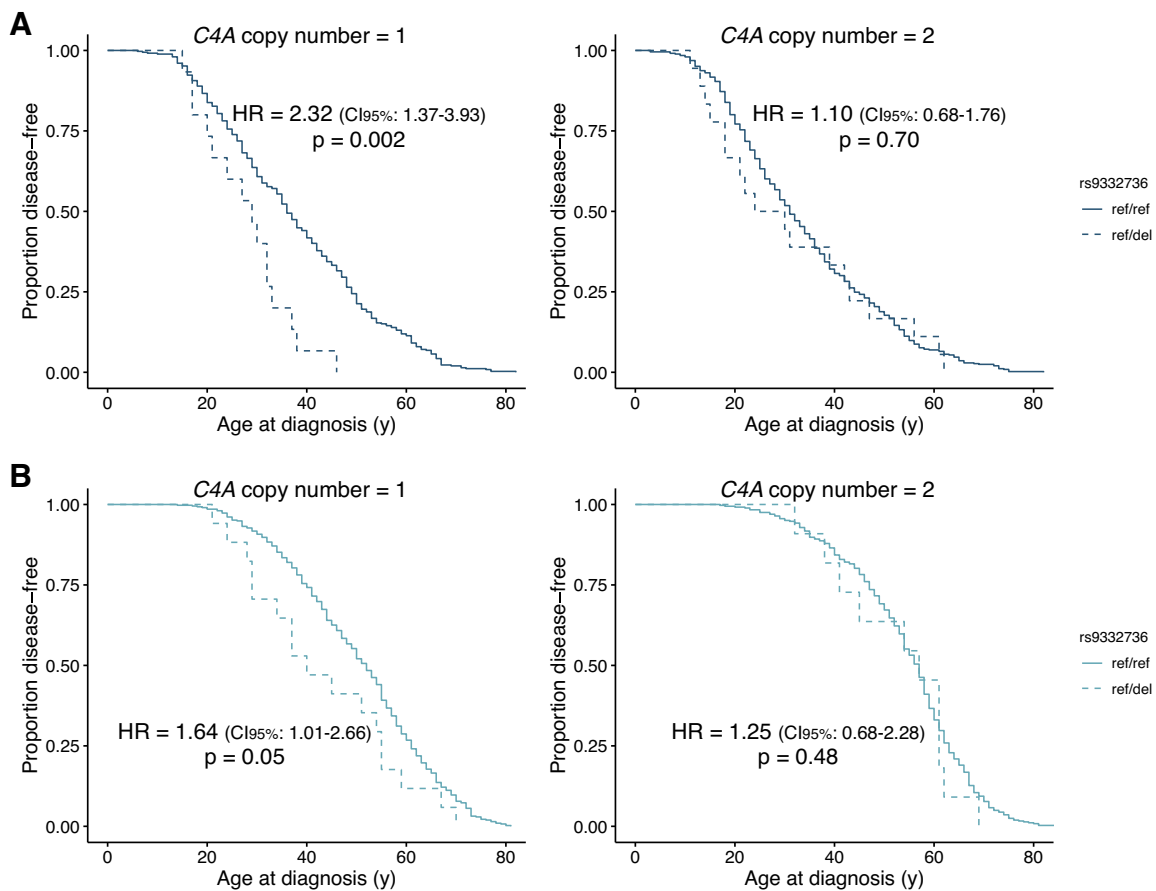


**Figure 3.** Age at diagnosis of systemic lupus erythematosus (SLE) and primary Sjögren's syndrome (SS) among patients with the 28-bp *C2* deletion rs9332736 (ref/del) relative to SLE patients and primary SS patients with normal *C2* (ref/ref). Kaplan-Meier plots depict the age at diagnosis of SLE in those with the 28-bp *C2* deletion rs9332736 and 1 *C4A* copy ( $n = 15$ ) or 2 *C4A* copies ( $n = 18$ ), relative to SLE patients with normal *C2* and 1 *C4A* copy ( $n = 352$ ) or 2 *C4A* copies ( $n = 446$ ) (A), and age at diagnosis of primary SS in those with the 28-bp *C2* deletion rs9332736 and 1 *C4A* copy ( $n = 17$ ) or 2 *C4A* copies ( $n = 11$ ), relative to primary SS patients with normal *C2* and 1 *C4A* copy ( $n = 412$ ) or 2 *C4A* copies ( $n = 363$ ) (B). Data were analyzed using a Cox proportional hazards regression model adjusted for sex and *C4B* copy number. HR = hazard ratio; 95% CI = 95% confidence interval. Color figure can be viewed in the online issue, which is available at <http://onlinelibrary.wiley.com/doi/10.1002/art.42270/abstract>.

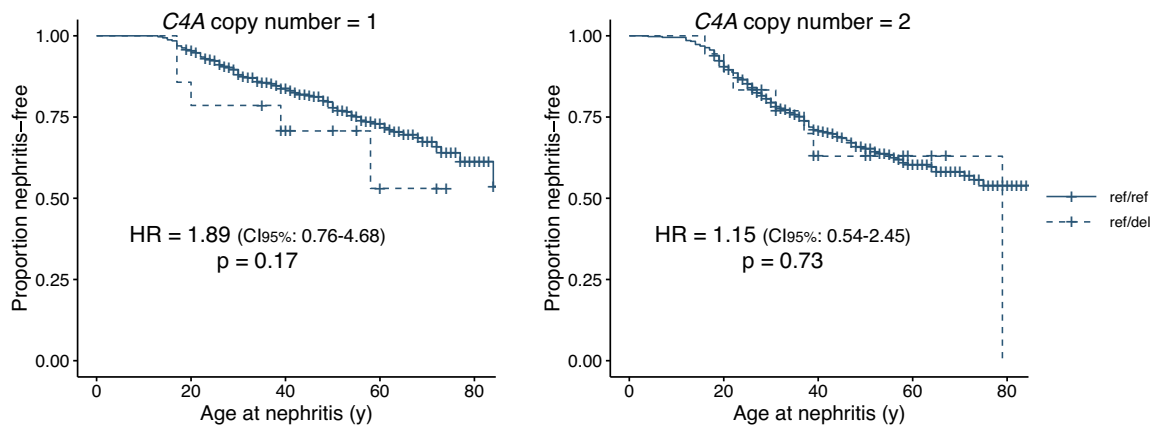


**Figure 4.** Age at first occurrence of nephritis in SLE patients. The Kaplan-Meier plot depicts age at first nephritis event in SLE patients with the 28-bp *C2* deletion rs9332736 and 1 *C4A* copy ( $n = 14$ ) or 2 *C4A* copies ( $n = 18$ ), and in SLE patients with normal *C2* and 1 *C4A* copy ( $n = 322$ ) or 2 *C4A* copies ( $n = 412$ ). Data were analyzed using a Cox proportional hazards regression model adjusted for sex and *C4B* copy number. See Figure 3 for definitions. Color figure can be viewed in the online issue, which is available at <http://onlinelibrary.wiley.com/doi/10.1002/art.42270/abstract>.

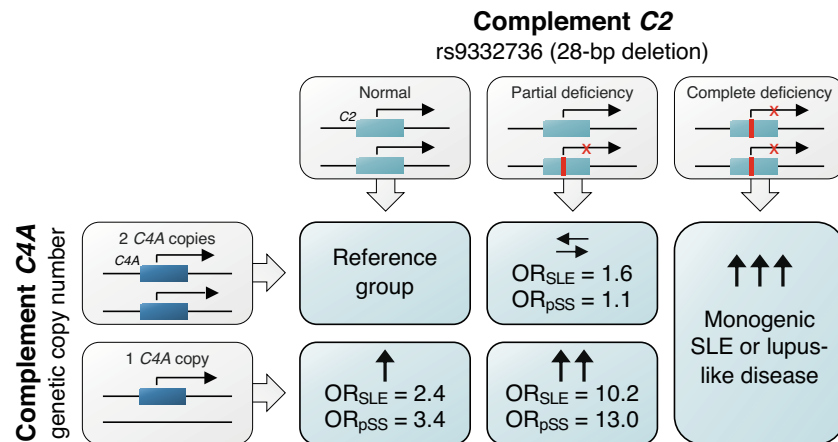


**Figure 5.** Summary of the conduct of the study. Homozygosity of the 28-bp deletion rs9332736 in C2 is associated with monogenic lupus. Heterozygous individuals are not at risk of SLE or primary SS if they have 2 or more copies of C4A, whereas individuals heterozygous for rs9332736 who have 1 copy of C4A are at substantial risk of both SLE and primary SS. OR = odds ratio (see Figure 3 for other definitions).

difference was seen in the age at first occurrence of nephritis between SLE patients with normal C2 and SLE patients heterozygous for 28-bp C2 deletion who had 2 copies of C4A ( $P$  for rs9332736 = 0.73) (Figure 4).

In a previous study by our group, we found a strong association between C4A copy number and the presence of autoantibodies against SSA/Ro and SSB/La in systemic inflammatory autoimmune diseases (18), and therefore, we evaluated whether rs9332736 affected the presence of autoantibodies in SLE and primary SS. However, analysis of SSA/Ro, SSB/La, anti-U1 RNP, anti-Sm, and antiphospholipid antibodies in SLE and primary SS patients only showed minor differences when evaluating the role of the 28-bp C2 deletion (Supplementary Figures 3A–E, <http://onlinelibrary.wiley.com/doi/10.1002/art.42270>). Further, the sex distribution of patients with heterozygous C2 deficiency did not differ from that of patients with normal C2 (Supplementary Figure 3F).

Overall, we detected earlier onsets of disease for both SLE and primary SS patients heterozygous for the 28-bp C2 deletion rs9332736 when present in combination with a C4A copy number of 1. A similar but not significant association was seen between heterozygous 28-bp C2 deletion and age at the first occurrence of nephritis in SLE patients, although this needs to be verified in a larger cohort.

**Monogenic SLE and primary SS due to complete C2 deficiency.** Complete C2 deficiency constitutes a major risk factor for monogenic SLE (6), and we identified 2 SLE patients homozygous for the 28-bp C2 deletion rs9332736. Interestingly, we also identified 1 primary SS patient with complete C2 deficiency due to the rs9332736 variant, and a brief clinical summary of the 3 C2-deficient patients is presented in Supplementary Figure 4 (<http://onlinelibrary.wiley.com/doi/10.1002/art.42270>). None of the population controls were homozygous for the rs9332736 deletion.

## DISCUSSION

In the current study, we observed that heterozygous C2 deficiency in combination with a low copy number of C4A substantially increases the risk of both SLE and primary SS (summarized in Figure 5). Further, this genetic combination was also found to be associated with lower age at diagnosis. Although only 1.5% of the patient cohort was observed to have heterozygous C2 deficiency in combination with a C4A copy number of 1, these characteristics still explain a likely genetic cause of disease at a much larger proportion of patients than can be explained by monogenic disease. In comparison, 0.18% of population controls carried the combination of rs9332736 heterozygosity and a C4A copy number of 1. As we had no clinical information for the population controls, we were not able to describe whether these individuals were diagnosed as having SLE or primary SS. Further, a previous study on combined heterozygous deficiencies of C2 and C4 involving 6 families did not find that all individuals with the C2/C4A risk combination had clinical symptoms (10), suggesting an incomplete penetrance.

In addition to heterozygous C2 deficiency, we also identified 3 patients with homozygous C2 deficiency. Interestingly, one of the patients with homozygous C2 deficiency was diagnosed as having primary SS. Homozygous C2 deficiency has mainly been associated with the risk of severe infections and SLE, but other rheumatic diseases, such as undifferentiated connective tissue disease and vasculitis, have also been described (5,6,11). Further, Sjögren's syndrome has been described as a condition secondary to SLE and vasculitis in patients with complete C2 deficiency, showing that the absence of C2 may cause a range of different manifestations (6,10). In the present study, low levels of anti-Scl-70 were observed in the patient with primary SS, suggesting a risk of developing systemic sclerosis or a potential overlap between primary SS and other systemic autoimmune diseases (31).

Both *C2* and *C4A* are located in the *HLA* region on chromosome 6, and previous studies have shown that the copy number of *C4A* is inversely correlated with the *DRB1\*03:01* allele that is a risk factor for both SLE and primary SS in populations of European ancestry (32). Still, the findings of recent studies involving participants of various ancestries suggest that the copy number of *C4A* is a causative factor for SLE and primary SS as it has consistently been found to be a risk factor across all populations studied (14,17). In addition, complete deficiency of the genes *C1Q*, *C1R*, *C1S*, *C4*, and *C2* are among the strongest risk factors for monogenic SLE. The apparent interaction between *C4A* copy number and heterozygous *C2* deficiency that was found in this study further strengthens the pivotal role of the classical complement pathway in the pathogenesis of both SLE and primary SS, indicating that impaired function of this pathway may lead to disease.

The increased risk of disease for individuals heterozygous for rs9332736 who also had a *C4A* copy number of 1 translated directly into lower age at diagnosis for both SLE and primary SS patients, whereas heterozygous *C2* deficiency did not affect the age of diagnosis among patients with 2 *C4A* copies. This is in line with the observation that heterozygous *C2* deficiency is only a genetic risk factor for SLE and primary SS when present in combination with a *C4A* copy number of 1. Also, we noted a weak tendency toward earlier development of nephritis for SLE patients with heterozygous *C2* deficiency and a low *C4A* copy number, although this was not significant and should be verified in a larger cohort. We did not see any associations between rs9332736 and specified autoantibodies and other clinical manifestations, which may have been due to low statistical power in the cross-sectional analyses.

The relationship between deficiencies in the early classical complement pathway and SLE has generally been ascribed to impaired clearance of apoptotic cells and defective handling of immune complexes, which may lead to the loss of self tolerance, the activation of self-reactive immune cells, and the production of autoantibodies (1,33). Alternatively, aberrant activation of the complement system may also lead to disease, and levels of *C3* and *C4* together with classical complement function (e.g., CH50) are currently used as biomarkers for complement activation in the classification of SLE (34) as well as in the evaluation of disease activity in patients with SLE (35). However, the common genetic causes of low complement, such as variation in *C4* copy number and heterozygous *C2* deficiency, obscure the diagnostic utility of these measures, and genetic analyses may add useful information in this regard. In patients with primary SS, the complement cascade has been studied to a lesser extent, but the results of the present study further highlight the role of the classical complement pathway in primary SS patients, and previous studies have shown that complement status may have prognostic value with regard to disease activity and adverse outcomes in primary SS (36,37).

Finally, while the 28-bp *C2* deletion rs9332736 exists in all populations of European descent, it is relatively uncommon in African and Asian populations (Supplementary Tables 2 and 3, [\[onlinelibrary.wiley.com/doi/10.1002/art.42270\]\(http://onlinelibrary.wiley.com/doi/10.1002/art.42270\)\), and therefore, the current results do not apply globally. However, other loss-of-function \*C2\* variants have been described \(38–40\), and as a low \*C4A\* copy number has been found to be common in all populations \(14,17\), the combination of heterozygous deficiencies of \*C2\* and \*C4A\* may also be a risk factor for patients of other ethnicities.](http://</a></p></div><div data-bbox=)

In conclusion, we report that heterozygous *C2* deficiency is a strong risk factor for SLE and primary SS when present together with a low *C4A* copy number. These results show that partial deficiencies affecting multiple genes of the classical complement pathway may increase the risk of disease substantially when present in combination, thereby emphasizing the role of the complement system in systemic inflammatory autoimmune diseases.

## ACKNOWLEDGMENTS

DNA sequencing and genotyping were performed at the SNP&SEQ Technology Platform in Uppsala, part of the National Genomics Infrastructure Sweden and Science for Life Laboratory. Computations were enabled by resources in projects sens2017142 and sens2020577, provided by the Swedish National Infrastructure for Computing at the Uppsala Multidisciplinary Center for Advanced Computational Science. Members of the DISSECT consortium and the ImmunoArray consortium are listed in the Supplementary Information.

## AUTHOR CONTRIBUTIONS

All authors were involved in drafting the article or revising it critically for important intellectual content, and all authors approved the final version to be published. Dr. Lundtoft had full access to all of the data in the study and takes responsibility for the integrity of the data and the accuracy of the data analysis.

**Study conception and design.** Lundtoft, Sjöwall, Rantapää-Dahlqvist, Bengtsson, Jönsen, Svenungsson, Leonard, Rönnblom.

**Acquisition of data.** Lundtoft, Sjöwall, Rantapää-Dahlqvist, Bengtsson, Jönsen, Pucholt, Wu, Lundström, Eloranta, Gunnarsson, Baecklund, Jonsson, Hammenfors, Forsblad-d'Elia, Eriksson, Mandl, Bucher, Norheim, Johnsen, Omdal, Kvarnström, Wahren-Herlenius, Truedsson, Nilsson, Kozyrev, Bianchi, Lindblad-Toh, Yu, Nordmark, Sandling, Svenungsson, Leonard, Rönnblom.

**Analysis and interpretation of data.** Lundtoft, Sjöwall, Rantapää-Dahlqvist, Bengtsson, Jönsen, Pucholt, Yu, Sandling, Svenungsson, Leonard, Rönnblom.

## ADDITIONAL DISCLOSURES


Author Pucholt is an employee of Olink Proteomics. Author Mandl is an employee of Novartis.

## REFERENCES

1. Sturfelt G, Truedsson L. Complement in the immunopathogenesis of rheumatic disease [review]. *Nat Rev Rheumatol* 2012;8:458.
2. Macedo ACL, Isaac L. Systemic lupus erythematosus and deficiencies of early components of the complement classical pathway [review]. *Front Immunol* 2016;7:55.
3. Lintner KE, Wu YL, Yang Y, et al. Early components of the complement classical activation pathway in human systemic autoimmune diseases [review]. *Front Immunol* 2016;7:36.

4. Truedsson L, Sturfelt G, Nived O. Prevalence of the type I complement C2 deficiency gene in Swedish systemic lupus erythematosus patients. *Lupus* 1993;2:325–7.
5. Jönsson G, Truedsson L, Sturfelt G, et al. Hereditary C2 deficiency in Sweden: frequent occurrence of invasive infection, atherosclerosis, and rheumatic disease. *Medicine (Baltimore)* 2005;84:23–34.
6. Jönsson G, Sjöholm AG, Truedsson L, et al. Rheumatological manifestations, organ damage and autoimmunity in hereditary C2 deficiency. *Rheumatology (Oxford)* 2007;46:1133–9.
7. Johnson CA, Densen P, Hurford RK, et al. Type I human complement C2 deficiency. A 28-base pair gene deletion causes skipping of exon 6 during RNA splicing. *J Biol Chem* 1992;267:9347–53.
8. Belot A, Rice GI, Omarjee SO, et al. Contribution of rare and predicted pathogenic gene variants to childhood-onset lupus: a large, genetic panel analysis of British and French cohorts. *Lancet Rheumatol* 2020;2:e99–109.
9. Sullivan KE, Petri MA, Schmeckpeper BJ, et al. Prevalence of a mutation causing C2 deficiency in systemic lupus erythematosus. *J Rheumatol* 1994;21:1128–33.
10. Hartmann D, Fremeaux-Bacchi V, Weiss L, et al. Combined heterozygous deficiency of the classical complement pathway proteins C2 and C4. *J Clin Immunol* 1997;17:176–84.
11. Lipsker DM, Schreckenberger-Gilliot C, Uring-Lambert B, et al. Lupus erythematosus associated with genetically determined deficiency of the second component of the complement. *Arch Dermatol* 2000;136:1508–14.
12. Yang WJ, Rich E, Saint-Cyr C, et al. Hereditary heterozygous C2 deficiency: variable clinical and serological manifestations among three sisters [review]. *Curr Rheumatol Rev* 2017;13:158–60.
13. Yang Y, Chung EK, Wu YL, et al. Gene copy-number variation and associated polymorphisms of complement component C4 in human systemic lupus erythematosus (SLE): low copy number is a risk factor for and high copy number is a protective factor against SLE susceptibility in European Americans. *Am J Hum Genet* 2007;80:1037–54.
14. Chen JY, Ling Wu Y, Yin Mok M, et al. Effects of complement C4 gene copy number variations, size dichotomy, and C4A deficiency on genetic risk and clinical presentation of systemic lupus erythematosus in East Asian populations. *Arthritis Rheumatol* 2016;68:1442–53.
15. Tsang-A-Sjoe MW, Bultink IE, Korswagen LA, et al. Comprehensive approach to study complement C4 in systemic lupus erythematosus: gene polymorphisms, protein levels and functional activity. *Mol Immunol* 2017;92:125–31.
16. Jüptner M, Flachsbarth F, Caliebe A, et al. Low copy numbers of complement C4 and homozygous deficiency of C4A may predispose to severe disease and earlier disease onset in patients with systemic lupus erythematosus. *Lupus* 2018;27:600–9.
17. Kamitaki N, Sekar A, Handsaker RE, et al. Complement genes contribute sex-biased vulnerability in diverse disorders. *Nature* 2020;582:577–81.
18. Lundtoft C, Pucholt P, Martin M, et al. Complement C4 copy number variation is linked to SSA/Ro and SSB/La autoantibodies in systemic inflammatory autoimmune diseases. *Arthritis Rheumatol* 2022;74:1440–50.
19. Sandling JK, Pucholt P, Rosenberg LH, et al. Molecular pathways in patients with systemic lupus erythematosus revealed by gene-centred DNA sequencing. *Ann Rheum Dis* 2021;80:109–17.
20. Thorlacius GE, Hultin-Rosenberg L, Sandling JK, et al. Genetic and clinical basis for two distinct subtypes of primary Sjögren's syndrome. *Rheumatology (Oxford)* 2021;60:837–48.
21. Tan EM, Cohen AS, Fries JF, et al. The 1982 revised criteria for the classification of systemic lupus erythematosus. *Arthritis Rheum* 1982;25:1271–7.
22. Vitali C, Bombardieri S, Jonsson R, et al. Classification criteria for Sjögren's syndrome: a revised version of the European criteria proposed by the American-European Consensus Group. *Ann Rheum Dis* 2002;61:554.
23. Eriksson D, Bianchi M, Landegren N, et al. Extended exome sequencing identifies BACH2 as a novel major risk locus for Addison's disease. *J Intern Med* 2016;280:595–608.
24. Ameer A, Dahlberg J, Olason P, et al. SweGen: a whole-genome data resource of genetic variability in a cross-section of the Swedish population. *Eur J Hum Genet* 2017;25:1253.
25. Xie C, Yeo ZX, Wong M, et al. Fast and accurate HLA typing from short-read next-generation sequence data with xHLA. *Proc Natl Acad Sci* 2017;114:8059.
26. Grosso G, Sandholm K, Antovic A, et al. The complex relationship between C4b-binding protein, warfarin, and antiphospholipid antibodies. *Thromb Haemost* 2021;121:1299–309.
27. Svenungsson E, Gustafsson JT, Grosso G, et al. Complement deposition, C4d, on platelets is associated with vascular events in systemic lupus erythematosus. *Rheumatology (Oxford)* 2020;59:3264–74.
28. Nilsson UR, Nilsson B. Simplified assays of hemolytic activity of the classical and alternative complement pathways. *J Immunol Methods* 1984;72:49–59.
29. Angioi A, Fervenza FC, Sethi S, et al. Diagnosis of complement alternative pathway disorders. *Kidney Int* 2016;89:278–88.
30. R Core Team. R: A language and environment for statistical computing; 2018. URL: <https://www.R-project.org/>.
31. Ramos-Casals M, Nardi N, Brito-Zerón P, et al. Atypical autoantibodies in patients with primary Sjögren Syndrome: clinical characteristics and follow-up of 82 cases. *Semin Arthritis Rheum* 2006;35:312–21.
32. Boteva L, Morris DL, Cortés-Hernández J, et al. Genetically determined partial complement C4 deficiency states are not independent risk factors for SLE in UK and Spanish populations. *Am J Hum Genet* 2012;90:445–56.
33. Leffler J, Bengtsson AA, Blom AM. The complement system in systemic lupus erythematosus: an update. *Ann Rheum Dis* 2014;73:1601.
34. Petri M, Orbai AM, Alarcón GS, et al. Derivation and validation of the Systemic Lupus International Collaborating Clinics classification criteria for systemic lupus erythematosus. *Arthritis Rheum* 2012;64:2677–86.
35. Gladman DD, Ibañez D, Urowitz MB. Systemic lupus erythematosus disease activity index 2000. *J Rheumatol* 2002;29:288.
36. Ramos-Casals M, Brito-Zerón P, Yagüe J, et al. Hypocomplementaemia as an immunological marker of morbidity and mortality in patients with primary Sjögren's syndrome. *Rheumatology (Oxford)* 2004;44:89–94.
37. Jordán-González P, Gago-Piñero R, Varela-Rosario N, et al. Characterization of a subset of patients with primary Sjögren's syndrome initially presenting with C3 or C4 hypocomplementemia. *Eur J Rheumatol* 2020;7:112–7.
38. Wetsel RA, Kulics J, Lokki ML, et al. Type II human complement C2 deficiency: allele-specific amino acid substitutions (Ser189 →Phe; Gly444 →Arg) cause impaired C2 secretion. *J Biol Chem* 1996;271:5824–31.
39. Wang X, Circolo A, Lokki M, et al. Molecular heterogeneity in deficiency of complement protein C2 type I. *Immunology* 1998;93:184.
40. El Sissy C, Rosain J, Vieira-Martins P, et al. Clinical and genetic spectrum of a large cohort with total and sub-total complement deficiencies. *Front Immunol* 2019;10:1936.

# Joint-Specific Memory and Sustained Risk for New Joint Accumulation in Autoimmune Arthritis

Margaret H. Chang,<sup>1</sup> Alexandra V. Bocharnikov,<sup>2</sup> Siobhan M. Case,<sup>3</sup> Marc Todd,<sup>1</sup> Jessica Laird-Gion,<sup>1</sup> Maura Alvarez-Baumgartner,<sup>2</sup> and Peter A. Nigrovic<sup>3</sup> 

**Objective.** Inflammatory arthritides exhibit hallmark patterns of affected and spared joints, but in each individual, arthritis affects only a subset of all possible sites. The purpose of this study was to identify patient-specific patterns of joint flare to distinguish local from systemic drivers of disease chronicity.

**Methods.** Patients with juvenile idiopathic arthritis followed without interruption from disease onset into adulthood were identified across 2 large academic centers. Joints inflamed at each visit were established by medical record review. Flare was defined as physician-confirmed joint inflammation following documented inactive disease.

**Results.** Among 222 adults with JIA, 95 had complete serial joint examinations dating from disease onset in childhood. Mean follow-up was 12.5 years (interquartile range 7.9–16.7 years). Ninety (95%) of 95 patients achieved inactive disease, after which 81% (73 patients) experienced at least 1 flare. Among 940 joints affected in 253 flares, 74% had been involved previously. In flares affecting easily observed large joint pairs where only 1 side had been involved before ( $n = 53$ ), the original joint was affected in 83% and the contralateral joint in 17% ( $P < 0.0001$  versus random laterality). However, disease extended to at least 1 new joint in ~40% of flares, a risk that remained stable even decades after disease onset, and was greatest in flares that occurred while patients were not receiving medication (54% versus 36% of flares occurring with therapy; odds ratio 2.09,  $P = 0.015$ ).

**Conclusion.** Arthritis flares preferentially affect previously inflamed joints but carry an ongoing risk of disease extension. These findings confirm joint-specific memory and suggest that prevention of new joint accumulation should be an important target for arthritis therapy.

## INTRODUCTION

Inflammatory arthritis encompasses a heterogeneous set of disorders affecting children and adults. While joint inflammation is the hallmark of these conditions, other tissues can also be involved, such as the lung in rheumatoid arthritis (RA) and the eye in early-onset juvenile idiopathic arthritis (JIA). Extensive study has therefore been dedicated to understanding the systemic immune drivers of autoimmune arthritis (1).

However, systemic autoimmunity is insufficient to explain the presentation of arthritis in the clinic. Beyond the broad disease patterns characterizing distinct forms of arthritis, each patient exhibits an individual pattern of joints that are involved or spared, both with respect to the type of joint (e.g., wrist, knee) and laterality. This phenomenon was first described more than 30 years ago by Roberts and colleagues, who found that most joints ever involved in an individual with RA, including all joints needing subsequent joint replacement, were already affected in the first year of disease (2). Consistent with this result, analysis of RA patients

---

Dr. Chang's work was supported by a Rheumatology Research Foundation Scientist Development Award, Boston Children's Hospital Lovejoy Award, the National Institute of Allergy and Infectious Diseases, NIH (award T32-AI-007512), the National Institute of Child Health and Human Development, NIH (award K12-HD-052896), the National Institute of Arthritis and Musculoskeletal and Skin Diseases, NIH (award K08-AR-080992), and a Translation Accelerator grant from the Human Skin Disease Research (award P30-AR-069625). Dr. Bocharnikov's work was supported by a Medical Student Preceptorship from the Rheumatology Research Foundation. Dr. Nigrovic's work was supported by an Innovative Research Grant from the Rheumatology Research Foundation, National Institute of Arthritis and Musculoskeletal and Skin Diseases, NIH (awards 2R01-AR-065538, R01-AR-075906, R01-AR-073201, and P30-AR-070253), the Fundación Bechara, and the Arbuckle Family Fund for Arthritis Research.

<sup>1</sup>Margaret H. Chang, MD, PhD, Marc Todd, BS, Jessica Laird-Gion, MD: Division of Immunology, Boston Children's Hospital, Boston, Massachusetts; <sup>2</sup>Alexandra V. Bocharnikov, MD, Maura Alvarez-Baumgartner, MD: Division of Rheumatology, Inflammation, and Immunity, Brigham and Women's Hospital, Boston, Massachusetts; <sup>3</sup>Siobhan M. Case, MD, MHS, Peter A. Nigrovic, MD: Division of Immunology, Boston Children's Hospital and Division of Rheumatology, Inflammation, and Immunity, Brigham and Women's Hospital, Boston, Massachusetts.

Author disclosures are available at <https://onlinelibrary.wiley.com/action/downloadSupplement?doi=10.1002%2Fart.42240&file=art42240-sup-0001-Disclosureform.pdf>.

Address correspondence via email to Peter A. Nigrovic, MD, at [peter.nigrovic@childrens.harvard.edu](mailto:peter.nigrovic@childrens.harvard.edu).

Submitted for publication February 16, 2022; accepted in revised form May 17, 2022.

in the Behandel Strategieën (BeSt) study showed that joints swollen at baseline were at higher risk of subsequent swelling, with wrists, metacarpophalangeal (MCP) joints, and metatarsophalangeal (MTP) joints reaching recurrence rates of 60% (3). These observations suggest that, in addition to systemic autoimmunity, factors local to individual joints render them susceptible to subsequent inflammation.

The pathogenic implications of such “joint-specific memory” are profound. If individual joints retain a predilection to flare, even through a period of remission, then there must exist long-lived site-specific mechanisms that drive disease chronicity in addition to the “original sin” of systemic autoimmunity. Identification and treatment of these local mechanisms could offer new avenues to durable joint-specific therapy.

To understand the relative contributions of joint-specific versus systemic factors to the localization of arthritis flares, we studied patients with JIA who were followed up without interruption from disease onset to adulthood at Boston Children’s Hospital and at a specialized clinic in the adjoining Brigham and Women’s Hospital (the Center for Adults with Pediatric Rheumatic Illness [CAPRI]). Historical and genetic evidence increasingly render a categorical division between childhood-onset and adult-onset arthritis biologically untenable (4,5). However, the patterns of arthritis observed in children differ from those observed in adults, including a greater prevalence of oligoarticular large-joint arthritis for which it is simpler to identify laterality than in RA, a highly polyarticular disease with a predilection for small joints (1,6). Further, the use of nonbiologic and biologic disease-modifying antirheumatic drugs (DMARDs) has enabled achievement of inactive disease in most patients with JIA, although flares remain common, affording an ideal opportunity to evaluate whether individual joints retain a tendency to flare through periods of remission (7).

In this study, we demonstrate that JIA flares display unambiguous joint-specific memory as reflected in preserved joint laterality. However, many patients continue to develop inflammation in new joints, even a decade or more after disease onset, confirming both local and systemic drivers of arthritis chronicity. Paired together, these findings suggest a new paradigm, termed here the joint accumulation hypothesis, which provides a rationale for arthritis control that is both rapid and sustained.

## PATIENTS AND METHODS

We conducted a review of the medical records of patients seen in the Brigham and Women’s Hospital’s CAPRI clinic between 2005 and 2017. Patients with JIA were evaluated to determine whether they also had medical records with the rheumatology clinic at Boston Children’s Hospital detailing their disease course since onset. Patients were excluded if care was interrupted, for example by care at another facility, or if insufficient documentation was available in the electronic medical record to determine clinical status at each clinic visit.

Patient records were reviewed for the following information for each patient: age at the time that JIA was diagnosed, age at transfer to CAPRI, the JIA classification assigned according to the International League of Associations for Rheumatology 2001 classification (8), treatments employed, and the joints inflamed at each visit. Inactive disease was defined as normal findings on physical examination, with no joint swelling or other evidence of active arthritis, in the judgement of the attending physician. Disease activity scales were not routinely employed by physicians and therefore were not considered. Arthritis flare was defined as an episode of physician-confirmed joint inflammation following physician-documented inactive disease. MCP and MTP joints within each hand or foot were counted as 1 joint, as were proximal interphalangeal (PIP) joints and distal interphalangeal (DIP) joints, since the individual joints affected in these groups were often not documented precisely by the treating clinician.

Statistical comparisons were performed using a 2-tailed exact binomial test, the Mantel-Cox test, or Spearman’s correlation, as indicated. Fisher’s exact test was used to evaluate the independence of 2 variables. *P* values less than 0.05 were considered statistically significant. This study was approved by the Institutional Review Boards of the Brigham and Women’s Hospital and Boston Children’s Hospital.

## RESULTS

**Patient cohort.** Of the 222 patients treated for JIA in CAPRI between 2005 and 2017, 109 had been cared for in the pediatric rheumatology program at Boston Children’s Hospital and had available medical records. Ten patients underwent care elsewhere before transferring to CAPRI, and 4 patients had insufficient records to assess which joints were involved throughout the disease course, leaving 95 patient records for detailed review (Figure 1).

**Patient demographics.** Most patients included in this study were female (77%). The mean age at JIA diagnosis was 11.5 years, and the mean age at transition to CAPRI was 21.5 years. The mean duration of follow-up was 12.5 years, with the longest patient continuity at 21.4 years. Of the 95 patients included in this study, 13% had oligoarticular JIA, 43% had polyarticular JIA (35% of whom were seropositive for rheumatoid factor [RF]), 12% had psoriatic JIA, 14% had enthesitis related arthritis, 7% had systemic JIA, and 11% had undifferentiated JIA. With regard to treatment, 79% of patients had received prescription nonsteroidal antiinflammatory drugs (NSAIDs) at any point during their disease course, 29% had received systemic steroids, and 24% had received intraarticular steroid injections. Additionally, 89% of patients had received conventional synthetic DMARDs (csDMARDs; methotrexate, leflunomide, hydroxychloroquine, or sulfasalazine) at any point during the course of their disease, while 70% had received a biologic DMARD (bDMARD;

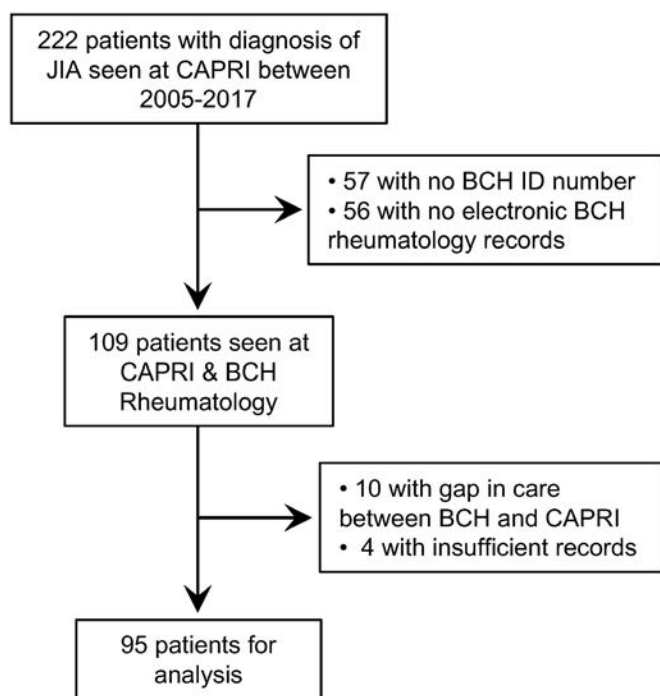


**Figure 1.** Flowchart showing juvenile idiopathic arthritis (JIA) patients initially evaluated in the Center for Adults with Pediatric Rheumatic Illness (CAPRI) who were followed up longitudinally from the rheumatology clinic at Boston Children's Hospital (BCH).

etanercept, adalimumab, infliximab, rituximab, abatacept, tocilizumab, anakinra, or canakinumab). Only 1 patient treated with bDMARDs never received csDMARDs at any point in their disease course (Table 1).

**Table 1.** Demographic and clinical characteristics of the JIA patients at baseline (n = 95)\*

Female sex, no. (%)	73 (77)
Age at diagnosis, mean $\pm$ SD years	11.5 $\pm$ 5.2
Age at transition to CAPRI, mean $\pm$ SD years	21.5 $\pm$ 2.5
Age at last follow-up visit, mean $\pm$ SD years	23.7 $\pm$ 3.4
Duration of follow-up, median (IQR) years	12.3 (7.9–16.7)
JIA diagnosis, final	
Oligoarticular, persistent	5 (5)
Oligoarticular, extended	8 (8)
Polyarticular, RF seronegative	27 (28)
Polyarticular, RF seropositive	14 (15)
Psoriatic	11 (12)
ERA	13 (14)
Systemic	7 (7)
Undifferentiated	10 (11)
Medications	
NSAIDs	75 (79)
Steroids, intraarticular	23 (24)
Steroids, systemic	28 (29)
DMARDs, nonbiologic	85 (89)
DMARDs, biologic	67 (70)

\* Except where indicated otherwise, values are the number (%) of patients. JIA = juvenile idiopathic arthritis; CAPRI = Center for Adults with Pediatric Rheumatic Illness; IQR = interquartile range; RF = rheumatoid factor; ERA = enthesitis related arthritis; NSAIDs = nonsteroidal antiinflammatory drugs; DMARDs = disease-modifying antirheumatic drugs.

### Association of the availability of bDMARDs with reduced time to inactive disease.

Ninety patients (95%) achieved inactive disease at some point in their disease course. We assessed the duration between presentation to a pediatric rheumatology clinic and first documented physical examination with normal results, finding that 50% of patients achieved inactive disease by 0.96 years after initial presentation (Figure 2A). Given the timeframe of this study, this cohort included patients diagnosed both before and after bDMARDs were available, since 45 patients (47%) were diagnosed as having JIA before etanercept was approved by the US Food and Drug Administration for the treatment of JIA in May 1999 (9). Given the gradual uptake of these treatments in pediatric rheumatology, the threshold at which 25% of patients in this cohort had received bDMARDs was achieved only in 2005 (see Supplementary Figure 1, available on the *Arthritis & Rheumatology* website at <http://onlinelibrary.wiley.com/doi/10.1002/art.42240>).

Considering those patients diagnosed as having JIA before 2005 to fall within the “pre-biologic era” and those diagnosed after 2005 to fall within the “biologic era”, we observed a substantially shorter time from first visit in a rheumatology clinic to the first recording of inactive disease in patients diagnosed during the biologic era (50% of patients diagnosed during the biologic era achieving inactive disease by 0.60 years versus 1.05 years for patients diagnosed during the pre-biologic era;  $P = 0.001$ ) (Figure 2B). Correspondingly, 56 of the 61 patients diagnosed during the pre-biologic era (92%) received prescribed NSAIDs while 21 (34%) received systemic glucocorticoids, and 19 of the 34 patients diagnosed during the biologic era (56%) received prescribed NSAIDs ( $P = 0.0001$  by 2-tailed Fisher's exact test) while 7 (21%) received systemic glucocorticoids ( $P = 0.24$  by 2-tailed Fisher's exact test) (Table 1). Since the CAPRI cohort is limited to patients who sought care as adults, these values do not reflect JIA as a whole but are consistent with the known efficacy of biologic agents and thus support the face validity of the data.

### Preferential flare of arthritis in previously inflamed joints.

Among the 90 patients who achieved inactive disease, 73 (81%) experienced at least 1 arthritis flare, totaling 253 distinct flares involving 940 joints. Flares were most common soon after diagnosis but could also be observed late in the disease course (Figure 3A). While the triggers for 51% of flares were unknown or not documented, 4% of flares followed missed doses of medication, 16% occurred during the weaning of medications, and 18% occurred after discontinuation of medication by either the patient or physician. Additionally, 9% of flares were coincident with or followed an infection, 2% were associated with trauma, and 4% were attributed to emotional stress.

Among the 940 flaring joints, 698 (74%) had been inflamed at some point before the patient entered inactive disease, while



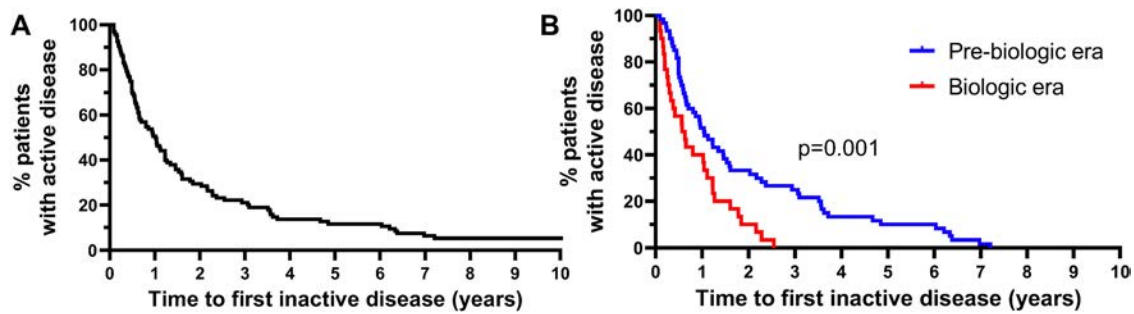


**Figure 2.** Percentage of patients attaining inactive disease over time, starting from first rheumatology clinic visit documenting active disease up to first visit documenting normal physical examination findings among all patients ( $n = 95$ , including 5 who never attained remission) (A) or first rheumatology clinic visit with active disease to first visit with documented inactive disease among patients diagnosed as having JIA before 2005 (pre-biologic era,  $n = 60$  patients) or after 2005 (biologic era,  $n = 30$  patients) (B), as assessed among the 90 patients in the cohort who attained inactive disease. The threshold of 25% of the patient cohort having received biologic therapy was reached in 2005.  $P = 0.001$  by Mantel-Cox test. Color figure can be viewed in the online issue, which is available at <http://onlinelibrary.wiley.com/doi/10.1002/art.42240/abstract>.

242 (26%) were new. Of the 253 documented flares, 151 (60%) involved no new joints, while flares that extended disease typically recruited only a few new joints (Figure 3B).

To evaluate for joint-specific memory, we analyzed flares involving paired joints wherein only 1 side had been inflamed previously ( $n = 116$  flares). In 30 (26%) of these events, inflammation developed on both sides; these flares were uninformative with respect to preserved laterality. However, in 86 (74%) of the flares involving paired joints, only 1 side became inflamed, allowing us to test whether flare distribution was stochastic (equal chance for either side) or skewed toward the side affected previously. Among these unilateral flares, 86% affected the side previously involved ( $P < 0.0001$  versus stochastic). Since DIP, PIP, MCP, and MTP joints were grouped in our analysis, prohibiting us from assessing individual joints, we repeated the analysis in flares involving paired large joints (i.e., shoulder, elbow, wrist, hips, knee, ankle), and found that 44 (83%) of 53 flares affected only the original joint, a strikingly nonrandom joint distribution ( $P < 0.0001$ ) (Figure 3C).

Intraarticular steroid injection did not evidently alter joint-specific memory. In the 13 patients with oligoarticular JIA, 11 of

12 distinct knee joints that were injected with intraarticular steroids flared again at least once. Several of the joints were injected multiple times but this did not prevent future flares from recurring in the same joint.

**New joint accumulation continues years after onset.** While recurrence of inflammation in established joints was a dominant pattern during flares, many patients continued to develop arthritis in previously uninvolved joints. This observation was illustrated by individual patients within each JIA category with the longest follow-up (Figure 4A) and was confirmed in the cohort as a whole (Figure 4B). Of the 73 patients who experienced at least 1 arthritis flare, 60 (82%) developed new joint involvement. Extension of inflammation to new joints was not restricted to early disease, as 1 patient developed arthritis in a previously spared joint 21.5 years after diagnosis. We evaluated the proportion of flares that affected new joints as a function of disease duration. Approximately 40% of flares involved at least 1 new joint, irrespective of time from diagnosis, which is consistent with a sustained propensity for recruitment of previously unaffected

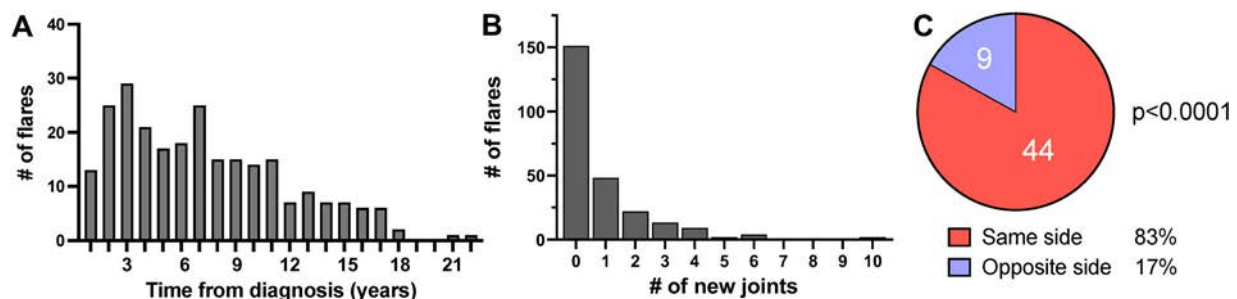


**Figure 3.** Preferential occurrence of arthritis flares over the follow-up in joints that were previously inflamed at the initial visit. A and B, Number of flares occurring at each year of follow-up after the diagnosis of juvenile idiopathic arthritis (JIA) (total number of flares = 253) (A) and distribution of number of new joints involved in each flare (B) among the 90 patients who achieved inactive disease. C, Distribution of joint inflammation in 53 flares involving paired large joints, of which only 1 joint had been affected prior to a period of inactive disease.  $P < 0.0001$  by 2-tailed exact binomial test against a stochastic 50/50 distribution. Color figure can be viewed in the online issue, which is available at <http://onlinelibrary.wiley.com/doi/10.1002/art.42240/abstract>.

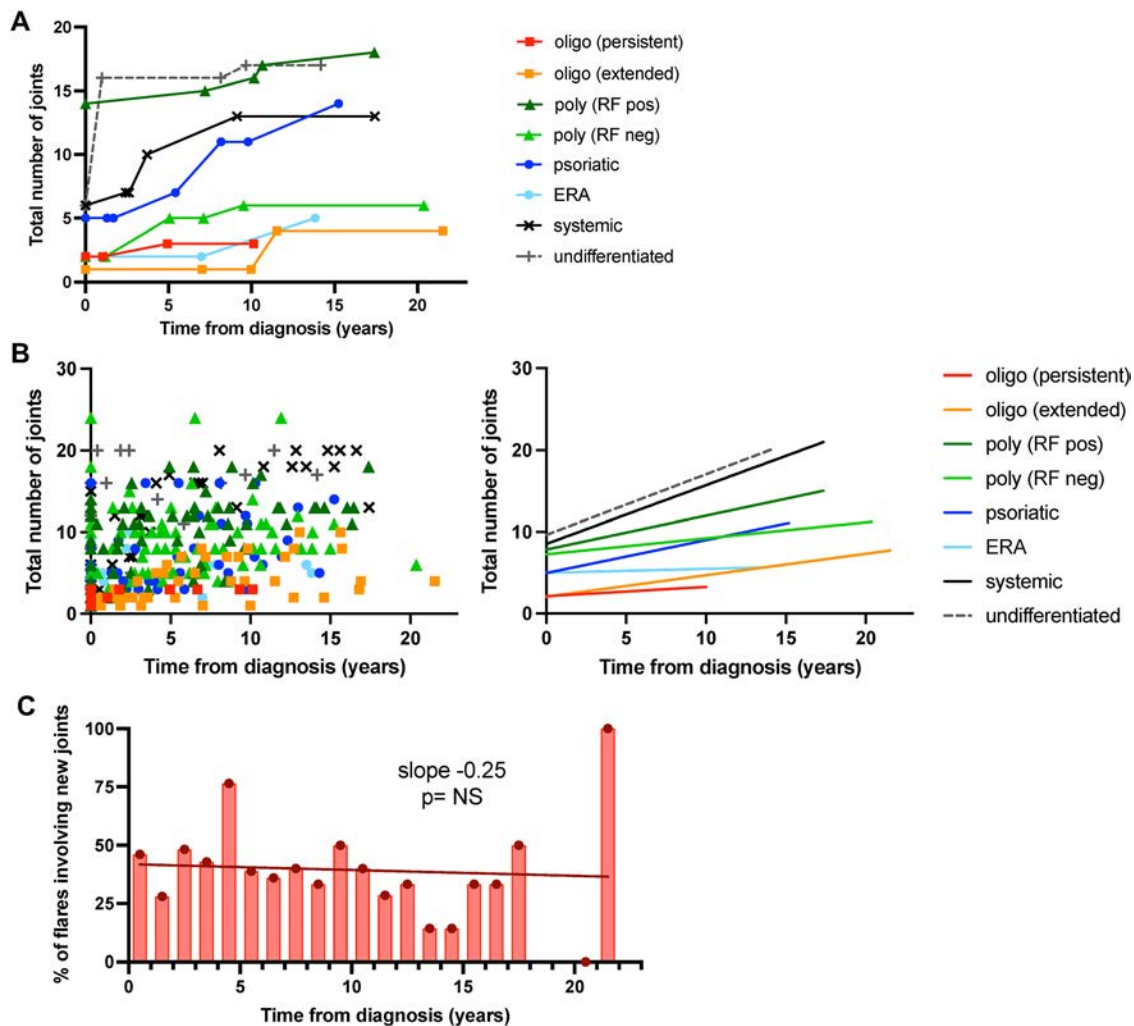


**Figure 4.** New arthritic joints accumulate during disease flares over time. **A**, Number of affected joints according to number of years from the diagnosis of juvenile idiopathic arthritis (JIA), assessed in representative patients with each JIA subtype over a follow-up of at least 10 years. Each data point reflects an encounter when a disease flare was assessed. **B**, Total number of arthritic joints involved over time. Left, Each patient contributes multiple data points and each dot represents an encounter for arthritis diagnosis or flare ( $n = 348$  encounters). Right, Linear regression curves showing the total number of affected joints over time in each JIA subtype. Correlations were assessed using Spearman's correlation test, and all correlations were significantly positive over time ( $P < 0.05$ ) except for enthesitis related arthritis (ERA). **C**, Proportion of flares involving new joints over time among all patients since diagnosis ( $n = 102$  newly affected joints,  $n = 253$  flares). Oligo = oligoarticular JIA; poly = polyarticular JIA; RF = rheumatoid factor; NS = not significant.

joints during periods of resurgent disease activity (Figure 4C and Supplementary Table 1, <http://onlinelibrary.wiley.com/doi/10.1002/art.42240>).

We found that 23% of arthritis flares occurred while patients were not receiving medications, while 77% occurred in patients receiving standing NSAIDs, oral steroids, and/or conventional or biologic DMARDs. Intriguingly, 54% of flares that occurred while patients were not receiving medications (32 of 59) involved previously unaffected joints, compared with only 36% of flares that occurred while patients were receiving medications (70 of 194) (for new joint involvement if the patient was not receiving medication at the time of flare, odds ratio 2.09 [95% confidence interval 1.16–3.80],  $P = 0.015$  by 2-tailed Fisher's exact test),

suggesting that recurrent arthritis in the absence of a protective agent poses a particularly high risk of disease extension to new sites.

## DISCUSSION

Here we provide a detailed analysis of the patterns of arthritis flares in patients with JIA who received uninterrupted longitudinal follow-up into adulthood. Our data demonstrate unambiguous joint-specific memory, reflected most clearly in the preserved laterality of flares in paired large joints through periods of remission. However, patients also exhibited ongoing risk for the accumulation of newly inflamed joints, revealing that

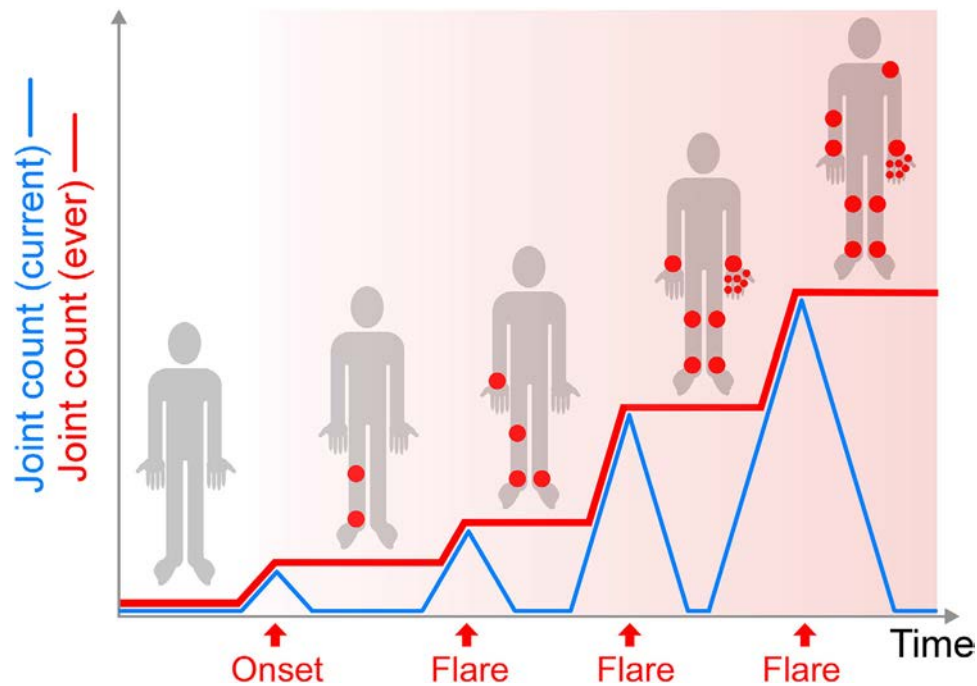


**Figure 5.** Joint accumulation hypothesis. Over the course of arthritis, the number of joints currently inflamed varies with disease activity (blue line), but the number of joints ever involved increases stepwise, leaving each patient with a progressively greater number of joints at elevated risk for subsequent flare (joints marked by red dots during periods of inactive disease). Rapid, sustained disease control that prevents accumulation of at-risk joints may render arthritis easier to control in the long term, irrespective of any “window of opportunity” in the underlying autoimmune process. Color figure can be viewed in the online issue, which is available at <http://onlinelibrary.wiley.com/doi/10.1002/art.42240/abstract>.

pathways mediating disease extension remain active in many patients even years into the course of arthritis.

Mechanisms of joint-specific memory are not yet fully elucidated. Friščić and colleagues showed that arthritis induces a persistent “primed” state in synovial fibroblasts, changing their function to intensify disease in previously inflamed joints (10). This work builds on the earlier demonstration that fibroblasts from RA joints exhibit epigenetic reprogramming (11,12). The role of local fibroblast priming in determining the location of arthritis flares is unknown.

In psoriasis and fixed drug eruptions, recurrent localized inflammation is mediated by infiltrating T cells that become anchored in tissues as resident memory T (Trm) cells (13–16). We recently identified Trm cells in RA synovium (17). Using several distinct murine arthritis models, we found that synovial Trm cells accumulate in inflamed joints and persist indefinitely during remission, nucleating site-specific recurrence when triggered by antigens through elaboration of the chemokine CCL5; correspondingly, Trm cell deletion abrogated local disease flares (17). These findings show that Trm cells form at least a part of the mechanism by which joint-specific memory arises, representing an interesting new target for site-specific disease ablation (18).

However, beyond local memory, many patients accrue newly affected joints during arthritis flares. Perhaps surprisingly, the propensity for recruitment of previously unaffected joints appeared not to wane, remaining at ~40% with each flare even decades

after disease onset in our cohort, with an even greater risk seen in patients not receiving therapy at the time of flare. These observations indicate that systemic factors underlying the development of arthritis persist even through periods of clinically inactive disease, and raise the possibility that suppressive therapy may limit disease extension even if control remains imperfect.

The paired findings of joint-specific memory and ongoing susceptibility to extension of disease have important implications for arthritis therapy. A leading model to conceptualize the benefit of early aggressive arthritis therapy in RA is the “window of opportunity hypothesis”, which postulates that effective early therapy induces a durable change in natural history by interrupting an autoimmune response that is not yet well established (19). Findings of clinical trials have suggested benefits to early intervention in terms of the prevention of structural injury and, to a much more modest extent, the achievement of drug-free remission, although a specific timeframe for intervention has proven difficult to define (20–22). Our data do not directly address whether such a window of opportunity exists, but do identify an important complementary principle that we term the joint accumulation hypothesis (Figure 5). Irrespective of any effect on the underlying autoimmune drivers of disease, effective and sustained treatment prevents inflammation from spreading to new joints that would then develop elevated risk for arthritis recurrence, such as through the acquisition of synovial Trm cells. Consistent with this possibility, delay in securing

inactive disease correlated in our cohort with a greater final number of joints accumulated, though this observation is difficult to interpret because some of this effect will reflect the greater difficulty of controlling highly polyarticular disease (data not shown). Nevertheless, since it is likely that joints that had ever been inflamed remain indefinitely at higher risk for recurrent disease than joints never affected, the prevention of disease extension is plausibly a key priority in arthritis care. This priority is independent of any theoretical window for systemic immune reprogramming and supports the importance not only of rapid achievement of inactive disease, but also of sustained maintenance of remission.

Our data provide observational evidence supporting the key role of bDMARDs in the achievement of remission in patients with JIA. We found that patients diagnosed in an era when biologics were in routine use (after 2005 in our center) achieved inactive disease 5.4 months earlier than those who did not have access to biologics and instead received more NSAIDs and, at least by trend, more systemic steroids. Other factors could have contributed to this finding, including evolving standards of care with respect to the use of csDMARDs. However, a central role for biologics in the treatment of JIA patients is consistent with their contribution to early achievement of good disease control, demonstrated in studies including the Aggressive Combination Drug Therapy in Very Early Polyarticular Juvenile Idiopathic Arthritis (ACUTE-JIA) study, the BeSt-for-Kids study, and the Start Time Optimization of Biologics in Polyarticular JIA (STOP-JIA) trial (23–27).

It is important to emphasize that our study population consisted of patients with JIA who sought rheumatology follow-up in CAPRI as adults. Among all JIA patients, ~15–20% have the polyarticular form, and only 15% of those patients are seropositive for RF (28). By contrast, in our CAPRI cohort 42% of patients had polyarticular JIA, 36% of whom were seropositive for RF, an enrichment that almost certainly reflects the fact that some children with less aggressive JIA “outgrow” their disease (29). For this reason, our data are not representative of JIA as a whole. However, since 81% of patients experienced at least 1 flare after achieving inactive disease, our cohort provided an optimal opportunity to characterize patterns of disease recurrence. The generalizability of the conclusions beyond JIA is supported by the broad clinical and biologic similarities between pediatric and adult arthritis and the concordance between our results and those found in studies of RA (2–5).

These findings suggest several directions for future investigation. It will be important to understand in detail the conceptually orthogonal mechanisms underlying local joint memory and the persistent drive to accumulate new joints. Our cohort included fewer patients with the least aggressive form of childhood arthritis, persistent oligoarticular JIA, underscoring the intriguing question of how some of these children succeed in maintaining drug-free remission. For example, it may be that

local arthritis memory fails to form, or that the triggering antigens disappear, or that memory mechanisms are somehow cleared or suppressed. Finally, since flares off medication appear to carry the highest risk for disease extension, it will be important to study whether patients in remission who are tolerating therapy should be continued on treatment rather than attempting to discontinue medications, especially if risk of relapse is predictably substantial, comparing outcomes including long-term remission, medication exposure, side effects, and cost.

Taken together, our data show 2 interwoven patterns in inflammatory arthritis: a predilection for joints that have been inflamed previously to flare again, which we term joint-specific memory, and an ongoing predilection in many patients to accumulate new joints with disease flares. These findings support therapeutic efforts targeting mechanisms of synovial memory while also defining a new paradigm of disease chronicity—the joint accumulation hypothesis—that may favor early and sustained treatment to forestall arthritis extension by preventing disease flares.

## AUTHOR CONTRIBUTIONS

All authors were involved in drafting the article or revising it critically for important intellectual content, and all authors approved the final version to be published. Dr. Nigrovic had full access to all of the data in the study and takes responsibility for the integrity of the data and the accuracy of the data analysis.

**Study conception and design.** Chang, Bocharnikov, Nigrovic.

**Acquisition of data.** Chang, Bocharnikov, Case, Todd, Laird-Gion, Alvarez-Baumgartner.

**Analysis and interpretation of data.** Chang, Nigrovic.

## REFERENCES

1. Chang MH, Nigrovic PA. Antibody-dependent and-independent mechanisms of inflammatory arthritis [review]. *JCI Insight* 2019;4:e125278.
2. Roberts WN, Daltroy LH, Anderson RJ. Stability of normal joint findings in persistent classic rheumatoid arthritis. *Arthritis Rheum* 1988; 31:267–71.
3. Heckert SL, Bergstra SA, Matthijssen XM, Goekoop-Ruiterman YP, Fodili F, Wolde ST, et al. Joint inflammation tends to recur in the same joints during the rheumatoid arthritis disease course. *Ann Rheum Dis* 2022;81:169–74.
4. Nigrovic PA, Raychaudhuri S, Thompson SD. Genetics and the classification of arthritis in adults and children [review]. *Arthritis Rheumatol* 2018;70:7–17.
5. Nigrovic PA, Colbert RA, Holers VM, Ozen S, Ruperto N, Thompson SD, et al. Biological classification of childhood arthritis: roadmap to a molecular nomenclature. *Nat Rev Rheumatol* 2021;17: 257–69.
6. Nigrovic PA, White PH. Care of the adult with juvenile rheumatoid arthritis. *Arthritis Rheum* 2006;55:208–16.
7. Guzman J, Oen K, Tucker LB, Huber AM, Shiff N, Boire G, et al. The outcomes of juvenile idiopathic arthritis in children managed with contemporary treatments: results from the ReACCh-Out cohort. *Ann Rheum Dis* 2015;74:1854–60.
8. Petty RE, Southwood TR, Manners P, Baum J, Glass DN, Goldenberg J, et al. International League of Associations for

- Rheumatology classification of juvenile idiopathic arthritis: second revision, Edmonton, 2001. *J Rheumatol* 2004;31:390–2.
9. United States Food and Drug Administration. Drugs@FDA: FDA-Approved Drugs. URL: <https://www.accessdata.fda.gov/scripts/cder/daf/index.cfm>.
  10. Friščić J, Böttcher M, Reinwald C, Bruns H, Wirth B, Popp SJ, et al. The complement system drives local inflammatory tissue priming by metabolic reprogramming of synovial fibroblasts. *Immunity* 2021;54:1002–21.
  11. Nakano K, Whitaker JW, Boyle DL, Wang W, Firestein GS. DNA methylome signature in rheumatoid arthritis. *Ann Rheum Dis* 2013;72:110–7.
  12. Ai R, Laragione T, Hammaker D, Boyle DL, Wildberg A, Maeshima K, et al. Comprehensive epigenetic landscape of rheumatoid arthritis fibroblast-like synoviocytes. *Nat Commun* 2018;9:1921.
  13. Gebhardt T, Palendira U, Tschärke DC, Bedoui S. Tissue-resident memory T cells in tissue homeostasis, persistent infection, and cancer surveillance. *Immunol Rev* 2018;283:54–76.
  14. Park CO, Kupper TS. The emerging role of resident memory T cells in protective immunity and inflammatory disease. *Nat Med* 2015;21:688–97.
  15. Mizukawa Y, Yamazaki Y, Teraki Y, Hayakawa J, Hayakawa K, Nuriya H, et al. Direct evidence for interferon-gamma production by effector-memory-type intraepidermal T cells residing at an effector site of immunopathology in fixed drug eruption. *Am J Pathol* 2002;161:1337–47.
  16. Boyman O, Hefti HP, Conrad C, Nickoloff BJ, Suter M, Nestle FO. Spontaneous development of psoriasis in a new animal model shows an essential role for resident T cells and tumor necrosis factor-alpha. *J Exp Med* 2004;199:731–6.
  17. Chang MH, Levescot A, Nelson-Maney N, Blaustein RB, Winden KD, Morris A, et al. Arthritis flares mediated by tissue-resident memory T cells in the joint. *Cell Rep* 2021;37:109902.
  18. Onuora S. Erasing the memory of arthritis in joints [review]. *Nat Rev Rheumatol* 2022;18:5.
  19. Boers M. Understanding the window of opportunity concept in early rheumatoid arthritis [review]. *Arthritis Rheum* 2003;48:1771–4.
  20. Van Nies JA, Krabben A, Schoones JW, Huizinga TW, Kloppenburg M, van der Helm-van Mil AH. What is the evidence for the presence of a therapeutic window of opportunity in rheumatoid arthritis? A systematic literature review. *Ann Rheum Dis* 2014;73:861–70.
  21. Bergstra SA, Van Der Pol JA, Riyazi N, Goekoop-Ruiterman YP, Kerstens P, Lems W, et al. Earlier is better when treating rheumatoid arthritis: but can we detect a window of opportunity? *RMD Open* 2020;6:e001242.
  22. Ebrahimian S, Salami A, Mahdavi AM, Esalatmanesh K, Khabbazi A, Hajjalilo M. Can treating rheumatoid arthritis with disease-modifying anti-rheumatic drugs at the window of opportunity with tight control strategy lead to long-term remission and medications free remission in real-world clinical practice? A cohort study. *Clin Rheumatol* 2021;40:4485–91.
  23. Tynjala P, Vahasalo P, Tarkiainen M, Kroger L, Aalto K, Malin M, et al. Aggressive combination drug therapy in very early polyarticular juvenile idiopathic arthritis (ACUTE-JIA): a multicentre randomised open-label clinical trial. *Ann Rheum Dis* 2011;70:1605–12.
  24. Hissink Muller P, Brinkman DM, Schonenberg-Meinema D, van den Bosch WB, Koopman-Keemink Y, Brederije IC, et al. Treat to target (drug-free) inactive disease in DMARD-naive juvenile idiopathic arthritis: 24-month clinical outcomes of a three-armed randomised trial. *Ann Rheum Dis* 2019;78:51–9.
  25. Kimura Y, Schanberg LE, Tomlinson GA, Riordan ME, Denny AC, Del Gaizo V, et al. Optimizing the Start time of biologics in polyarticular juvenile idiopathic arthritis: a comparative effectiveness study of childhood arthritis and Rheumatology Research Alliance Consensus Treatment Plans. *Arthritis Rheumatol* 2021;73:1898–909.
  26. Muller PC, Brinkman DM, Schonenberg D, Koopman-Keemink Y, Brederije IC, Bekkering WP, et al. A comparison of three treatment strategies in recent onset non-systemic juvenile idiopathic arthritis: initial 3-months results of the BeSt for Kids-study. *Pediatr Rheumatol Online J* 2017;15:11.
  27. Ong MS, Ringold S, Kimura Y, Schanberg LE, Tomlinson GA, Natter MD, et al. Improved disease course associated with early initiation of biologics in polyarticular juvenile idiopathic arthritis: trajectory analysis of a childhood arthritis and Rheumatology Research Alliance Consensus Treatment Plans Study. *Arthritis Rheumatol* 2021;73:1910–20.
  28. Petty RE, Laxer RM, Lindsley CB, Wedderburn LR, Mellins E, Fuhlbrigge R. *Textbook of pediatric rheumatology*. Philadelphia: Elsevier, Inc; 2020.
  29. Wallace CA, Huang B, Bandeira M, Ravelli A, Giannini EH. Patterns of clinical remission in select categories of juvenile idiopathic arthritis. *Arthritis Rheum* 2005;52:3554–62.

## LETTERS

DOI 10.1002/art.42294


### Duloxetine and osteoarthritis, a herd of elephants in the room: comment on the article by van den Driest et al

To the Editor:

Dr. van den Driest and colleagues must be commended for their cluster-randomized trial, which showed that duloxetine had no added value in patients with chronic knee or hip osteoarthritis (OA)-related pain (1). This confirmed a recent meta-analysis (2).

However, we question whether van den Driest and colleagues could have provided a rationale for their conclusion: “Another trial including patients with centralized pain symptoms should be conducted.” Indeed, duloxetine has no advantages versus other antidepressants but does have specific serious adverse effects, such as life-threatening liver injury (3) and severe skin reactions, including Stevens-Johnson syndrome (4). Both of these complications are mentioned in the summary of the product characteristics. Furthermore, duloxetine ranks worst among antidepressants for causing hyponatremia (5). Finally, duloxetine is listed among “105 drugs to avoid” (drugs that are more harmful than beneficial in all of their approved indications or drugs having an alternative with a better harm-to-benefit balance) in the yearly independent drug publication *Prescrire* (6). This “choosing wisely initiative” remains deliberately ignored by regulatory agencies and by prescribers, as duloxetine is ranked 26 of the 50 most commonly prescribed medications in the US (7).

Author disclosures are available at <https://onlinelibrary.wiley.com/action/downloadSupplement?doi=10.1002%2Fart.42294&file=art42294-sup-0001-Disclosureform.pdf>.

Alain Braillon, MD, PhD   
[braillon.alain@gmail.com](mailto:braillon.alain@gmail.com)  
Previously senior consultant  
Amiens, France

1. Van den Driest JJ, Schiphof D, Koffeman AR, et al. No added value of duloxetine in patients with chronic pain due to hip or knee osteoarthritis: a cluster-randomized trial. *Arthritis Rheumatol* 2022;74:818–28.
2. Osani MC, Bannuru RR. Efficacy and safety of duloxetine in osteoarthritis: a systematic review and meta-analysis. *Korean J Int Med* 2019;34:966–73.
3. Wernicke J, Pangallo B, Wang F, et al. Hepatic effects of duloxetine-I: non-clinical and clinical trial data. *Curr Drug Saf* 2008;3:132–42.
4. Strawn JR, Whitsel R, Nandagopal JJ, et al. Atypical Stevens-Johnson syndrome in an adolescent treated with duloxetine. *J Child Adolesc Psychopharmacol* 2011;21:91–2.
5. Revol R, Rault C, Polard E, et al. Hyponatremia associated with SSRI/NRSI: descriptive and comparative epidemiological study of the incidence rates of the notified cases from the data of the French

National Pharmacovigilance Database and the French National Health Insurance. *Encephale* 2018;44:291–6. In French.

6. *Prescrire*. Towards better patient care: drugs to avoid in 2022. *Prescrire Int* 2022;31:50-1–50-10. URL: <https://english.prescrire.org/en/OA3B7E6B94F2B2EAE84F816CDBA3D5EE/Download.aspx>
7. ClinCalc.com. Duloxetine. Drug usage statistics, United States, 2013–2019. URL: <https://clincalc.com/DrugStats/Drugs/Duloxetine>.

DOI 10.1002/art.42293

### Duloxetine may have clinical value: comment on the article by van den Driest et al

To the Editor:

We read with interest the article by Dr. van den Driest and colleagues (1), who reported a pragmatic trial of duloxetine in patients with knee and hip OA. This study adds to the extensive information confirming that currently available therapy for painful OA is hardly ideal, and we agree that treatments found to add no benefit at all should be discarded. We suggest, however, that this trial does not provide sufficient evidence to remove duloxetine from our OA armamentarium, and we are concerned that the title, which includes the phrase, “no added value of duloxetine,” may be used by payers to deny patients a therapy who many (albeit a minority) may find efficacious. We list our concerns regarding some of the details of the article.


First, although this trial was designed as a pragmatic trial, only 3% of those screened (133 of 4,748) were enrolled, which raises issues of generalizability. Moreover, whereas pragmatic trials generally enroll large groups of patients to overcome inherent heterogeneity, this study included group sizes of only 66 patients, even though OA is overwhelmingly the most prevalent form of arthritis. The difficulty in enrollment for an OA trial that used a conventional and approved medication raises questions regarding the possible experiences of the study population with neuroactive agents in general.

Second, every one of the 29 outcome parameters listed in Table 2 in the article by van den Driest et al yielded superior responses in the duloxetine group compared with the group with usual care alone. None of the responses were statistically significant, likely due to high variance with small group sizes, but it would be unlikely that this remarkably consistent pattern occurred by chance alone, and a Type 2 statistical error seems likely. This is exacerbated by the fact that the investigators enrolled only two-thirds of the patients that their prospective power analyses suggested were required (66 instead of 102 participants per group).

Third, the authors recognized that OA-related pain is multifactorial, including nociceptive pain and peripheral and central sensitization; however, they did not address myofascial pain, which is common in OA and for which duloxetine may provide relief. Coexisting fibromyalgia in OA has a reported prevalence of 30–40% (2). In this trial, 23 of 56 patients (41%) continued duloxetine for 12 months, suggesting that they experienced a benefit. Perceived improvement, which may address all factors in a patient's experience that are not covered by specific questionnaires, was reported by 15 of 66 patients in the duloxetine group versus 4 of 66 in the usual care (control) group (chi-square with Yates' correction = 7.4392,  $P = 0.013$ ).

This trial provides evidence that duloxetine, like all currently available options, is suboptimal for OA pain. However, we believe it is premature to conclude on the basis of these results that it is of no clinical value for OA.

Author disclosures are available at <https://onlinelibrary.wiley.com/action/downloadSupplement?doi=10.1002%2Fart.42293&file=art42293-sup-0001-Disclosureform.pdf>.

Joel A. Block, MD   
jblock@rush.edu  
Theodore Pincus, MD  
Division of Rheumatology  
Rush University Medical Center  
Chicago, IL

1. Van den Driest JJ, Schiphof D, Koffeman AR, et al. No added value of duloxetine in patients with chronic pain due to hip or knee osteoarthritis: a cluster-randomized trial. *Arthritis Rheumatol* 2022;74:818–28.
2. Schmukler J, Jamal S, Castrejon I, et al. Fibromyalgia Assessment Screening Tools (FAST) based on only Multidimensional Health Assessment Questionnaire (MDHAQ) scores as clues to fibromyalgia. *ACR Open Rheumatol* 2019;1:516–25.

DOI 10.1002/art.42291

## Reply

To the Editor:

We thank Dr. Braillon and Drs. Block and Pincus for their comments on our recent article.

The first comment concerned the generalizability of our results. In The Netherlands, duloxetine is not registered for use in patients with OA-related pain and therefore is not a common treatment for general practitioners (GPs) to prescribe for OA-related pain (1). In our cluster-randomized trial, patients were eligible when acetaminophen and nonsteroidal antiinflammatory drugs (NSAIDs) did not reduce symptoms of pain or if these medications had side effects or were contraindicated. Treatment with duloxetine is not indicated for all patients with OA. For our trial, GPs asked their patients to participate based on their medical records to avoid introducing bias. The indication for prescribing duloxetine was difficult to assess based on the medical records,

especially with regard to presence of pain. GPs could only examine for the presence of certain exclusion criteria, like comorbidities or use of certain medications, in the medical records. Therefore, the number of patients suitable for inclusion was much lower than the 4,748 patients registered with OA in the GPs' medical records. Only 205 patients were eligible for the trial, and only 133 (65%) of these patients who were suitable for the intervention participated in the trial. Despite these limitations, we believe our trial included a representative sample of patients for whom duloxetine can be prescribed.

The second remark addressed the results of our trial in the context of current prescription practices of duloxetine and future research. Our results showed only small, not clinically relevant effects in the outcome parameters. Based on the 95% confidence intervals, we even could rule out the presence of a clinically relevant effect for the complete group of patients with OA. This result is in accordance with a more recent meta-analysis on the efficacy and safety of antidepressants for low back pain and OA, which also demonstrated no effect of duloxetine for OA-related pain, although the investigators could not rule out the possibility of a relevant effect (2). We note that pain in OA is multifactorial (3) and can consist of nociceptive pain from the joint or from alterations in central pain processing, and duloxetine may only be beneficial for a specific subtype of OA. A possible disadvantage of a pragmatic trial can be that the effect of the intervention is not found, because it is predominantly found in a specific phenotype of OA (4). For this reason, we specified a subgroup analysis a priori. We hypothesized that the effect of duloxetine would be predominantly found in patients with symptoms of central sensitization. In this subgroup analysis, we did not observe this effect (in fact, the estimate was about the same as in the total group); however, this finding was based on smaller numbers and we could not rule out a clinically relevant effect. For this reason, we advised a more extensive study of duloxetine's effectiveness in this specific subgroup.

The final comment addressed the side effects of duloxetine. The current American College of Rheumatology guidelines conditionally recommend the use of duloxetine for patients with knee, hip, and/or hand OA and specifically mention issues about the tolerability of duloxetine (5). In our trial, the presence of side effects from duloxetine was high; during follow-up, 57% of the patients who quit taking duloxetine had stopped because of the presence of side effects. No serious adverse events occurred during our trial. Furthermore, 39% (28 of 72) of the eligible patients declined to participate because of fear of side effects, indicating a concern among patients.

So that an effective treatment is not withheld from patients, research is needed to assess if and for which subgroup duloxetine may be useful, rather than prescribing duloxetine to all patients with OA who have moderate or worse pain and who do not respond satisfactorily to paracetamol or oral NSAIDs or cannot use such medications. However, the tolerability and risks of serious side effects should be considered when assessing the use of duloxetine for OA-related pain.

Jacoline J. van den Driest, MD  
[j.vandendriest@erasmusmc.nl](mailto:j.vandendriest@erasmusmc.nl)  
 Dieuwke Schiphof, PhD  
 Patrick J. E. Bindels, MD, PhD  
*Department of General Practice,  
 Erasmus MC, University Medical Center  
 Rotterdam, The Netherlands*  
 Aafke R. Koffeman, MD, PhD  
*Department of Public Health and Primary Care  
 Leiden University Medical Center  
 Leiden, The Netherlands*  
 Marc A. Koopmanschap, PhD  
*Department of Health Policy and Management  
 Erasmus University Rotterdam  
 Rotterdam, The Netherlands*  
 Sita M. A. Bierma-Zeinstra, PhD  
*Department of General Practice  
 and Department of Orthopedics  
 Erasmus MC, University Medical Center  
 Rotterdam, The Netherlands*

1. Dutch College of General Practitioners (NHG). NHG Standaard Niet-traumatische knieklachten. 2016. URL: [https://www.nhg.org/standaarden/volledig/nhg-standaard-niet-traumatische-knieklachten#Richtlijnen\\_diagnostiek](https://www.nhg.org/standaarden/volledig/nhg-standaard-niet-traumatische-knieklachten#Richtlijnen_diagnostiek)
2. Ferreira GE, McLachlan AJ, Lin CC, et al. Efficacy and safety of antidepressants for the treatment of back pain and osteoarthritis: systematic review and meta-analysis. *BMJ* 2021;372:m4825.
3. Deveza LA, Loeser RF. Is osteoarthritis one disease or a collection of many? *Rheumatology (Oxford)* 2018;57:iv34–iv42.
4. Pawson R. The shrinking scope of pragmatic trials: a methodological reflection on their domain of applicability. *J Clin Epidemiol* 2019;107:71–6.
5. Kolasinski SL, Neogi T, Hochberg MC, Oatis C, Guyatt G, Block J, et al. 2019 American College of Rheumatology/Arthritis Foundation guideline for the management of osteoarthritis of the hand, hip, and knee. *Arthritis Rheumatol* 2020;72:220–33.

DOI 10.1002/art.42275

### Differences in definitions and prevalence of hand osteoarthritis: comment on the article by Eaton et al

To the Editor:

We read with great interest the article by Dr. Eaton et al (1) in which they discussed their findings from a study of hand osteoarthritis (OA), utilizing data from the Osteoarthritis Initiative (OAI), which included individuals with or at risk for knee OA. The contributions of their study to the broader research on the understudied areas of hand OA and multiple joint OA are appreciated. As with any study, there are several items to consider when interpreting the results of this work, particularly the available data, the population, and the stated definitions. Hand OA was not an initial focus of the OAI, so the data were limited, including the use of an overall question on hand pain (rather than joint-specific information) and the examination of radiographs for only the dominant hand in most participants. A standard definition of hand OA is not available, although bilateral involvement is so common in patients that

its presence is often incorporated into robust case definitions (2). The exclusion of the carpometacarpal joints from the definitions diminishes the impact of these results, given the disproportionate effects of carpometacarpal OA on function and quality of life.

Importantly, although the authors highlighted lower frequencies of OA in Black participants as “noteworthy and relatively novel,” the authors missed an opportunity to compare their results with highly relevant publications from the Johnston County Osteoarthritis Project, a diverse population-based cohort that oversampled Black participants. Using data from the Johnston County Osteoarthritis Project, we have previously reported differences by race for multiple joint OA (3). Compared with the findings in White participants, we found that Black participants had lower frequencies of hand OA, with or without other joints involved, but more often had multiple large joint involvement (4,5). We also observed a higher incidence for most definitions of hand OA among White participants (6). White participants had significantly greater progression at the thumb base, but progression was otherwise not statistically different by race (6).

We look forward to continued work by the OA community to explore these important variations in hand OA by sex, race and ethnicity, and other individual factors as we unravel this complex and heterogeneous condition.

Author disclosures are available at <https://onlinelibrary.wiley.com/action/downloadSupplement?doi=10.1002%2Fart.42275&file=art42275-sup-0001-Disclosureform.pdf>.

Amanda E. Nelson, MD, MSCR   
[aenelson@med.unc.edu](mailto:aenelson@med.unc.edu)  
 Todd A. Schwartz, DrPH   
 Carolina Alvarez, MS  
*Thurston Arthritis Research Center  
 University of North Carolina at Chapel Hill  
 Chapel Hill, NC*  
 Yvonne M. Golightly, PT, PhD   
*Thurston Arthritis Research Center  
 University of North Carolina at Chapel Hill  
 Chapel Hill, NC  
 and College of Allied Health Professions  
 University of Nebraska Medical Center  
 Omaha, NE*

1. Eaton CB, Schaefer LF, Duryea J, et al. Prevalence, incidence, and progression of radiographic and symptomatic hand osteoarthritis: the Osteoarthritis Initiative. *Arthritis Rheumatol* 2022;74:992–1000.
2. Kraus VB, Jordan JM, Doherty M, et al. The Genetics of Generalized Osteoarthritis (GOGO) study: study design and evaluation of osteoarthritis phenotypes. *Osteoarthritis Cartilage* 2007;15:120–7.
3. Gullo TR, Golightly YM, Cleveland RJ, et al. Defining multiple joint osteoarthritis, its frequency and impact in a community-based cohort. *Semin Arthritis Rheum* 2019;48:950–7.
4. Nelson AE, Golightly YM, Renner JB, et al. Brief report: differences in multijoint symptomatic osteoarthritis phenotypes by race and sex: the Johnston County Osteoarthritis Project. *Arthritis Rheum* 2013;65:373–7.
5. Nelson AE, Renner JB, Schwartz TA, et al. Differences in multijoint radiographic osteoarthritis phenotypes among African Americans and



Caucasians: the Johnston County Osteoarthritis project. *Arthritis Rheum* 2011;63:3843–52.

- Snyder EA, Alvarez C, Golightly YM, et al. Incidence and progression of hand osteoarthritis in a large community-based cohort: the Johnston County Osteoarthritis Project. *Osteoarthritis Cartilage* 2020;28:446–52.

DOI 10.1002/art.42276



## Reply

*To the Editor:*

We agree with Dr. Nelson et al that hand OA is understudied and that each cohort provides a unique perspective that adds to our knowledge base of the natural history and etiology of hand OA. We also agree that there are limitations in studying hand OA epidemiology in the OAI. In our study, we excluded robust measures of hand-related work injuries and trauma and joint-specific pain; instead, we relied on participants to use a homunculus to indicate the site of hand pain, which we then matched to the participant's radiograph to define hand OA. Although the OAI lacked bilateral hand imaging for many participants, we believe our hand OA definition, which required  $\geq 2$  affected joints on different fingers, to be a robust definition. Our definition is more conservative than the Framingham OA study, which defined presence of hand OA at the individual level as  $\geq 1$  affected joint (1).

Over 95% of our study sample had dominant hand radiographs, so it is unlikely that the small number of participants with unknown hand dominance affected our results. In addition, although we observed carpometacarpal OA to be highly prevalent in our participants, as shown in our prevalence figures by sex, the epidemiology of carpometacarpal OA differs from interphalangeal joint OA. Similar to our results, carpometacarpal OA appears to be more common in women (2), is related to hypermobility (3–5), and is more prevalent in the nondominant hand (6). Because we measured hand OA in the dominant hand, we did not include carpometacarpal OA in our definition of hand OA. Recently, we focused on thumb-based OA (7); an area of future investigation could be a focus on the etiology of thumb-based OA as a separate phenotype.

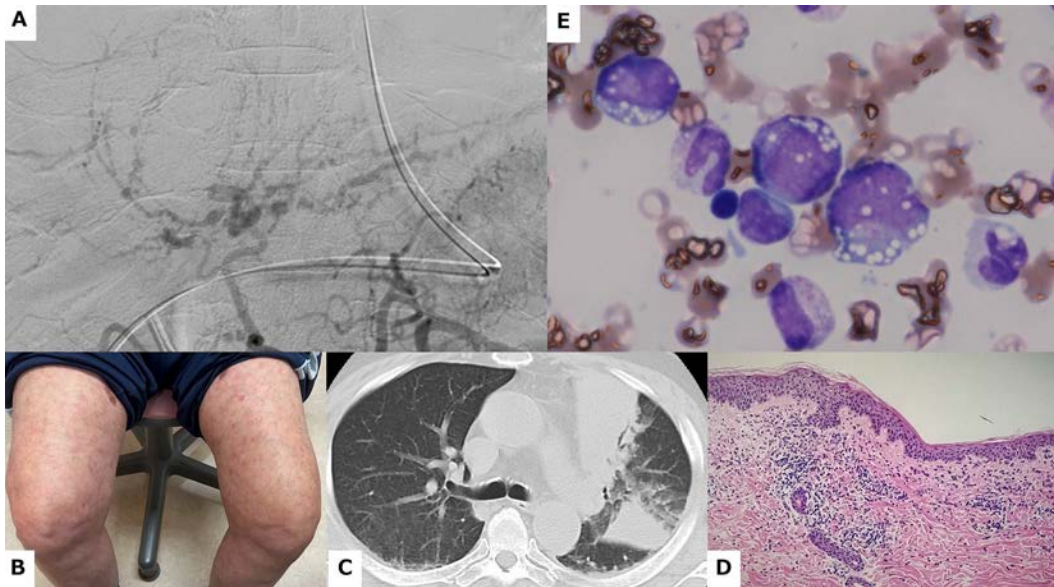
We did compare our results to the important information in the Johnston County cohort (8). Still, we appreciate the more complete summary of results from Johnston County provided by Nelson et al. The interesting finding in the Johnston County cohort that Black participants more frequently had multiple large joint OA but less frequently had hand OA could be replicated in the OAI cohort. We also found an interesting age–sex–race interaction that could be replicated in the Johnston County Cohort. We look forward to further exploring the complex etiology of hand OA and multiple joint OA in the larger OA community.

Charles B. Eaton, MD, MS   
[Cbeaton51@gmail.com](mailto:Cbeaton51@gmail.com)  
 Center for Primary Care and Prevention  
 Alpert Medical School of Brown University  
 Pawtucket, RI  
 Tim McAlindon, MD, MPH  
 Jeffrey Driban, PhD   
 Tufts Medical Center  
 Boston, MA

- Haugen IK, Englund M, Aliabadi P, et al. Prevalence, incidence and progression of hand osteoarthritis in the general population: the Framingham Osteoarthritis study. *Ann Rheum Dis* 2011;70: 1581–6.
- Haara MM, Heliövaara M, Kröger H, et al. Osteoarthritis in the carpometacarpal joint of the thumb. Prevalence and associations with disability and mortality. *J Bone Joint Surg Am* 2004;86:1452–7.
- Jónsson H, Eliasson GJ, Jónsson A, et al. High hand joint mobility is associated with radiological CMC1 osteoarthritis: the AGES-Reykjavik study. *Osteoarthr Cartilage* 2009;17:592–5.
- Jónsson H, Valtýsdóttir ST, Kjartansson O, et al. Hypermobility associated with osteoarthritis of the thumb base: a clinical and radiological subset of hand osteoarthritis. *Ann Rheum Dis* 1996;55:540–3.
- Hunter DJ, Zhang Y, Sokolove J, et al. Trapeziometacarpal subluxation predisposes to incident trapeziometacarpal osteoarthritis (OA): the Framingham Study. *Osteoarthr Cartilage* 2005;13:953–7.
- Acheson RM, Chan YK, Clemett AR. New Haven survey of joint diseases. XII. Distribution and symptoms of osteoarthritis in the hands with reference to handedness. *Ann Rheum Dis* 1970;29:275–86.
- Driban JB, Lo GH, Roberts MB, et al. Racket or bat sports: no association with thumb-base osteoarthritis. *J Athl Train* 2022;57(4):341–51.
- Qin J, Barbour KE, Murphy LB, et al. Lifetime risk of symptomatic hand osteoarthritis: the Johnston County Osteoarthritis Project. *Arthritis Rheumatol* 2017;69:1204–12.

DOI 10.1002/art.42257


### Clinical images: VEXAS syndrome presenting as treatment-refractory polyarteritis nodosa



The patient, a 74-year-old man, presented with fever, chest pain, and pruritic rash. One year earlier, the patient was diagnosed as having polyarteritis nodosa after he developed fever, weight loss, and cholangitis, with multiple hepatic aneurysms shown on angiography (A). The patient was started on a regimen of high-dose prednisolone with cyclophosphamide, rituximab, and mycophenolate mofetil, but prednisolone could not be tapered below 15 mg once daily. After treatment initiation, erythema developed on the patient's trunk and extremities (B), but there was no evidence of auricular or nasal chondritis. Electrocardiogram findings were unremarkable and showed no ST changes. Laboratory investigations revealed elevated levels of inflammatory markers as well as presence of leukopenia and macrocytic anemia. Results of a computed tomography scan indicated the presence of a pulmonary infarction (C). A skin biopsy revealed erythematous lesions indicative of neutrophilic dermatitis (D). Vacuoles were present in myeloid precursor cells from bone marrow aspirates (E). With the Sanger method, DNA sequencing of leukocytes from the patient's peripheral blood demonstrated the presence of a somatic *UBA1* variant, c.121A>G resulting in p.Met41Val, which established a diagnosis of VEXAS (vacuoles, E1 enzyme, X-linked, autoinflammatory, somatic) syndrome (1). After the patient was started on treatment with intravenous tocilizumab, his symptoms improved, and steroids could be tapered (2). VEXAS syndrome is a late adulthood-onset autoinflammatory disease, which most often presents as relapsing polychondritis (1). Polyarteritis nodosa has been infrequently reported. This case highlights the importance of broadening the differential diagnosis for treatment-refractory vasculitis with skin rash and hematologic abnormalities, as VEXAS syndrome is an evolving acquired inflammatory condition associated with vasculitides that requires different types of therapy (1,2).

We thank Rita McGill, MD, MS (Department of Nephrology, University of Chicago), for the English correction of a draft of this article. Author disclosures are available at <https://onlinelibrary.wiley.com/action/downloadSupplement?doi=10.1002%2Fart.42257&file=art42257-sup-0001-Disclosureform.pdf>.

1. Beck DB, Ferrada MA, Sikora KA, et al. Somatic mutations in *UBA1* and severe adult-onset autoinflammatory disease. *N Engl J Med* 2020;383:2628–38.
2. Kirino Y, Takase-Minegishi K, Tsuchida N, et al. Tocilizumab in VEXAS relapsing polychondritis: a single-center pilot study in Japan. *Ann Rheum Dis* 2021;80:1501–2.

Masaki Itagane, MD   
[m.itagane@gmail.com](mailto:m.itagane@gmail.com)  
Department of Rheumatology  
Okinawa Chubu Hospital  
Okinawa, Japan  
Hiroyuki Teruya, MD

*Clinical Images (Cont'd)*

*Department of Allergy and Rheumatology  
The University of Tokyo  
Graduate School of Medicine  
Tokyo, Japan*  
Tomohiro Kato, MD  
*Department of Rheumatic Diseases  
Tokyo Metropolitan Tama Medical Center  
Tokyo, Japan*  
Naomi Tsuchida, MD, PhD   
*Department of Stem Cell and Immune Regulation  
and Department of Human Genetics  
Yokohama City University Graduate School of Medicine  
and Department of Rare Disease Genomics  
Yokohama City University Hospital  
Yokohama, Japan*  
Ayaka Maeda, MD  
Yohei Kirino, MD, PhD 

*Department of Stem Cell and Immune Regulation  
Yokohama City University Graduate School of Medicine  
Yokohama, Japan*  
Yuri Uchiyama, MD, PhD   
*Department of Human Genetics  
Yokohama City University Graduate School of Medicine  
and Department of Rare Disease Genomics  
Yokohama City University Hospital  
Yokohama, Japan*  
Naomichi Matsumoto, MD, PhD   
*Department of Human Genetics  
Yokohama City University Graduate School of Medicine  
Yokohama, Japan*  
Mitsuyo Kinjo, MD, MPH   
*Department of Rheumatology  
Okinawa Chubu Hospital  
Okinawa, Japan*

# Arthritis & Rheumatology

An Official Journal of the American College of Rheumatology  
www.arthritisrheum.org and wileyonlinelibrary.com

## GENERAL INFORMATION

### TO SUBSCRIBE

#### Institutions and Non-Members

Email: wileyonlinelibrary.com  
Phone: (201) 748-6645  
Write: Wiley Periodicals LLC  
Attn: Journals Admin Dept  
UK  
111 River Street  
Hoboken, NJ 07030

Volumes 74, 2022:  
Institutional Print Only:

Institutional Online Only:  
Institutional Print and  
Online Only:

**Arthritis & Rheumatology and Arthritis Care & Research:**  
\$2,603 in US, Canada, and Mexico  
\$2,603 outside North America

\$2,495 in US, Canada, Mexico, and outside North America  
\$2,802 in US, Canada, and Mexico; \$2,802 outside  
North America

For submission instructions, subscription, and all other information visit: wileyonlinelibrary.com.

Arthritis & Rheumatology accepts articles for Open Access publication. Please visit <https://authorservices.wiley.com/author-resources/Journal-Authors/open-access/hybrid-open-access.html> for further information about OnlineOpen.

Wiley's Corporate Citizenship initiative seeks to address the environmental, social, economic, and ethical challenges faced in our business and which are important to our diverse stakeholder groups. Since launching the initiative, we have focused on sharing our content with those in need, enhancing community philanthropy, reducing our carbon impact, creating global guidelines and best practices for paper use, establishing a vendor code of ethics, and engaging our colleagues and other stakeholders in our efforts.

Follow our progress at [www.wiley.com/go/citizenship](http://www.wiley.com/go/citizenship).

Access to this journal is available free online within institutions in the developing world through the HINARI initiative with the WHO. For information, visit [www.healthinternetwork.org](http://www.healthinternetwork.org).

### Disclaimer

The Publisher, the American College of Rheumatology, and Editors cannot be held responsible for errors or any consequences arising from the use of information contained in this journal; the views and opinions expressed do not necessarily reflect those of the Publisher, the American College of Rheumatology and Editors, neither does the publication of advertisements constitute any endorsement by the Publisher, the American College of Rheumatology and Editors of the products advertised.

### Members:

#### American College of Rheumatology/Association of Rheumatology Professionals

For membership rates, journal subscription information, and change of address, please write:

American College of Rheumatology  
2200 Lake Boulevard  
Atlanta, GA 30319-5312  
(404) 633-3777

### ADVERTISING SALES AND COMMERCIAL REPRINTS

**Sales:** Kathleen Malseed, National Account Manager  
E-mail: [kmalseed@pminy.com](mailto:kmalseed@pminy.com)  
Phone: (215) 852-9824  
Pharmaceutical Media, Inc.  
30 East 33rd Street, New York, NY 10016

**Production:** Patti McCormack  
E-mail: [pmccormack@pminy.com](mailto:pmccormack@pminy.com)  
Phone: (212) 904-0376  
Pharmaceutical Media, Inc.  
30 East 33rd Street, New York, NY 10016

**Publisher:** Arthritis & Rheumatology is published by Wiley Periodicals LLC, 101 Station Landing, Suite 300, Medford, MA 02155

**Production Editor:** Ramona Talantor, [artprod@wiley.com](mailto:artprod@wiley.com)

ARTHRITIS & RHEUMATOLOGY (Print ISSN 2326-5191; Online ISSN 2326-5205 at Wiley Online Library, wileyonlinelibrary.com) is published monthly on behalf of the American College of Rheumatology by Wiley Periodicals LLC, a Wiley Company, 111 River Street, Hoboken, NJ 07030-5774. Periodicals postage paid at Hoboken, NJ and additional offices. POSTMASTER: Send all address changes to Arthritis & Rheumatology, Wiley Periodicals LLC, c/o The Sheridan Press, PO Box 465, Hanover, PA 17331. **Send subscription inquiries care of** Wiley Periodicals LLC, Attn: Journals Admin Dept UK, 111 River Street, Hoboken, NJ 07030, (201) 748-6645 (nonmember subscribers only; American College of Rheumatology/Association of Rheumatology Health Professionals members should contact the American College of Rheumatology). **Subscription Price:** (Volumes 74, 2022: Arthritis & Rheumatology and Arthritis Care & Research) Print only: \$2,603.00 in U.S., Canada and Mexico, \$2,603.00 rest of world. For all other prices please consult the journal's website at wileyonlinelibrary.com. All subscriptions containing a print element, shipped outside U.S., will be sent by air. Payment must be made in U.S. dollars drawn on U.S. bank. Prices are exclusive of tax. Asia-Pacific GST, Canadian GST and European VAT will be applied at the appropriate rates. For more information on current tax rates, please go to [www.wileyonlinelibrary.com/tax-vat](http://www.wileyonlinelibrary.com/tax-vat). The price includes online access to the current and all online backfiles to January 1st 2018, where available. For other pricing options including access information and terms and conditions, please visit <https://onlinelibrary.wiley.com/library-info/products/price-lists>. Terms of use can be found here: <https://onlinelibrary.wiley.com/terms-and-conditions>. **Delivery Terms and Legal Title:** Where the subscription price includes print issues and delivery is to the recipient's address, delivery terms are Delivered at Place (DAP); the recipient is responsible for paying any import duty or taxes. Title to all issues transfers Free of Board (FOB) our shipping point, freight prepaid. We will endeavor to fulfill claims for missing or damaged copies within six months of publication, within our reasonable discretion and subject to availability. **Change of Address:** Please forward to the subscriptions address listed above 6 weeks prior to move; enclose present mailing label with change of address. **Claims** for undelivered copies will be accepted only after the following issue has been received. Please enclose a copy of the mailing label or cite your subscriber reference number in order to expedite handling. Missing copies will be supplied when losses have been sustained in transit and where reserve stock permits. Send claims care of Wiley Periodicals LLC, Attn: Journals Admin Dept UK, 111 River Street, Hoboken, NJ 07030. If claims are not resolved satisfactorily, please write to Subscription Distribution c/o Wiley Periodicals LLC, 111 River Street, Hoboken, NJ 07030. **Cancellations:** Subscription cancellations will not be accepted after the first issue has been mailed. **Journal Customer Services:** For ordering information, claims and any enquiry concerning your journal subscription please go to <https://wolsupport.wiley.com/s/contactsupport?tabset-a7d10=2> or contact your nearest office. **Americas:** Email: [cs-journals@wiley.com](mailto:cs-journals@wiley.com); Tel: +1 877 762 2974. **Europe, Middle East and Africa:** Email: [cs-journals@wiley.com](mailto:cs-journals@wiley.com); Tel: +44 (0) 1865 778315; 0800 1800 536 (Germany). **Asia Pacific:** Email: [cs-journals@wiley.com](mailto:cs-journals@wiley.com); Tel: +65 6511 8000. **Japan:** For Japanese speaking support, Email: [cs-japan@wiley.com](mailto:cs-japan@wiley.com). **Visit our Online Customer Help** at <https://wolsupport.wiley.com/s/contactsupport?tabset-a7d10=2>. **Back Issues:** Single issues from current and prior year volumes are available at the current single issue price from [csjournals@wiley.com](mailto:csjournals@wiley.com). Earlier issues may be obtained from Periodicals Service Company, 351 Fairview Avenue-Ste 300, Hudson, NY 12534, USA. Tel: +1 518 822-9300, Fax: +1 518 822-9305, Email: [psc@periodicals.com](mailto:psc@periodicals.com). Printed in the USA by The Sheridan Group.